

This document was produced
by scanning the original publication.

Ce document est le produit d'une
numérisation par balayage
de la publication originale.



**GEOLOGICAL SURVEY OF CANADA
COMMISSION GÉOLOGIQUE DU CANADA**

**PAPER / ÉTUDE
90-1B**

**CURRENT RESEARCH, PART B
EASTERN AND ATLANTIC CANADA**

**RECHERCHES EN COURS, PARTIE B
EST ET RÉGION ATLANTIQUE DU CANADA**



Energy, Mines and
Resources Canada

Energie, Mines et
Ressources Canada

Canada

THE ENERGY OF OUR RESOURCES - THE POWER OF OUR IDEAS

L'ÉNERGIE DE NOS RESSOURCES - NOTRE FORCE CRÉATRICE

NOTICE TO LIBRARIANS AND INDEXERS

The Geological Survey's Current Research series contains many reports comparable in scope and subject matter to those appearing in scientific journals and other serials. Most contributions to Current Research include an abstract and bibliographic citation. It is hoped that these will assist you in cataloguing and indexing these reports and that this will result in a still wider dissemination of the results of the Geological Survey's research activities.

AVIS AUX BIBLIOTHÉCAIRES ET PRÉPARATEURS D'INDEX

La série Recherches en cours de la Commission géologique paraît une fois par année; elle contient plusieurs rapports dont la portée et la nature sont comparables à ceux qui paraissent dans les revues scientifiques et autres périodiques. La plupart des articles publiés dans Recherches en cours sont accompagnés d'un résumé et d'une bibliographie, ce qui vous permettra, nous l'espérons, de cataloguer et d'indexer ces rapports, d'où une meilleure diffusion des résultats de recherche de la Commission géologique.

**GEOLOGICAL SURVEY OF CANADA
COMMISSION GÉOLOGIQUE DU CANADA**

PAPER/ÉTUDE 90-1B

**CURRENT RESEARCH, PART B
EASTERN AND ATLANTIC CANADA**

**RECHERCHES EN COURS, PARTIE B
EST ET RÉGION ATLANTIQUE DU CANADA**

1990

© Minister of Supply and Services Canada 1990
Available in Canada through
authorized bookstore agents and other bookstores
or by mail from

Canadian Government Publishing Centre
Supply and Services Canada
Ottawa, Canada K1A 0S9

and from

Geological Survey of Canada offices :

601 Booth Street
Ottawa, Canada K1A 0E8

3303-33rd Street N.W.
Calgary, Alberta T2L 2A7

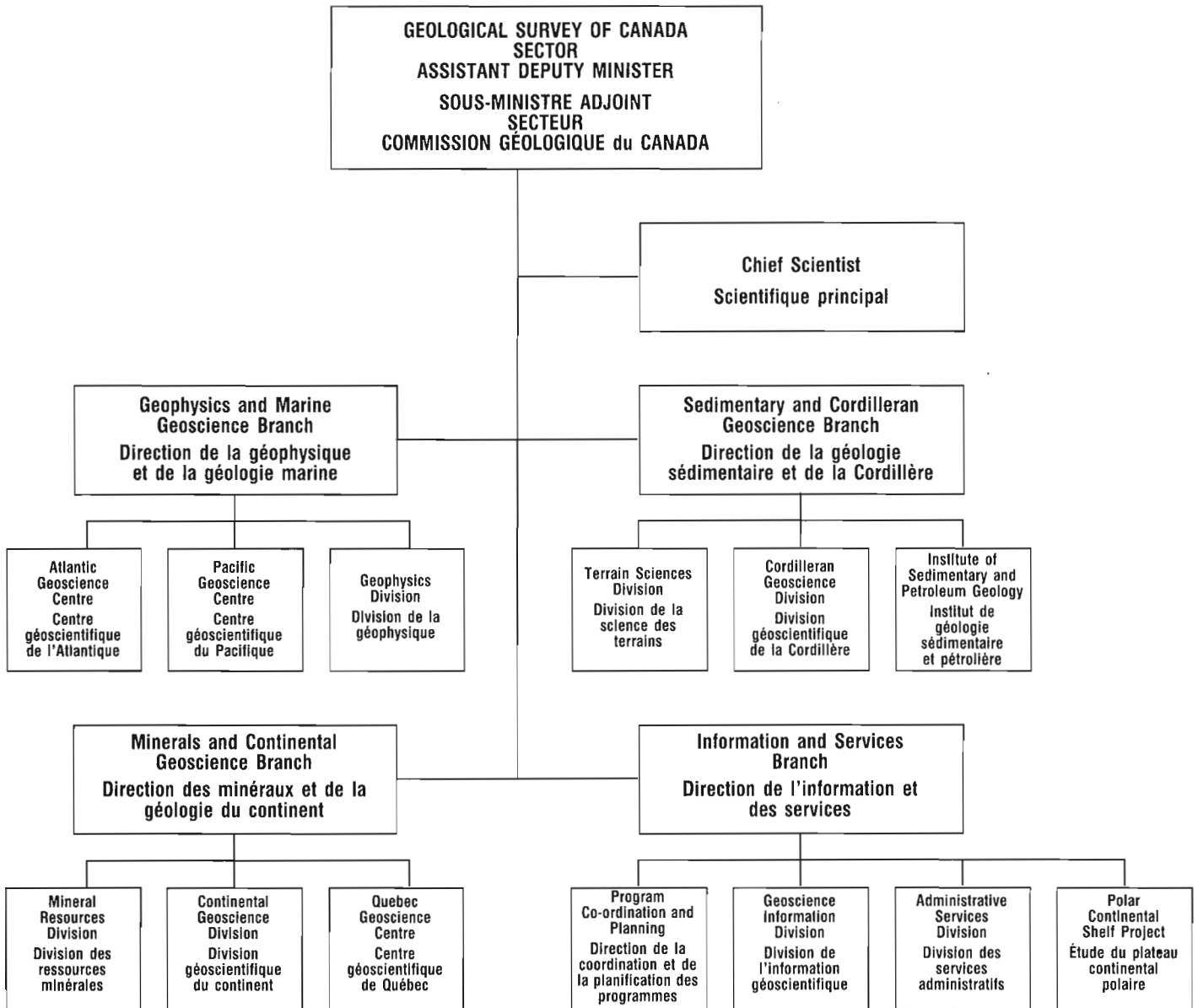
100 West Pender Street
Vancouver, British Columbia V6B 1R8

A deposit copy of this publication is also available
for reference in public libraries across Canada

Cat. No. M44-90/1B
ISBN 0-660-55678-2

Cover description

Pillar Rock: an erosional remnant of the Faribault Brook metavolcanic unit, Jumping Brook metamorphic suite, western Cape Breton Highlands, Nova Scotia. The site is near the Cabot Trail within Cape Breton Highlands National Park.



Separates

A limited number of separates of the papers that appear in this volume are available by direct request to the individual authors. The addresses of the Geological Survey of Canada offices follow:

601 Booth Street,
OTTAWA, Ontario
K1A 0E8
(FAX: 613-996-9990)

Institute of Sedimentary and Petroleum Geology,
3303-33rd Street N.W.,
CALGARY, Alberta
T2L 2A7
(FAX: 403-292-5377)

Cordilleran Division,
100 West Pender Street,
VANCOUVER, B.C.
V6B 1R8
(FAX: 604-666-1124)

Pacific Geoscience Centre
P.O. Box 6000,
9860 Saanich Road
SIDNEY, B.C.
V8L 4B2
(FAX: 604-356-6565)

Atlantic Geoscience Centre
Bedford Institute of Oceanography,
P.O. Box 1006
DARTMOUTH, N.S.
B2Y 4A2
(FAX: 902-426-2256)

Québec Geoscience Centre
2700, rue Einstein
C.P. 7500
Ste-Foy, Québec
G1V 4C7
(FAX: 418-654-2615)

When no location accompanies an author's name in the title of a paper, the Ottawa address should be used.

Tirés à part

On peut obtenir un nombre limité de « tirés à part » des articles qui paraissent dans cette publication en s'adressant directement à chaque auteur. Les adresses des différents bureaux de la Commission géologique du Canada sont les suivantes:

601, rue Booth
OTTAWA (Ontario)
K1A 0E8
(facsimilé: 613-996-9990)

Institut de géologie sédimentaire et pétrolière
3303-33rd St. N.W.,
CALGARY (Alberta)
T2L 2A7
(facsimilé: 403-292-5377)

Division de la Cordillère
100 West Pender Street,
VANCOUVER (Colombie-Britannique)
V6B 1R8
(facsimilé: 604-666-1124)

Centre géoscientifique du Pacifique
B.P. 6000,
9860 Saanich Road
SIDNEY (Colombie-Britannique)
V8L 4B2
(facsimilé: 604-356-6565)

Centre géoscientifique de l'Atlantique
Institut océanographique de Bedford
B.P. 1006
DARTMOUTH (Nouvelle-Écosse)
B2Y 4A2
(facsimilé: 902-426-2256)

Centre géoscientifique de Québec
2700, rue Einstein
C.P. 7500
Ste-Foy (Québec)
G1V 4C7
(facsimilé: 418-654-2615)

Lorsque l'adresse de l'auteur ne figure pas sous le titre d'un document, on doit alors utiliser l'adresse d'Ottawa.

CONTENTS

- 1 S. PARADIS, T.C. BIRKETT and R. GODUE
Preliminary investigations of the Upton sediment-hosted barite deposit, southern Quebec Appalachians
- 9 D. LAVOIE
Stratigraphy of the upper Cambrian-lower Ordovician barite and sulphide hosted limestones of the Acton Vale-Upton area, Québec
- 17 D. LAVOIE, N. TASSÉ and E. ASSELIN
Lithostratigraphic framework of the Upper Gaspé Limestones (Early Devonian) in eastern Gaspé Basin, Québec
- 29 D.J.W. PIPER, M.R. GIPP and K. MORAN
Radiocarbon dating evidence for the age of deglaciation of LaHave Basin, Scotian Shelf
- 33 B.V. SANFORD and A.C. GRANT
Bedrock geological mapping and basin studies in the Gulf of St. Lawrence
- 43 D.R. PARROTT, C.F.M. LEWIS, E. BANKE, G.B.J. FADER and G.V. SONNICHSEN
Seabed disturbance by a recent (1989) iceberg grounding on the Grand Banks of Newfoundland
- 49 G. VILKS, B. MACLEAN and C. RODRIGUES
Late Quaternary high resolution seismic and foraminiferal stratigraphy in the Gulf of St. Lawrence
- 59 H. JOSEPHANS, J. ZEVENHUIZEN and B. MACLEAN
Preliminary seismostratigraphic interpretations from the Gulf of St. Lawrence
- 77 B. DUBÉ
A preliminary report on contrasting structural styles of gold-only deposits in western Newfoundland
- 91 A.N. RENCZ and D.F. SANGSTER
Characterizing vegetation response to an alteration halo using LANDSAT Thematic Mapper imagery and aeromagnetic data in the Murdochville area, Gaspésie, Québec
- 95 W.D. SINCLAIR and D.M. KINGSTON
Rare-earth-bearing apatite near Benjamin River, northern New Brunswick
- 105 R.J. WETMILLER and J. ADAMS
An earthquake doublet in the Charlevoix seismic zone, Québec
- 115 M. LAMONTAGNE, R.J. WETMILLER and R. DU BERGER
Some results from the 25 November, 1988 Saguenay, Québec earthquake
- 123 R.E. MCCALLUM and J.S. BELL
In situ stress magnitudes at Whiterose, Jeanne d'Arc Basin, Grand Banks of Newfoundland
- 131 H.M. STEELE-PETROVICH
Lithostratigraphy of upper Middle Ordovician sedimentary rocks, lower Ottawa Valley, Ontario and Quebec

Preliminary investigations of the Upton sediment-hosted barite deposit, southern Quebec Appalachians

Suzanne Paradis, T.C. Birkett, and R. Godue
Quebec Geoscience Centre, Quebec

Paradis, S., Birkett, T.C., and Godue, R., Preliminary investigations of the Upton sediment-hosted barite deposit, southern Quebec Appalachians in Current Research, Part B, Geological Survey of Canada, Paper 90-1B, p. 1-8, 1990.

Abstract

The Upton stratabound barite deposit is hosted in carbonate rocks of the Upton group of the Cambro-Ordovician flyschoid belt of the Quebec Appalachians. It contains approximately 950 000 tons grading 46.5 % BaSO₄, 1.9 % Zn, 0.6 % Pb, 0.15 % Cu, 0.11 % Cd and 13.5 g/t Ag.

The mineralization consists of blade-like crystals, rosettes, fine grained aggregates, nodules and veins of barite, and disseminations, aggregates, and veinlets of sphalerite, chalcopyrite, pyrite and galena in a brecciated, massive, grey, locally fossiliferous limestone of probable late Cambrian or early Ordovician age.

The mineralized limestone is interbedded with black calcareous shales, mafic volcanic rocks, mudstones, siltstones, and barren white limestones here named the Upton Group. The Upton Group is exposed as windows within the tectonically overlying Cambrian Granby nappe.

The Upton barite deposit may be the result of a submarine exhalative process contemporaneous to sedimentation or of an epigenetic process involving emplacement/replacement into a brecciated, porous limestone aquifer.

Résumé

Le gisement de barytine d'Upton contenu au sein d'une couche unique, est logé dans les roches carbonatées du groupe d'Upton de la zone de flysch du Cambrien-Ordovicien des Appalaches du Québec. Il contient approximativement 950 000 tonnes titrant 46,5 % d'BaSO₄, 1,9 % de Zn, 0,6 % de Pb, 0,15 % de Cu, 0,11 % de Cd et 13,5 g/t d'Ag.

La minéralisation consiste en barytine de teinte grisâtre à blanchâtre, de blende, de chalcopyrite, de pyrite et de galène incluses dans un calcaire massif d'âge cambrien supérieur à Ordovicien inférieur, fossilifère par endroits, et parfois bréchique. La barytine se présente sous forme de bâtonnets, de rosettes, d'aggrégats de fins cristaux, de nodules et de filons.

Le calcaire à barytine est interstratifié avec des shales noirs calcaires, des roches volcaniques mafiques, des mudstones, des siltstones et des calcaires blancs massifs non minéralisés, connus sous le nom de Groupe d'Upton. Les roches de ce groupe forment des fenêtres dans les roches cambriennes de la nappe susjacent de Granby.

Le gisement de barytine d'Upton est possiblement le résultat d'un processus sousmarin de type exhalatif, contemporain à la sédimentation ou d'un processus épigénétique postérieur à la sédimentation, et impliquant une mise en place dans un calcaire poreux et bréchifié.

INTRODUCTION

Carbonate rocks of the Cambro-Ordovician Flyschoid belt of the Quebec Appalachians (St-Julien and Hubert, 1975) have been known since the nineteenth century to host vein- and breccia-type copper deposits (Gauthier et al., 1989). The discovery of the stratabound Upton barite deposit in the late 1960s opened new perspectives for mineral exploration in the external nappe zone of the Appalachians.

The Upton deposit, located 3 km northeast of the town of Upton (Fig. 1), is an unusual stratabound limestone-hosted barite deposit containing minor Zn, Pb, Cu, Cd and Ag. This assemblage contrasts markedly with better known carbonate-, shale-hosted mineralization elsewhere in the world such as Silvermines and Tynagh, Ireland, and Meggen, West Germany, where massive sulphide mineralization (Pb-Zn) is generally predominant over sulphate mineralization (Brown, 1967; Routhier, 1980; Anderson and Macqueen, 1982; Dawson, 1985).

The information presented in this paper represents the first phase of a metallogenic study of the Upton deposit and is based mainly on detailed examination and sampling of drill cores from twenty-two drill holes of Ressources Robex Inc. (Fig. 2), and reconnaissance geological mapping of the Upton-Acton Vale area.

GEOLOGICAL SETTING

The Upton deposit is located within the Flyschoid belt (Fig. 3), which represents one of the five major tectonostratigraphic units of the Quebec Appalachians (St-Julien and Hubert, 1975). The Flyschoid belt consists of several imbricated nappes piled up in the inverse order of their ages and separated by major thrust faults (St-Julien 1968, 1972; St-Julien and Hubert, 1975). The nappes were emplaced during the Taconic orogen of middle Ordovician age. The polarity of the stratigraphic sequence within each nappe are upright. The Granby nappe, with the oldest sedimentary sequence (early Cambrian), corresponds to one of the farthest-travelled nappes and lies on nappes with younger sequences (late Cambrian to early and middle Ordovician;

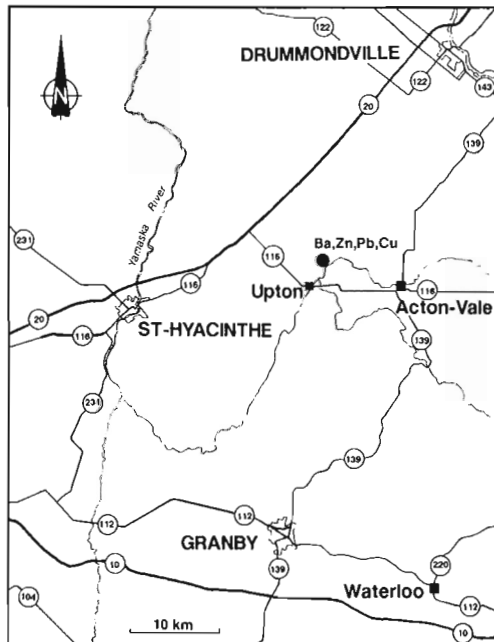


Figure 1. Location of the Upton barite deposit.

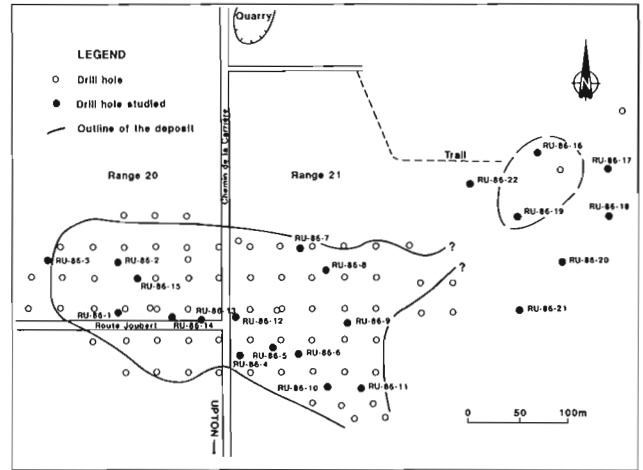


Figure 2. Outline of the Upton barite deposit and collar locations of the drillholes studied. From Ressources Robex Inc. (1988).

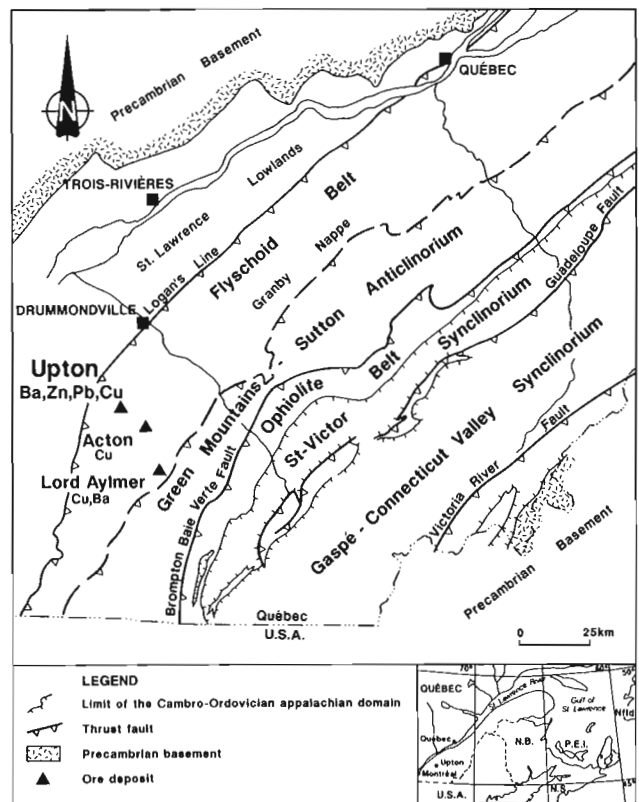


Figure 3. Location of the Upton barite deposit within the Flyschoid belt of the Quebec Appalachians.

St-Julien and Hubert, 1975). The Upton Group which hosts the Upton barite deposit, is exposed as a series of windows (the "island-like" areas of Kumarapeli et al., 1988) within the tectonically overlying Granby nappe. The Upton Group consists of an unmetamorphosed assemblage of limestones, mudstones, shales, siltstones, volcanic rocks and gabbroic rocks of probable late Cambrian-early Ordovician age. The age of the Upton Group is not well constrained. Only pelmatozoan plates and other skeletal fossil debris were

reported in carbonate rocks of the Upton Group by Kumarapeli et al. (1988). A late Cambrian-early Ordovician age has been assigned because of its possible correlation with carbonate units of the Phillipsburg slice (Beaupré, 1975). $^{87}\text{Sr}/^{86}\text{Sr}$ initial values of rocks of the Upton Group are consistent with an early Ordovician age (Hoy, pers. comm., 1989).

GEOLOGY OF THE UPTON DEPOSIT

Host rock

The Upton barite deposit is hosted by a grey massive, brecciated, and locally fossiliferous limestone that varies in thickness from 0.5 to 20 m. The mineralized limestone consists of recrystallized fine-to coarse-grained calcite (greyish sparry calcarenite with grainstone texture), up to 75 vol. % barite and 1-5 vol. % sulphides (Fig. 4a). Black calcareous

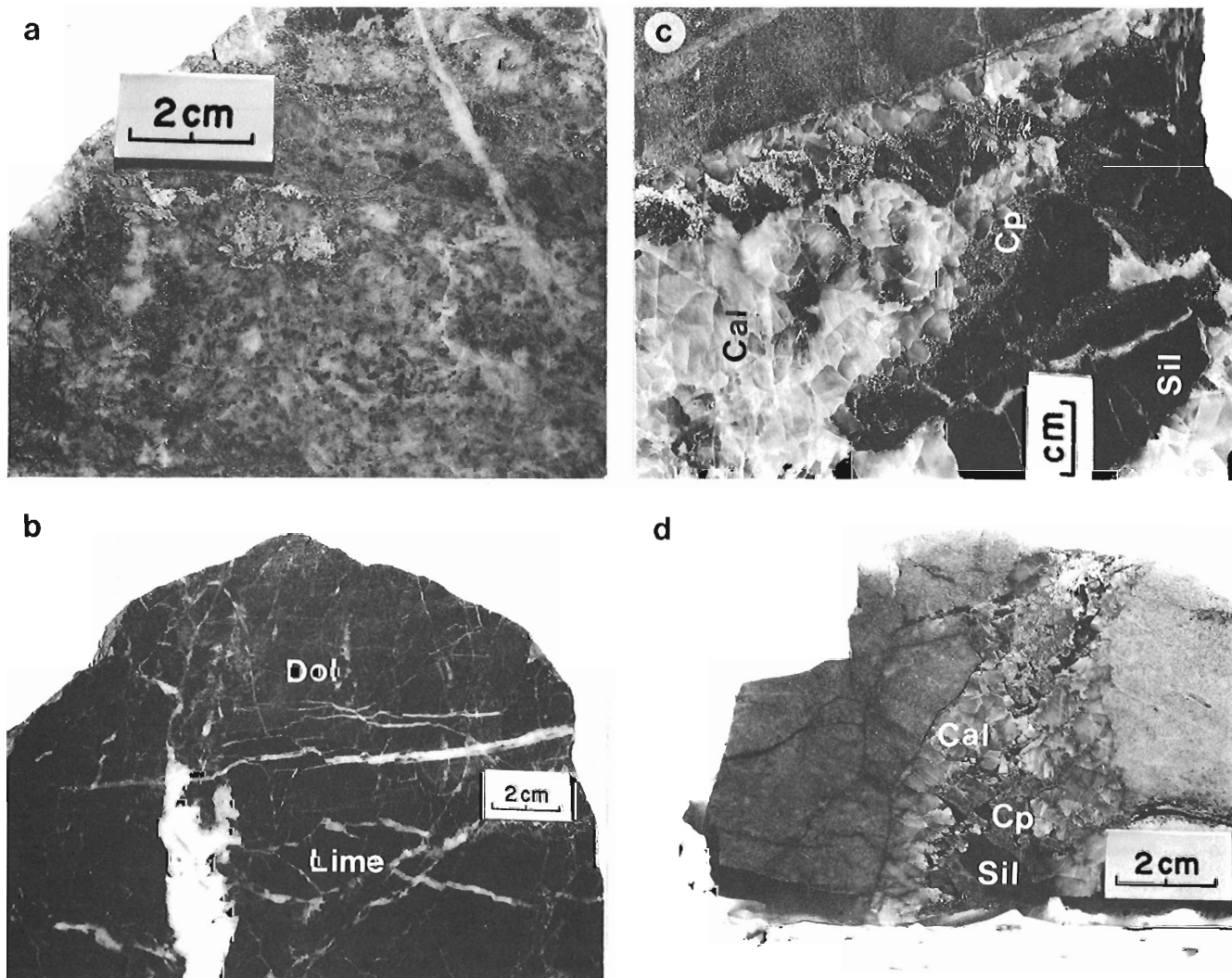


Figure 4. Polished rock slabs illustrating some characteristics of the mineralization from the Upton barite deposit and from an outcrop located 100 m north of the deposit.

(a) Polished rock slab showing barite crystals and sulphide aggregates interspersed with calcite crystals. Barite is light grey, calcite is white and sulphides are the reflective material. (b) Polished rock slab showing dolomitization following fractures and forming discordant zones that display sharp contacts with the nondolomitized limestone. Dol = dolomitization, Lime = limestone (c) Polished rock slab of a copper-sulphide vein from the Upton area. Cal = calcite, Sil = silica, Cp = chalcopyrite. (d) Symmetrical banding within a sulphide vein (Cal = calcite, Cp = chalcopyrite, Sil = silica).

shales are interbedded with and stratigraphically overlie the mineralized limestone (Fig. 5). These shales are finely bedded, fissile, locally brecciated and contain finely disseminated pyrite crystals and aligned barite nodules. Mudstones and volcanic rocks stratigraphically underlie the mineralized limestone. The distinctive mudstone unit consists of interlayered bands of massive black and green mudstones, some siltstones that exhibit normal graded bedding and thin beds (< 10 cm thick) of mudstone breccia interpreted as debris flows. The volcanic rocks, interbedded with the mineralized limestone near the northeastern margin of the deposit, consist of 85 % mafic lava flows and 15 % mafic tuffs. The lava flows are massive, amygdaloidal and porphyritic. The massive flows are light green to red, and contain up to 40 % amygdules of calcite and chlorite concentrated near the flow tops. The porphyritic lava flows are light to dark green, and contain 5-10 % variably altered

phenocrysts of clinopyroxene, plagioclase and amphibole. A white barren micritic limestone underlies the sequence of shales, mudstones, and baritic limestone. This limestone is characterized by the presence of white bleached spots and reddish spots that attain a few centimetres in diameter, and by thin anastomosing argillaceous and manganiferous seams. An outcrop located 100 m north of the Upton deposit is similar to the white barren limestone identified in the drill cores. This limestone consists mainly of recrystallized, non-fossiliferous, massive, locally brecciated sparry calcarenite with a grainstone texture. According to Lavoie (pers. comm., 1989), the limestone is of secondary origin and results from the recrystallization of a micritic precursor with a mudstone texture. Preserved dolomitic and non-recrystallized textures suggest that the limestone underwent an incomplete dedolomitization process at some time. Numerous zones bleached to a light grey are present and

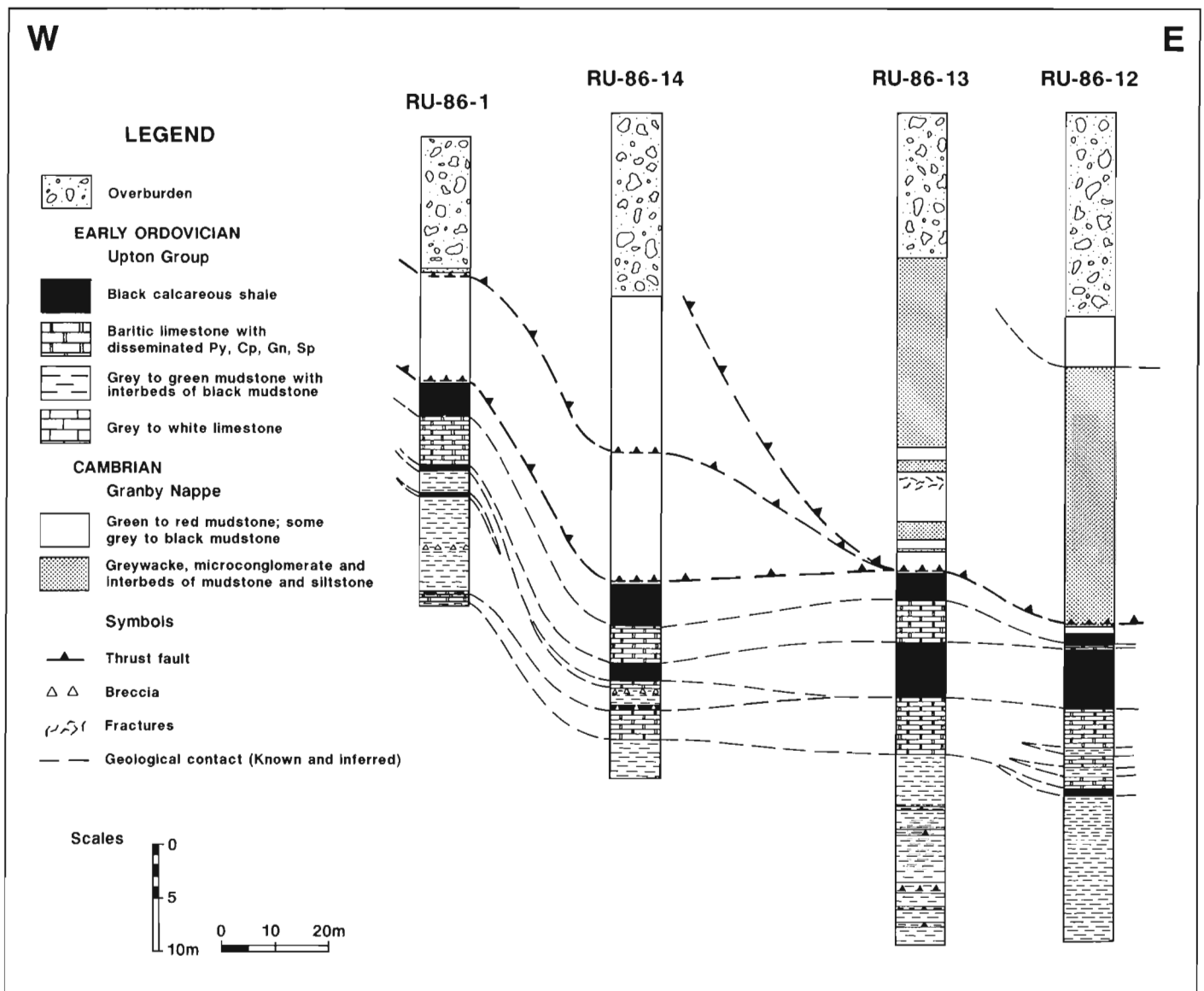


Figure 5. Geological W-E cross-section of the Upton barite deposit. Location of the drillholes is shown in Figure 2.

suggest a subsequent period of partial dolomitization which was accompanied by some silicification. Dolomitization seems to follow fractures and forms numerous patchy and discordant zones that display sharp contacts with the non-dolomitized limestone (Fig. 4b). The nature and timing of the recrystallization, diagenesis and the different alteration

processes that affected the carbonate rocks have yet to be established.

The stratigraphic sequence of the Upton deposit (Fig. 5, 6) is similar to that at the Acton Vale quarry described by Sassano and Procyshyn (1988). Detailed stratigraphic

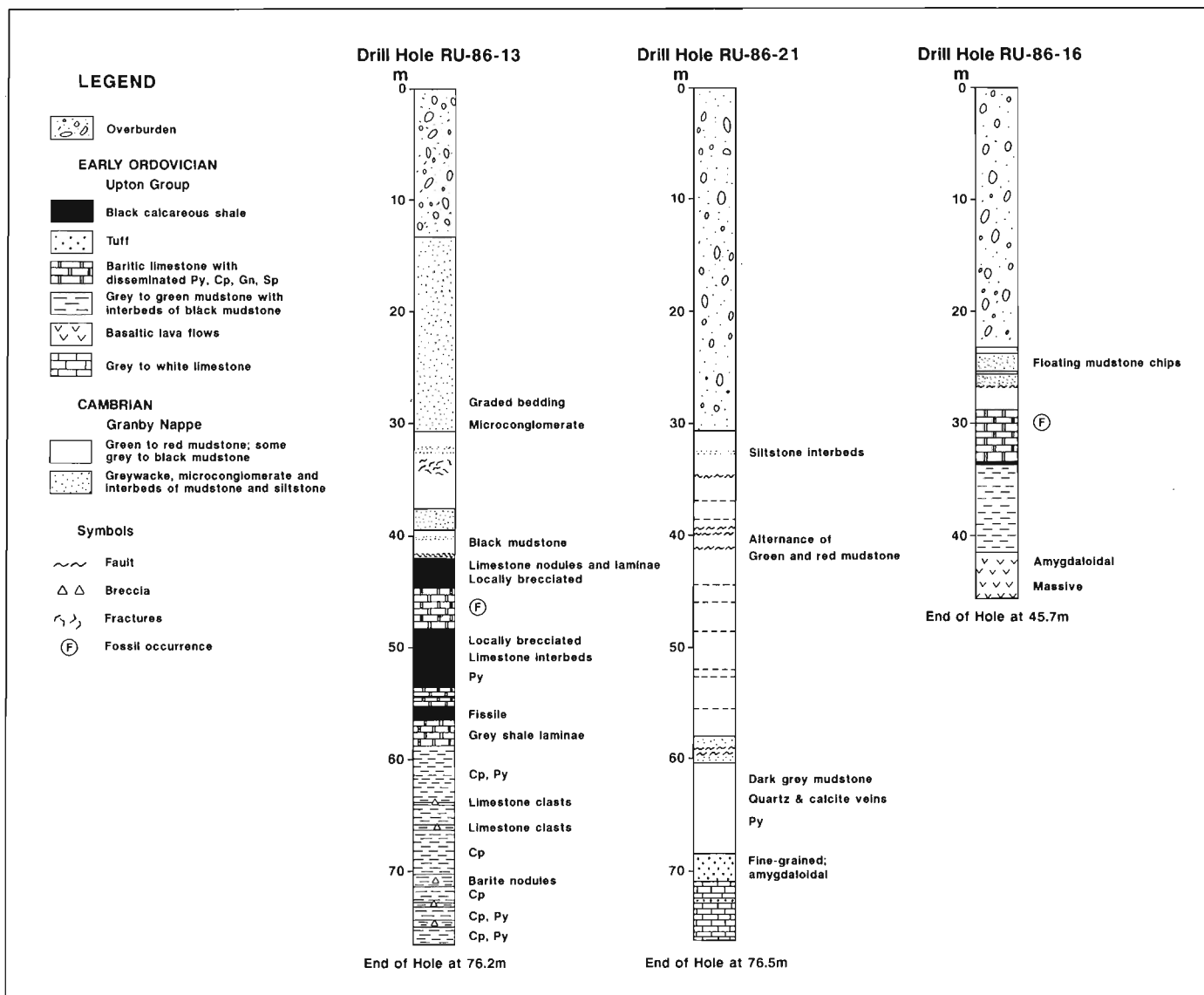


Figure 6. Three selected drill holes showing the stratigraphy of the Upton barite deposit area. Drill holes located in Figure 2. Note that although lithological contacts are shown as horizontal, the core bedding angle varies from 20 to 80°.

correlation between the Upton deposit and the Acton Vale quarry is difficult because of the numerous faults present in the region, the lack of exposure and the presence of overlying rocks of the Granby nappe.

The Upton deposit consists of one main tabular body having a length, width, and thickness dimensions of 350, 200 and 0.5 to 20 m, respectively and a smaller lens (76 m in length) located 200 m to the northeast (Fig. 2). The main body strikes northwest and dips 20 to 30° southeast. The mineralized limestone is thicker in the central portion of the deposit and becomes thinner (< 3 m) towards the southeast. The mineralization is open down-dip to the southeast.

Mineralization

The Upton deposit contains proven reserves (after dilution) of 950 000 tons grading 46.5 % BaSO₄, 1.94 % Zn, 0.59 % Pb, 0.15 % Cu, 0.11 % Cd, and 13.5 % g/t Ag (Ressources Robex Inc., 1988). Probable and possible reserves have been estimated at 350 000 tons of comparable grade (Northern Miner, Dec. 19, 1988).

The mineralization consists of barite, sphalerite, chalcopyrite, pyrite, and galena. Barite commonly occurs as fine- to coarse-grained blade-like crystals, rosettes, and fine-grained aggregates interspersed with fine- to coarse-grained calcite crystals. Nodules of barite are locally present within the black calcareous shale and veins of coarse-grained blade-like crystals cut the mineralized limestone.

Sulphide minerals are disseminated through the limestone and form aggregates and veinlets. Sphalerite is the most common sulphide mineral. It is medium grey, contains traces of pyrite, galena and chalcopyrite and occurs as aggregates of fine grained crystals sporadically distributed in the limestone and concentrated along barite and calcite crystal boundaries. Pyrite and chalcopyrite disseminations appear ubiquitous in all Upton Group lithologies.

The limestone outcrop situated 100 north of the Upton barite deposit contains subvertical northwest and northeast striking mineralized and nonmineralized veins that are up to 10 cm wide. The mineralized veins appear to be preferentially associated with zones of dolomitization described previously. The sulphide mineralogy of these veins consists mainly of chalcopyrite, bornite, covellite and malachite (Fig. 4c), but sphalerite, pyrite, and minor galena are also present. Many of the mineralized veins are symmetrically banded with coarse calcite at the wall, followed inwards by copper-sulphides and a bluish silica phase at the centre (Fig. 4d). Vein morphology suggests that they formed by open space sequential filling with bluish silica being the latest phase to precipitate. Nonmineralized veins consist of coarse-grained milky calcite crystals intergrown with quartz. The mineralogy and paragenesis of similar veins at the Acton Vale quarry have been described by Sassano and Procyshyn (1988). In addition to the sulphide-bearing veins, abundant (1-15 vol. %) disseminated pyrite and chalcopyrite are present within the dolomitized limestone.

Due to the lack of outcrops and the presence of numerous faults, the relationship between the outcropping sulphide-bearing veins situated 100 m north of the deposit and the stratabound barite deposit is not clear. If the white barren

micritic limestone identified in the drill cores of the Upton deposit corresponds to the outcropping limestone host of the sulphide-bearing veins, these sulphide veins may represent pathways of ascending hydrothermal fluids that could possibly have generated the stratabound barite deposit.

DISCUSSION

Hypotheses concerning the structural framework of the Upton Group and the genesis of the Upton barite deposit are briefly discussed in this section.

As previously noted, the Upton Group forms windows within the tectonically overlying Granby nappe. These windows may represent exposed parts of a tectono-stratigraphic package or of a nappe sandwiched between an underlying nappe and the older overlying Granby nappe (Baldwin, 1973; Sassano and Procyshyn, 1988). Alternatively, the Upton Group may correspond to allochthonous blocks or slabs derived from the continental shelf margin and incorporated into the cratonward-moving nappes during the Taconic orogen (St-Julien and Hubert, 1975; Beaupré, 1975; Globensky, 1978; Kumarapeli et al., 1988). Although more information is necessary to understand the structural framework of the Upton Group, increasing development of the schistosity in the mudstones and shales of the Upton Group towards the south, the presence of low angle thrust faults at the contacts between the lithologies of the Granby nappe and the Upton Group, and similar strikes and dips of the lithologies of the Granby nappe and the Upton Group suggest that the group represents exposed parts of another allochthonous sheet or nappe. Also, the lithological character of rocks of the Upton Group contrasts with those of the Granby nappe but resembles the lithological character of rocks of the Stanbridge nappe.

Several constraints can be placed on a genetic model for the Upton barite deposit and the parameters that must be considered are listed in Table 1.

Two genetic models are briefly considered; a sediment-hosted submarine exhalative process and an epigenetic process. The Upton barite deposit may possibly result from a submarine exhalative process contemporaneous with sedimentation and involving deep circulation along faults (or fracture zones) of barium and base metal-rich brine. This model is based on (1) the stratabound, quasi-stratiform nature of the mineralized limestone, (2) the occurrence of diffuse laminae of barite, calcite, and sulphides, and (3) the presence of calcareous, bedded, fissile, black shales containing finely disseminated pyrite crystals and aligned barite nodules.

Alternatively, an epigenetic origin for the Upton barite deposit, involving the focussed discharge of hydrothermal solutions along faults into a porous limestone aquifer and/or into a brittle-fractured massive limestone, precipitation of the mineralization in open spaces of the limestone, and subsequent replacement of the limestone, also appears viable. This model is based on the assumption that the unmineralized limestone precursor was originally vuggy and porous (or developed a secondary porosity) or brecciated, and that it had a favourable composition to trap ascending mineralized fluids. Geological evidence for this

Table 1. Characteristics of the Upton barite deposit.

1. The Upton barite deposit is a relatively small deposit having a uniform, tabular shape.
2. Mineralization is confined to a recrystallized fossiliferous massive, locally brecciated limestone interbedded with black calcareous shale, and nonmineralized mudstones, and volcanic rocks.
3. Barite and sulphides are intermixed within the mineralized limestone unit.
4. The presence of volcanic rocks suggests an anomalously high geothermal gradient.
5. The fining and thinning of some beds and the presence of debris flows may be indicative of contemporaneous fault movement during sedimentation. Numerous minor thrust faults occur in the area, and these thrusts may be occupying growth faults that were originally established by tilting of fault blocks in early Ordovician time.
6. Sulphide-bearing veins and associated hydrothermal alteration zones [dolomitization, silicification (?)] underlie the mineralized limestone. This suggests that the Upton barite deposit may be of proximal type with an underlying or proximal feeder zone.
7. Chert nodules and fragments are present within the limestone that host the sulphide-bearing veins and may represent an exhalative-hydrothermal silica phase presumably of the same origin as the silicification.
8. No metal zonation seems to be present within the deposit.

model includes: (1) the occurrence of up to 75 vol. % barite as fine- to coarse-grained blade-like crystals, rosettes, and fine-grained aggregates interspersed with calcite crystals, suggesting that mineralization was formed by open-space filling, and (2) the brecciated aspect of most of the mineralized limestone.

Kumarapeli et al. (1989) considered the Upton barite deposit and the sulphide-bearing veins of the Upton-Acton Vale area as epigenetic and formed largely by open-space filling and replacement in parts of the limestone which had undergone ground preparation by brecciation and/or karsting.

SUMMARY AND CONCLUSION

The potentially economic Upton stratabound barite deposit occurs in carbonate rocks of the external nappe zone of the Appalachians. Older rocks of the Granby nappe have overriden the Upton Group assemblage and only windows of the Upton Group are now observable. Though the Upton barite deposit displays many of the parameters listed by Large (1983) of typical sediment-hosted submarine exhalative (sedex) deposits, an epigenetic origin for the deposit cannot be dismissed. Substantiation of either a syngenetic or epigenetic origin for the Upton deposit will have significant implications for subsequent mineral exploration in the Appalachians. The potential for the discovery of Zn-Pb-Ag-Ba deposits would seem most favourable in the early Ordovician carbonate assemblage of the Upton Group and its stratigraphic equivalents. Elsewhere in the world, mineralization similar to the Upton deposit is associated with mas-

sive sulphide mineralization of commercial importance (Silvermines, Ireland; Walton, Nova Scotia; Battle Mountain, Nevada; Meggen, West Germany). Therefore, the down-dip extension of the Upton baritic lens should be further investigated as it may grade into a sulphide-bearing facies.

ACKNOWLEDGMENTS

We are grateful to I.R. Jonasson and D.G. Richardson for critical reading of the manuscript and providing constructive comments. Drafting was done by L. Dubé. Robex Inc. allowed us to sample and study the drill core from the Upton deposit and provided pertinent information on the deposit. N. Marchildon and M. Tellier were field assistants.

REFERENCES

- Anderson, G.M. and MacQueen, R.W.**
1982: Ore deposit models-6. Mississippi Valley type lead-zinc deposits; *Geoscience Canada*, v. 9, p. 108-117.
- Baldwin, A.B.**
1973: Report recommending mineral exploration for 1973-1974 in an area located in the St. Lawrence Lowlands; Ministère de l'Énergie et des Ressources du Québec, Service du Potentiel Minéral.
- Beaupré, M.**
1975: Stratigraphie et structure du « Complexe Saint-Germain » et de la partie frontale des Appalaches de Drummondville; M.Sc. thesis, Université de Montréal.
- Brown, J.S.**
1967: Genesis of stratiform lead-zinc-barite-fluorite deposits in carbonate rocks; *Economic Geology*, monograph 3, 433 p.
- Dawson, K.R.**
1985: Geology of barium, strontium and fluorine deposits in Canada; Geological Survey of Canada, *Economic Geology Report* 34, 136 p.
- Gauthier, M., Auclair, M., Bardoux, M., Blain, M., Boisvert, D., Brassard, B., Chartrand, F., Darimont, A., Dupuis, L., Durocher, M., Gariépy, C., Godue, R., Jébrak, M., et Trottier, J.**
1989: Synthèse métallogénique de l'Estrie et de la Beauce; Ministère de l'Énergie et des Ressources du Québec, MB 89-20, 631 p.
- Globensky, Y.**
1978: Région de Drummondville; Ministère des Richesses Naturelles du Québec, rapport géologique 192.
- Kumarapeli, P.S., St. Seymour, K., Pinton, H., and Hasselgren, E.**
1988: Volcanism on the passive margin of Laurentia: an early Paleozoic analogue of Cretaceous volcanism on the northeastern American margin; *Canadian Journal of Earth Sciences*, v. 25, p. 1824-1833.
- Kumarapeli, P.S., Hoy, L., and Pinton, H.**
1989: Origin of Cu and Cu-Ba mineralization in the Acton Vale limestone, southeastern Quebec: evidence from sulphur and strontium isotopes; *Geological Association of Canada, Program with Abstracts*, v. 14, p. 121A.
- Large, D.E.**
1983: Sediment-hosted massive sulphide lead-zinc deposits: an empirical model; in *Sediment-hosted Stratiform Lead-zinc Deposits*, ed. D.F. Sangster and D. MacIntyre; *Mineralogical Association of Canada, Short Course Handbook*, v. 8, p. 1-29.
- Ressources Robex Inc.**
1988: Baryte-zinc, Upton: Etude finale d'évaluation; Internal report, v. 1,2,3, no. 12.
- Routhier, P.**
1980: Où sont les métaux pour l'avenir? Les provinces métalliques - Essai de métallogénie globale; Bureau de Recherches Géologiques et Minières (BRGM), mémoire no. 105, 410 p.
- Sassano, G.P. and Procyshyn, E.**
1988: Mineralogy and paragenesis of the cupriferous deposits of the Acton Vale-Upton sector, Klippen Belt, Quebec; *Mineralium Deposita*, v. 23, p. 123-131.

St-Julien, P.

1968: Les « argiles-à-blocs » du sud-ouest des Appalaches du Québec. *Le Naturaliste Canadien*; v. 95, pp. 1345-1356.

1972: La tectonique appalachienne dans les cantons de l'Est de la province de Québec. 24^{ème} Congrès géologique international; livret-guide de l'excursion B-21, 22 pages.

St-Julien, P. and Hubert, C.

1975: Evolution of the Taconian Orogen in the Quebec Appalachians; *American Journal of Science*; v. 275 A, p. 337-362.

Stratigraphy of the upper Cambrian – lower Ordovician barite and sulphide hosted limestones of the Acton Vale – Upton area, Québec

D. Lavoie

Centre géoscientifique de Québec, Québec

Lavoie, D. *Stratigraphy of the upper Cambrian-lower Ordovician barite and sulphide hosted limestones of the Acton Vale-Upton area, Quebec; in Current Research, part B, Geological Survey of Canada, Paper 90-1B, p. 9-15, 1990.*

Abstract

Cambro-Ordovician volcano-sedimentary sequences of the Acton Vale-Upton area outcrop within the Ordovician Drummondville olistostrome. Stratigraphy of the mineralized (barite and sulphides) carbonates embodied in the Upton Group, is established at various places. Preliminary field observations show that most of these carbonates are strongly recrystallized (recrystallized grainstone) and, in part, dedolomitized. Peritidal lithofacies (laminated calcilutite and calcareous siltstone) with associated diagenetic features (sulphate pseudomorphs, crusts) were identified. Limestone breccias are rare. A peculiar siliciclastic lithofacies assemblage (black mudstone with dolomitic mudstone and carbonates concretions) is developed at one section.

Résumé

Des séquences volcanosédimentaires d'âge cambrien et ordovicien de la région d'Acton Vale et d'Upton (Québec) affleurent dans l'olistostrome ordovicien de Drummondville. La stratigraphie des roches carbonatées minéralisées (barytine, sulfures) présentes dans le Groupe d'Upton, a été établie dans un certain nombre de secteurs de la région. L'analyse préliminaire des observations de terrain indique que la majeure partie de ces roches carbonatées a été fortement recristallisée (grainstone recristallisé) et, en partie, très certainement dédolomitisée. On a également identifié des lithofaciès péritidaux (calcilutite feuilletée et siltstone calcaireux) ainsi que des phénomènes diagénétiques connexes (pseudomorphes de sulfates, croûtes). De rares horizons de brèches calcaires intraformationnelles ont été relevés. Un assemblage particulier de lithofaciès silicoclastiques (mudstones noirs et mudstones dolomitiques avec concrétions carbonatées) a été observé par endroits.

INTRODUCTION

The sedimentology and diagenesis of carbonates in the Acton-Vale – Upton area are being studied as part of a wider metallogenic study of the Upton barite deposit and carbonate hosted sulphide mineralization (S. Paradis, pers. comm.). This preliminary contribution presents field data dealing with both stratigraphy and megascopic diagenetic phenomena of the carbonates. This paper also provides some work-

ing hypothesis on the sedimentary depositional environments and diagenetic events. Sedimentological and diagenetic laboratory work (petrography and geochemistry) will be performed later.

GEOLOGICAL SETTING

The studied area (Fig. 1) is part of the external nappe zone of St-Julien and Hubert (1975). This tectonostratigraphic

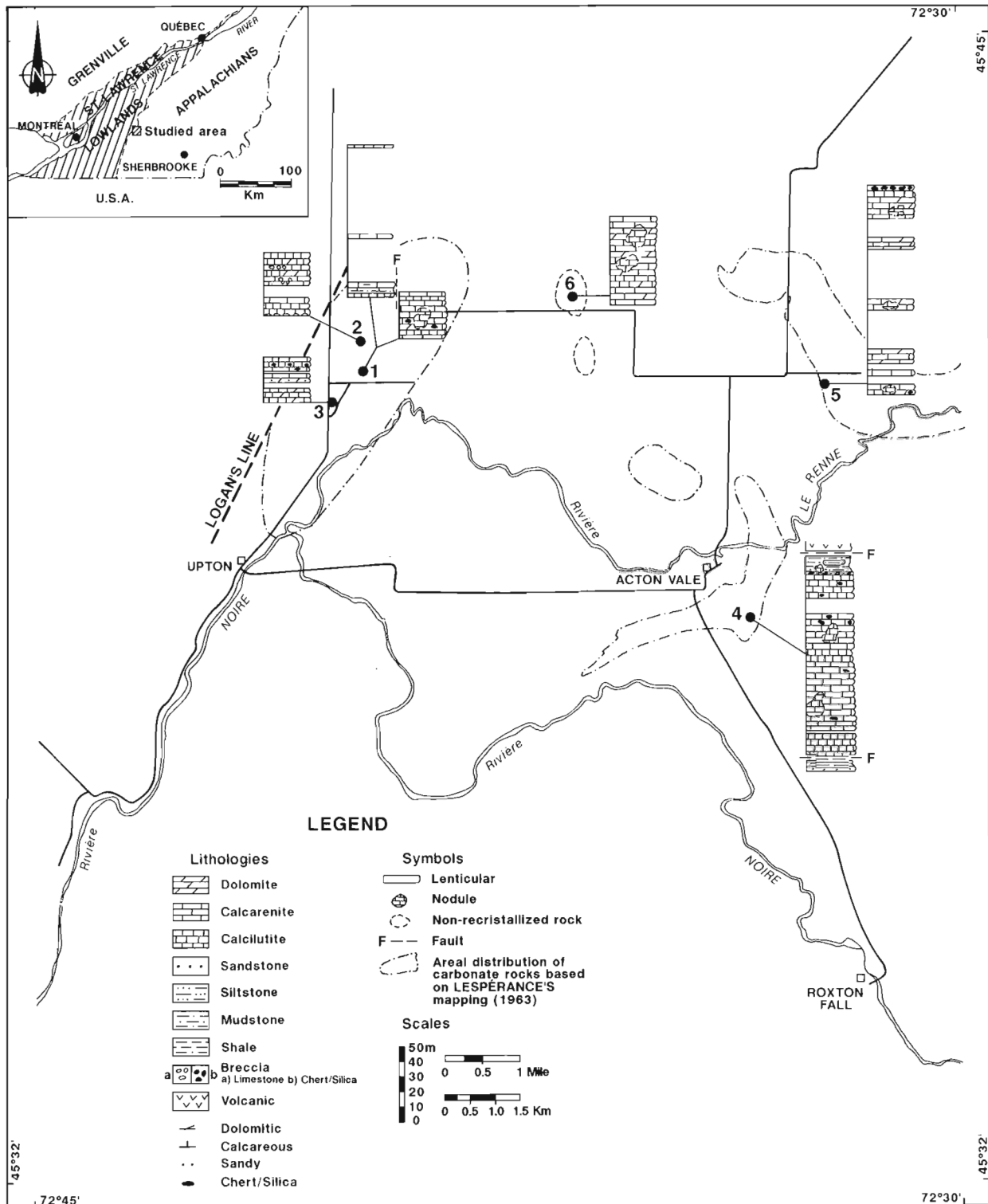


Figure 1. Geological map of the studied area with locations and general stratigraphy of the discussed sections.

domain is characterized by stratigraphically inverted structural stacking of nappes set in place by gravity sliding during the mid-Ordovician partial closure of Iapetus. This domain is bordered to the west by Logan's line which separates it from the foreland thrust belt and to the east by the more tectonically deformed and metamorphosed internal nappe belt (St-Julien and Hubert, 1975). Geology of the studied area was examined by Lespérance (1963) and Globensky (1978, 1987) among others.

The Drummondville Olistostrome (Slivitzky and St-Julien, 1987), previously part of the Granby Nappe of St-Julien and Hubert (1975) and also known as the Drummondville Wildflysch of Globensky (1978) is the main tectonostratigraphic unit of this area. It is composed of a shale-sandstone succession containing mid-Ordovician graptolites (Riva, 1966). This succession is interpreted as a continental rise prism in which some allochthonous blocks of various sizes and shapes are scattered. These blocks comprise sedimentary and volcanic rocks (limestones-shales-lavas-tuffs) of late Cambrian-early Ordovician age. They are interpreted as large olistoliths disrupted from the continental platform and incorporated in the nappes during the Taconian orogeny (Globensky, 1978; Slivitzky and St-Julien, 1987). Preliminary data on the volcanic rocks of these successions were recently presented by Kumaparelli et al. (1988).

STRATIGRAPHY OF CARBONATE ROCKS

Carbonates of the area were only briefly considered by previous workers. Beaupré (1975) correlated them with those of the southern Québec Phillipsburg Slice, giving them a late Cambrian-early Ordovician age. Lespérance (1963) briefly described them as recrystallized grey limestones with a possible dolomitic precursor. More recently, Kumaparelli et al. (1988) suggested that these carbonates are of relatively deep-water origin but close to a shallow-water platform in a fault bordered active basin. In ongoing metallogenic study of the area, Paradis et al. (1990) defined the Upton Group as a formal unit of the volcano-sedimentary package. The studied carbonates are part of that group and occur at various stratigraphic levels (Kumaparelli et al., 1988). No formal designation of these carbonates will be introduced until precise correlations are better established. Carbonates field terminologies are from Grabau (1904) and Dunham (1962).

Upton Area

Three stratigraphic sections were studied in the area north-east of Upton (Fig. 1 and 2, sections 1 to 3). This area showed the greatest number of lithofacies.

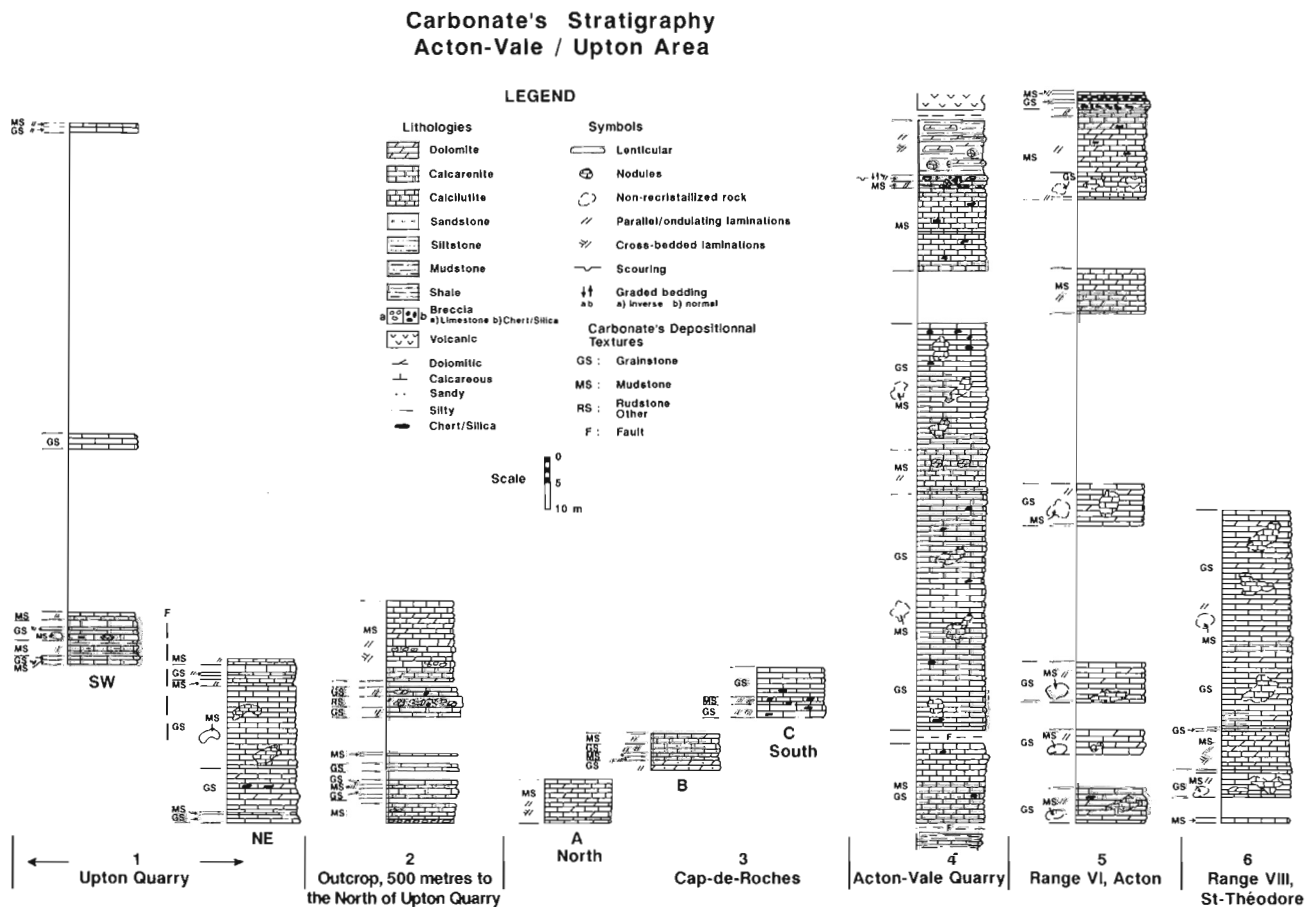


Figure 2. Detailed stratigraphic sections of the studied carbonates. Location of the sections in Figure 1.

Recrystallized grainstone

This is the most abundant lithofacies. It is a greyish sparry calcarenite with grainstone texture occurring in beds ranging in thickness from 10 cm to 1.5 m (average of 30 cm). This lithofacies, almost devoid of fossils and sometimes sandy, is of secondary origin resulting from recrystallization of a calcilutite precursor with a mudstone texture, the latter being preserved in fairly abundant, irregularly shaped zones showing gradual contacts with the surrounding grainstone.

The outcrop north of Upton quarry (Fig. 1 and 2, section 2) shows evidence of incomplete dedolomitization as dark dolomitic laminations become progressively more calcareous and ultimately disappear in the structureless sparry calcarenite (Fig. 3). The calcarenite grainstones frequently display silica and chert crusts of various sizes and shapes, but often concentric with isopachous habit. Evidence of syndepositional reworking was also observed. Rare geotrophic infillings of echinoderm rich calcarenite were observed within these crusts. Some of the recrystallized calcarenites are bleached. The distribution and shape of this phenomenon are irregular. It is associated with tiny black fractures (Fig. 4).

Laminated calcilutite

This lithofacies comprises calcilutite with a mudstone texture in beds ranging from 6 to 30 cm thick (average of 12 cm). Millimetre-scale parallel laminations and subordinate cross-bedded laminations are present. Some beds display imbricated rip-up clasts. No fossils, silica crusts, or bleached zones were observed in this lithofacies. Small millimetre- to centimetre-wide dolomite nodules or crusts (Fig. 5) were sometimes seen on bedding planes.



Figure 3. Incompletely dedolomitized carbonates. Dark dolomitic laminations become progressively more calcareous to ultimately disappear in the structureless limestone. Section 2.

Limestone breccia

Intraformational limestone breccias are almost exclusively restricted to the outcrop north of Upton quarry (Fig. 1, 2, section 2). The clast-supported and structureless breccia (Fig. 6) is composed of angular to sub-rounded fragments of calcarenite grainstone. Clasts comprise up to 60% of the rock and their sizes range from 2 mm to 18 cm (average of 6 cm). The matrix of the breccia consists of variably silty calcarenite. These breccias are no more than a few metres thick and wide.



Figure 4. Irregularly shaped bleached limestone (light area) set within darker recrystallized but unbleached limestone. Note thin black fractures occurring within bleached areas. Section 1.



Figure 5. Slightly calcareous dolomitic crust of variable thickness occurring within faintly laminated calcilutite mudstone. Section 3.

Calcareous siltstone

This is the least common lithofacies in the area. Beds are 5 to 15 cm thick (average of 8 cm) and commonly display parallel and cross-bedded laminations. The calcareous siltstone is interbedded with the laminated calcilutite.

Acton Vale Area

The excellent exposure at the Acton Vale quarry (Fig. 1, 2, section 4) shows the most complete section of the Upton Group. This section displays the recrystallized grainstone and laminated calcilutite lithofacies in addition to siliciclastic lithofacies near the top of the section.

The recrystallized grainstone comprises more than 90 % of the total carbonates and like the exposures in Upton area, it displays numerous non-recrystallized, irregularly shaped zones of calcilutite. The grainstone is bleached at numerous places and is associated locally with spectacular silica/chert crusts (Fig. 7). At this section, the recrystallized grainstone displays small pinkish zones due to tiny red inclusions, the nature of which is unknown.

The laminated calcilutite lithofacies is restricted to the middle part of the section where it forms an 8-m thick succession. The lithofacies is very similar to that of the Upton area with the addition of small parallel dolomitic nodules.

Impure laminated limestone

This lithofacies is restricted to the uppermost metres of carbonates at Acton Vale quarry. It consists of recrystallized grainstone with silty and sandy laminations becoming thicker upward.



Figure 6. Structureless limestone breccia with fairly angular clasts set in calcarenite matrix. Note razor-sharp contact with surrounding recrystallized grainstone. Bed top is indicated by the head of the hammer. Section 2.

Conglomerate

The transition between the carbonates and siliciclastic parts of the section is characterized by numerous lenses of conglomerate of 50 cm thick at the most. This clast-supported conglomerate is composed of clasts of various lithologies. They are in decreasing abundance: black mudstone, calcarenite, impure laminated limestone. Quartz and echinoderms were also observed. These fragments, up to 85 % of the rock, are sub-rounded to angular. The black mudstone commonly displays a platy shape. The size of the clasts ranges from 2 mm to 30 cm (average of 6 cm). The clasts are embodied in a calcareous sandstone matrix. The conglomerate displays numerous sedimentary structures such as scouring, inverse and normal graded bedding, and cross-bedded laminations with imbricated clasts.

Mudstones

The top of the stratigraphic section in the Acton Vale quarry is marked by an alternating sequence of black siliciclastic mudstone and greyish dolomitic mudstone with an average ratio of 60 to 40. The black mudstone forms beds 2 to 6 cm thick and the dolomitic mudstone forms centimetre-thick lenses that are a few metres wide. This dolomitic mudstone shows numerous parallel and cross-bedded millimetric laminations. The lowermost succession is represented by abundant (up to 15 %) carbonates nodules (Fig. 8) up to 75 cm in diameter (average of 25 cm), characterized by septarian dykes.

This siliciclastic unit is overlain, in locally faulted contact, by volcanic rocks which are overlain by poorly exposed recrystallized grainstone and black mudstone.

Other areas

Two more stratigraphic sections were described in the studied area, one north of Acton Vale (Fig. 1, 2, section 5)



Figure 7. Irregularly shaped, more or less concentric and isopachous multilayered silica crust and associated chert (darker areas). Note bleached limestone overlying the crust. Section 4.

and one in St-Théodore area (Fig. 1, 2, section 6). Carbonates lithofacies are similar to the previously described recrystallized grainstone and laminated calcilutite.

DISCUSSION

This section presents some working hypothesis regarding the paleoenvironments and carbonates diagenesis.

Sedimentary environments

Recrystallized grainstone

Because of the pervasive recrystallization and dedolomitization that affected this lithology, paleoenvironmental information such as depositional textures, sedimentary structures and fossils were systematically erased or masked (see Fig. 3 for example). The non-recrystallized (but dedolomitized?) precursor seems to invariably be an unfossiliferous structureless calcilutite with a mudstone texture but whether this was the case for the whole recrystallized grainstone lithofacies has yet to be determined. Such a micritic precursor could be interpreted either as tidal flat lime mud, or as muddy subtidal sediments in a restricted lagoon, or as offshore mud deposited below fairweather wave base or as pelagic carbonate muds. However, the occurrence of syn-sedimentary reworked silica crusts, interpreted (see below) as a replacement of sulphate precursors, might indicate the possible presence of tidal flat muds in the recrystallized lithofacies.

Laminated calcilutite and calcareous siltstone

These two lithofacies are closely associated in the field. The laminated calcilutite resembles a cryptocyanobacterial laminite (Shinn, 1983) which strongly suggests a peritidal (tidal flat) setting for those rocks. Furthermore, the dolomite nodules, which are generally found parallel to bedding planes, are interpreted as sulphate pseudomorphs. This suggests hypersaline conditions, which commonly characterize tidal flats environments.



Figure 8. Almost perfectly rounded carbonate concretion embodied in black crumbling mudstone. The concretion is structureless and lime carbonate rich. Section 4.

Occurrences of imbricated rip-up clasts and cross-bedded laminations in some of these rocks are likely the result of occasional energetic pulses on the tidal flat that perhaps storm-related events. The calcareous siltstone could represent episodic influx of siliciclastic sediments on the flat.

Other lithofacies

Limestone breccias will be carefully examined in order to assess a mechanism for its formation. Our working hypothesis include karst-related subaerial dissolution or evaporite-related dissolution. Understanding the origin of the breccias may have metallogenic implications for the area.

The Acton Vale quarry conglomerate shows many characteristics of a debris flow unit. Finally, the black mudstones of that same section suggest an anoxic sedimentary setting. In this environment, small scales energetic sediment influx (dolomitic mudstone) episodically occurred. These anoxic settings are best suited for the formation of carbonate concretions due to CO₂ production by various anaerobic bacterias (Irwin et al., 1977).

Carbonates diagenesis

Recrystallization affected most of the carbonates of the Upton Group, but the nature and timing of this process have yet to be established. Moreover, there is evidence of a previous dolomite mineralogy. Carbonates of the Upton Group are fairly pure limestones (Goudge, 1935) but they could be the product of dedolomitization. The latter could have been related to fresh water circulation associated with subaerial exposures, or it could have been favoured by presence of high concentration of sulphate ions in pore fluids related to some evaporite dissolution.

Occurrence of nodules/crusts of silica or dolomite could also indicate the former presence of sulphate minerals. This hypothesis relies, for now, upon the observation of such nodules/crusts within peritidal-like lithologies. Silica and carbonates replacement of sulphates are fairly common in such lithologies (Shinn, 1983).

CONCLUSIONS

Carbonates within the Upton Group of the Acton Vale-Upton area are mostly characterized by intense recrystallization and possibly dedolomitization. Peritidal carbonates and associated diagenetic features were identified and are likely present in the recrystallized lithologies.

Many questions are still unanswered and various sedimentological and diagenetic working hypothesis will be tested petrographically and geochemically.

ACKNOWLEDGMENTS

Discussions with S. Paradis, A. Chagnon, R. Godue, Y. Héroux and N. Tassé were of great help. Critical review of the manuscript by B. Beauchamp greatly improved it. L. Dubé skilfully redrafted our sections and typing of the manuscript was done by L. Michard, their help is acknowledged.

REFERENCES

Beaupré, M.

1975: Stratigraphie et structure du "Complexe St-Germain" et la partie frontale des Appalaches, de Drummondville au lac Champlain, Québec; Mémoire de maîtrise, Université de Montréal, Montréal (Québec).

Dunham, R.J.

1962: Classification of carbonate rocks according to depositional texture; *in* W.E. Ham (ed.). Classification of Carbonate Rocks, a Symposium, American Association of Petroleum Geologists, Memoir 1, p. 108-121.

Globensky, Y.

1978: Région de Drummondville; Ministère des Richesses naturelles du Québec, Geological Report 192.

Globensky, Y.

1987: Géologie des Basses-Terres du Saint-Laurent; Ministère de l'Énergie et des Ressources du Québec, MM 85-02.

Gouge, M.F.

1935: Les calcaires du Canada, partie III, Québec; Bureau des Mines du Canada, Publication 758.

Grabau, A.W.

1904: On the classification of sedimentary rocks; *American Geologists*, v. 33, p. 228-247.

Irwin, H.C., Curtis, C.D. and Coleman, M.L.

1977: Isotopic evidence for source of diagenetic carbonates formed during burial of organic-rich sediments; *Nature*, v. 269, p. 209-213.

Kumaparelli, P.S., St. Seymour, K., Pintson, H. and Hasselgren, E.

1988: Volcanism on the passive margin of Laurentia: an Early Paleozoic analogue of Cretaceous volcanism on the northeastern American margin; *Canadian Journal of Earth Sciences*, v. 25, p. 1824-1833.

Lespérance, P.J.

1963: Région d'Acton; Ministère des Richesses naturelles du Québec, DP-677.

Paradis, S., Birkett, T.C. and Godue, R.

1990: Preliminary investigations of the Upton sediment-hosted barite deposit, southern Québec Appalachians; *in* Part B, Geological Survey of Canada, Paper 90-1B.

Riva, J.

1966: New assemblages of Middle Ordovician graptolites from the Appalachian region; *Le Naturaliste canadien*, v. 93, p. 153-156.

Shinn, E.A.

1983: Tidal flat environment; *in* P.A. Scholle, D.G. Bebout and C.H. Moore (ed.) Carbonate Depositional Environments, American Association of Petroleum Geologists, Memoir 33, p. 172-210.

Slivitzky, A. and St-Julien, P.

1987: Compilation géologique de la région de l'Estrie-Beauce; Ministère de l'Énergie et des Ressources du Québec, MM 85-04.

St-Julien, P. and Hubert, C.

1975: Evolution of the Taconian orogen in Quebec Appalachians; *American Journal of Sciences*, v. 275A, p. 337-362.

Lithostratigraphic framework of the Upper Gaspé Limestones (Early Devonian) in eastern Gaspé basin, Québec

D. Lavoie, N. Tassé¹ and E. Asselin
Quebec Geoscience Centre, Quebec

Lavoie, D., Tassé, N., and Asselin, E. Lithostratigraphic framework of the Upper Gaspé Limestones (Early Devonian) in eastern Gaspé basin, Québec; in *Current Research, Part B, Geological Survey of Canada, Paper 90-1B*, p. 17-27, 1990.

Abstract

The Upper Gaspé Limestones (Early Devonian) were studied in the eastern part of Gaspésie. We recognized the Forillon (with newly defined Mont Saint-Alban and Cap Gaspé Members), the Shiphead and the Indian Cove Formations. This threefold framework has proved to be easily applicable in the type-area (Forillon peninsula) and in the northern outcrop belt of the Upper Gaspé Limestones. In the southern and southwestern areas, this lithostratigraphic framework becomes difficult to apply due to facies homogenization, thickening of the formations and disappearance of the middle unit (Shiphead Formation). These changes are likely linked to accelerated subsidence of that part of the basin coupled with synsedimentary movement along the Bras Nord-Ouest fault.

Résumé

On a étudié les Calcaires supérieurs de Gaspé (Dévonien inférieur) dans le secteur est de la péninsule gaspésienne. Cette unité se compose des Formations de Forillon (avec les nouveaux Membres de Mont Saint-Alban et de Cap Gaspé), de Shiphead et d'Indian Cove. Cette division tripartite est aisément reconnue dans la région-type (péninsule de Forillon) et dans la zone septentrionale d'affleurements des Calcaires supérieurs de Gaspé. Vers le sud et le sud-ouest, ces divisions lithostratigraphiques deviennent difficilement applicables vu l'homogénéisation des faciès, l'épaississement des formations et la disparition de l'unité intermédiaire (Formation de Shiphead). Ces changements latéraux semblent liés à une subsidence accélérée de cette partie du bassin associée à une activité synsédimentaire de la faille de Bras Nord-Ouest.

¹ INRS-Géoresources, CGQ, 2700, rue Einstein, C.P. 7500, Sainte-Foy, Québec G1V 4C7

INTRODUCTION

Basin analysis of a lower Devonian (Emsian) sedimentary succession in the Gaspé basin was initiated during the 1989 field season. The studied unit, the Upper Gaspé Limestones, outcrops over most of Gaspésie (Fig. 1). During the 1989 field season, an area of more than 3000 km² was covered over which 20 stratigraphic sections were described and 800 samples collected.

This paper presents the lithostratigraphy of the Upper Gaspé Limestones in their type-area (Forillon peninsula) and tries to extend the lithostratigraphic framework defined in the western and southern adjacent areas. The ultimate goal of the project is to present paleogeographic and diagenetic evolution that could then be compared to those observed in the coeval Appalachian-Caledonian sedimentary sequences.

GEOLOGICAL SETTING

The Gaspé basin was characterized during the latest Silurian (Pridolian) — earliest Devonian (Lockhovian) by fine grained siliciclastic sedimentation (Chaleurs Group; Bourque et al., in press). Carbonate sedimentation extended over most of the actual eastern Gaspésie, during Early Devonian. A return to a siliciclastic dominated regime happened in late Early to Mid-Devonian (Gaspé Sandstones). The carbonate dominated horizon, known as the Upper Gaspé Limestones (Lespérance, 1980a) is one of the few pauses in the siliciclastic sedimentation that characterized the post-Taconic basin history (Bourque et al., in press).

PREVIOUS WORK

Logan (1845) first described the sedimentary sequence outcropping on Forillon peninsula. He divided it into nine informal units forming two informal groups, the Gaspé Limestones and the overlying Gaspé Sandstones. Clarke (1908) divided the informal units of Logan's Gaspé Limestones into three formations (St-Alban, Cap Bon Ami, Grande Grève). Problems of correlation during preliminary mapping carried inland by McGerrigle and co-workers prior the final report (McGerrigle, 1950) lead to a re-examination of Logan's and Clarke's stratigraphy of the Forillon peninsula. Russel (1946) divided Clarke's three formations into various members, following closely Logan's subdivisions. The three uppermost (Forillon, Shiphead and Indian Cove Members) were later given formation status and included under the term Upper Gaspé Limestones by Lespérance (1980a). He ranked them as a sub-group of the Gaspé Limestones, they are now considered as a formal group. Those last three formations were recognized inland by Lespérance (1980b) and Rouillard (1986). Besides those studies, the sedimentology of this lower Devonian carbonate succession is poorly known. Lespérance (1980a) and later workers concluded that the prevailing carbonate muds are an offshore type of a deep to medial platform with a locally fairly abundant sponge fauna.

LITHOSTRATIGRAPHY

Forillon Peninsula

The peninsula is the type-area of the Upper Gaspé Limestones where the threefold subdivision into Forillon, Shiphead and Indian Cove Formations was established (Lespérance, 1980a). Seven stratigraphic sections (Fig. 1, 2) were described. The easily recognizable Shiphead/Indian Cove contact is used as datum line for all lithostratigraphic correlations (Fig. 2, 8). We agree that its value as an isochron can be questionable. Readers interested in the biostratigraphy of the Forillon peninsula succession are referred to Lespérance (1980a).

Forillon Formation

No complete stratigraphic section of the lowermost unit of the Upper Gaspé Limestones is known on the peninsula. Thickness (290 m; Lespérance, 1980a) was estimated on structural data. The Forillon Formation is herein preliminary divided into two new formal members: the Mont Saint-Alban Member and the Cap Gaspé Member. Their respective thickness on the peninsula are estimated at 150 and 140 m.

Mont Saint-Alban Member

Most of this member is exposed at its type section, in an accessible gully cut into Mont Saint-Alban vertical cliffs (section E, Fig. 1, 2). Its base, which is also the base of the Forillon Formation, is fixed at the first carbonate-bearing mudstone bed overlying the purely siliciclastic mudstone of the Cape Road Member (Indian Point Formation; section D, Fig. 1, 2). The passage from the Cape Road to the Forillon is abrupt. The upper limit of the Mont Saint-Alban Member is fixed at the first appearance of more or less siliceous and cherty calcilutite of the Cap Gaspé Member. This contact, exposed at Mont Saint-Alban, is gradational over 4 m but partly faulted at this locality. The Mont Saint-Alban Member is mostly composed of dolomitic to rarely calcareous mudstones. These mudstones, in some cases sandy or silicified, range from 3 to 50 cm in thickness (average of 15 cm), and frequently show parallel and cross-bedded laminations, small current ripples and scour channels. Occasionally small beds and lenses of shaly calcilutite with mudstone texture are seen.

Cap Gaspé Member

The Cap Gaspé section, although incomplete (Section A, Fig. 1, 2), is chosen as the type section. The upper limit of this member, which is the upper limit of the Forillon Formation, is fixed where siliceous calcilutites with mudstone to packstone textures pass abruptly to thickly bedded calcareous sandstones assigned to the Shiphead Formation (Fig. 3). The Cap Gaspé Member is mostly made of partly dolomitized and silicified or cherty calcilutite with a mudstone texture. It occurs in planar to undulating beds 5 to 20 cm thick (average of 12 cm) with generally less than 10 % of

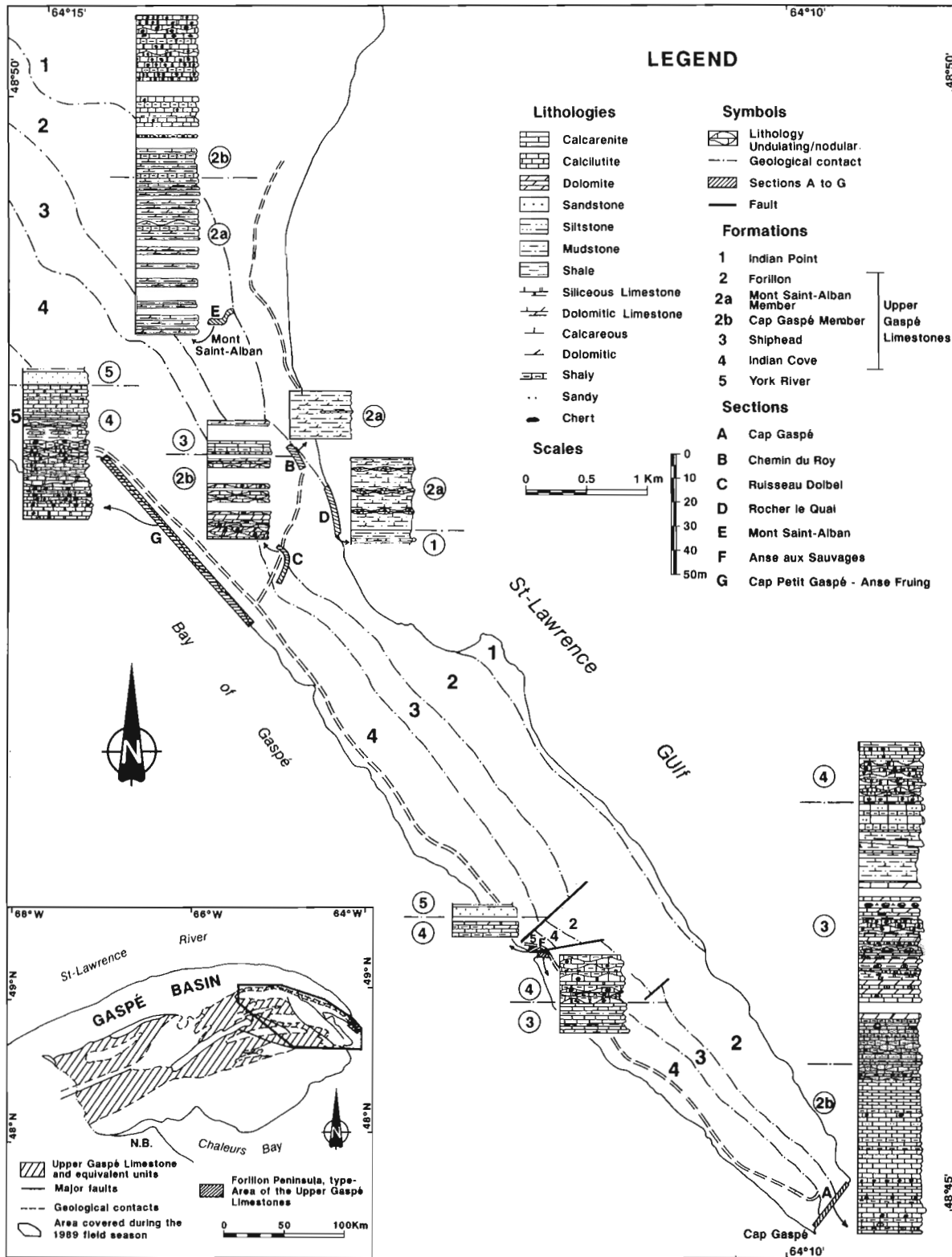


Figure 1. Geology of the Forillon peninsula with locations and general stratigraphy of studied sections.

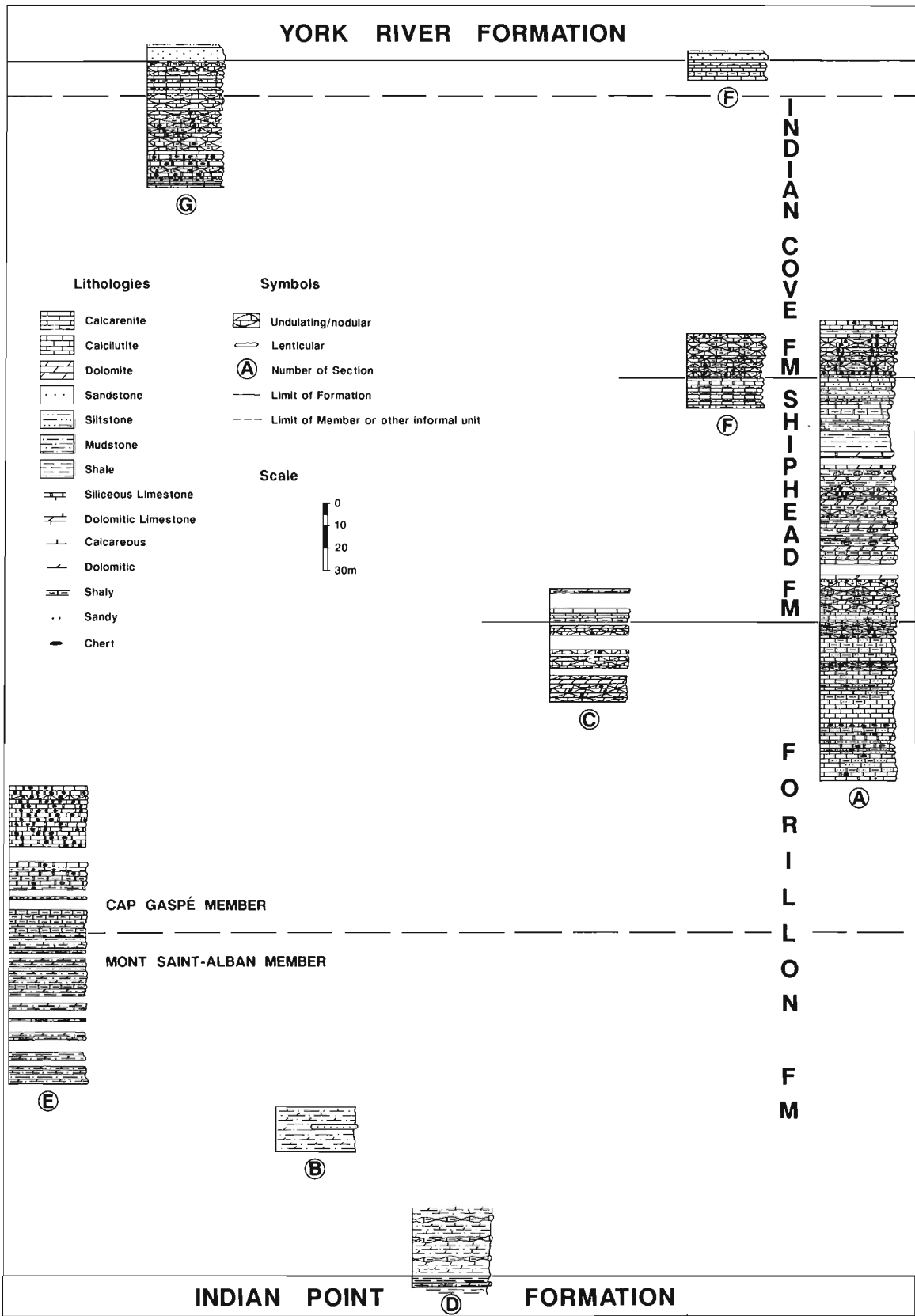


Figure 2. Lithostratigraphic framework for the Upper Gaspé Limestones. Location of sections in Figure 1.

interbeds of shaly calcilitite or calcareous mudstone. Besides the ubiquitous calcilitite mudstone, some beds of fossiliferous calcilitite wackestone and calcarenite packstone are also found but represent less than 5% of the member. One of the main characteristics of this unit is the ubiquitous silicification and chertification that has affected the calcilitite (see below).

Shiphead Formation

The Shiphead Formation is entirely exposed (106 m) at Cap Gaspé (Fig. 1, 2). The upper limit of the formation is set at its last sandstone bed (Fig. 4). The Shiphead Formation is an heterogeneous assemblage of more or less dolomitized and impure limestones interbedded with siliciclastics. Limestones comprise calcilitites with mudstone and wackestone textures (with very rare chert) and calcarenites with grain-



Figure 3. Contact (outlined in black) between underlying Cap Gaspé Member calcilitites and overlying Shiphead Formation sandstones. Section A.

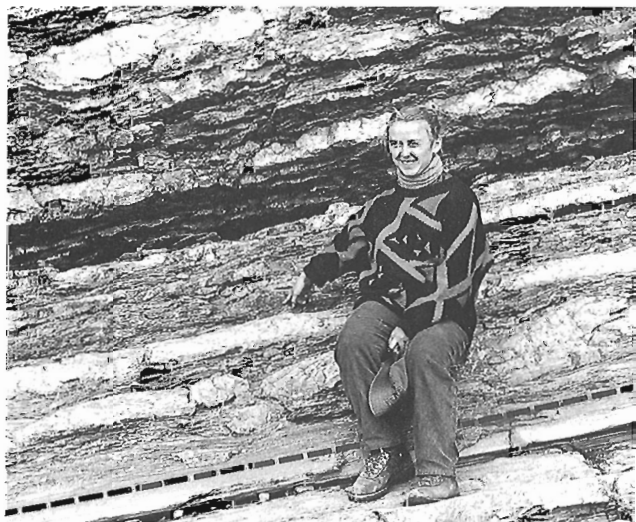


Figure 4. Contact (outlined in black) between underlying Shiphead Formation sandstones and overlying Indian Cove Formation calcilitites. Section A.

stone or packstone textures. Siliciclastics are represented by mudstones with common carbonate (calcite and dolomite) concretions (Fig. 5), and greenish or greyish calcareous lithic sandstones with low-angle cross-bedded and parallel laminations. Bentonite layers are also present. All those lithologies are in beds of millimetre to metre in thickness and are commonly bioturbated (*Zoophycos sp.* and *Scalarituba sp.*).

Indian Cove Formation

No complete stratigraphic section for the Indian Cove Formation could be found on the peninsula. Its thickness is estimated at 140 m (Lespérance, 1980a). The upper limit of the formation is set at the first non-calcareous siliciclastic bed (siltstone or sandstone) of the York River Formation (Gaspé Sandstones). The contact is abrupt. The Indian Cove Formation is almost exclusively composed of siliceous and cherty bioturbated calcilitite with a mudstone to wackestone texture (Fig. 6). The beds are planar to undulating and generally less than 25 cm thick. These limestones are, by far, the most chertified and silicified of the Upper Gaspé Limestones (see below). Besides siliceous calcilitite, beds of frequently sandy dolomites and calcarenites with a packstone to grainstone textures are found near the top of the formation. The uppermost beds were referred to as the "platy facies" by Lespérance (1980a). He later gave them member status (Champou Member; Lespérance, 1980b) west of Forillon peninsula. Because this member is highly irregular and lenticular in its regional distribution, we will not use this nomenclature, but only consider the unit as a particular lithosome of the Indian Cove Formation.

Eastern Gaspésie

Previous geological studies have shown that there are major changes in the nature and thickness of the Upper Gaspé Limestones inland in the eastern peninsula (McGerrigle, 1950; Mason, 1971; Lespérance, 1980a, b; Amyot, 1984; Rouillard, 1986). These changes are linked to presence of fault bordered acadian tectonic blocks. These blocks are



Figure 5. Mudstone with structureless dolomite concretions. Shiphead Formation, section A.



Figure 6. Cherty area with preserved *Zoophycos* trail. Indian Cove Formation, section A.

(Fig. 7): the area north of Bras Nord-Ouest (BNO) fault; the area between Bras Nord-Ouest and Third Lake (TL) faults, and the area between Third Lake and Grande Rivière faults.

Area north of Bras Nord-Ouest (BNO) fault

In this sector, the Upper Gaspé Limestones are part of the sequence forming the northwest border of the Connecticut Valley-Gaspé Synclinorium. Sections 1 to 11 described in this structural block are sketched and correlated in Figure 8.

North of the Bras Nord-Ouest fault, the Upper Gaspé Limestones sequence is the extension of the one seen on Forillon peninsula. The twofold division of the Forillon Formation is recognized along the entire length of this structural belt. The Mont Saint-Alban Member is composed of more or less carbonate-bearing and siliceous mudstones while the Cap Gaspé Member is again dominated by calcilitites with a mudstone texture, but far less cherty and fossiliferous than in the Forillon peninsula. The Shiphead Formation is here again an heterogeneous unit. Figure 8 shows that the base of the Shiphead Formation is almost invariably made of mudstones, overlying the Cap Gaspé Member calcilitites. A more or less dolomitic and impure limestone succession usually marks the uppermost metres of the formation. The Shiphead Formation in this area is almost devoid of fossils. Slumps and truncated surfaces are locally seen. The Indian Cove Formation is similar in lithology to its extension on Forillon peninsula, being composed almost entirely of highly siliceous and cherty calcilitites with a mudstone texture. The sandy and silty limestone lithosome is irregularly present at the top of the formation in that area. The Upper Gaspé Limestones are overlain in the easternmost area (Fig. 8) by the York River Formation whereas in the remaining area, a transitionnal unit (York Lake Formation; Lespérance, 1980b) composed of limestones and siliciclastics is developed. Its stratigraphic assignment is unsettled yet (D. Brisebois, pers. comm. to D. Lavoie).

Area between or close to the Bras Nord-Ouest and Third Lake (TL) faults

Section 12 (Mississippi River area) and the Sunny Bank drill hole (SB) are located in that structurally complex area. Our description of Sunny Bank core is taken from Lespérance (1980a) and Amyot (1984).

Figure 7 shows, for sections south of Bras Nord-Ouest fault, important changes in the Upper Gaspé Limestones. The rock succession being more homogeneous, the three units are difficult to recognize. South of the Bras Nord-Ouest fault, the thicknesses of units are almost twice that of the northern sections. The Forillon Formation is a succession of slightly dolomitized, uncommonly cherty calcilitites with a mudstone texture that cannot be subdivided. The calcilitite is silty and shaly, contains parallel and cross bedded laminations and is devoid of fossils. The Shiphead Formation is almost entirely composed of dolomitized siliciclastic-rich calcilitites with a mudstone texture and occurs generally in thicker beds (up to 75 cm) than the Forillon calcilitites. Tuffaceous mudstones are observed in the Mississippi River area. The Indian Cove Formation is composed of slightly siliceous and seldom cherty (except Sunny Bank) calcilitites. The thickness of this last unit is much greater than the one in the northern sections.

Area between Third Lake and Grande Rivière faults

The area in which sections 13 and 14 (Fig. 7) were described is structurally complex. Faults are most abundant and obvious at the Grande Rivière section (no. 14) where numerous stratigraphic repetitions are likely to be present.

The undivided Forillon Formation is almost exclusively composed of a thick unfossiliferous dolomitic and shaly calcilitites with a mudstone texture interbedded with beds and lenses of limy mudstones and lithic sandstones. The formation is also characterized by some truncated surfaces, slumps (Fig. 9) and debris flow units associated with slumped beds. The Indian Cove Formation is represented by slightly siliceous, shaly to silty calcilitites with a mudstone texture. The unfossiliferous limestone contains parallel and cross-bedded laminations, small scale slumps and truncated surfaces. The most obvious change in this area is the disappearance of the Shiphead Formation, as it is known in the northern part of Gaspésie, which is replaced by a thick siliciclastic unit dominated by slumped dark sandy mudstones with thin silty laminations. Beds and lenses of commonly dolomitic lithic sandstones and conglomerates (Fig. 10) are interlayered with the mudstones. This succession is lithologically identical to the lithology of the nearby Fortin Group (D. Brisebois, pers. comm. to D. Lavoie and D. Lavoie, pers. obser.), a time equivalent unit of the Upper Gaspé Limestones (Bourque *et al.*, in press) which outcrops in the western Gaspé basin. Rouillard (1986), in the Grande Rivière area (section 14), introduced a fourth unit in the Upper Gaspé Limestones under the Forillon Formation. The Joncas facies is a 500 m rock succession lithologically similar to the unit sandwiched between the Forillon and Indian Cove Formations.

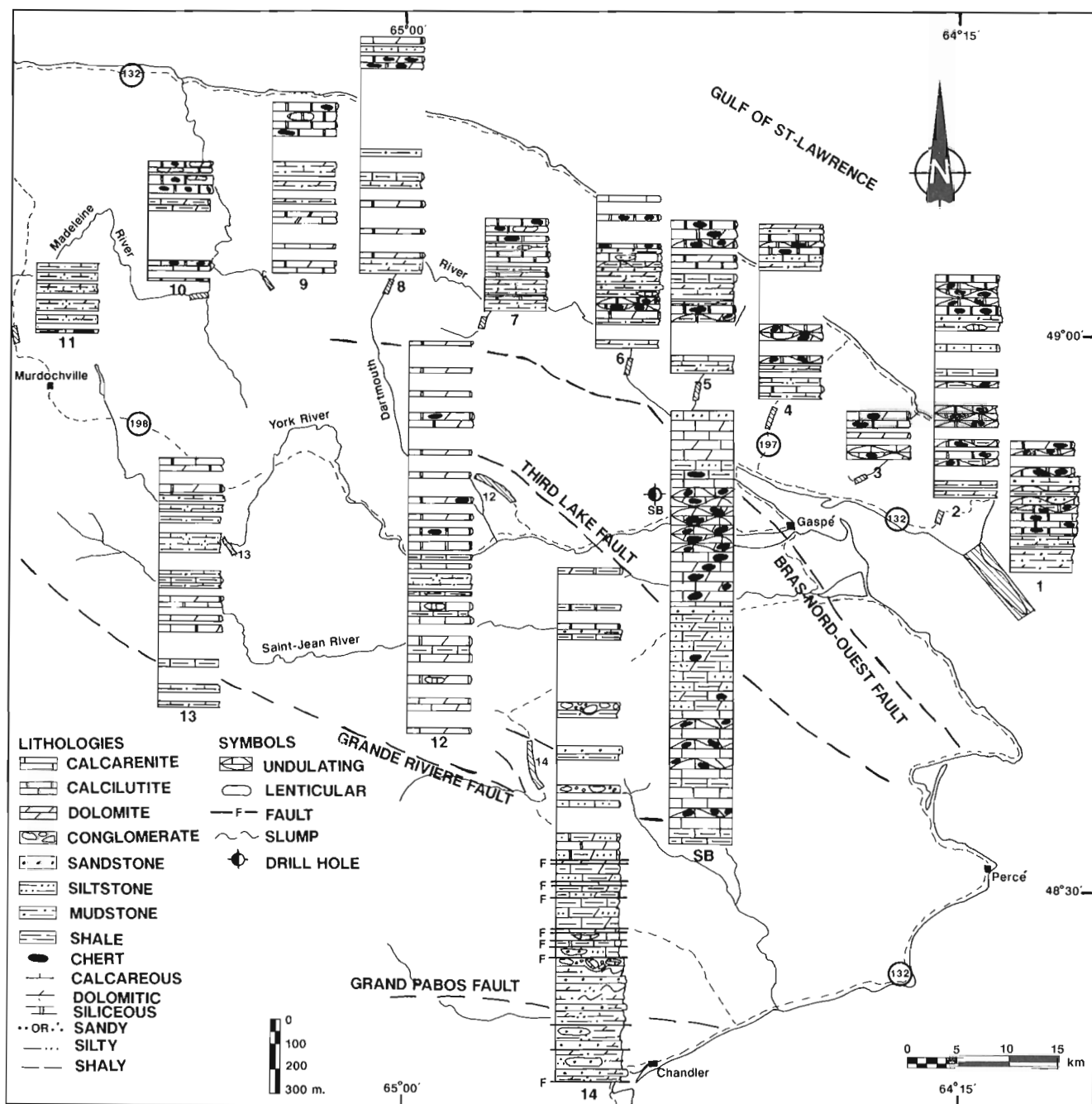


Figure 7. General stratigraphy of the studied horizon in the Gaspé Basin with major faults. Sections 1: Forillon peninsula; 2: Road 132; 3: Anse au Griffon River; 4: Road 197; 5: Petite Fourche River; 6: Dartmouth River (Blanchet twp); 7: Logan Creek; 8: Dartmouth River (Beaujeu twp); 9: Roburn Camp Creek; 10: Madeleine River area; 11: Road 198 (Murdochville); 12: Mississippi River area; 13: Oatcake Creek area; 14: Grande Rivière area; SB: Sunny Bank.

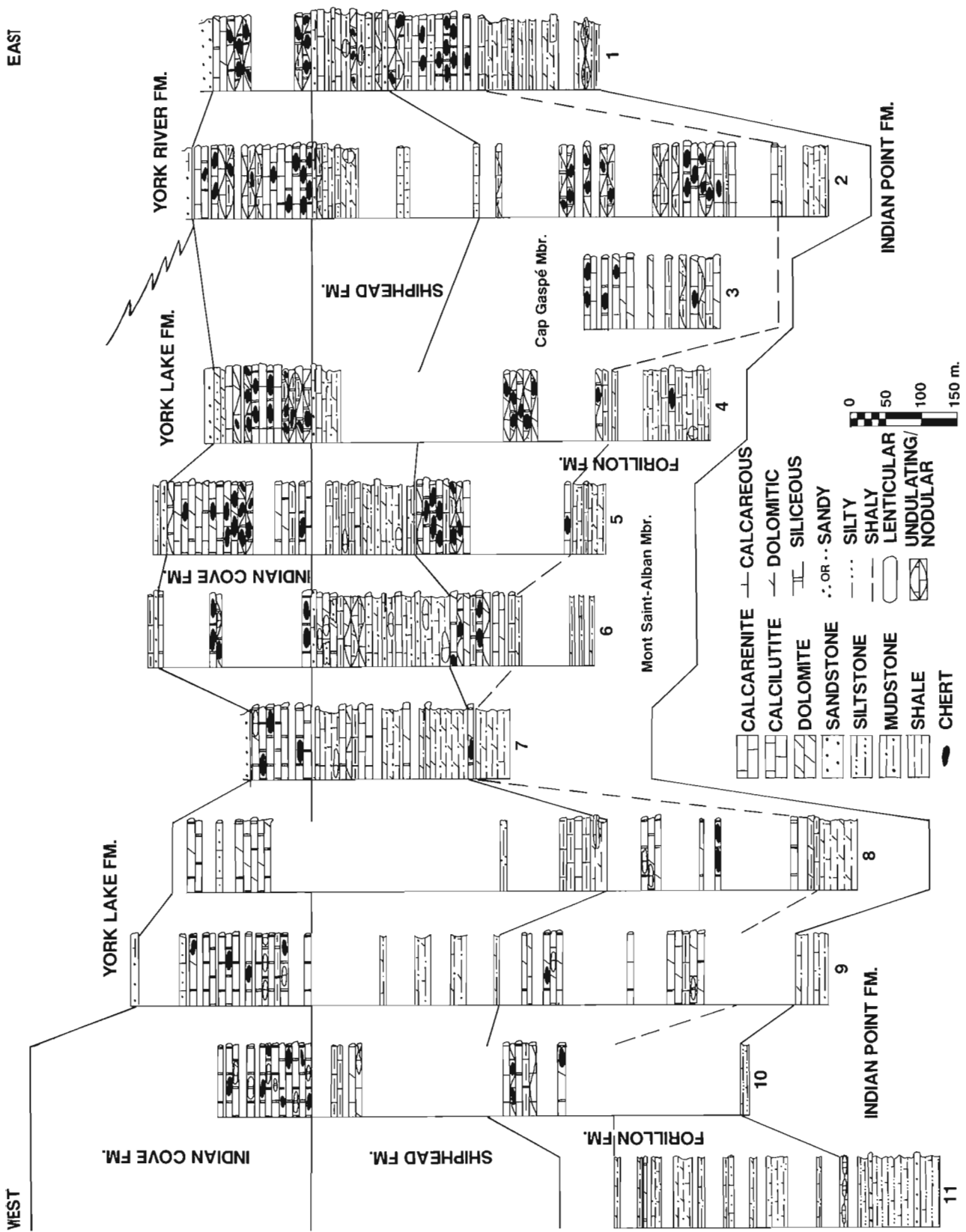


Figure 8. Lithostratigraphic correlations for the northern area. Location of sections on Figure 12.



Figure 9. Slumped dolomitic calcilutite of the Forillon Formation. Section 14.



Figure 10. Graded lithic and quartz-rich conglomerate lense in dark dolomitic mudstone with occasional conglomeratic laminations. Quarter for scale. Fortin Group, section 14.



Silica in the Upper Gaspé Limestones

Silica is certainly one of the most obvious components of the Upper Gaspé Limestones. Its recognition was as early as stratigraphic study of the horizon (Clark, 1908; Parks, 1931). Russel (1946) and Lespérance (1980a, b) dealt to some extent with the origin and distribution of the silica. However, questions related to the source, control mechanisms and relations between silicification and carbonate diagenesis are still unsettled. Silicification of the Upper Gaspé Limestones is almost entirely restricted to the Forillon and Indian Cove Formations. Our preliminary work shows that it is almost absent outside the northern segment, our study



Figure 12. Small black chert nodules set in unevenly silicified calcilutite. Cap Gaspé Member, section A.



Figure 13. Silicified calcilutite with unaltered core. Note black laminated border of the silicified area. Cap Gaspé Member, section A.

Figure 11. Silicified calcilutite with depressed lens of un-silicified carbonates (top of picture). Indian Cove Formation, section 1G.

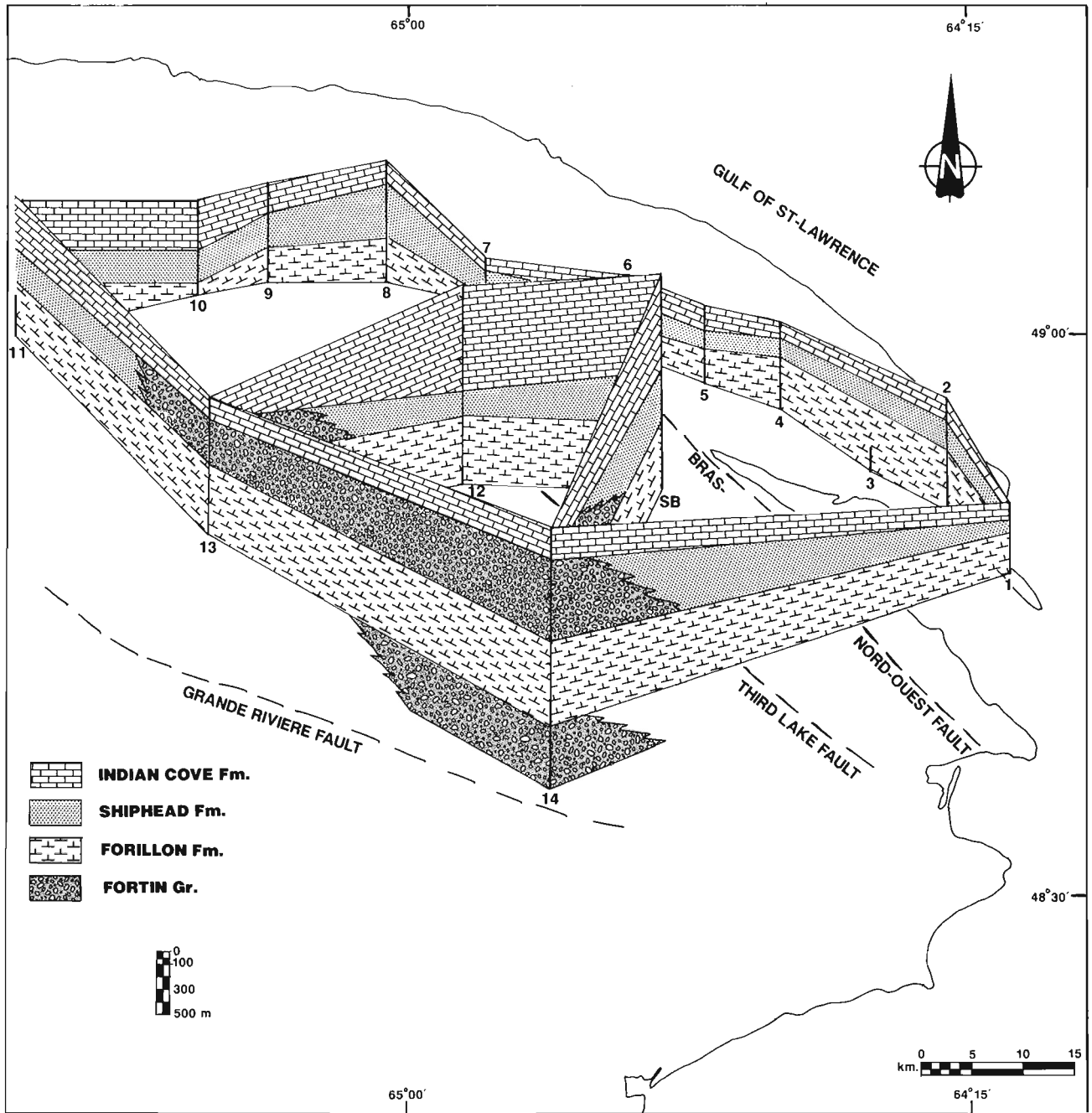


Figure 14. Early Devonian megafacies distribution with major faults of the Gaspé Basin.

is focused on that part of the basin (Fig. 7). Field observations show that the Indian Cove Formation is more uniformly silicified than the Forillon. Intensity of silicification varies within single section and is more pronounced in the western part of the northern segment. Silicification, with minor dolomitization, is mostly developed in shaly limestone interbeds resulting in well indurated beds with more or less abundant chert. Chert occurs in irregularly shaped, black or grey centimetre-sized nodules or ribbons within silicified areas. Silicification has frequently left unaltered, depressed, lenticular areas of carbonates (Fig. 11). The Forillon Formation is significantly less silicified than the Indian Cove and also shows important local and regional variations that are more intense in the eastern part of the northern segment. At Cap Gaspé (Fig. 1, section A), silicification of Cap Gaspé Member calcilutites produces more or less coalescive nodules of varied size and lateral extent (Fig. 12) with tiny black laminated margins (Fig. 13). Chert is developed as black irregularly shaped nodules of varied size (from 1×3 cm to 3×15 cm) concentrated in closely spaced (20 to 40 cm apart) horizons. Elsewhere, silicification gradually increases away from the top of Mont Saint-Alban Member with local high chert concentrations.

DISCUSSIONS AND CONCLUSIONS

The lithostratigraphic framework of the Upper Gaspé Limestones, as established on Forillon peninsula, is composed of the Forillon (with newly defined Mont Saint-Alban and Cap Gaspé Members), Shiphead and Indian Cove Formations. This stratigraphy has proven to be easily applicable to the area north of the Bras Nord-Ouest fault. Sections immediately south of it are characterized by thickening of the units and by homogenization of the sequence. Farther south and west, a new threefold division is seen but with major facies changes in the middle unit. Figure 14 summarizes all those relations in a fence diagram of that part of the Gaspé basin.

The following working sedimentological hypothesis are based on the previous lithostratigraphic considerations.

— The Upper Gaspé Limestones offer a wider spectrum of sedimentary environments than previously thought (Lespérance, 1980a; Bourque et al., in press).

— Shallower sedimentary conditions seemed to have prevailed in the northern sequence (greater number of sedimentary facies with relatively rapid facies changes, more fossiliferous units). The conditions seemed to have been even shallower in the Forillon peninsula area.

— The Bras Nord-Ouest fault was, as previously suggested by Amyot (1984), probably active in Early Devonian time. This resulted in a relatively fast subsiding basin located south and southwest of this structure, leading to thick lime mud accumulation.

— Farther south and southwest, as suggested by Bourque et al. (in press), tongues of the Upper Gaspé Limestones muds interlayer with the siliciclastic deposits of the Fortin Group.

— Movements along major acadian faults in that part of the studied area are thought to be of a few kilometres only (Brisebois, 1981; Kirkwood, 1986). Actual geographic distribution of facies would give a preliminary picture of Early

Devonian paleogeography with shallower conditions (shelf?) to the north-northeast and deeper conditions (subsiding basin?) to the south-southwest.

ACKNOWLEDGMENTS

Discussions with many people helped us in planning and initial fieldwork for this project. Among those, special thanks are expressed to D. Brisebois of the Ministère de l'Énergie et Ressources du Québec and P.J. Lespérance of Montréal University. L. Dubé, L. Michard and P. Vaillancourt respectively are thanked for redrafting of some figures, typing of the manuscript and an invaluable help on the field. Special thanks are due to Parks Canada for allowing us to work and collect samples in Forillon National Park.

Critical review by F.W. Chandler (GSC) and D. Brisebois (MERQ) has greatly improved the manuscript.

REFERENCES

- Amyot, G.
1984: Lithostratigraphie de sous-surface de l'est de la Gaspésie; Ministère de l'Énergie et des Ressources du Québec, ET 83-11, 75 p.
- Bourque, P.-A.
1975: Lithostratigraphic framework and unified nomenclature for Silurian and basal Devonian rocks in Eastern Gaspé Peninsula, Québec; Canadian Journal of Earth Sciences, v. 12, p. 858-872.
- Bourque, P.-A., Brisebois, D. and Malo, M.
in press Middle Paleozoic rocks of Québec and adjacent New-Brunswick; in H. Williams (ed.). The Appalachian/Caledonian Region: Canada and Greenland, Geological Survey of Canada, Geology of Canada, no. 6 (also Geological Society of America, The Geology of North American, Volume F-1.)
- Brisebois, D.
1981: Géologie de la région de Gaspé; Ministère de l'Énergie et des Ressources du Québec, DPV-824, 19 p.
- Clarke, J.M.
1908: Early Devonian history of New York and eastern North America; New York State Museum, Memoir 9, parts 1 and 2.
- Kirkwood, D.
1986: Géologie structurale de la région de Percé, Gaspésie, Québec; M.Sc. thesis University of Montréal, Lespérance, P.J.
- 1980a: Calcaires Supérieurs de Gaspé. Les aires-types et le prolongement vers l'ouest; Ministère de l'Énergie et des Ressources du Québec, DPV-595, 98 p.
- Lespérance, P.J.
1980b: Les Calcaires Supérieurs de Gaspé (Dévonien inférieur) dans le nord-est de la Gaspésie; Ministère de l'Énergie et des Ressources du Québec, DPV-751, 35 p.
- Logan, W.E.
1845: Coupes géologiques de la Baie des Chaleurs et de la côte de Gaspé; Geological Survey of Canada, Progress Report, p. 85-119.
- Mason, G.D.
1971: A stratigraphical and paleoenvironmental study of the Upper Gaspé Limestone and Lower Gaspé Sandstone Groups (Lower Devonian) of eastern Gaspé Peninsula, Québec; Ph.D. thesis, Carleton University, Ottawa.
- McGerrigle, H.W.
1950: The geology of eastern Gaspé, Québec; Ministère des Mines, Québec, RG-35, 168 p.
- Parks, W.A.
1931: Geology of the Gaspé peninsula; Bulletin of the Geological Society of America, v. 42, p. 785-800.
- Rouillard, M.
1986: Les Calcaires Supérieurs de Gaspé (Dévonien inférieur), Gaspésie; Ministère de l'Énergie et des Ressources du Québec, MB 86-15, 94 p.
- Russel, L.S.
1946: Stratigraphy of the Gaspé Limestone Series, Forillon Peninsula, Cap-des-Rosiers township, county of Gaspé south; Ministère des Richesses naturelles du Québec, DPV-347, 96 p.

Radiocarbon dating evidence for the age of deglaciation of LaHave Basin, Scotian Shelf

**David J.W. Piper, Michael R. Gipp¹ and Kate Moran
Atlantic Geoscience Centre, Dartmouth**

Piper, D.J.W., Gipp, M.R. and Moran, K., Radiocarbon dating evidence for the age of deglaciation of LaHave Basin, Scotian Shelf; in Current Research, Part B, Geological Survey of Canada, Paper 90-1B, p. 29-32, 1990

Abstract

Three new radiocarbon dates from LaHave Basin confirm that ice retreat on the outer part of the central Scotian Shelf began about 18 ka. The deglaciation chronology of LaHave Basin is similar to that of the nearby Emerald Basin, but physical properties of sediments are quite different.

Résumé

Trois nouvelles datations au carbone radioactif provenant du bassin de LaHave confirment que le retrait de la glace sur la périphérie de la partie centrale de la plate-forme Néo-Écossaise a commencé il y a environ 18 ka. L'histoire de la déglaciation du bassin de LaHave est similaire à celle du bassin d'Emerald avoisinant, mais les propriétés physiques des sédiments sont assez différentes.

¹ Department of Geology, University of Toronto, Scarborough Campus, 1265 Military Trail, Scarborough, Ontario M1C 1A4

INTRODUCTION

Accelerator mass spectrometry (AMS) dating has made it possible to date small mollusc shells in offshore glaciomarine sediments and thus help to derive a reliable deglaciation chronology for the eastern Canadian continental shelf.

A series of dates in Emerald Basin on the Scotian Shelf (Gipp and Piper, 1989) showed that deglaciation took place between about 18 and 14 ka, not much earlier as proposed by previous workers (King and Fader, 1986). Subsequently, King and Fader (1988) have presented further evidence for the deglaciation chronology proposed by Gipp and Piper (1989). In our study of Emerald Basin, we saw evidence in seismic reflection profiles for the deposition of diamict or other coarse ice-proximal sediment in southwestern Emerald Basin synchronous with deposition of proglacial muds within the basin. This could have been explained either by ice remaining in LaHave Basin longer than in Emerald Basin, or by the development of ice rises on some of the outer banks. Gipp (1989) has presented seismic and textural evidence for the latter hypothesis.

On C.S.S. Hudson cruise 88-010 we collected four piston cores (Fig. 1) in order to: 1) date the oldest sediments overlying till in LaHave Basin; 2) compare the lithologies present with those in Emerald Basin and 3) evaluate our hypothesis that ice remained later in LaHave Basin.

RESULTS

Four cores (6 - 9) were collected along high-resolution (Huntec DTS) seismic lines (Fig. 2). The seismostratigraphy was interpreted following the nomenclature of King and Fader (1986). Acoustically transparent or weakly stratified LaHave Clay thins towards the basin margin and overlies, in places unconformably, acoustically well-stratified Emerald Silt. The Emerald Silt overlies acoustically incoherent sediments interpreted as Scotian Shelf Drift (till or diamict).

All four cores penetrated to approximately the base of the Emerald Silt. Much of the Emerald Silt in the cores con-

sisted of muds with numerous dispersed clasts of unconsolidated sediment and stones seen on the split core face and in X-radiographs. Some of the clay clasts were twisted. These deposits resemble debris flow deposits that we have seen elsewhere, although the possibility that they are in part ice-rafted deposits cannot be excluded.

Although the seismic reflection profiles are similar to those from Emerald Basin, the sediment physical properties are quite different in the two basins. In Emerald Basin, cores from the central part of the basin show that both the Emerald Silt and LaHave Clay have low density and acoustic velocity and high water content (Moran et al., 1989). In our cores from the margin of LaHave Basin, the physical properties are distinctly different in the Emerald Silt (sandy silt unit in Fig. 3), with very low water content (mean $\approx 50\%$ dry weight) and high density and acoustic velocity. The magnetic susceptibility signature in the cores from the two basins is similar, which suggests that the source of sediment is from the same general area. The difference in properties therefore implies a difference in depositional environment, or possibly post-depositional processes such as ice loading or iceberg scouring.

Shells suitable for radiocarbon dating were found only in cores 7 and 8. In core 7, an age of 17.5 ka (Table 1) was obtained from a shell immediately above a unit of thick debris flow deposits. The seismic reflection profile suggests that the base of this unit occurs just below the base of the core and rests directly on till. A shell 2 m higher in the core yielded a date of 16.3 ka, suggesting a high rate of deposition for the lower part of the Emerald Silt. Linear extrapolation of this deposition rate gives an age of 18.5 ka for the top of the till in this core. This is probably a maximum age, since the depositional rate at the base of the core, immediately after ice retreat, is likely to have been greater than higher in the core.

In core 8, an age of 13 ka was obtained from a shell 40 cm above the base of a unit of olive grey laminated silty mud (?LaHave Clay), which overlies brown sandy sediments containing debris flow deposits. This date probably shortly follows the retreat of proximal ice from the area, marked by the cessation of debris flow deposition. Ice retreat is constrained to lie between 16.3 and 13 ka.

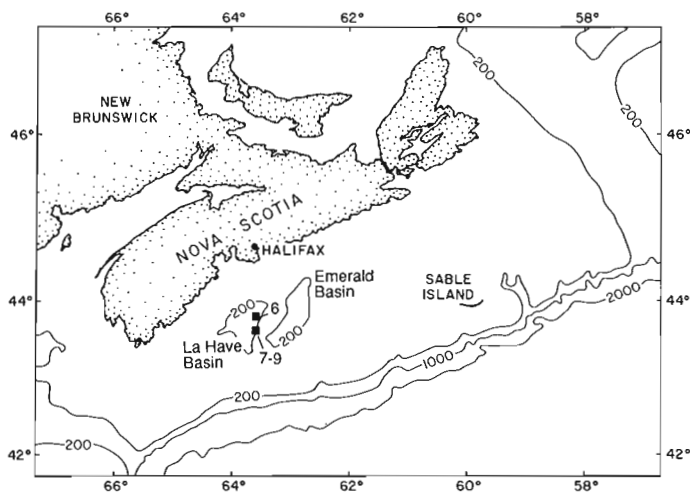


Figure 1. Map showing location of cores (6-9) from LaHave Basin.

Table 1. Radiocarbon dates

Core	depth	Material	Lab No	Date
007	187-198	<i>Nuculana pernula</i> single valve, intact periostracum, in sandy layer	B27228	16320 \pm 145
007	393-396	<i>Macoma calcareo</i> paired valves, slightly worn periostracum	B27229	17450 \pm 155
008	85-87	<i>Nucula delphinodonta</i> fresh-looking paired valves	B27230	12950 \pm 130

Dates by AMS technique adjusted by C-13 for total isotope effects. Age reported in Radiocarbon years BP.

DISCUSSION

The deglaciation chronology inferred for LaHave Basin is very similar to that in Emerald Basin. Gipp and Piper (1989) extrapolated an age of 17.5 - 18 ka for the top of till in Emerald Basin from a greatest age of 17.4 ka. In LaHave Basin, an age for the top of the till of < 18.5 ka is extrapolated from a greatest age of 17.5 ka. Ice retreat from the central Scotian Shelf was dated as younger than 15 ka from Emerald Basin;

the similar event in LaHave Basin took place between 16.3 and 13 ka. This evidence does not support the hypothesis that ice remained longer in LaHave Basin than in Emerald Basin. The difference in physical properties in the Emerald Silt in the two basins may result from the abundance of debris flows in the LaHave Basin cores. This abundance may be related to the location of the cores closer to the former ice margin, compared with more distal cores in Emerald Basin.

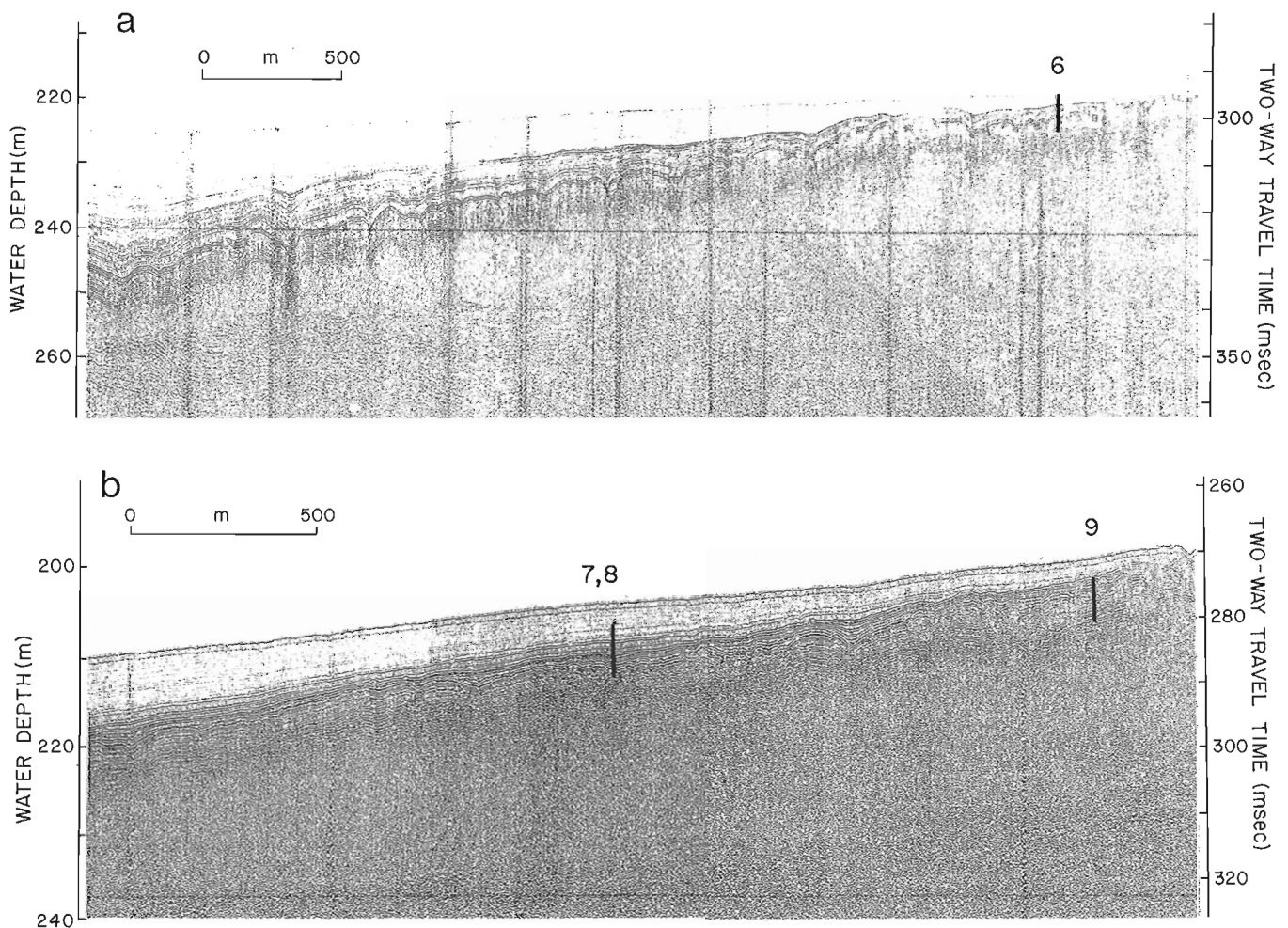


Figure 2. Hunttec DTS boomer profiles through the core sites. Note that because of different instrument settings the LaHave Clay appears extremely transparent near core site 6. The acoustic velocity profiles in the cores have been used to position them relative to the acoustic stratigraphy: note that some cores did not sample the uppermost part of the stratigraphic section.

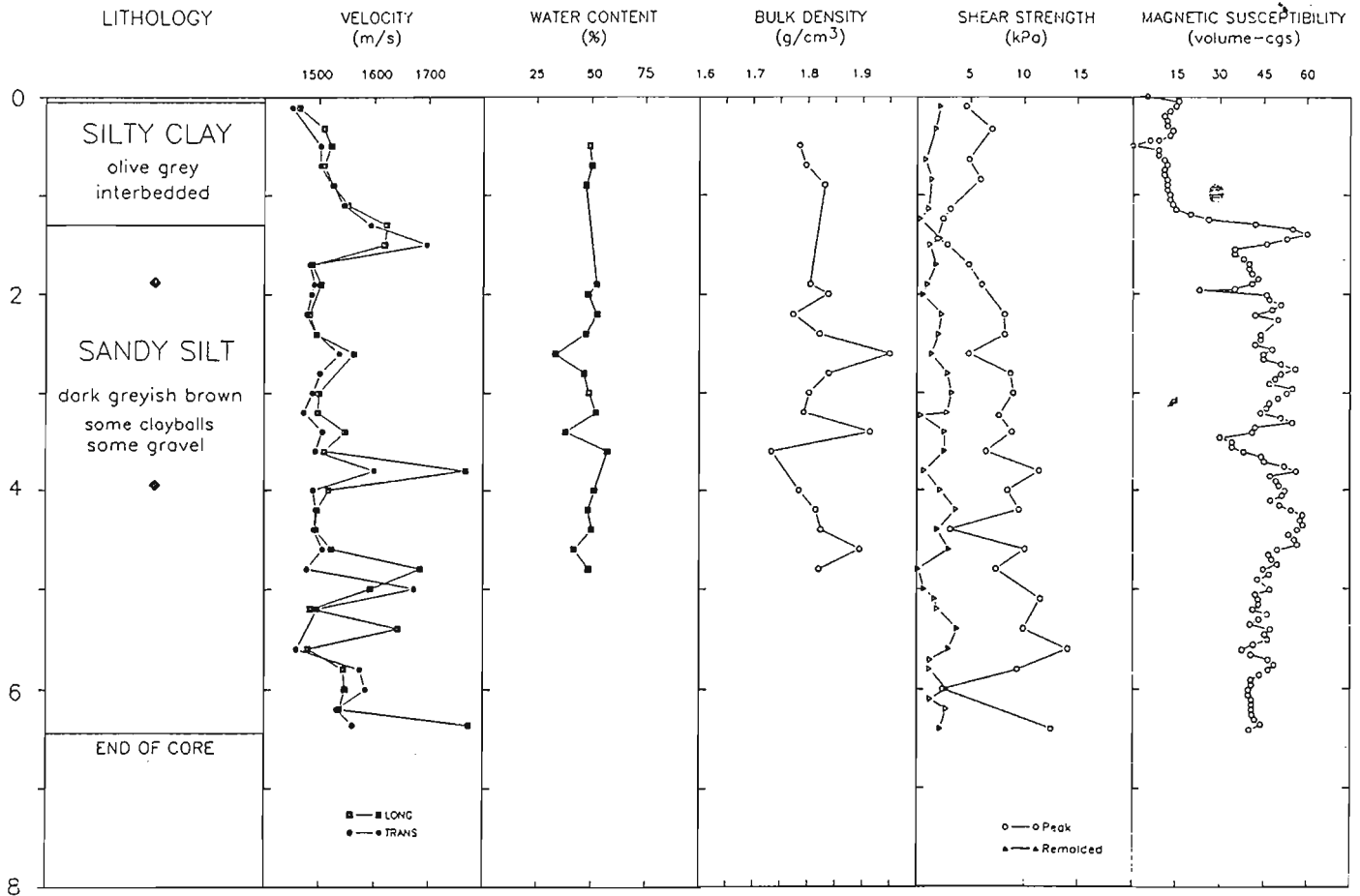


Figure 3. Down-core logs of sediment properties for core 7. This core is representative of the other cores collected. The silty clay unit is interpreted as the lower part of the LaHave Clay; the sandy silt unit as Emerald Silt. ♦ shows location of radiocarbon dated samples.

REFERENCES

Gipp, M.R.

1989: Late Wisconsinan deglaciation of Emerald Basin, Scotian Shelf; unpublished M.Sc. thesis, Memorial University of Newfoundland.

Gipp, M.R. and Piper, D.J.W.

1989: Chronology of Late Wisconsinan glaciation, Emerald Basin, Scotian Shelf; Canadian Journal of Earth Sciences, v. 26, p. 333-335.

King, L.H. and Fader, G.B.

1986: Wisconsinan glaciation of the continental shelf, southeastern Atlantic Canada; Geological Survey of Canada, Bulletin, 363, 72 p.

1988: Late Wisconsinan ice on the Scotian Shelf; Geological Survey of Canada, Open File 1972, 13 p.

Moran, K., Piper, D.J.W., Mayer, L.A., Courtney, R.C., Driscoll, A.H. and Hall, F.R.

1989: Scientific results of long coring on the eastern Canadian continental margin; Proceedings of the 21st Annual Offshore Technology Conference, Houston, OTC 5963, p. 65-71

Bedrock geological mapping and basin studies in the Gulf of St. Lawrence

B.V. Sanford¹ and A.C. Grant²

Sanford, B.V. and Grant, A.C., *Bedrock geological mapping and basin studies in the Gulf of St. Lawrence*; in *Current Research, Part B, Geological Survey of Canada, Paper 90-1B*, p. 33-42, 1990.

Abstract

High resolution reflection seismic profiles collected in 1989 have been analyzed in conjunction with coverage from previous surveys to produce a revised, preliminary bedrock geological map of the Gulf of St. Lawrence region. A significant result indicated by this map is that Carboniferous strata extend farther northward onto the Lower Paleozoic terrane of the Anticosti Basin than previously recognized. Windsor and Canso-Riversdale sequences are interpreted to extend northeastward off the west coast of Newfoundland, and northwestward between Anticosti Island and Gaspé into the St. Lawrence Estuary. This superposition of structured and reservoir-rich Carboniferous sequences on potential source rocks of the Anticosti Basin may present targets for hydrocarbon exploration.

Résumé

Des profils de sismique réflexion de haute résolution recueillis en 1989 ont été analysés conjointement avec des profils tirés au cours de levés antérieurs afin de produire une carte préliminaire révisée de la géologie de la roche en place de la région du golfe du Saint-Laurent. Un détail important ressort de cette carte, soit que les couches carbonifères se prolongent, en direction nord, beaucoup plus loin au-dessus du terrane du bassin d'Anticosti, datant du Paléozoïque inférieur, antérieurement présumé. On interprète les séquences de Windsor et de Canso-Riversdale comme étant un prolongement nord-est s'étendant au large de la côte ouest de Terre-Neuve, et un prolongement nord-ouest s'étendant entre l'île d'Anticosti et la Gaspésie jusque dans l'estuaire du Saint-Laurent. Cette superposition de séquences carbonifères à structure favorable et riches en roches réservoirs au-dessus de roches mères potentielles dans le bassin d'Anticosti pourrait indiquer la présence de cibles se prêtant à l'exploration pétrolière.

¹ Continental Geoscience Division, Ottawa

² Atlantic Geoscience Centre, Dartmouth

INTRODUCTION

Purpose of the study

Multidisciplinary surveys were carried out in the Gulf of St. Lawrence from C.S.S. BAFFIN and C.S.S. DAWSON between May and June, 1989 to collect data on bedrock and surficial geology (Fig. 1). Principal objectives of these cruises were to upgrade knowledge of the geology of the Gulf toward compilation of a "basin atlas" for this region, outline new exploration plays for oil and gas, and collect data to assist in assessment of hydrocarbon potential. The information from this survey will be integrated with existing geological and geophysical data to prepare maps of bedrock geology, subsurface structure and interval thickness maps, lithofacies maps, and relevant structure sections.

This paper presents a revised map of bedrock geology (Fig. 2) based on preliminary analysis of available data, and discusses some of the significant new findings indicated by

this map. Studies of Quaternary geology deriving from the 1989 BAFFIN and DAWSON cruises are reported by Josehans et al. (1990) and Vilks et al. (1990).

The Database

The 1989 BAFFIN cruise (BA 89-008) collected a grid of approximately 5000 km of single channel seismic coverage in the Gulf of St. Lawrence (Fig. 1) utilizing a 655 cm³ sleeve gun energy source for bedrock penetration, Huntect DTS and 3.5 khz systems for resolving surficial deposits, and sidescan sonars for definition of seafloor morphology. The survey by C.S.S. DAWSON (Vilks et al., 1990) collected 2200 km of additional seismic coverage (Fig. 1), and bedrock cores at a number of locations in the northern part of the Gulf using an underwater electric drill. Previous cruises by the Geological Survey of Canada (Fig. 1, thin lines) provided coverage in the west Gulf of St. Lawrence

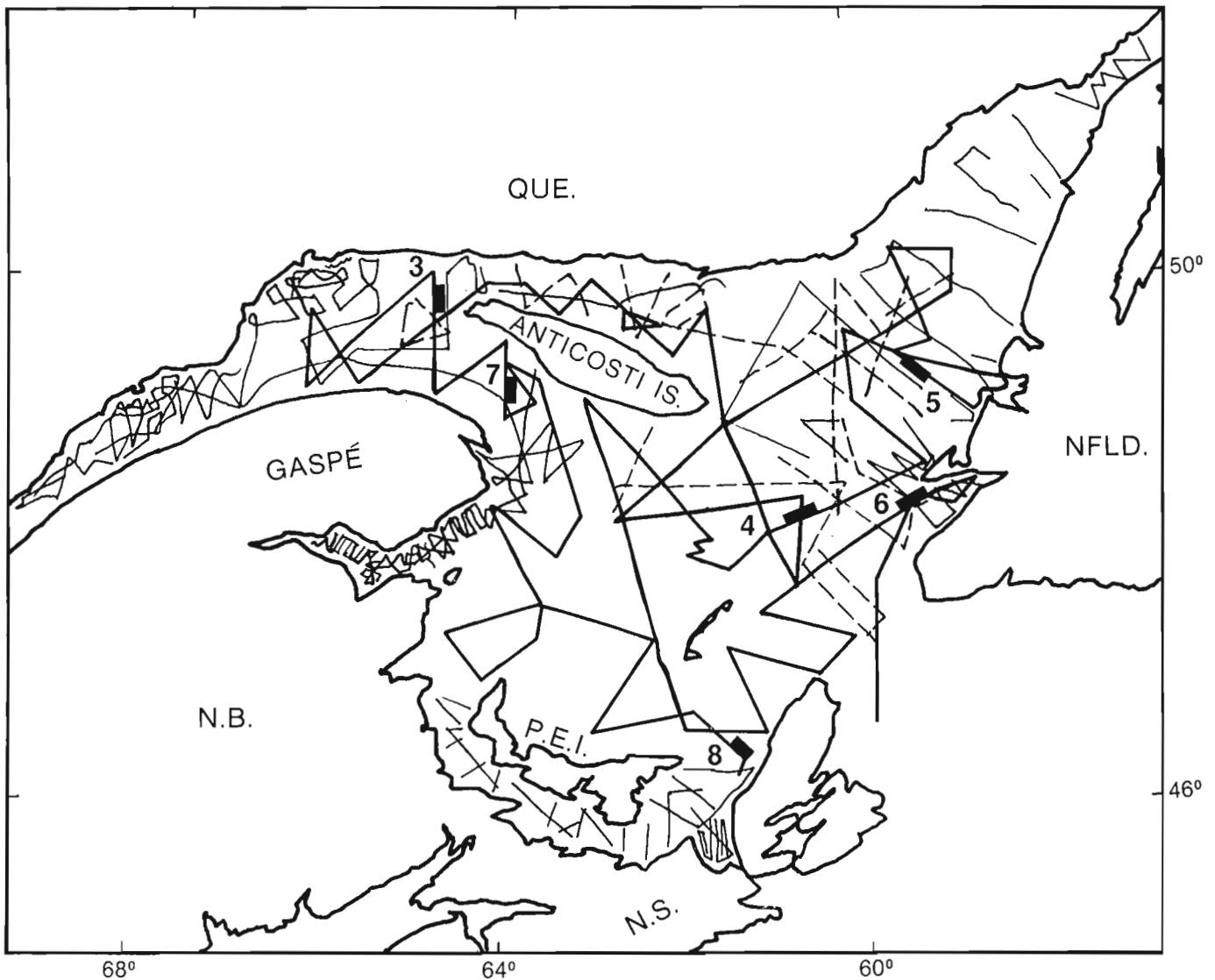


Figure 1. Lines of seismic coverage by the Geological Survey of Canada. Heavy lines are BAFFIN cruise 89-008; dotted lines are DAWSON cruise 89-007. Sources of remaining coverage are given in text. Numbered line segments locate specimen seismic profiles in Figures 3 to 8.

region (Syvitski et al., 1987; Syvitski and Praeg 1989a, b), the northeast Gulf (Shearer, 1973; Haworth and Sanford, 1976), and in the southern Gulf (Kranck, 1971). Bedrock cores have been collected previously in the northeast Gulf (Haworth and Sanford, 1976), and immediately east of Anticosti Island (Loring, 1975). Nine exploratory wells have been drilled in the Gulf of St. Lawrence by oil companies, and a number of relevant wells are located on Anticosti Island, Prince Edward Island, and in Carboniferous strata along the southwestern coast of the Gulf. Non-confidential industry multichannel seismic coverage in the Gulf of St. Lawrence amounts to some 40 000 km.

REGIONAL GEOLOGY

The Gulf of St. Lawrence is underlain by relatively flat-lying Paleozoic strata, ranging from Early Cambrian to Permian (Fig. 2). The rocks are contained in two principal sedimentary basins; the Anticosti Basin underlying the northern part of the Gulf, containing up to 6 km of lower Paleozoic (Cambrian to Upper Silurian) carbonates and lesser terrigenous clastics, and the Magdalen Basin centred beneath the southern Gulf of St. Lawrence, containing more than 10 km of upper Paleozoic (Mississippian to Permian)

terrigenous clastics, evaporites and carbonates (Wade et al., 1977). The rocks of Anticosti Basin rest on a Precambrian basement complex of Grenvillian age; strata of the Magdalen Basin overlie a Lower Paleozoic basement deformed by the Taconian and Acadian orogenies in Ordovician and Devonian time respectively.

The following outline of tectonostratigraphic events affecting the Gulf of St. Lawrence region is the background for offshore bedrock mapping based on extrapolation of geology from land, analysis of seafloor physiography and subsurface seismic character, and ties to offshore boreholes. This summary is drawn mainly from work by Howie (1988), Petryk (1976), Poole (1967), Poole et al. (1970) and Sanford et al. (1985). Geology of land areas around the Gulf of St. Lawrence is compiled from published maps (eg., Bolton, 1972; Cumming et al., 1982; Hibbard, 1983; Keppie, 1979; McGerrigle, 1953; Potter et al., 1968; Skidmore, 1967).

The sediments of the Anticosti Basin were initially (Cambrian to Early Ordovician) deposited on a broad continental shelf, which progressively evolved into a foreland basin as allochthons were emplaced in western Newfoundland in the early Middle Ordovician, and in Gaspésie in

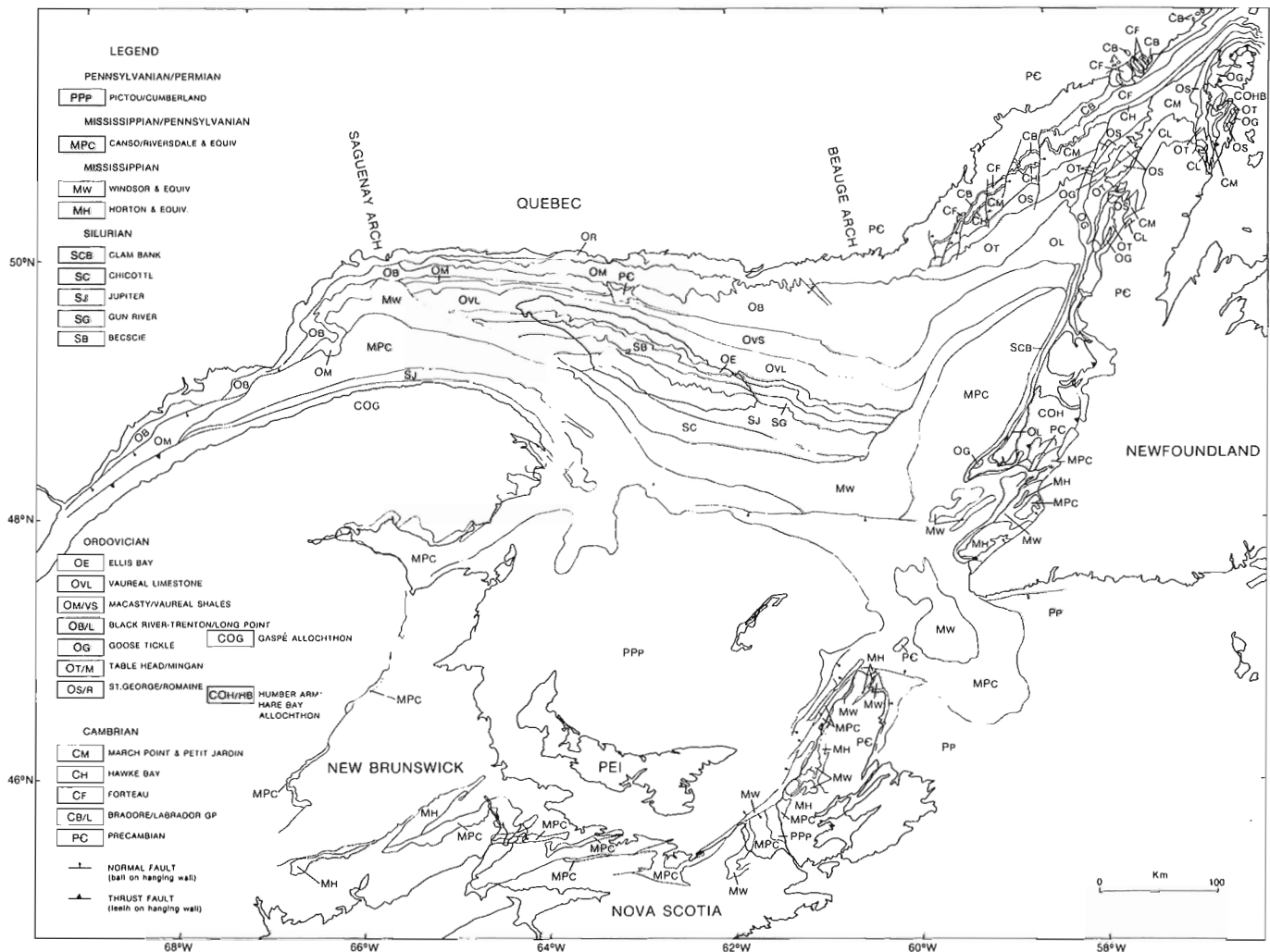


Figure 2. Preliminary revised map of bedrock geology in the Gulf of St. Lawrence region.

early Late Ordovician, to form the Appalachian Structural Front. Near the close of the Ordovician the seaway was again open to the south and contiguous with the Appalachian geosyncline, a connection that continued to the close of the Late Silurian. Because Silurian rocks are succeeded unconformably by Carboniferous strata, the region apparently was emergent through most, if not all, of Devonian time. The Mississippian to Permian Magdalen Basin was centred in the Iles de la Madeleine region of the Gulf of St. Lawrence, but extended into broad regions of the Atlantic Provinces and overlapped onto lower Paleozoic platform terrane of the Anticosti Basin.

Anticosti Basin

The Cambrian to Silurian succession is summarized under five principal tectono-stratigraphic cycles:

(i) Lower Cambrian to Lower Ordovician (Canadian) cycle: initiated in latest Precambrian Hadrynian to Early Cambrian, with deposition of coarse redbed clastics and volcanics (Bradore, Fig. 2). Of probable non marine origin, the beds reflect rifting processes. A succeeding marine invasion brought deposition of carbonates and craton-derived shales and sandstones (Forteau, Hawke Bay, March Point, Petite Jardin, St. George, Romaine). These were deposited on a broad continental shelf extending from western Newfoundland to southern Gaspésie, its southern edge and adjacent slope and rise now obscured beneath allochthons of the Appalachian Orogen.

(ii) Lower Middle Ordovician (Whiterockian to Chazyan) cycle: a sequence containing a thin basal sand and composed locally of fine, crystalline limestones (Table Head/Mingan), changing in their upper part to black shales and flysch (Goose Tickle) towards the southern edge of the shelf. The clastics are orogen-derived and represent the thick wedge of sediments deposited along the leading edges of advancing (Humber Arm/Hare Bay) allochthons.

(iii) Upper Middle Ordovician (Blackriverian/Trentonian) to lower Upper Ordovician (Maysvillian) cycle: a sequence of limestones (Long Point) with a basal orthoquartzitic sand unit in the eastern part of the embryonic Anticosti Basin where the beds unconformably onlap the Humber Arm allochthon. These merge with limestones (Black River/Trenton) in the western part of the basin, and in turn give way vertically and laterally southward to black shales and flysch (Macasty), the latter a product of the advancing Gaspé allochthon, presumably emplaced in early Late Ordovician time. Shale deposition (lower Vaureal, Upper Long Point) continued throughout the Anticosti basin in the mid-Late Ordovician, the detritus derived from the newly emplaced Appalachian Structural Front immediately to the south.

(iv) Upper Ordovician (Richmondian) to Lower Silurian (Llandovery) cycle: a dominant limestone succession (upper Vaureal, Ellis Bay, Becscie, Gun River, Jupiter, Chicotte) of shallow water origin containing bioherms. It onlaps Gaspésie (Fig. 2) and would appear to confirm the stable nature of that segment of the orogen, and the final date of emplacement of the allochthons.

(v) Lower Silurian (Wenlock) to Upper Silurian (Pridolian) cycle: a thick redbed unit (Clam Bank) with interbeds of limestone at the top of the succession. The sudden influx of

orogen-derived clastics onto the platform points to intensive and probably widespread tectonic activity within the orogen. Renewed epeirogeny has been recorded at this period in widely separated parts of the Canadian craton, which probably relates to orogenic events in progress along the continental margins. The Clam Bank Formation is the youngest of the early Paleozoic sequences recorded in the Anticosti Basin.

Throughout the early Paleozoic, The Beaugé and Saguenay arches were tectonically active structural elements. The Beaugé Arch affected sedimentation processes across its axis, and obviously controls the present day distribution of the Cambrian to Silurian and Carboniferous rock units (Fig. 2). The arch also played an important role in the emplacement of the segmented Appalachian Front; first, of the Hare Bay/Humber Arm allochthons along its southeast margin in the early Middle Ordovician (Chazyan), and secondly, the somewhat later emplacement of the Gaspé allochthon along its southwest margin in the early Late Ordovician (Edenian) time.

The Saguenay Arch, its southern extremity now buried beneath the Gaspé allochthon, was also a major tectonic element throughout the Paleozoic, and is currently active as indicated by the anomalous level of earthquake activity along its east and west margins (Sanford et al., 1985; Adams and Basham, 1989).

Magdalen Basin

The sedimentary sequences deposited in the Magdalen Basin are largely coarse to fine redbed terrigenous clastics of continental origin, with some marine carbonates and evaporites. These have been divided into a number of formational units of local significance where mapped in detail onshore. In offshore mapping (Fig. 2) and in regional geological compilation of the Atlantic provinces and adjacent offshore (Sanford et al., 1979), it has proved more practical to combine these into four principal units, namely Horton, Windsor, Riversdale/Canso and Pictou/Cumberland groups and equivalents in that respective order of succession. These units, nearly everywhere bounded by unconformities, represent four major tectonostratigraphic cycles of deposition:

(i) Lower Mississippian (Tournaisian) cycle: red and grey sandstone, siltstones, shales, conglomerates and volcanics of the Horton Group and equivalents. The transport and deposition of these sediments into the southern part of the Magdalen Basin presumably was due to renewed, albeit somewhat subdued, orogenic activity (Alleghenian Orogeny) confined largely to the southern margin of the previously stabilized Acadian Geosyncline. Following this depositional cycle, the southernmost margins of the basin were again uplifted and block-faulted, a process that also affected wide segments of the Magdalen Basin itself as shown by industry seismic data.

(ii) Upper Mississippian (Visean) cycle: salt, gypsum, carbonates, fine to coarse clastics, and volcanics of both continental and marine origins of the Windsor Group and equivalents. Marine invasion of the Magdalen Basin was extensive, as recorded by the thick evaporite deposits over a wide region of the Gulf of St. Lawrence and in onshore

areas of the Atlantic Provinces. The thick salt deposits that underlie the southern part of the Gulf from southwestern Newfoundland to northern Nova Scotia are highly structured, the bedded deposits having migrated into ridges, walls and diapirs of variable shapes and sizes. Some of these have penetrated overlying Pennsylvanian/Permian strata to form the bedrock surface beneath Quaternary deposits on the seafloor.

(iii) Upper Mississippian (Visean) and Lower Pennsylvanian (Westphalian) cycle: continental red and grey shales, sandstones, conglomerates and volcanics of the Canso/Riversdale and equivalents. They unconformably succeed the Windsor Group, and in many localities overlap the latter to rest directly on lower Paleozoic terranes, mainly the deformed rocks of the Appalachian Orogen. Coal deposits are an important component of this cycle in the onshore regions of the Magdalen Basin and probably have widespread distribution in the offshore as well.

(iv) Middle Pennsylvanian (Westphalian) to Permian (Wolfcampian) cycle: continental red and grey sandstones, conglomerates and shales of the Cumberland and Pictou Groups. As in the preceding cycle, coal deposits are an important component in onshore regions of the basin, and drilling results indicate they also have widespread distribution offshore (Hacquebard, 1986). In the southern part of the basin the strata locally overlap older Carboniferous strata to lie directly on deformed lower Paleozoic rocks. Their distribution in the northern part of the basin has been greatly reduced by erosion along the St. Lawrence River channel, and probably subsequent glacial scouring during the Quaternary.

RESULTS

Preliminary interpretation of the grid of seismic coverage (Fig. 1) has indicated some substantial changes to existing geological maps of this region (e.g., Sanford et al., 1979).

Undoubtedly there will be further revisions when this data set is more thoroughly examined and integrated with industry multichannel seismic data and available stratigraphic information.

The Lower Paleozoic rocks of the Anticosti Basin (Fig. 2) include resistant carbonate sequences that have prominent erosional relief (Fig. 3), so that seafloor physiography in that region is an invaluable guide in mapping bedrock geology. The resistant beds frequently outcrop through the surficial deposits and afford targets for sampling with underwater electric drilling techniques.

Carboniferous strata beneath the Gulf of St. Lawrence generally show good seismic energy penetration and detailed resolution of stratification (Fig. 4 to 8). Structuring of these beds throughout much of the Gulf relates to effects of evaporite flowage or dissolution. In the St. Lawrence Estuary, and off the coasts of Newfoundland and Cape Breton Island structuring may relate primarily to regional tectonism (Fig. 6 to 8), with ancillary evaporite displacement.

Perhaps the most significant new finding of the 1989 BAFFIN cruise is the recognition that Carboniferous strata extend farther northward onto the Paleozoic terrane of the Anticosti Basin (Fig. 2) than previously mapped. Windsor and Canso-Riversdale sequences are interpreted to extend northwest into the St. Lawrence estuary, and northeastward off the west coast of Newfoundland. The mapped area of Carboniferous rocks in the Gulf of St. Lawrence is thus increased by about 30 000 square km² (Fig. 9).

An interpretation of the structure of these Carboniferous strata in the St. Lawrence Estuary is shown by cross-section in Figure 10. Reflectors immediately beneath the seafloor are drawn from a single channel seismic profile along this line. The inferred Precambrian surface is based on information from industry multichannel seismic data in this area. Dashed lines in the subsurface are interpretative projec-

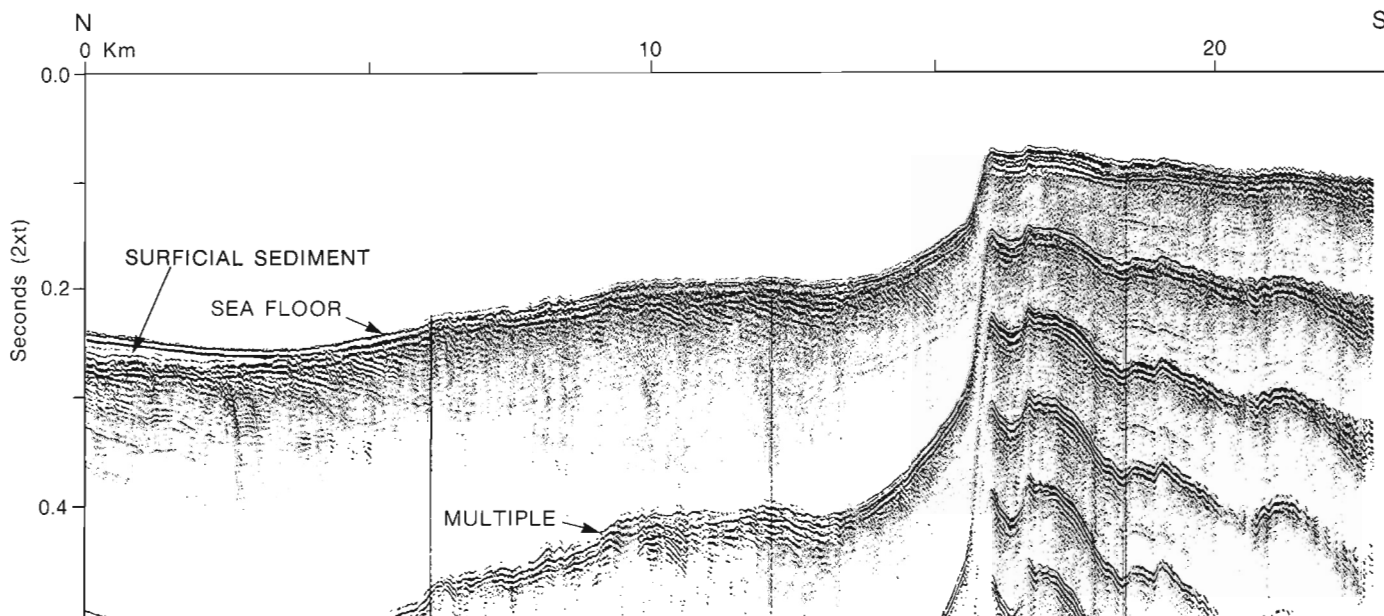


Figure 3. Seismic profile showing erosional (+ fault?) scarp in Lower Paleozoic strata. Location in Figure 1.

tions; the observed structure of the inferred Carboniferous strata is tentatively attributed to deformation of underlying evaporites. Probable faults are indicated by dashed vertical lines. Applying velocities of 4000 m/s and 5000 m/s for Carboniferous and Lower Paleozoic rocks respectively yields a depth to the base of the Carboniferous of approximately 2100 m, and 6200 m to the Precambrian surface. The superposition of these salt-structured and reservoir-rich Carboniferous sequences on potential source rocks of the Anticosti Basin may present attractive targets for hydrocarbon exploration.

ECONOMIC GEOLOGY

Anticosti Basin

Shows of oil and gas have been reported from wells drilled on Anticosti Island and western Newfoundland. Some of the best shows were reported in the Lower Ordovician Romaine Formation on Anticosti (Roliff, 1968; Petryk, 1976), and some small commercial production was obtained from the equivalent St. George Group in western Newfoundland in the early 1900s (Department of Mines and Energy, Newfoundland, 1989). An oil show was found in one of the cores recovered by C.S.S. DAWSON (Vilks et al., 1990) north of Anticosti Island (B. MacLean, pers. comm. 1989).

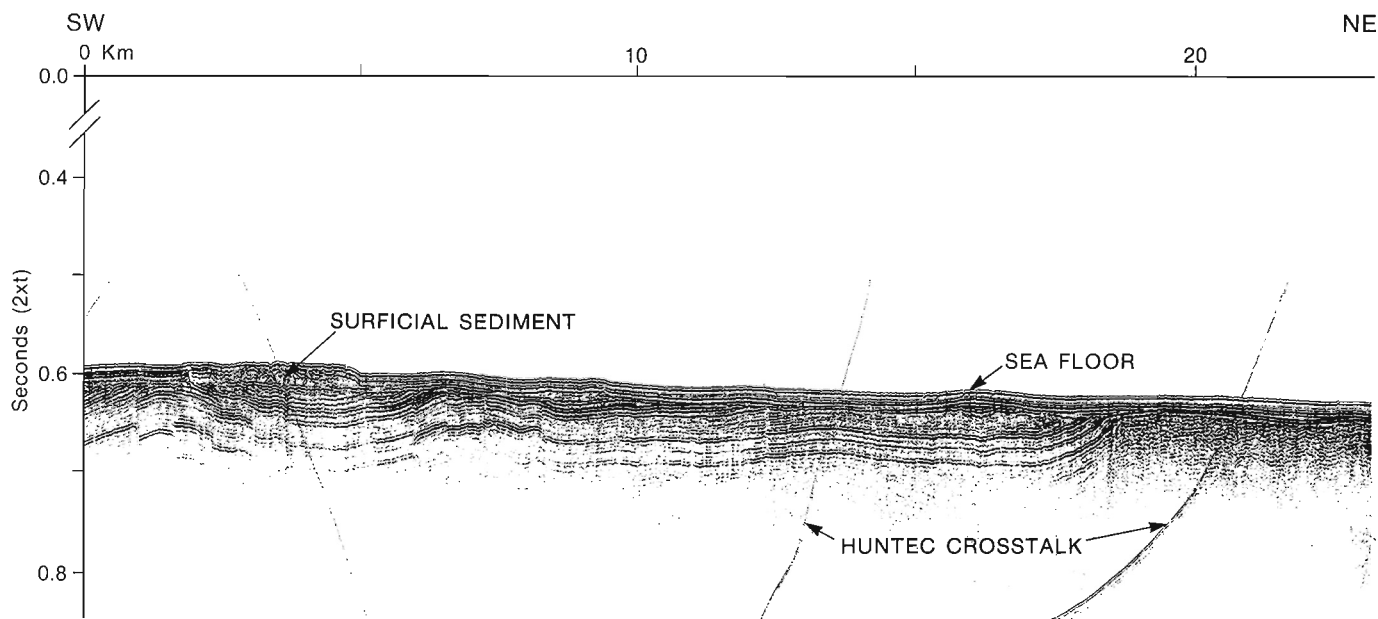


Figure 4. Seismic profile showing interpreted Carboniferous/Lower Paleozoic contact (18 km). Location in Figure 1.

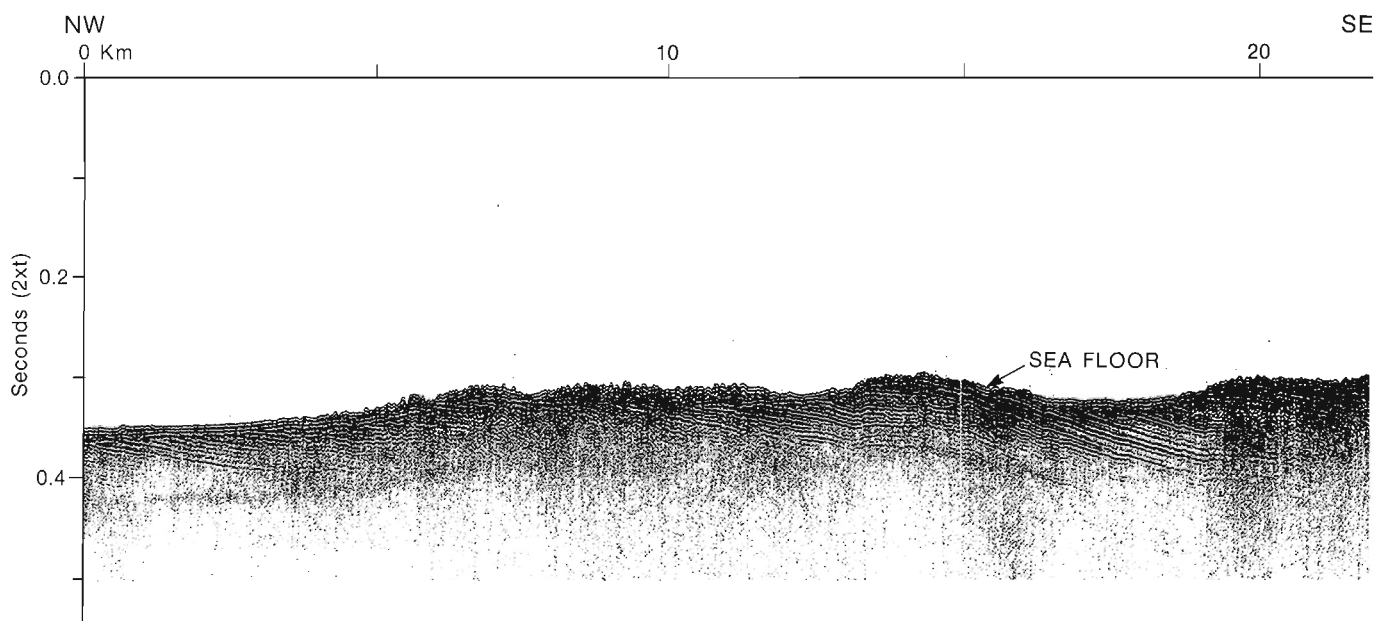


Figure 5. Seismic profile showing interpreted Carboniferous strata in northeast Gulf of St. Lawrence. Location in Figure 1.

The lower Paleozoic strata of the Anticosti Basin offer a number of possibilities for entrapment of oil and gas. Sandstones in the Lower Cambrian (Bradore/Hawke Bay) and Middle and Upper Ordovician (Long Point/Vaureal/Ellis Bay) appear to have fair to good reservoir characteristics. Shales and shaly carbonate units in the Lower Cambrian (Forteau) and Upper Ordovician (Macasty/Vaureal/Long Point) undoubtedly contain good source rocks, although this has not yet been fully assessed. Potential trap-

ping mechanisms include fault-bounded blocks associated with Taconian emplacement of allochthons and later Acadian deformation; stratigraphic traps — sandstones derived from both the craton and orogen that intertongue with shale and/or carbonate units; Ordovician and Silurian reefs that may have formed along the outer rapidly subsiding margins of the Anticosti Basin in transition zones to deeper water facies of the Appalachian geosyncline.

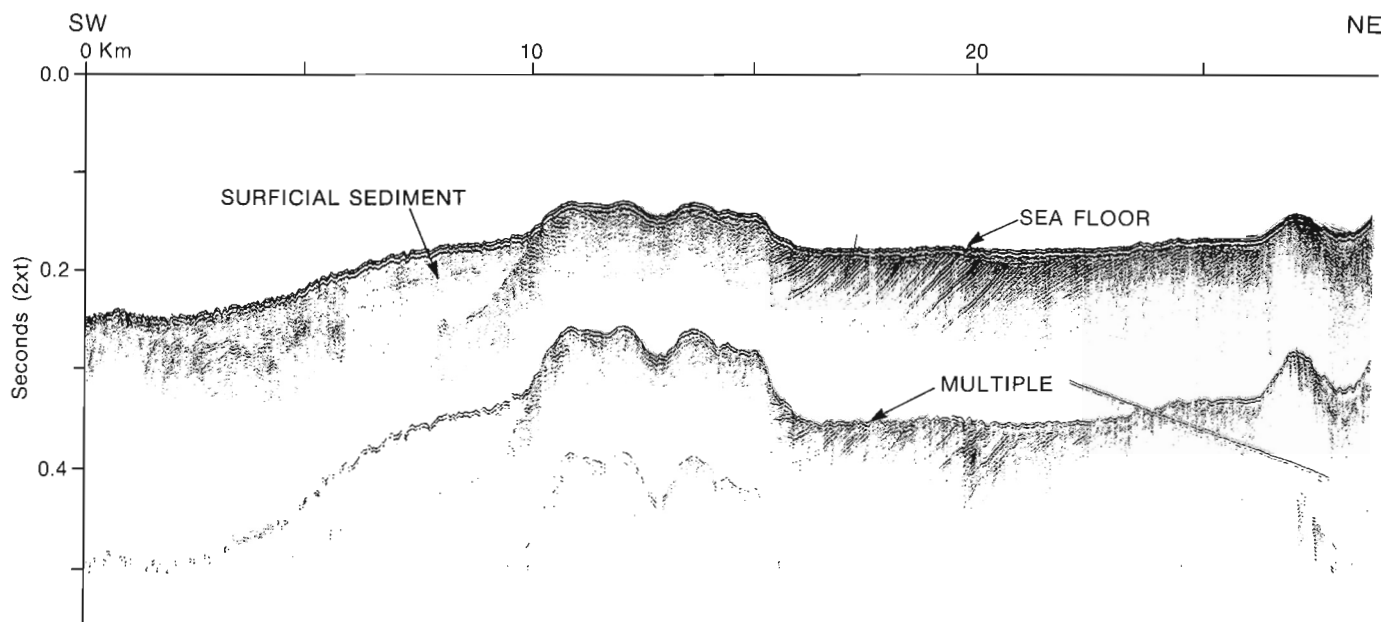


Figure 6. Seismic profile showing erosional escarpment in interpreted Carboniferous (Windsor?) strata. Location in Figure 1.

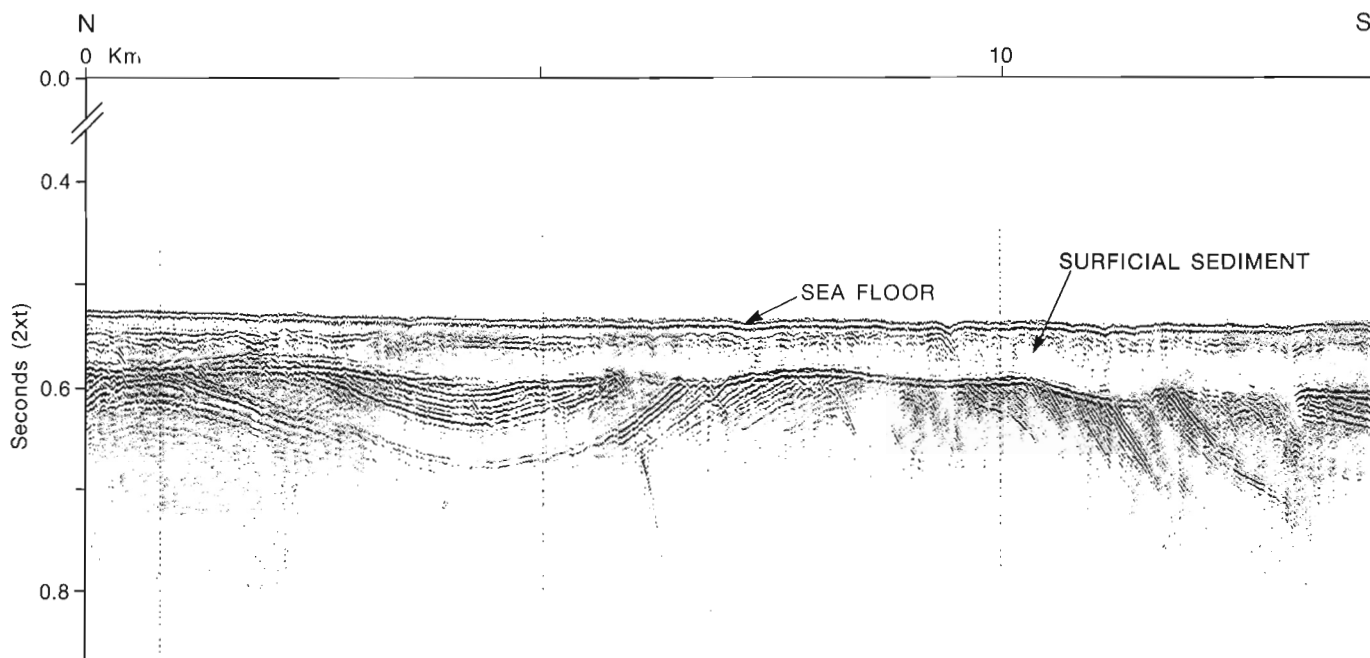


Figure 7. Seismic profile showing structure in interpreted Carboniferous strata southwest of Anticosti Island. Location in Figure 1.

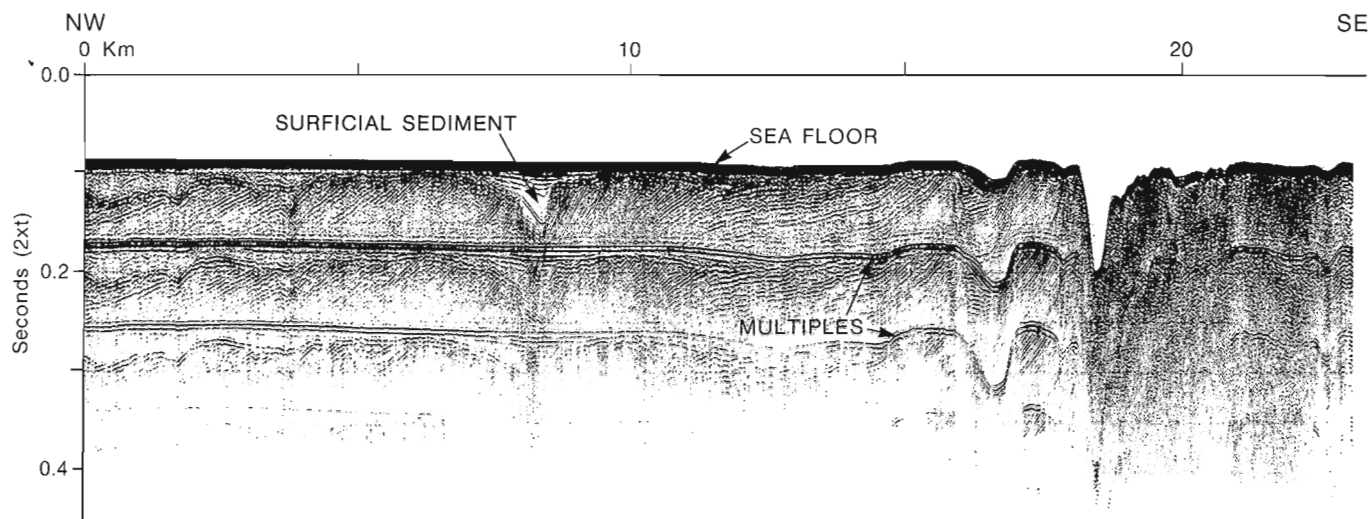


Figure 8. Seismic profile showing deformation of Carboniferous strata along west coast of Cape Breton Island. Location in Figure 1.

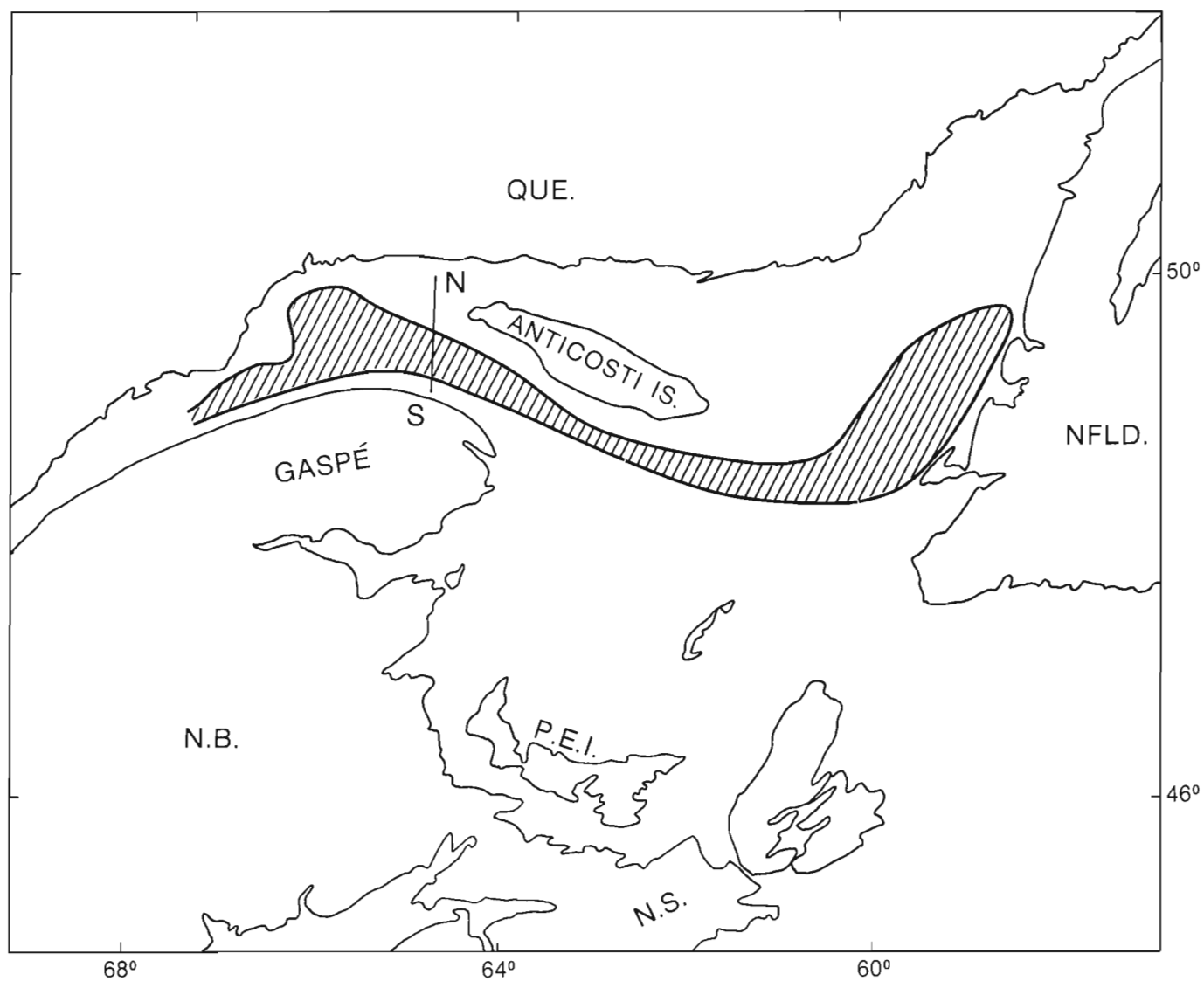


Figure 9. Cross-hatched zone indicates extent of additional Carboniferous strata tentatively identified in Gulf of St. Lawrence region. Line N-S indicates location of cross-section in Figure 10.

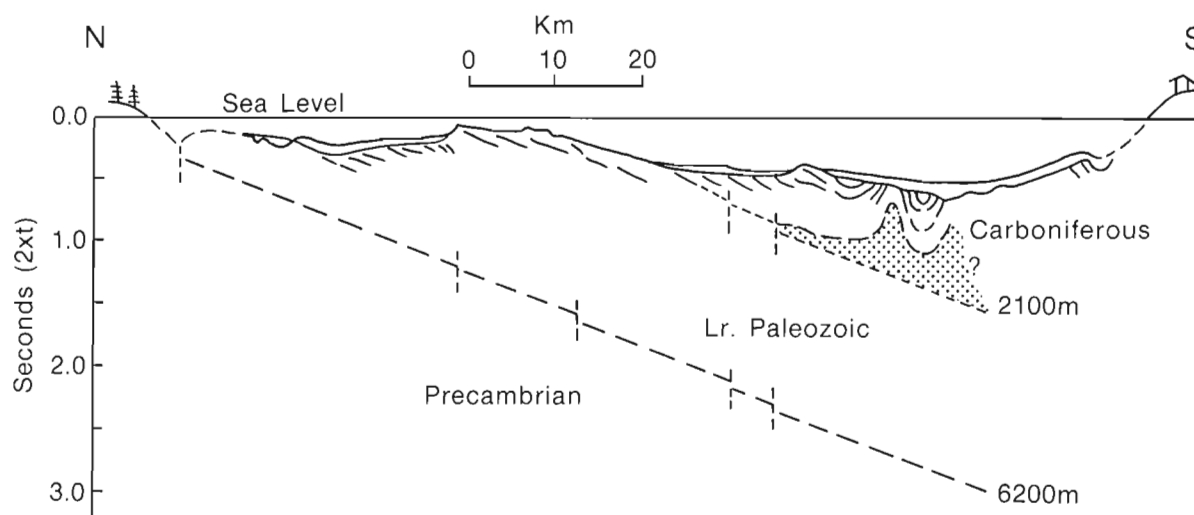


Figure 10. Interpretative cross-section compiled from single channel seismic line and multichannel seismic data. Stipple indicates inferred salt.

Magdalen Basin

Exploration for oil and gas in Carboniferous rocks of the Atlantic provinces has been sporadically carried out for more than a century, but so far only one field of commercial significance has been developed. The Stony Creek oil and gas field near Moncton, New Brunswick (Howie, 1968), is a combination structural/stratigraphic trap in sandstone reservoirs within Horton Group equivalent rocks.

Potential source and reservoir rocks undoubtedly have widespread distribution throughout the Magdalen Basin, but are sparsely tested in the offshore regions of the Gulf of St. Lawrence. The principal offshore oil and gas exploration plays relate to reservoir pinchout against halokinetic structures, and possibly also some of the more subtle structures that may have formed by simple salt dissolution and collapse. Diapiric structures are widespread throughout the Magdalen Basin, but occur in greatest numbers and complexity along the southern margins of the basin extending from western Newfoundland to northern Nova Scotia. Several of these have been drilled; the HB Fina East Point E-49 well, off Prince Edward Island, was reported as an "uneconomic" gas discovery (Hudson's Bay Oil and Gas Company Limited, 1974), but a follow-up well (HB et al., East Point E-47) was unsuccessful. Salt structures suspected north of Gaspésie in the St. Lawrence Estuary may constitute a significant exploration play that has been overlooked by the petroleum industry.

Fault-bounded structures that are abundant in the Horton Group beneath a wide segment of the southern Magdalen Basin are another important exploration play that should be further evaluated.

ACKNOWLEDGMENTS

We thank Captain J.N. Lewis and the officers, crew, and scientific staff of the C.S.S. BAFFIN for dedicated and gracious support during the 1989 cruise. We are especially

grateful to H.W. Josenhans, chief scientist, for his efficient planning and direction of this expedition. Thanks are extended to H.W. Josenhans and B. MacLean for helpful review of this manuscript.

REFERENCES

- Adams, J. and Basham, P.**
1989: The seismicity and seismotectonics of Canada east of the Cordillera; *Geoscience Canada*, v. 16, p. 3-16.
- Bolton, T.E.**
1972: *Geology of Anticosti Island*; Geological Survey of Canada, Map 2-1971.
- Cumming, L.M., Bostok, H.H., and Williams, H.**
1982: *Geology, Strait of Belle Isle area*; Geological Survey of Canada, Map 1495A (sheet 1 of 3).
- Department of Mines and Energy, Government of Newfoundland and Labrador.**
1989: *Hydrocarbon potential of the western Newfoundland Area*; Department of Mines and Energy, Government of Newfoundland and Labrador, 20 p.
- Hacquebard, P.A.**
1986: *The Gulf of St. Lawrence Carboniferous Basin; the largest coalfield of eastern Canada*; Canadian Institute of Mining and Metallurgy, *Bulletin*, v. 79, p. 67-78.
- Haworth, R.T. and Sanford, B.V.**
1976: *Paleozoic geology of northeast Gulf of St. Lawrence*; in *Report of Activities, Part A*, Geological Survey of Canada, Paper 76-1A, p. 1-6.
- Hibbard, J.**
1983: *Geology of the Island of Newfoundland (preliminary version)*, Department of Mines and Energy, Government of Newfoundland and Labrador, Map 83-06.
- Howie, R.D.**
1968: *The Stony Creek oil and gas field, New Brunswick*; in *Natural Gases of North America*; American Association of Petroleum Geologists, *Memoir* 9, v. 2, p. 1819-1832.
1988: *Upper Paleozoic evaporites of southeastern Canada*; Geological Survey of Canada, *Bulletin* 380, 120 p.
- Hudson's Bay Oil and Gas Company Limited.**
1974: *Well history report, HB Fina East Point E-49*.
- Josenhans, H., Zevenhuizen, J., and MacLean, B.**
1990: *Preliminary seismostratigraphic interpretations from the Gulf of St. Lawrence*; in *Current Research, Part B*, Geological Survey of Canada, Paper 90-1B.

- Keppie, J.D.**
1979: Geological map of the Province of Nova Scotia; Nova Scotia Department of Mines and Energy.
- Kranck, K.**
1971: Surficial geology of Northumberland Strait; Marine Science Paper 5, Geological Survey of Canada, Paper 71-53, 10 p.
- Loring, D.H.**
1975: Surficial geology of the Gulf of St. Lawrence; *in* Offshore Geology of Eastern Canada, ed. W.J.M. van DerLinden and J.A. Wade; Geological Survey of Canada, Paper 74-30, p. 11-34.
- McGerrigle, H.W.**
1953: Geological map of Gaspé Peninsula; Department of Mines, Province of Quebec, Map no. 100.
- Petryk, A.A.**
1976: Geology and oil and gas exploration of Anticosti Island, Gulf of St. Lawrence, Quebec; preliminary reconnaissance; Quebec Department of Natural Resources, Preliminary Report No. 1, 25 p.
- Poole, W.H.**
1967: Tectonic evolution of Appalachian region of Canada; Geological Association of Canada, Special Paper no. 4, Geology of the Atlantic Region, p. 9-51.
- Poole, W.H., Sanford, B.V., Williams, H. and Kelley, D.G.**
1970: Geology of southeastern Canada; *in* Geology and Economic Minerals of Canada, ed. R.J. Douglas; Geological Survey of Canada, Economic Geology Report No. 1, p. 229-304.
- Potter, R.R., Jackson, E.V. and Davies, J.L.**
1968: Geological map of New Brunswick; New Brunswick Department of Mines, Map no. N.R.-1.
- Roliff, W.A.**
1968: Oil and gas exploration — Anticosti Island, Quebec; Geological Association of Canada, Proceedings, v. 19, p. 31-36.
- Sanford, B.V., Grant, A.C., Wade, J.A. and Barss, M.S.**
1979: Geology of Eastern Canada and adjacent areas; Geological Survey of Canada, Map 1401A (4 sheets, scale 1:2 000 000).
- Sanford, B.V., Thompson, F.J. and McFall, G.H.**
1985: Plate tectonics — a possible controlling mechanism in the development of hydrocarbon traps in southwestern Ontario; Bulletin of Canadian Petroleum Geology, v. 33, p. 52-71.
- Shearer, J.M.**
1973: Bedrock and surficial geology of the northern Gulf of St. Lawrence as interpreted from continuous seismic reflection profiles, *in* Earth Science Symposium on Offshore Eastern Canada, ed. P.J. Hood; Geological Survey of Canada, Paper 71-23, p. 285-303.
- Skidmore, W.B.**
1967: Geological map of Gaspé; Quebec Department of Natural Resources, Map no. 1642.
- Syvitski, J.P.M. and Praeg, D.B.**
1989a: Quaternary sedimentation in the St. Lawrence Estuary and adjoining areas, Eastern Canada: an overview based on high-resolution seismo-stratigraphy; *Geographie physique et Quaternaire*, v. 43.
1989b: Quaternary seismo-stratigraphy of the lower St. Lawrence Estuary; Geological Survey of Canada, Open File (10 sheets).
- Syvitski, J.P.M., Beattie, D.D., Praeg, D.B. and Schafer, C.T.**
1987: Marine geology of Baie des Chaleurs; Geological Survey of Canada, Open File 1375 (5 sheets).
- Vilks, G., MacLean, B. and Rodrigues, C.**
1990: Late Quaternary high resolution seismic and foraminiferal stratigraphy in the Gulf of St. Lawrence; *in* Current Research, Part B, Geological Survey of Canada, Paper 90-1B.
- Wade, J.A., Grant, A.C., Sanford, B.V. and Barss, M.S.**
1977: Basement structure of eastern Canada and adjacent areas; Geological Survey of Canada, Map 1400A (4 sheets, 1:2 000 000).

Seabed disturbance by a recent (1989) iceberg grounding on the Grand Banks of Newfoundland

D.R. Parrott, C.F.M. Lewis, E. Banke¹, G.B.J. Fader,
and G.V. Sonnichsen
Atlantic Geoscience Centre, Dartmouth

Parrott, D.R., Lewis, C.F.M., Banke, E., Fader, G.B.J., and Sonnichsen, G.V., Seabed disturbance by a recent (1989) iceberg grounding on the Grand Banks of Newfoundland, in Current Research, Part B, Geological Survey of Canada, Paper 90-1B, p. 43-48, 1990.

Abstract

Up to 4000 icebergs are calved annually from glaciers in Greenland and eastern Arctic Canada. Each year some of these drift southward to the Grand Banks of Newfoundland. A portion of this flux contacts the seafloor resulting in scouring of seafloor sediments. To provide a case history of this process a recent iceberg grounding which resulted in the formation of a linear scour and a large pit has been documented on the eastern Grand Banks following an oil-industry iceberg monitoring program in 1989.

A sidescan sonar and high resolution seismic reflection survey was conducted at the site of the grounding on northeastern Grand Bank. A fresh iceberg scour, varying from 20-30 m in width and less than 1 m in depth was traced for about 14 km. The scour terminated in a pit 5 m deep and 90 m wide, with a berm up to 3 m above the original seafloor.

Résumé

Jusqu'à 4 000 icebergs sont formés chaque année par les glaciers du Groenland et dans l'est de l'Arctique canadien. Chaque année certains d'entre eux dérivent vers le sud jusqu'aux Grands Bancs de Terre-Neuve. Parfois, ils raclent le fond marin et y inscrivent des cicatrices dans les sédiments. Afin d'établir un cas type de ce processus, l'échouage récent sur la partie est des Grands Bancs d'un iceberg qui a produit une cicatrice d'affouillement linéaire et creusé un grand trou, a été étudié (en 1989) dans le cadre d'un programme de surveillance des icebergs de l'industrie pétrolière.

Un levé combiné au sonar à balayage latéral et de sismique réflexion à haute résolution a été exécuté à l'emplacement de l'échouage, sur la partie nord-est du Grand-Banc. Une cicatrice d'affouillement fraîche faite par un iceberg, d'une largeur allant de 20 m à 30 m et de moins d'un mètre de profondeur, a été suivie sur environ 14 km. La cicatrice se termine par un trou de 5 m de profondeur et de 90 m de large dont le rebord s'élève 3 m au-dessus du fond marin original.

¹ Erik Banke Consulting, P.O. Box 32, Bedford, Nova Scotia, B4A 2X1

INTRODUCTION

Iceberg keels which scour the seabed of the Grand Banks of Newfoundland raise questions regarding the burial depth of potential oil and gas seabed facilities such as wellheads and pipelines (Lewis et al., 1988). These icebergs produce long linear scours as well as circular depressions termed iceberg pits. The pits have been documented in numerous site specific and regional geophysical surveys on the Grand Banks of Newfoundland (Amos and Barrie, 1980; Fader and King, 1981; Lewis and Barrie, 1981; Fader et al, 1985; Barrie et al., 1986). Typically, the pits are larger (by up to a factor of seven) than the iceberg scours found in the area and have widths in the range of 30 to 350 m and depths of 0.5 to 10 m (Mobil, 1985; Barrie et al., 1986). The process by which icebergs form scours and pits as well as the

processes controlling their persistence on the seafloor need to be better understood.

To provide information on the processes of initial seabed disturbance and the subsequent degradation of iceberg scours and pits under different environments and geological conditions, a series of case histories of recent scouring events is being assembled with the assistance of the offshore oil and gas industry. Early in 1989, observations associated with drilling activities at the Texaco Springdale M-29 well site documented a large (1.3 million tonnes) iceberg which drifted southward from loose pack ice into a grounded position in 110 m water depth. The iceberg remained grounded for 45 days, drifting free on 24 April, 1989 (J. Spaapen, pers. comm., 1989). This grounding provided a unique opportunity to study a scour and grounding pit produced by

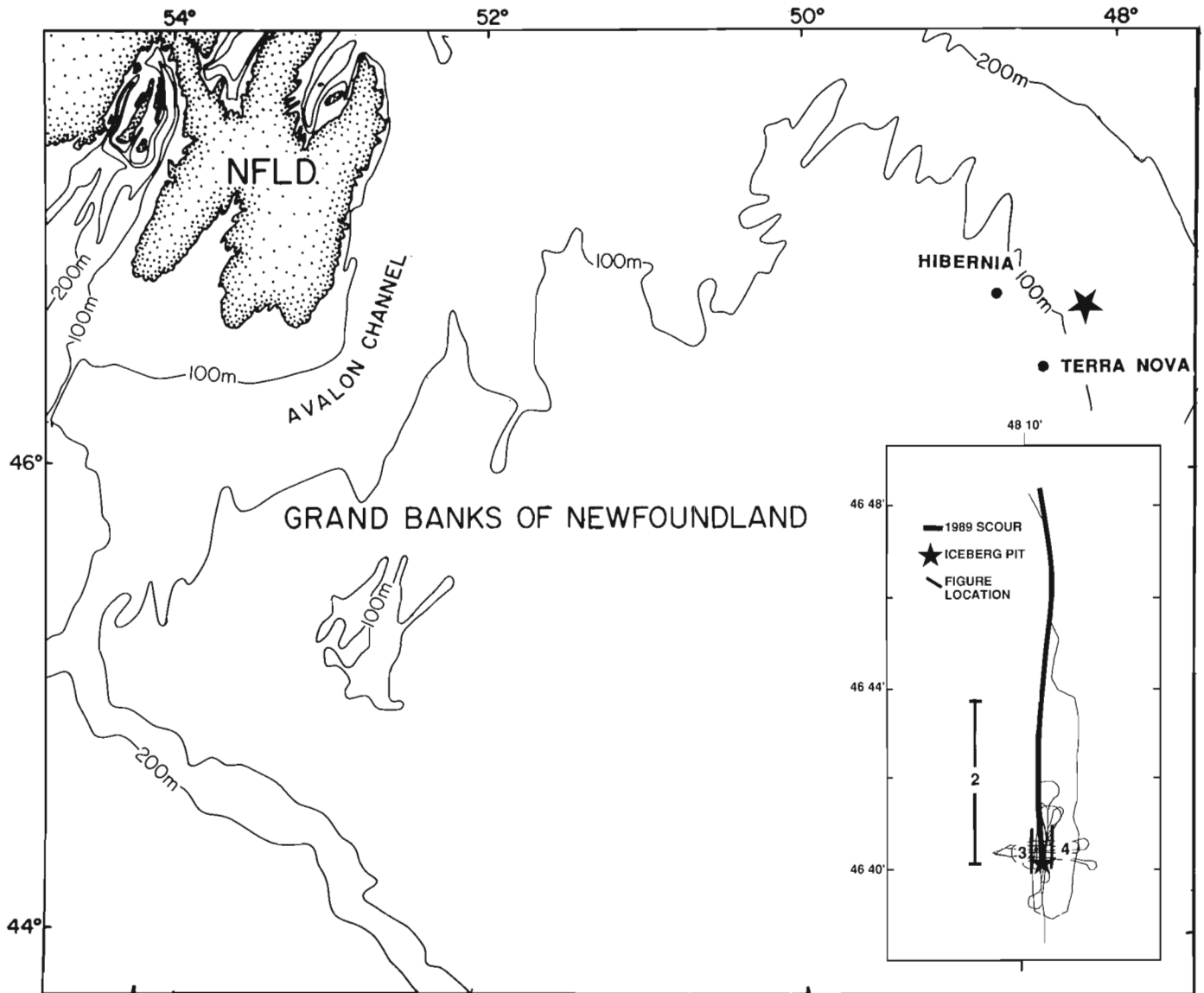


Figure 1. Location map showing the Grand Banks of Newfoundland and the iceberg grounding site. Inset shows the ship's track and the mapped fresh iceberg scour.

a well-documented iceberg. A geophysical survey to collect sidescan sonar, seismic reflection and echo sounder data was conducted on 9 May, 1989 by the Atlantic Geoscience Centre (Fader, 1989) along part of the recorded trajectory of the iceberg to determine the nature of seafloor disruption at the grounding site. In this note, we present preliminary results of the seabed survey.

SURVEY TECHNIQUE

The primary tool used for the field investigations was the Bedford Institute of Oceanography (BIO) 70 kHz sidescan sonar (Jollimore, 1974). This sidescan, with a nominal swath of 1500 m (1-s firing rate) was towed at 9-11 km/hr. The sidescan sonar data were displayed on a conventional 2-channel, 45.7-cm wet paper recorder. This display results in an aspect ratio of about 1:2 for the paper rates and ship's speeds used (Fig. 2 and 3). An additional EPC Labs model 4800 three channel graphic recorder also presented the two channels of sidescan sonar data in a scale-corrected (but not slant-range corrected) format. This unit provided microprocessor control of both paper advance rate and swath display width so that data can be presented at a scale of 1:15 000 with an aspect ratio of 1:1 for subsequent analysis of seabed features.

A Klein 100 kHz sidescan sonar with an altimeter, operated at 0.15 s sweep (105 m range each side), provided higher resolution sidescan sonar images and details on the depth of the scour and pit and sediment texture. The Klein sidescan sonar data were displayed on a 3-channel, 45.7-cm wet paper recorder (Fig. 4). This display results in an aspect ratio of about 1.5:1 for the paper rates and ship's speeds used.

In addition, high-resolution seismic reflection and echo sounder data were collected to provide information on the depths and morphology of the iceberg scours and the subsurface geology. Navigation for the survey was provided by LORAN-C and Transit satellite.

RESULTS

The geophysical survey was successful in locating and following the scour associated with the iceberg grounding. The survey began about 14 km north of the grounding site (Fig. 1). A fresh iceberg scour (20-30 m wide and less than 1 m deep) was located which followed the recorded trajectory of the iceberg for at least 14 km, where it terminated in a large pit (Fig. 1 and 2). The scour was longer than 14 km as its starting point lay beyond the survey area. The iceberg pit is estimated to be 90 m wide, with a depth of 5 m below the original seafloor, and a berm rising 1 to 3 m above the seafloor. This yields a maximum relief of 8 m from the crest of the berm to the base of the pit.

A smaller pit-like feature can be seen about 75 m north-east of the deep pit in Figures 3 and 4. This feature appears to be about 30-40 m wide and consists of a central circular area and two smaller elongated features which are connected to the centre.

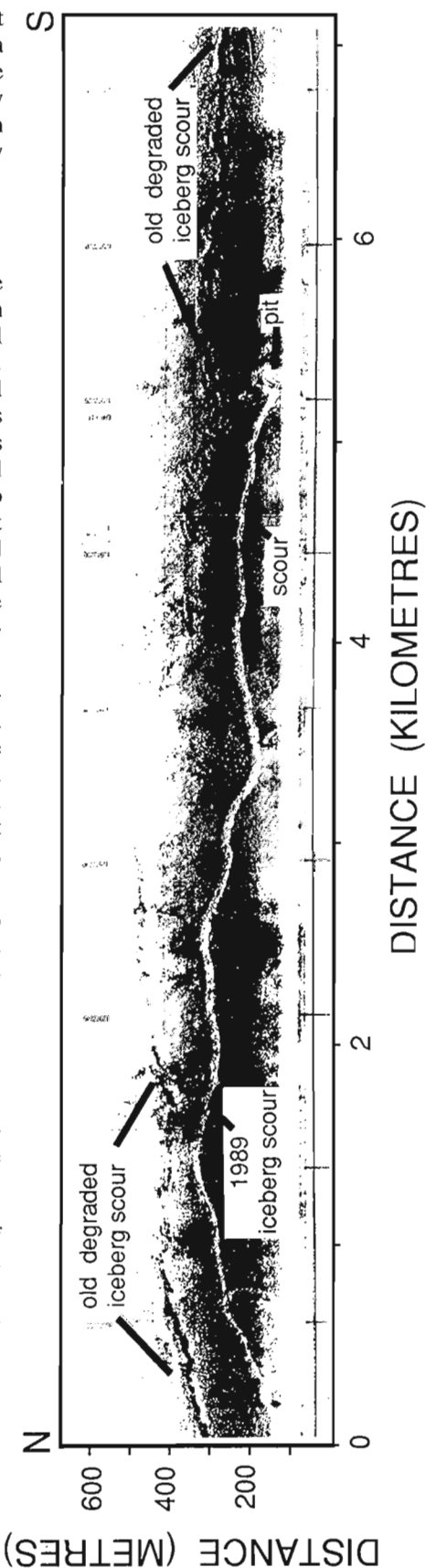


Figure 2. Sidescan sonar record (uncorrected) showing the scour and pit created in March 1989. The pit is much wider than the scour. Also, note the older scour (exact age unknown) located to the east.

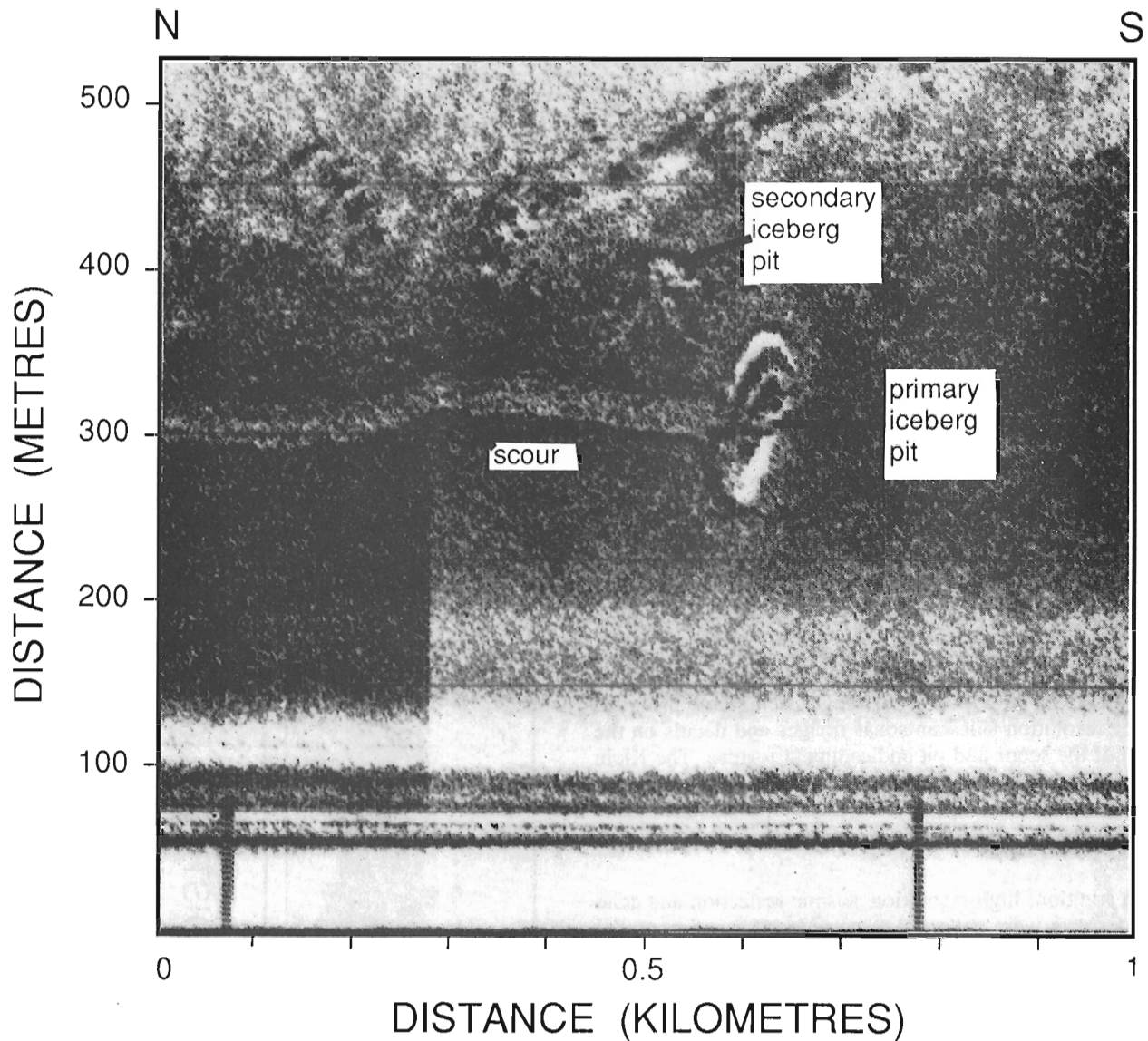


Figure 3. Sidescan sonar image produced with the Bedford Institute of Oceanography medium range sidescan sonar system of the scour and pit. The small feature directly southeast of the deep pit may have formed when the iceberg was rolling free of the pit. Note that the berm completely surrounds the pit.

The Klein 100 kHz sidescan sonar system showed increased detail of the nature of the scour and the pit (Fig. 4). The interior of the scour consists of linear ridges parallel to the track of the iceberg, and the terminal pit is clearly 4-5 times as wide as the scour. The interior of the pit shows a complex structure with internal ridges (seen on the sidescan sonar records as highly reflective dark-toned zones) parallel to the exterior berm. The berm completely surrounds the pit and has been built across the scour leading into the pit. A large (0.3 m³) grab sample near the site of the iceberg pit showed the undisturbed seafloor to consist of a thin (less than 30 cm) layer of medium grained, well sorted sand over a subsurface layer of grey silty sand to sandy silt.

Another scour, of unknown age, lies 100-200 m east of the fresh scour and can be traced for over 16 km. A portion of this scour can be seen on the sidescan sonar record shown in Figure 2. The trajectory and shape of this scour are quite prominent although the detailed morphology of the scour appears much less distinct and well defined than that of the fresh (1989) iceberg scour.

DISCUSSION

This study has provided an unique opportunity to obtain geophysical data on a fresh iceberg scour and pit. The sidescan sonar data has shown lineations within the scour paral-

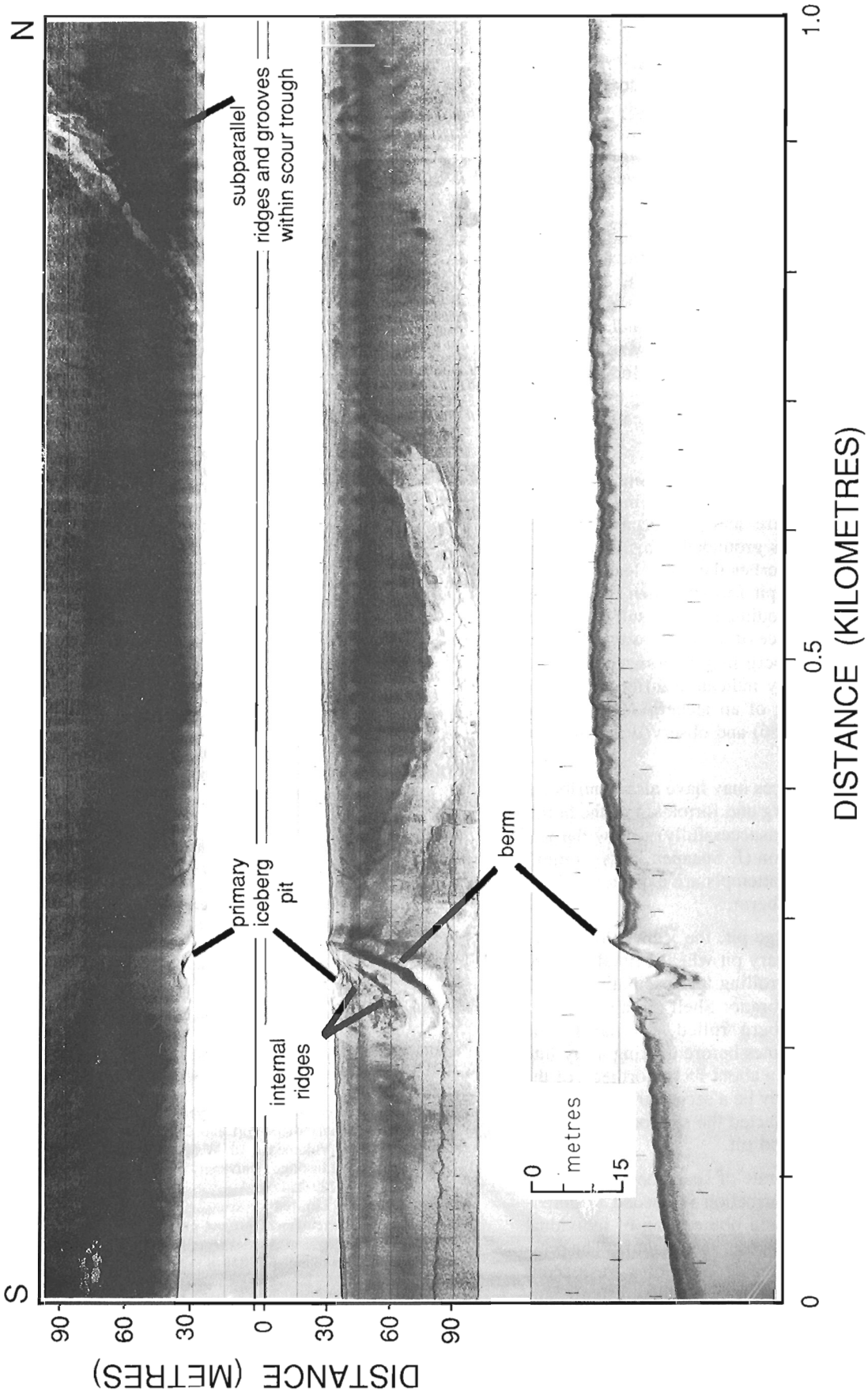


Figure 4. High resolution sidescan sonar and altimeter record of the scour and pit. These records are not corrected for slant range or fish motion so that some distortion exists on the records. The apparent change in the water depth on the altimeter record was caused by a slow change in the height of the tow fish due to changes in the ship's speed. Echo soundings show the undisturbed seafloor to be flat.

lel to the scour berms. This suggests that the bottom of the iceberg keel was irregular and that these irregularities shaped the seafloor sediment into subparallel ridges and grooves as it scoured in a manner similar to conditions reported by Hodgson et al. (1989) on the Labrador shelf. Since the lineations remain parallel to the berm, the iceberg appears to have remained stable with very little rotation about its vertical axis as it dragged its keel along the seafloor.

Barrie et al. (1986) described a relict iceberg pit on Grand Bank and suggested that the pit was formed when the centre of gravity of an iceberg changed due to calving or splitting. This would have resulted in the iceberg rolling to a new stable position, increasing its draught and impacting the seafloor. The sediment below the seafloor was suggested to have failed by a bearing capacity failure. Hodgson et al. (1989) also described a splitting and grounding event on the Labrador shelf which was interpreted to have caused a large pit as a result of a bearing capacity failure.

The pit produced at the 1989 grounding site is substantially wider and deeper than the scour leading to the pit indicating considerable failure and displacement of the seabed while the iceberg was grounded. This is also suggested by the berm which overlies the scour leading to the pit. It is suggested that the pit formed when the iceberg grounded and reworked the sediment as a result of the iceberg wallowing under influence of the wind, wave and tidal forces. Wallowing of an iceberg may be a mechanism for producing a deep pit and may indicate a different process than the splitting and rolling of an iceberg suggested for Bowers Pit (Barrie et al., 1986) and observed in Labrador (Hodgson et al., 1989).

In this case additional forces may have also contributed to the wallowing of the iceberg and formation of the berm, when attempts were made (unsuccessfully) to tow the iceberg from its grounded position (J. Spaapen, pers. comm., 1988). However, the towing attempts are expected to have had a minimal effect on the berm.

After formation of the large pit, the iceberg may have also created a smaller secondary pit when it finally drifted clear of the seabed. Iceberg rolling and oscillating events have been documented on Labrador Shelf (Hodgson et al., 1989). In that case an iceberg rolled, oscillated, and impacted the seafloor three times before drifting away into deeper water. The feature seen about 75 m northeast of the deep pit in Figures 3 and 4 may be a secondary feature that formed when the iceberg contacted the seafloor as it rolled free of its large berm-enclosed pit.

At present the nature and rate of scour degradation are poorly known, yet much information is needed to understand the rates of formation and obliteration of individual scours within the population of observable scours. The present study provides baseline measurement of a fresh scour and pit which may be compared to the results of future surveys to study scour degradation.

ACKNOWLEDGMENTS

We thank the Captain and staff of the CSS DAWSON and the Program Support Subdivision of the Atlantic Geoscience Centre for their assistance in acquiring, processing and archiving data for this study. We also thank J. Spaapen of Texaco Canada Resources Ltd. and T.J. Murphy of Husky Oil for advising us of the iceberg grounding. Colleagues H.W. Josenhans and J.V. Barrie made helpful comments on the manuscript. This is a contribution of the Offshore Geotechnics Program 63201 and 63202 of the federal Panel on Energy Research and Development.

REFERENCES

- Amos, C.L. and Barrie, J.V.**
1980: Hibernia and Ben Nevis seabed study - POLARIS V cruise report, June 1980; C-CORE Data Report 80-17, 40 p.
- Barrie, J.V., Collins, W.T., Clark, J.I., Lewis, C.F.M. and Parrott, D.R.**
1986: Submersible observations and origin of an iceberg pit on the Grand Banks of Newfoundland; *in* Current Research, Part A, Geological Survey of Canada, Paper 86-1A, p. 251-258.
- Fader, G.B.J.**
1989: Cruise Report Dawson 89-006; Geological Survey of Canada, Internal Report.
- Fader, G.B. and King, L.H.**
1981: A reconnaissance of the surficial geology of Grand Banks of Newfoundland; *in* Current Research, Part A, Geological Survey of Canada, Paper 81-1A, p. 45-56.
- Fader, G.B., Lewis, C.F.M., Barrie, J.V., Parrott, D.R., Collins, W., Miller, R.O. and d'Apollonia, S.J.**
1985: Quaternary Geology of the Hibernia area of northeast Grand Bank, Map 14968QC; Geological Survey of Canada, Open File 1222.
- Hodgson, G.J., Lever, J.H., Woodworth-Lynas, C.M.T. and Lewis, C.F.M.**
1989: The dynamics of iceberg grounding and scouring (DIGS) experiment and the repetitive mapping of the eastern Canadian continental shelf; Environmental Studies Research Funds, Report No. 094, Ottawa, 315 p.
- Jollimore, P.G.**
1974: A medium range sidescan sonar for use in coastal waters; design criterion and operational experiences; *in* Oceans '74, Proceedings of the Institute of Electrical and Electronics Engineers, International Conference on Engineering in the Ocean Environment, Halifax, Nova Scotia, p. 108-114.
- Lewis, C.F.M. and Barrie, J.V.**
1981: Geological evidence of iceberg groundings and related seafloor processes in the Hibernia discovery area of the Grand Bank, Newfoundland; *in* Proceedings of the Symposium on Production and Transportation Systems for the Hibernia Discovery, ed. W.E. Russell and D.B. Muggerridge; Newfoundland and Labrador Petroleum Directorate, St. John's, Newfoundland, p. 146-147.
- Lewis, C.F.M., Parrott, D.R., d'Apollonia, S.J., Gaskill, H.S. and Barrie, J.V.**
1988: Methods of estimating iceberg scouring rates on the Grand Banks of Newfoundland; *in* Port and Ocean Engineering under Arctic Conditions, Volume III, ed. W.M. Sackinger and M.O. Jefferies, Geophysical Institute, University of Alaska Fairbanks, Fairbanks, Alaska, p. 229-254.
- Mobil Oil Canada Limited**
1985: Hibernia development project environmental impact statement; v. IIIa Biophysical Assessment; Mobil Oil Canada Limited, St. John's, Newfoundland, 258 p.

Late Quaternary high resolution seismic and foraminiferal stratigraphy in the Gulf of St. Lawrence

G. Vilks, B. MacLean and C. Rodrigues¹
Atlantic Geoscience Centre, Dartmouth

Vilks, G., MacLean, B., and Rodrigues, C., Late Quaternary high resolution seismic and foraminiferal stratigraphy in the Gulf of St. Lawrence, in Current Research, Part B, Geological Survey of Canada, Paper 90-1B, p. 49-58, 1990.

Abstract

Glacial to post glacial marine environments are described in the Gulf of St. Lawrence on the basis of 1300 km of high resolution seismic profiles and foraminiferal assemblages from eight piston cores. Salinity was highest in the lower and upper parts of the marine sequence. The high salinity intervals are related to the presence of Atlantic water. The lower salinity interval in the middle of the marine sequence may be related to a meltwater discharge.

Résumé

Les auteurs décrivent dans le présent article des milieux marins glaciaires et post-glaciaires se trouvant dans le golfe du Saint-Laurent à partir de 1300 km de profils sismiques à haute résolution et d'assemblages de foraminifères provenant de huit carottes prélevées par carottier à piston. La salinité était plus élevée dans les sections inférieures et supérieures de la série marine. Les intervalles à forte salinité sont liés à la présence de l'eau de l'Atlantique. L'intervalle de faible salinité, situé au milieu de la série marine, peut être lié à un débit d'eau de fonte.

¹ Department of Geology, University of Windsor, Windsor, Ontario N9B 3P4

INTRODUCTION

The Younger Dryas, a short period (11 – 10 ka BP) of climate deterioration in Europe and North American maritime areas, has been related to the switching of glacial meltwater drainage from Gulf of Mexico to Gulf of St. Lawrence (Johnson and McClure, 1976; Broecker, et al., 1988). The paleoclimatic model calls for sufficient dilution of the surface waters of the North Atlantic to disrupt the flow of warm water to the northeast Atlantic and thus the transfer of heat to Europe. Evidence for the presence of large volumes of meltwater in Gulf of St. Lawrence during that period has not been documented to a sufficient accuracy to provide constraints to the meltwater - climate model. This paper discusses preliminary results of high resolution seismic and piston core analysis in the Gulf of St. Lawrence. The study shows that during deglaciation there were several intervals of relatively fresh bottom waters, and one of these could be linked to the Younger Dryas event.

Previous work

Major sedimentological processes and depositional history of the Gulf of St. Lawrence were described by Loring and Nota (1973) and Loring (1975) who recognized the presence of glacial tills, glaciomarine, glaciolacustrine and postglacial marine sediments. Initial glacial deposition was followed by sediment reworking, and accumulating of mud in the large troughs that characterize the seafloor of the Gulf of St. Lawrence. Syvitski and Praeg (1989) recognized five seismostratigraphic units related to the advance and retreat of the Laurentide Ice Sheet in the St. Lawrence Estuary and Chaleur Bay. The units represent ice — contact sediments, ice proximal and distal glaciomarine sediments, as well as paraglacial deltaic and post glacial sediments.

Bartlett and Molinsky (1972) examined 9 cores in the Gulf of St. Lawrence and reported alternating marine and nonmarine faunas downcore. The presence of the subtropical *Globigerinoides ruber* and *Globorotalia menardii* in one of the cores in the Laurentian Channel was interpreted as indicating an early postglacial incursion of subtropical offshore waters. Rodrigues and Hooper (1982) recognized 179 benthic species of foraminifera in surface sediments between water depths of 55 and 528 m. They related eight foraminiferal associations and 5 taxa groups to three major water masses at different water depths: the upper layer, the transitional and the deep water. This is baseline information for the interpretation of foraminifera in cores collected during Cruise 89007.

Materials and methods

During May and June, 1989, Quaternary sediments and bedrock geology were investigated in Gulf of St. Lawrence from CSS BAFFIN, Cruise 89008 and CSS DAWSON, Cruise 89007. (see Josenhans, et al., 1990, and Sandford and Grant, 1990 for preliminary results of regional surficial and bedrock surveys, respectively). During Phase I, DAWSON Cruise 89007, 11 piston cores and 1340 km of high resolution Huntec and airgun survey lines were collected in Esquiman, Anticosti and parts of Laurentian Channel (Fig. 1) (Vilks and Rodrigues, 1989). Cores were

collected using a Benthos 800 kg piston corer with a 6.7 cm plastic liner, and a 9.14 m core barrel. Average penetration, estimated from visible mud on the core barrel, was 8.33 m, and the average core recovery was 6.28 m. Thus, average core recovery was 2 m less than core penetration. The discrepancy is important when comparing the relationship between measured parameters in the cores, such as lithologies and faunal boundaries, with the depth of seismostratigraphic boundaries. The comparison of trigger weight and piston core top data, e.g. foraminifera and lithology, suggests the loss of material from the piston core tops could be in the order of 0.25 – 0.5 m. Thus loss of material takes place downcore, and compression of the more liquid surface muds during the coring process is a possibility.

PRELIMINARY RESULTS

Lithologies and colour of sediment cores

Major sediment units are described from core logs and X-radiographs (Fig. 2, 3). Cores from Anticosti and Esquiman channels contain an upper layer of dark brown mud overlying a pebbly sandy mud. In most cores the lower unit appears about half way down the core (Fig. 2), except for Esquiman Channel core 36, where it is close to the bottom. In Esquiman Channel core 26, dark red and dark brown mud interchange throughout the core, with brown pebbly sediments at the bottom.

The major lithologies in cores from the Laurentian Channel vary irregularly downcore (e.g., Core 092, Fig. 3) Zones of mud and pebbly sandy mud interchange throughout the cores beneath the surface layer of mud. In core 092 the olive grey surface muds grade to reddish brown sediments with occasional red (2.5YR 4/3) zones. Sediments in core 006, at the junction of Laurentian and Esquiman channels, contain progressively more pebbles towards the bottom of the core. The top of the core is dark grey and changes to red (10R 4/2) at about 1.5 m downcore. The change coincides with the top of foraminiferal interval C defined later in the text. In core 106, farther south in the Cabot Strait area, the surface mud is greyish brown, changing to brown or reddish brown downcore coincident with the appearance of the coarser sediments. A number of red (2.5YR 4/3) layers are present.

Seismostratigraphy

The acoustic units recognized in the study area are in general similar to acoustic units recognized by Syvitski and Praeg (1989) and we retain their unit designations and regional interpretation. Their unit IV, designating deltaic deposits, is not present at the localities described in this report.

Four seismic units are recognized: unit I is a basal acoustically unstratified and unstructured sequence interpreted as ice contact sediment (glacial drift). Unit II represents acoustically strongly stratified sediments interpreted to be glaciomarine, tentatively ice proximal. Unit III is acoustically moderately stratified and tentatively represents ice distal glaciomarine sediments. The uppermost unit V consists of acoustically transparent postglacial sediments.

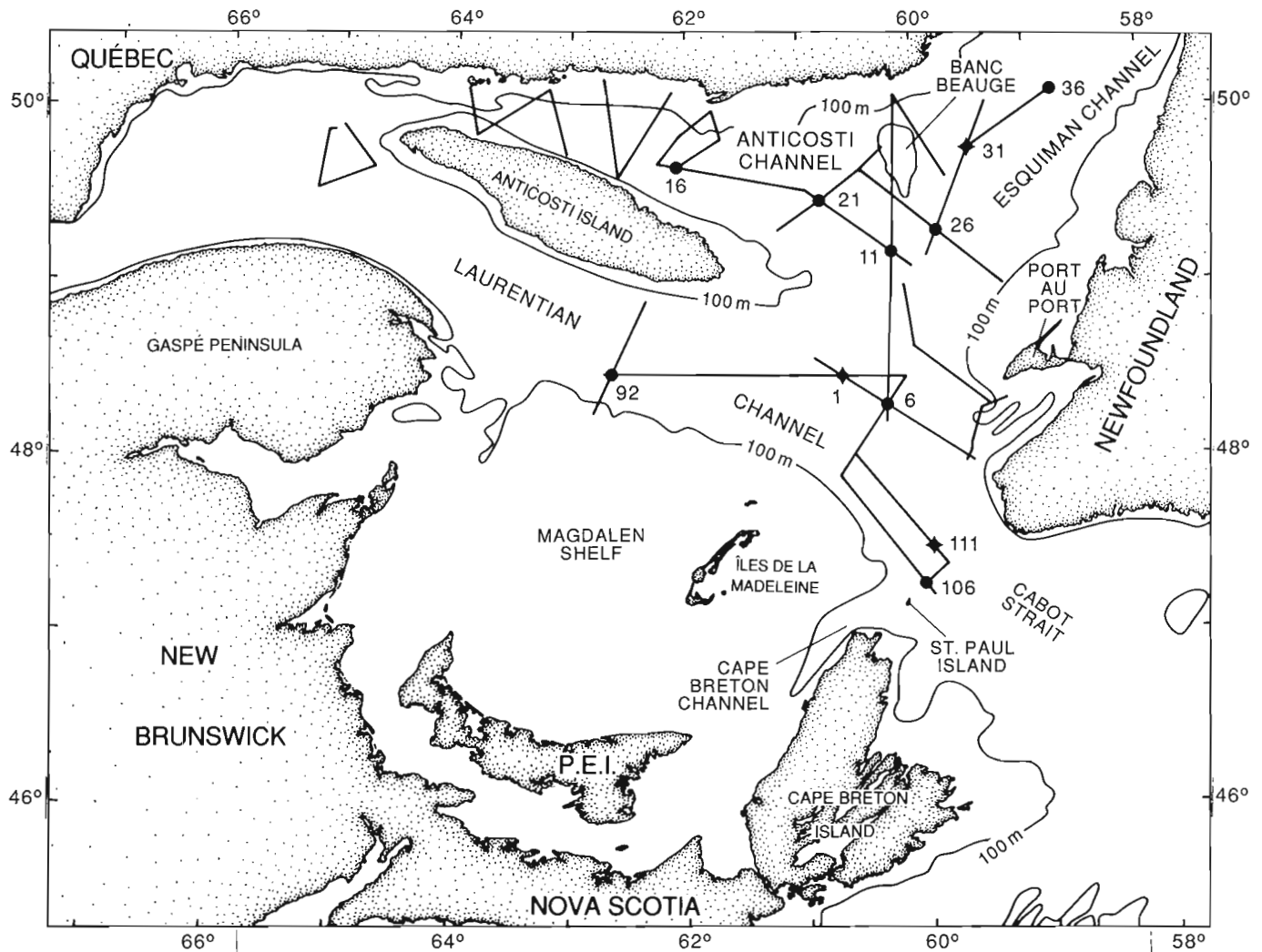


Figure 1. Location of seismic lines and piston core stations.

In Anticosti Channel basal unit I ranges in thickness from discontinuous deposits of a few metres or less to massive morainal deposits (Fig. 4, 5). Southeast of Banc Beauge adjacent to the junction with Esquiman Channel a moraine reaches a thickness of 20 metres and extends along the axis of Anticosti Channel for 63 km. Unit II is not present in Anticosti Channel. The acoustically moderately stratified unit III rests on unit I and may locally interfinger with these sediments, e.g., east of station 16 (Fig. 5). The lower part of unit III commonly is conformable with the basal boundary, but upward the succession displays basin-fill characteristics and in places appears to be gradational with the overlying weakly stratified sediments of the lower part of unit V.

Unit V is commonly 3 – 5 m thick. The faintly stratified sediments fill depressions or gently conform with the underlying topography. Small surface depressions are tentatively interpreted as pockmarks (Fig. 6).

In Esquiman Channel unit I is acoustically similar to unit I in Anticosti Channel. Moraines up to 27 m thick occur across Esquiman Channel in water depths below 100 m between Port au Port Peninsula and Banc Beauge. Moraines

up to 9 m thick also occur along part of the northern flank of Esquiman Channel east and northeast of Banc Beauge. These are up to 10 m thick between stations 31 and 36. Figures 7 and 8 illustrate the seismic stratigraphy at these stations.

In Esquiman Channel unit III appears to be composed of two parts. Twenty-two kilometres northwest of station 26 a prominent acoustic reflector separates beds in the lower part of the sequence from those above. The acoustic character of the lower beds, referred to as IIIa, is variable, in places it closely resembles the beds above (IIIb) (e.g. in the main basin to the northeast in Esquiman Channel), but in others, beds of the lower zone fill local depressions where they mimic the shape of the underlying surface and are unconformably overlain by the pervasive beds above (e.g. as at station 36, Fig. 8) In places the reflector marking the top of IIIa becomes coincident with the top of adjacent mounds of ice-contact sediments in a manner suggesting some equivalency between the two. This acoustic horizon appears to coincide with the beginning of gritty sediments in core 36 and appears to indicate a change in depositional style.

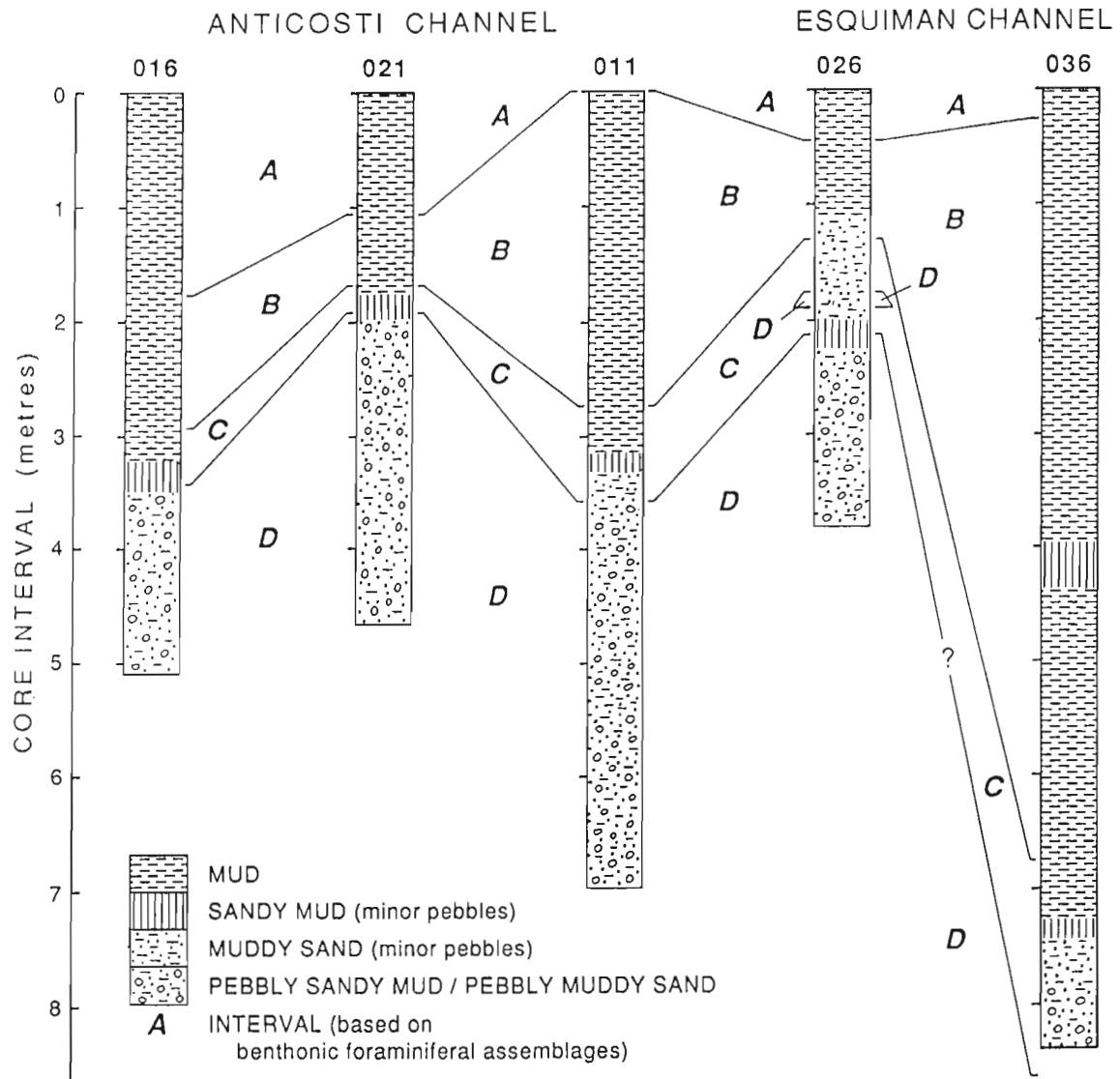


Figure 2. Preliminary lithological and biostratigraphic correlation of piston cores from Anticosti and Esquiman channels. Core sites are shown in Figure 1; seismic sections at each core site are illustrated in Figures 4-9.

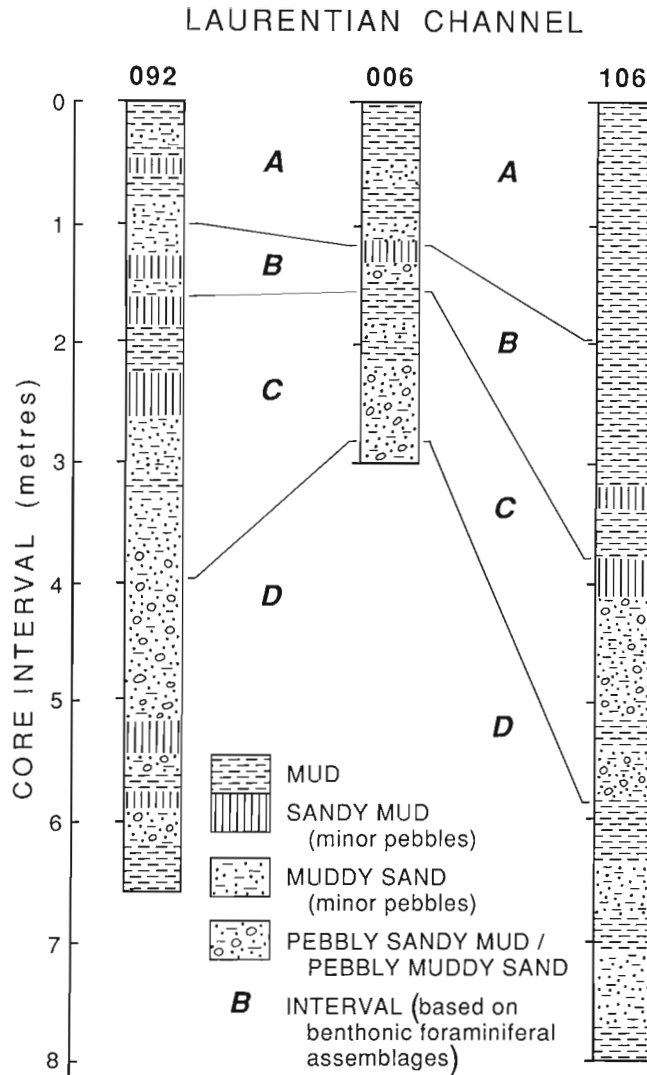


Figure 3. Preliminary lithological and biostratigraphic correlation of piston cores from Laurentian Channel. Core sites are shown in Figure 1; seismic sections at each core site are illustrated in Figures 10-12.

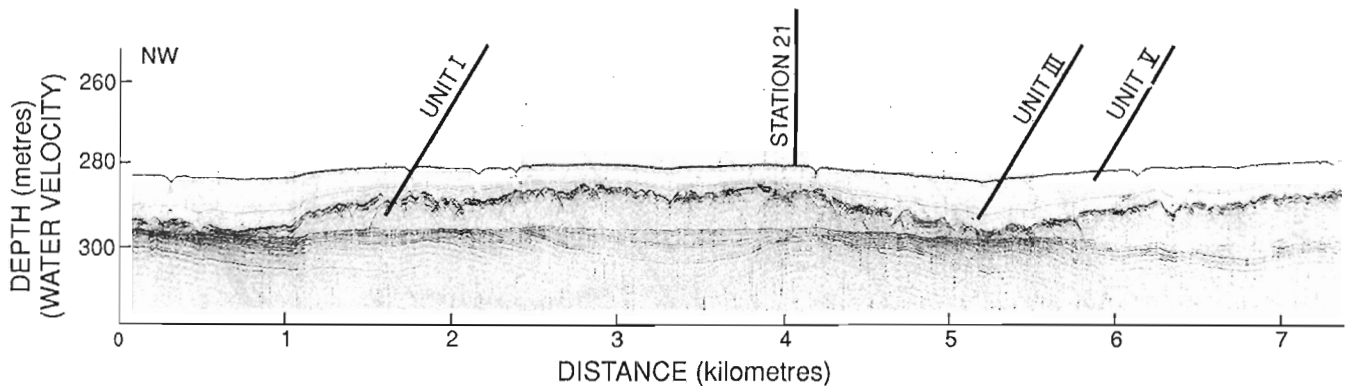


Figure 4. Huntec high resolution seismic reflection profile across station 21. A thick deposit of unit I (moraine) is overlain by variable thickness of unit III and a continuous cover of unit V. At the core site unit I is 9 m, unit III 1.5 m and unit V is 4 m thick. unit II is absent.

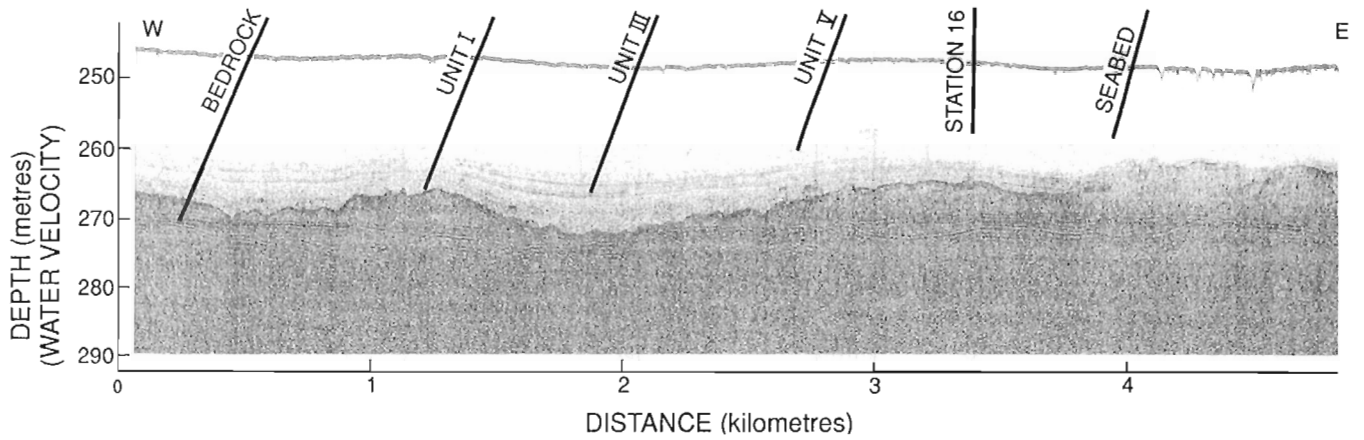


Figure 5. Hunttec high resolution seismic reflection profile across station 16. Note the hummocky unstratified unit I, the discontinuous (basin fill) unit III and a thick sequence of unit V. At the core site unit I is 5 m, unit III 3 m and unit V is 4.5 m thick.

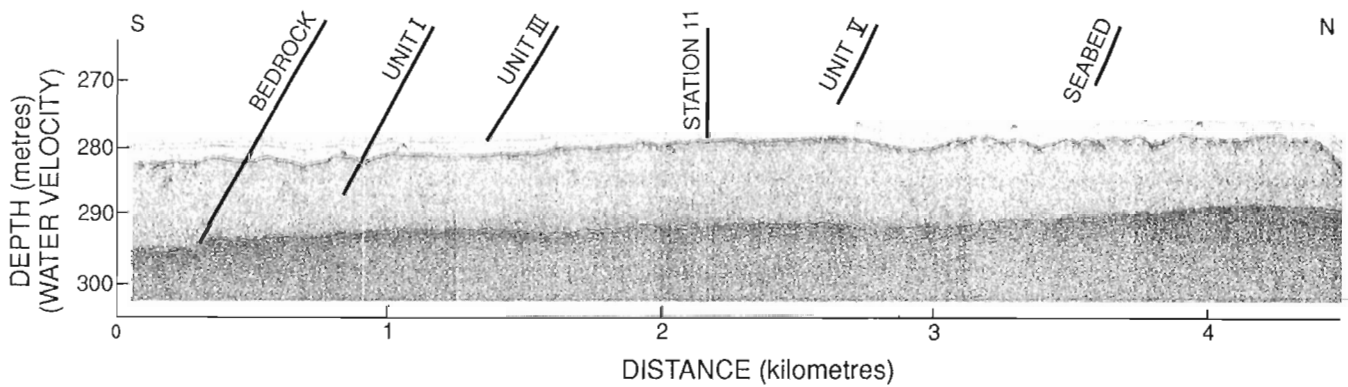


Figure 6. Hunttec high resolution seismic reflection profile across station 11. Unit I is a thick and continuous sheet on the flat bedrock surface, overlain by relatively thin glaciomarine deposits of unit III and thick postglacial deposits of unit IV. At the core site unit I is 12 m, unit II is absent, unit III is 4.0 m and unit IV is 2.5 m thick.

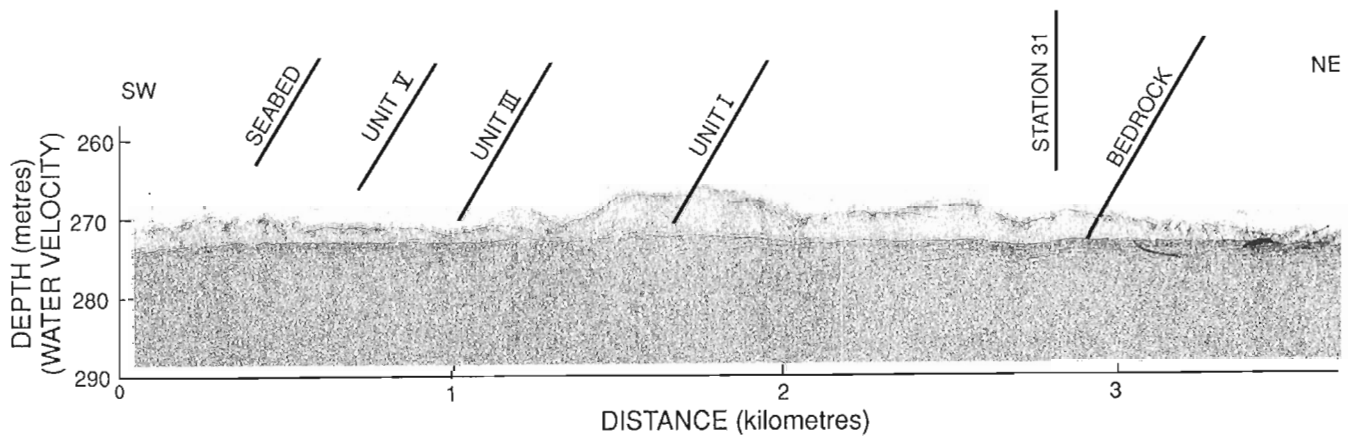


Figure 7. Hunttec high resolution seismic reflection profile across station 31. At the core site unit I is 3.5 m, unit IIIa 1.0 m, unit IIIb 3.1 m and unit III 3.0 m thick. Unit II is absent.

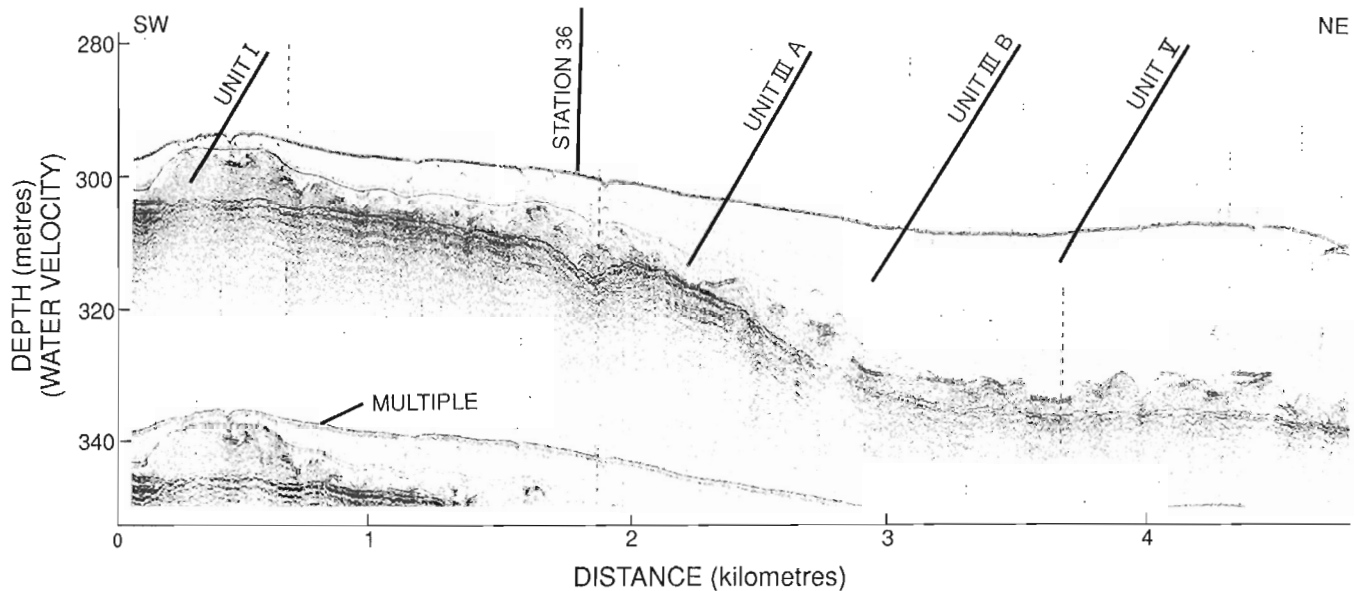


Figure 8. Huntec high resolution seismic reflection profile across station 36. The depression filling character of unit IIIa and unconformable boundary with unit IIIb in the western part of the section contrast with the more complete section deeper in the basin to the southwest. At the core site unit I is 2.5 m, unit IIIa 1.8 m, unit IIIb 3.1 m and unit V is 4 m thick.

Unit IIIa commonly is 1 – 2 m thick, but reaches 9 m in the basin of the northeastern part of the channel. Unit IIIb commonly ranges from <1 to 5m, but is 9 m thick in the northeastern basin.

Unit V resembles the Anticosti Channel unit V with weak stratification in the lower part and a relatively transparent upper part. The sediments of this unit generally range between 2.5 and 3.5 m in thickness. The surface is smooth to gently undulating with some V - shaped notches interpreted as pockmarks.

In Laurentian Channel / Cabot Strait the sediment sequence includes units I, II, III and V (Fig. 10, 11, 12 and 13). Unit I ranges in thickness between 0 and 7 m, commonly between 1 – 4 m, south of eastern Anticosti Island between stations 92 and 1 (Fig. 1). Major accumulations occur on the south flank of the channel adjacent to the Magdalen Shelf, where unit I reaches 50 m or more in thickness. The greatest thicknesses of unit I, locally in excess of 100 m, are in Cabot Strait northeast of St. Paul Island. Multiple sequences of unit I occur adjacent to Cape Breton Channel (Fig. 13) and are thought to be related at least in part to glacial ice advances emanating from that channel.

Unit II is prominent in the Laurentian Channel (Fig. 10), although absent in Anticosti and Esquiman channels. It is up to 12 m thick in the middle of the Channel northeast of station 92, while to the southwest it is transitional to unit I. Along the line between stations 92 and 1, unit II directly overlies unit I, and locally bedrock. It commonly is 3 – 5 m thick in the western part of this area and 1 – 2 m thick in the east. Unit II sediments commonly are 3 – 4 m thick in Cabot Strait northeast of St. Paul Island where they locally interfinger with unit I adjacent to Cape Breton Channel. These relationships are interpreted to mark a glacial ice margin / liftoff position.

Unit III is very thin or absent in the vicinity of station 92 south of Anticosti Island, thickens to 8 m to the northeast and east, but thins again to 4 m at station 1 and to 1 – 2 m in near station 6. Northeast of St. Paul Island in Cabot Strait unit III mainly ranges between 4 and 8 m in thickness.

Unit V is 3m thick in the vicinity of station 92, thickens eastward to 15 m south of eastern Anticosti Island and thins to 3 m at Station 1. To the southeast, the unit ranges up to 10 m in thickness in Cabot Strait. As in Anticosti and Esquiman Channels, the lower part of unit 5 often displays weak stratification and the contact with the upper part of unit III commonly appears to be gradational on the acoustic profiles.

Foraminiferal fauna

Cores from Anticosti and Esquiman channels (Fig. 2) were sampled at 5 cm intervals and cores from the Laurentian Channel (Figure 3) at 20 cm intervals. The abundance of key benthonic foraminiferal species in residues was estimated visually and used to subdivide the cores into intervals. Four intervals are recognized (Fig. 2, 3).

Interval A: *Brizalina subaenariensis*, *Buccella arctica*, *Bulimina aculeata*, *B. exilis*, *Elphidium excavatum clavatum*, *Islandiella norcrossi*, *Nonionellina labradorica* and *Pullenia osloensis* are abundant. *Bulimina exilis* is most abundant in the cores from the deeper Laurentian Channel, whereas *Buccella arctica* and *Bulimina aculeata* are most abundant in the cores from the shallower Anticosti and Esquiman channels. *Brizalina subaenariensis* is most abundant in the middle part of the interval in all channels.

Interval B: The assemblages are characterized by large numbers of *Islandiella helenae*, *Elphidium excavatum* and *Cassidulina reniforme*. *Nonionellina labradorica* is abundant in some levels and *Haynesina orbicularis* is present in low numbers.

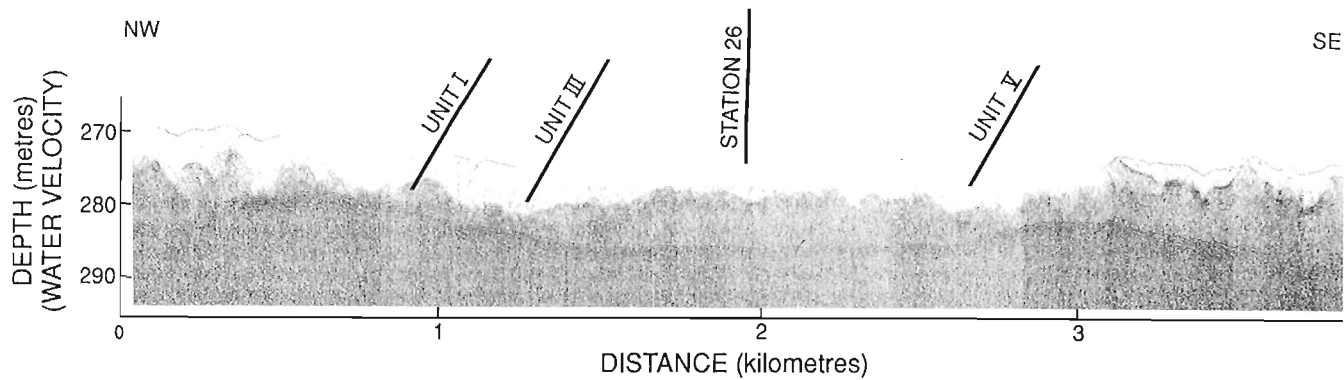


Figure 9. Hunttec high resolution seismic reflection profile across station 26 near the junction of Anticosti and Esquiman channels. At the core site the approximate thickness of unit I is 6 m, unit III 1 m and unit V 3 m.

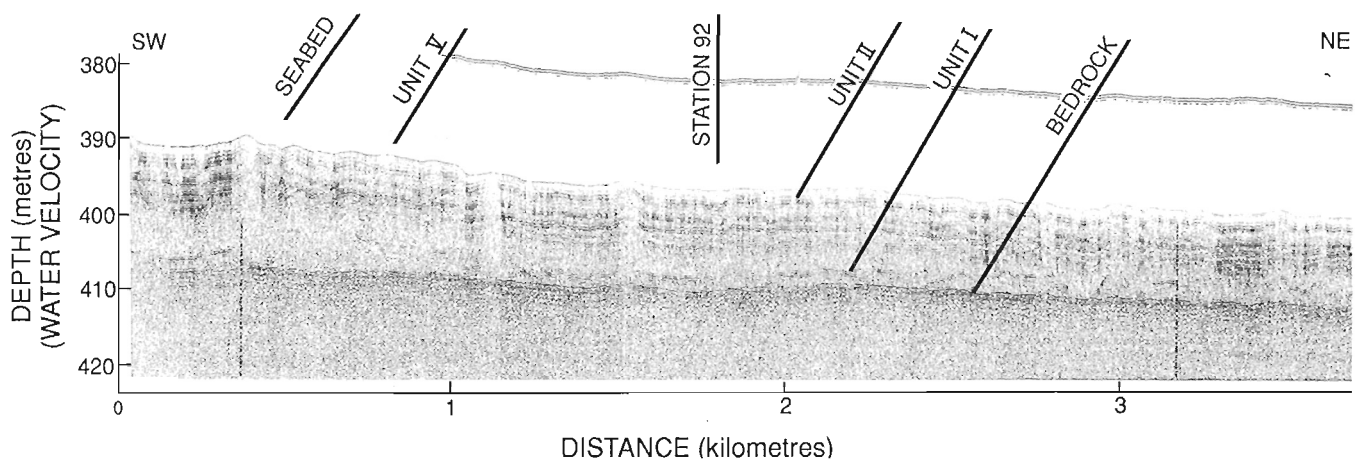


Figure 10. Hunttec high resolution seismic reflection profile across station 92 in Laurentian Channel south of Anticosti Island. Unit II sediments interfinger with and are transitional to, ice contact sediments of unit I. Approximate thicknesses at the core site are: unit I 4 m, unit II 8 m and unit V 3 m.

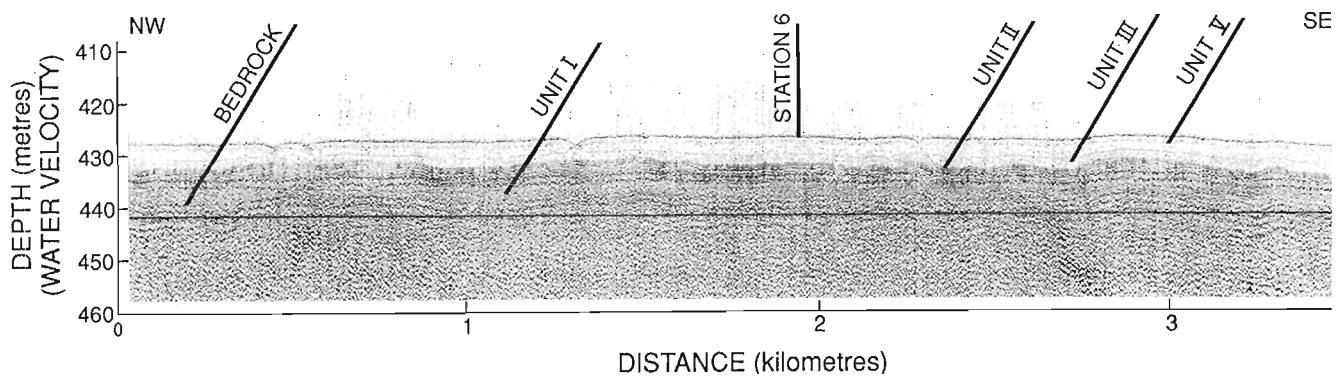


Figure 11. Hunttec high resolution seismic reflection profile across station 6 in Laurentian Channel south of the junction with Esquiman Channel. Approximate thicknesses at the core site are: unit I 4 m, unit II 3 m, unit III 1.5 m and unit V 3 m.

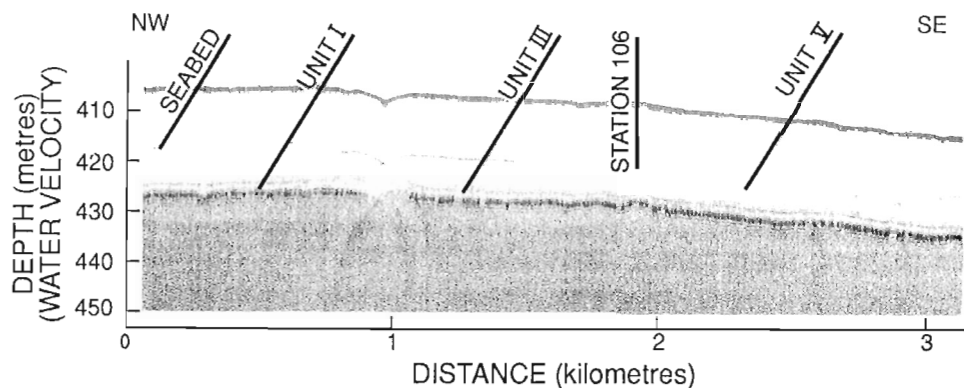


Figure 12. Hunttec high resolution seismic reflection profile across station 106 in Cabot Strait. Approximate thicknesses at the core site are: unit I 95 m, unit II 1 m, unit III 2 m and unit V 4 m.

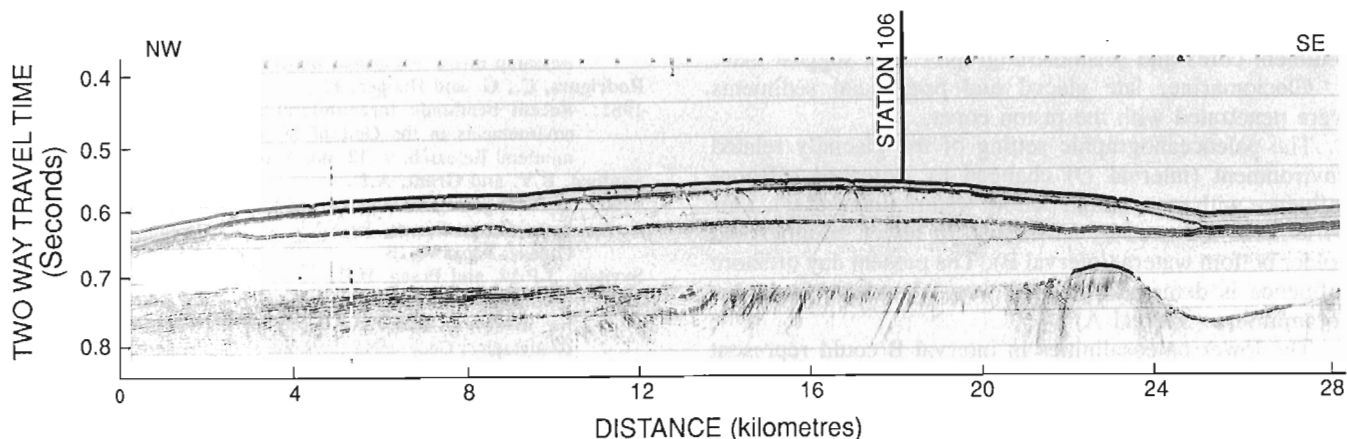


Figure 13. Airgun seismic reflection profile across station 106. The sediments are interpreted to be mainly ice contact deposits in Cabot Strait east of Cape Breton Channel. These overlie bedrock strata deformed by folding and possible diapirism.

Interval C: *Melonis zaandamae* and *Cibicides lobatulus* are abundant in the upper part, and *Cassidulina laevigata*, *Pullenia bulloides* and *Oridorsalis* sp. cf. *O. umbonatus* are abundant in the lower part of the interval. *Cassidulina reniforme* and *Astrononion gallowayi* are abundant throughout.

Interval D: Benthonic foraminifera are absent or in some samples present in low numbers. *Cassidulina reniforme* and *Elphidium excavatum clavatum* are the abundant species in the fossiliferous portions of the interval.

Planktonic foraminifera in the cores are characterized by sinistrally coiled *Neogloboquadrina pachyderma*. Low numbers of *Globigerina bulloides* and *G. quinqueloba* are present in interval A. Planktonic foraminiferal tests are most abundant in interval A and in the lower part of interval C; they are absent or present in low numbers in intervals B and D.

Preliminary paleo-oceanographic interpretation

The cores were collected in water depths ranging between 258 and 503 m, i. e., within the depth range of the modern deep water mass with temperature 4 - 6°C and salinity 34 - 35‰. Benthonic foraminiferal assemblages in the

upper part of the cores (interval A; Fig. 2, 3) are dominated by some of the deep water species reported by Rodrigues and Hooper (1982) from modern sediments in the Gulf of St. Lawrence. Interval B contains species that are characteristic of waters colder than 4°C and less saline than 34‰, e.g., *Islandiella helenae*. In the lower part of Interval C the presence of *Pullenia bulloides* is probably related to an incursion of saline Atlantic deep water into the Gulf of St. Lawrence shortly after deglaciation. *Pullenia bulloides* is not present in the modern sediments of the Gulf of St. Lawrence. The low foraminiferal abundances in interval D is probably related to glaciomarine conditions with salinities lower than in the overlying interval C.

The benthonic foraminiferal assemblages in the cores indicate that the salinity of the bottom water in the channels was highest in the lower part of interval C and in interval A. This higher-salinity bottom water is related to the presence of Atlantic water (slope or deep water) in the Gulf of St. Lawrence. Lower-salinity bottom water was present in the Gulf of St. Lawrence during deposition of the sediments in intervals D and B. The lower-salinity interval B, which occurs between intervals C and A (Fig. 2, 3), is present in all cores, including water depth of 503 m. The regional

persistence of interval B suggests that it may represent a major event of meltwater discharge. ^{14}C dates are needed to relate this event to any specific documented glacial lake drainage through the St. Lawrence valley.

Assemblages characteristic of the lower part of interval C (*Cassidulina laevigata*, *Oridorsalis* sp. cf. *O. umbonatus* – *Pullenia bulloides* dominant) appear to be absent on the Scotian Shelf (cf. Vilks and Rashid, 1976) and on the Labrador Shelf (cf. Vilks and Deonarine, 1988). However, *Cassidulina laevigata* — dominant assemblages were reported from early postglacial sediments in Hudson Strait (Vilks, et al., 1989).

SUMMARY

The presence of ice contact (glacial drift), glaciomarine and postglacial sediments is interpreted from acoustic data. On the basis of dominant species, foraminiferal intervals A, B, C and D were established. Foraminiferal assemblages in sediment cores and seismostratigraphic data suggest that:

1. Glaciomarine, late glacial and postglacial sediments were penetrated with the piston cores.
2. The paleoceanographic setting of the glacially related environment (interval D) changed to increased offshore influence with more saline bottom waters (interval C). This period was followed by an interval of lower salinities and colder bottom waters (interval B). The present day offshore influence is demonstrated with very abundant planktonic foraminifera (interval A).
3. The lower paleosalinities in interval B could represent a major event of glacial runoff that eventually could be related to the Younger Dryas. A recently obtained ^{14}C date (TO1848) on foraminifera at the bottom of zone B is $11\,480 \pm 290$ à BP (core 21, 165-167 cm).

ACKNOWLEDGMENTS

We thank the officers and crew of CSS DAWSON for work performed during Cruise 98007, and the technical staff of the program Support Subdivision, AGC, for faultless operation of the seismic equipment. H. Josenhans and D.B. Praeg reviewed the manuscript.

REFERENCES

- Bartlett, A. and Molinsky, L.**
1972: Foraminifera and the Holocene history of the Gulf of St. Lawrence; Canadian Journal of Earth Sciences, v. 9, no. 9, p. 1204-1215.
- Broecker, W.S., Andre, M., Wolfli, W., Oeschger, H., Bonani, G., Kennet, J., and Peteet, D.**
1988: The chronology of the last deglaciation: Implications to the cause of the Younger Dryas; Paleoceanography, v. 3, no. 1, p. 1-19.
- Johnson, R.G. and McClure, B.T.**
1976: A model for northern hemisphere continental icesheet variation; Quaternary Research, v. 6, p.325-353
- Josenhans, H., Zevenhuisen, J., and MacLean, B.**
1990: Preliminary seismostratigraphic interpretations from the Gulf of St. Lawrence in Current Research, Part B, Geological Survey of Canada, Paper 90-1B.
- Loring, D.H.**
1975: Surficial geology of the Gulf of St. Lawrence in Offshore Geology in Eastern Canada, ed. W.J.M. van der Linden and J. Wade; Geological Survey of Canada, Paper 74-30, v. 2, Regional Geology, p. 11-34.
- Loring, D.H. and Nota, D.J.G.**
1973: Morphology and Sediments of the Gulf of St. Lawrence; Fisheries Research Board of Canada, Bulletin 182, 147 p.
- Rodrigues, C., G. and Hooper, K.**
1982: Recent benthonic foraminiferal associations from offshore environments in the Gulf of St. Lawrence; Journal of Foraminiferal Research, v. 12, no. 4, p. 327-352.
- Sanford, B.V. and Grant, A.C.**
1990: Bedrock geological mapping and basin studies in the Gulf of St. Lawrence in Current Research, Part B, Geological Survey of Canada, Paper 90-1B.
- Syvitski, J.P.M. and Praeg, D.B.**
1989: Quaternary sedimentation in the St. Lawrence Estuary and adjoining areas: an overview based on high-resolution seismostratigraphy; Géographie Physique et Quaternaire, v. 43, no. 3, p. 291-310.
- Vilks, G. and Rashid, M.A.**
1976: Post-glacial paleoceanography of Emerald Basin, Scotian Shelf. Canadian Journal of Earth Sciences, v. 13, no. 9, p. 1256-1267.
- Vilks, G. and Deonarine, B.**
1988: Labrador shelf benthic Foraminifera and stable oxygen isotopes of *Cibicides lobatulus* related to Labrador Current; Canadian Journal of Earth Sciences, v. 25, p. 1240-1255.
- Vilks, G. and C. Rodrigues.**
1989: Dawson Cruise 89007, Gulf of St. Lawrence; GSC Open File 2119, 113 p.
- Vilks, G., MacLean, B., Deonarine, B., Currie, C.G., and Moran, K.**
1989: Late Quaternary paleoceanography and sedimentary environments in Hudson Strait; Géographie Physique et Quaternaire, v. 43, no. 2, p. 161-178.

Preliminary seismostratigraphic interpretations from the Gulf of St. Lawrence

Heiner Josenhans, John Zevenhuizen¹ and Brian MacLean
Atlantic Geoscience Centre, Dartmouth

Josenhans, H., Zevenhuizen, J., and MacLean, B. Preliminary seismostratigraphic interpretations from the Gulf of St. Lawrence; in Current Research, Part B, Geological Survey of Canada, Paper 90-1B, p. 59-75, 1990.

Abstract

The results from a two ship seismic and sampling survey in the Gulf of St. Lawrence are illustrated and discussed. Regional coverage of the surficial and bedrock geology of the entire gulf was obtained and the major features of the surficial geology and geomorphology of the region, is presented. Comparison of the acoustic character of the seismic sections from the Gulf of St. Lawrence shows clear similarities with other well studied areas from the east coast of Canada and the St. Lawrence estuary. Based on these similarities we tentatively interpret the presence of glacial till(s), glaciomarine sediments and post-glacial muds and sands.

Résumé

Les résultats d'un levé sismique et d'échantillonnage exécuté au moyen de deux bateaux dans le golfe du Saint-Laurent sont expliqués et étudiés dans le présent rapport. On a obtenu une couverture régionale de la géologie des formations en surface et du socle de tout le golfe; on présente en outre les principales structures de la géologie des formations en surface et de la géomorphologie de la région au moyen de 22 coupes sismiques. La comparaison du caractère acoustique des coupes sismiques provenant du golfe du Saint-Laurent révèle clairement les similarités qui existent avec d'autres régions bien étudiées de la côte est du Canada et de l'estuaire du Saint-Laurent. À partir de ces similarités, on essaie d'interpréter la présence de tills, de sédiments glacio-marins ainsi que de vases et de sables post-glaciaires.

¹ Orca Marine Geological Consultants, 3609 Rosemeade Avenue, Halifax, Nova Scotia, B3K-4L8.

INTRODUCTION

The Canadian oceanographic research vessels CSS Baffin cruise 89-008 and CSS Dawson cruise 89-007 collected a 7100 km grid (Fig 1) of high resolution seismic data over the Gulf of St. Lawrence which will form the basis of a new series of Frontier Geoscience Program Eastcoast Basin Atlas maps of the bedrock (Sanford and Grant, 1990) and surficial geology. Seismic sources included a 655 cm³ sleeve gun and airgun for bedrock penetration, Hunttec DTS and 3.5 kHz subbottom profilers for resolution of unconsolidated sediments as well as 50 and 100 kHz sidescan sonars for definition of the seafloor morphology. Regional seismic coverage was obtained mainly from C.S.S. Baffin and site specific data in the vicinity of piston and bedrock core sites were, together with some supporting regional lines, collected from C.S.S. Dawson. Seismic profiles representative of the core sites have been interpreted in more detail and subdivided into units 1-5. Those profiles which have no nearby piston core data have tentatively been interpreted as representing glacial till (unit 1), glaciomarine sediments (units 2 and 3) and postglacial sediments (unit 5). These seismic units are similar to those proposed for the St. Lawrence Estuary by Syvitski and Praeg (1989). Our observations on the Magdalen Plateau include some of the detailed surficial geological observations presented by Loring and Nota (1973).

Knowledge of the lateral distribution of the unconsolidated sediments helps to determine the flux of modern sediments. The regional data grid will be combined with the paleo-environmental data provided by the micropaleontological analysis of the piston cores (Vilks et al., 1990), and combined with results of geotechnical and age analyses to define the occurrence, mode of deposition and history of the glacial and post glacial sediments.

RESULTS

Description of acoustic stratigraphic units

The lateral distribution of the acoustic surficial stratigraphic units is shown by the map (Fig. 2). These units have the following characteristics.

Glacial till/ice contact sediments (unit 1)

Unit 1 is a basal, massive, acoustically unstratified sediment that lies on bedrock and is interpreted to represent glacial till or ice contact sediments deposited by grounded glacial ice. It is variable in occurrence, ranging in places from discontinuous deposits a few metres or less in thickness to multiple sequences forming morainal deposits up to 180 m in composite thickness.

Glaciomarine sediments (units 2 and 3)

Unit 2 comprises a very strongly laminated acoustic unit that forms the lower part of what is interpreted to represent ice proximal glaciomarine sediments. The unit locally inter-fingers with the glacial till/ice contact deposits and reaches thicknesses up to 15 m near former ice marginal positions.

Unit 3, is a sequence of moderately stratified sediments, that overlies glacial till and ice proximal glaciomarine sediments. Locally the unit contains some point source reflectors, which are attributed to ice rafted particles. The lower part of the unit commonly fills depressions and mimics the shape of the underlying surface; upward the unit displays basin fill characteristics. Deposits up to 15 m thick were found in deep basins. The unit thins and pinches out over subbottom elevations. In such instances the unit is condensed and in places incomplete relative to that in the depressions.

Iceberg turbate

The iceberg turbate represents an acoustically unstratified deposit which has been reworked by scouring of the seabed by grounded icebergs. It is characteristically undulating at its surface. These deposits are thought to comprise glaciomarine sediments, but may include some glacial till. The lack of (acoustic) stratification makes these deposits difficult to differentiate from glacial till/ice contact deposits but their lateral transition into glaciomarine sediments leads us to designate this as a separate map unit.

Paraglacial deltaic (unit 4)

Unit 4 represents localized, coarse grained deposits (similar to marine sandars) which are generally found near the present coastline. The unit is interpreted by Syvitski and Praeg (1989) to be the product of fluvial discharge from a nearby, rapidly ablating, ice sheet.

Postglacial ponded muds (unit 5a)

Unit 5a represents acoustically near-transparent sediments that display some weak stratification primarily in the lower part of the unit. Unit 5 is approximately 10 m thick near Cabot Strait and thickens up to 60 m at the mouth of the St. Lawrence River. The surface of the unit is smooth to gently undulating reflecting the underlying surface. Pockmarks locally form depressions to a depth of 6 m on the surface of the unit. The unit is deposited in a basin fill manner.

Postglacial reworked (transgressive (?)) sands and gravels (unit 5b)

This unit represents sands and gravels partially derived by reworking of pre-existing sediments during the transgression produced by sea level recovery following the last glaciation. Modern wave and tidally generated currents continue to winnow and transport sediments of this unit. In Figure 2 these sands and gravels are subdivided into five subunits based on the type of material which they overlie. These subunits are: 1) thin discontinuous deposits of sand/gravel directly overlying bedrock (sections 17 and 18), 2) deposits sand/gravel over paleo-channels (section 19, 21, 22), 3) deposits of sand/gravel over thick ice contact/ till deposits (section 3), 4) accretional sand bodies forming constructional features ranging from 5 to greater than 20 m in thickness and, 5) a Laurentian Channel slope spillover sand which occurs from the slope crest to approximately 200 m water depths.

STRATIGRAPHIC AND GEOMORPHIC HIGHLIGHTS

A Huntec DTS profile of the typical seismic type section in the Gulf of St. Lawrence (section 1) shows the acoustic character of the units discussed in the text.

Major morainal deposits and ice marginal sequences were identified throughout various areas of the Gulf. These are illustrated by sections 2-12 and the locations of these and all other seismic sections are shown in figure 1. These sections show variations in depositional setting in the shallow and deep waters of the gulf which will be used to define the ice margins and depositional styles of the late Wisconsinan glaciation. Till tongues (sections 6, 7, 9 and 12) which are interpreted to mark the bouyancy line (King and Fader, 1986) of the former ice sheets, are shown throughout numerous areas of the gulf. These ice marginal settings are significant because they provide ideal sites for future stratigraphic sampling below the ice contact/till deposits.

Seafloor geomorphic features identified from sidescan sonar and Huntec DTS data include active gas venting features called "pockmarks" and "mudlumps" (sections 13-15). These were found in most deep areas of the gulf, often in areas overlying Carboniferous bedrock. These ubiquitous gas venting features suggest that significant quantities of hydrocarbons are released. Recent studies (Hovland and Judd, 1988) have shown that the gases venting from pockmarks are absorbed by the food chain and ultimately released to the global carbon cycle.

Post Quaternary faulting occurs within the modern sediments in the St. Lawrence Estuary as illustrated by section 16. The 3 m offset which is still reflected in the weak muds of the seafloor suggests that this faulting has recently occurred.

Faults in outcropping bedrock (sections 17-18) are revealed on the Magdalen Plateau by sidescan sonar data. The data show the lateral trends and structural complexity of these bedrock features, which is helpful in understanding the regional (bedrock) geology.

Active sand wave fields (section 19) with heights up to 11 m (trough to crest), were mapped between the Magdalen Islands and Cape Breton Island. Current indicators in the form of "comet marks" and megaflutes were observed within the sand wave fields, indicating a strong dominant current flow to the east-southeast. Accretionary sand deposits up to 20 m thick, restricted to water depths less than 40 m, were identified southeast of the Magdalen Islands, these could provide large volumes of aggregate. The lateral distribution of this sand body is shown in Figure 2.

Fishing trawl marks of variable size and depth were observed on sidescan sonar images (section 20) throughout most of the gulf in depths less than 165 m. In some areas 100 % of the seafloor has been disturbed by the trawling activity. In one area off Cape North (Cape Breton Island) (Fig. 1, section 20) these trawl marks had incised and disturbed the seafloor to a depth of up to 1.5 m.

A large, partially eroded and buried paleochannel system up to 50 km in width (sections 21-22) was found between Cape Breton Island and the Magdalen Islands. Numerous smaller infilled channels were also found throughout the Magdalen Plateau. These fluvial sediments were deposited directly on materials interpreted as glacial tills. The association with glacial materials suggests that they may represent subglacial channel systems.

ACKNOWLEDGMENTS

We thank the officers, crews of the CSS Baffin and CSS Dawson and Atlantic Geoscience Centre technical support staff for their able assistance at sea. Gus Vilks and Al Grant reviewed the manuscript.

REFERENCES

- Dyke, A.S. and Prest, V.K.
1987: Paleogeography of northern North America 18000-5000 years ago; Geological Survey of Canada, Map 1703A, Scale 1:12 500 000.
- Hovland, M. and Judd, A.J.
1988: Seabed Pockmarks and Seepages; Graham and Trotman, London, 293 pages.
- King, L.H. and Fader, G.B.
1986: Wisconsinan glaciation of the Atlantic continental shelf of south-east Canada. GSC Bulletin 363, 72 pages.
- Loring, D.H. and Nota, D.J.G.
1973: Morphology and sediments of the Gulf of St. Lawrence; Fisheries Research Board of Canada Bulletin 182, 147 pages plus maps and interpreted sections.
- Sanford, B.V. and Grant, A.C.
1990: Bedrock geological mapping and basin studies in the Gulf of St. Lawrence; *in* Current Research, Part B, Geological Survey of Canada, Paper 90-1B.
- Syvitski, J.P.M. and Praeg, D.
1989: Quaternary sedimentation in the St. Lawrence estuary and adjoining areas, eastern Canada: an overview based on high-resolution seismo-stratigraphy; *Geographie Physique et Quaternaire*, v. 43, p. 291-310.
- Vilks, G., MacLean, B. and Rodrigues, C.
1990: Late Quaternary high resolution seismic stratigraphy and foraminiferal zones in the Gulf of St. Lawrence; *in* Current Research, part B, Geological Survey of Canada, Paper 90-1B.

Figures 1-22 to follow

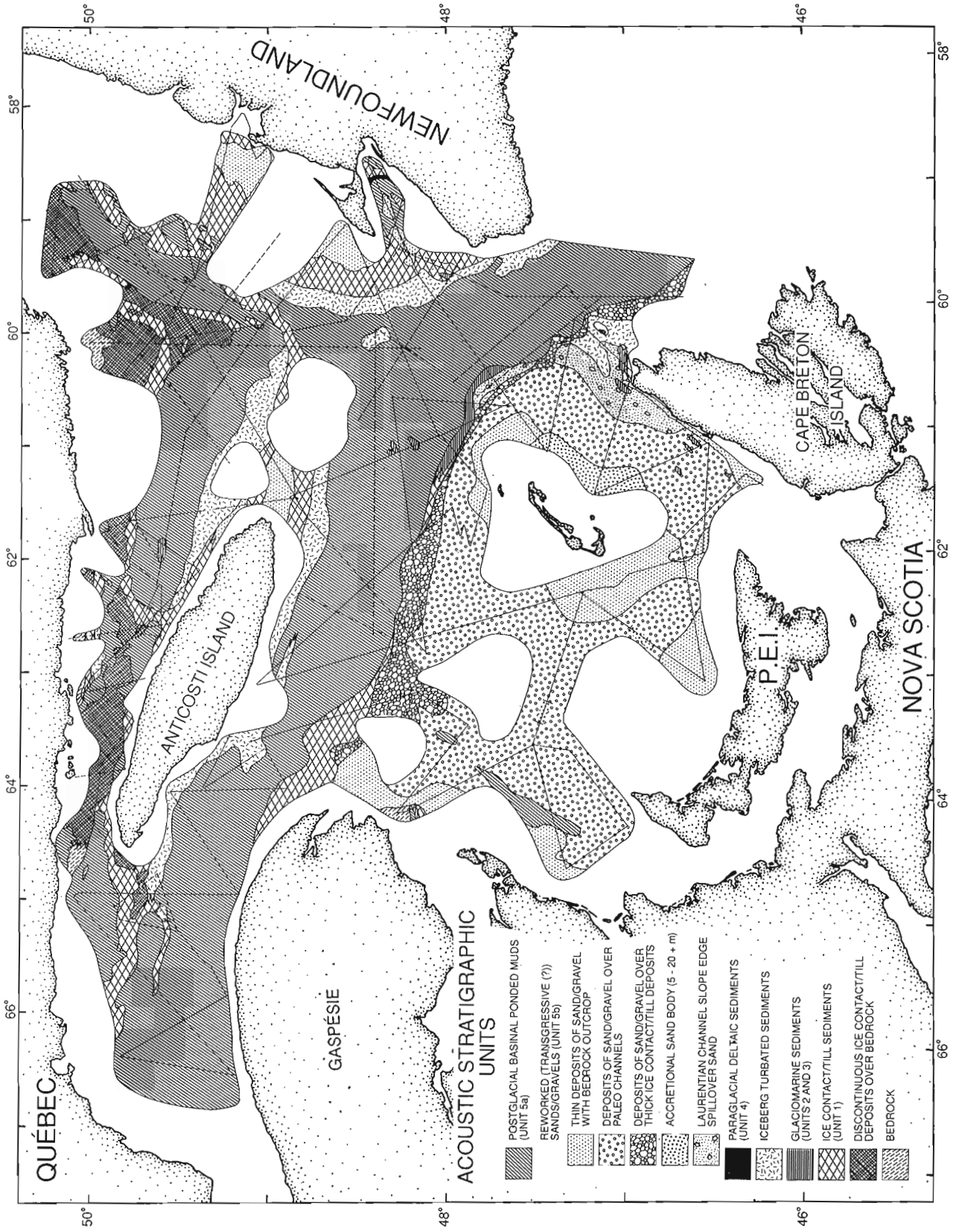


Figure 1. Location map of sections illustrated in text, generalized bathymetry and seismic control from CSS Baffin 89-008 (solid lines) and CSS Dawson 89-007 (dashed lines).

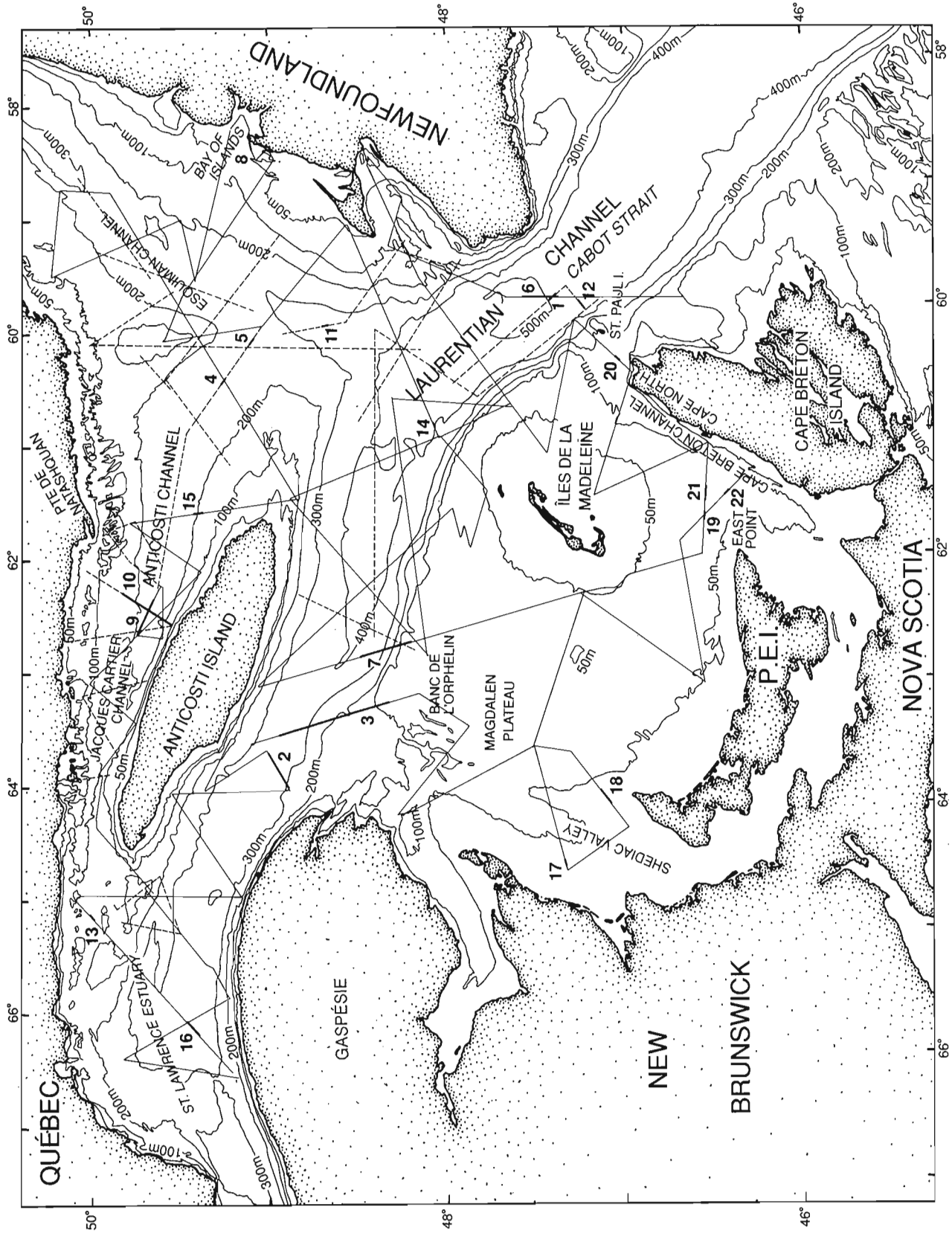
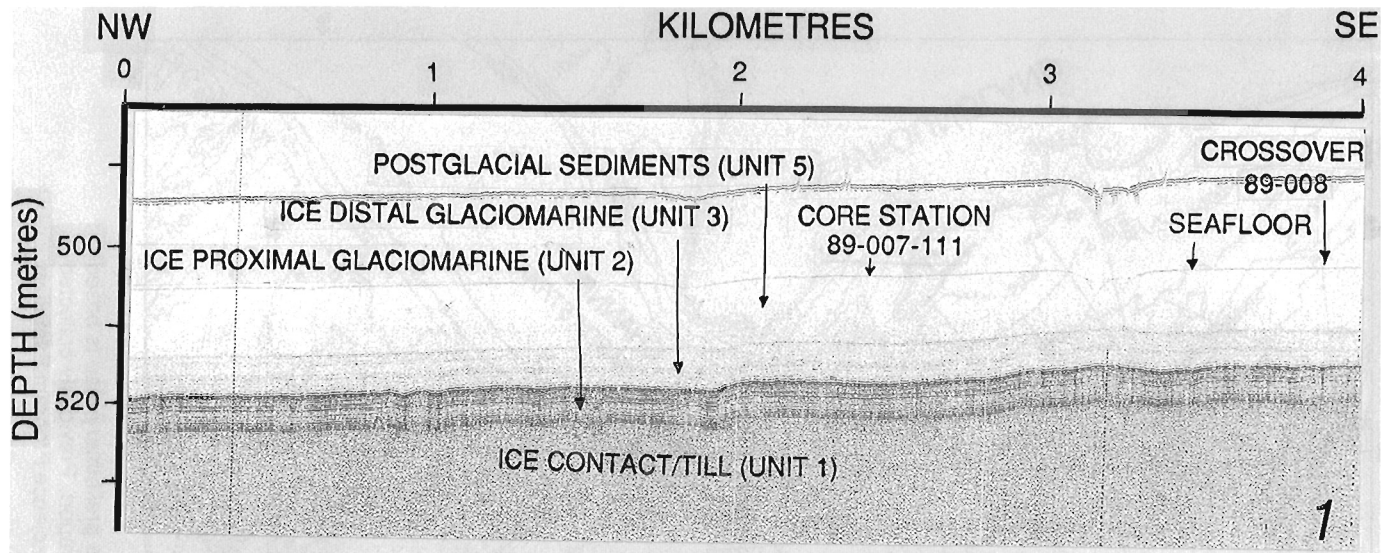
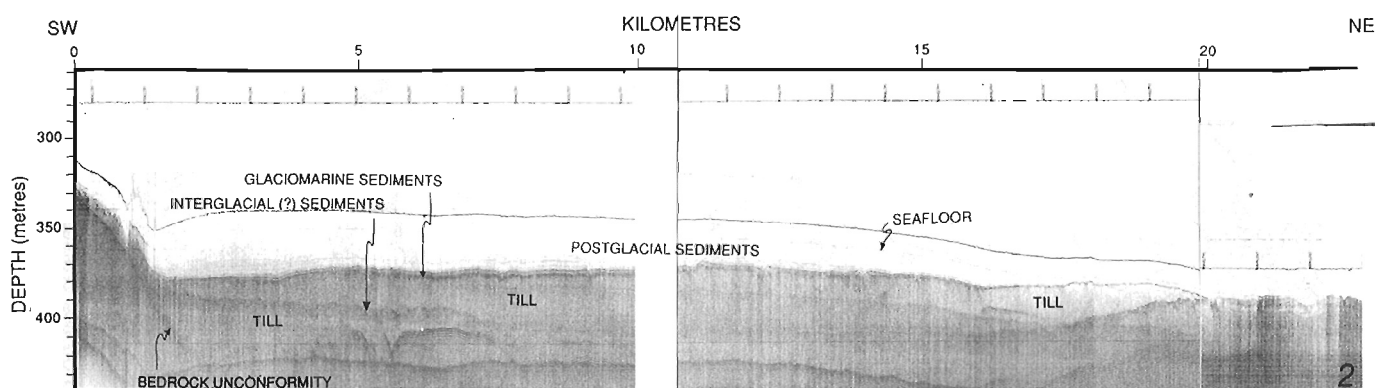


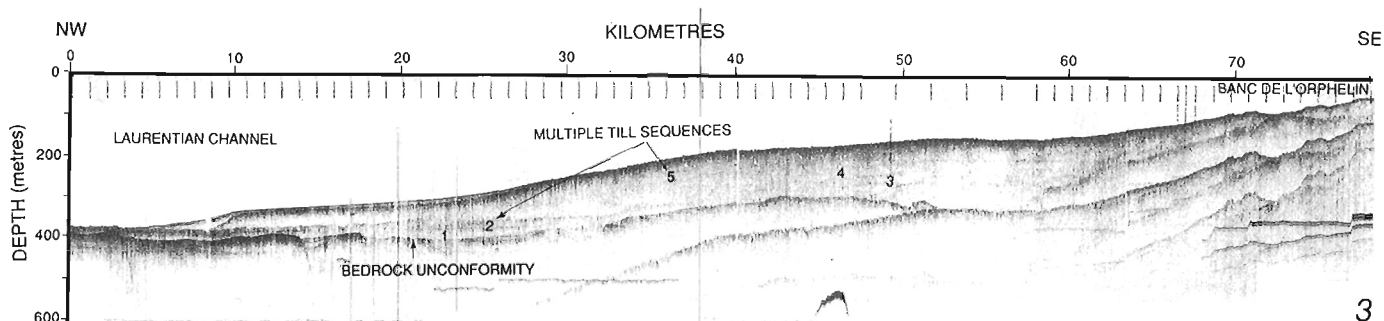
Figure 2. Regional distribution of surficial acoustic stratigraphic units. This preliminary map is based only on the data collected on the cruises (subdued lines) described in this report. Previously collected data is presently being incorporated and will be published in the Frontier Geoscience Program Eastcoast Basin Atlas Series format. Areas of insufficient seismic coverage are blank.



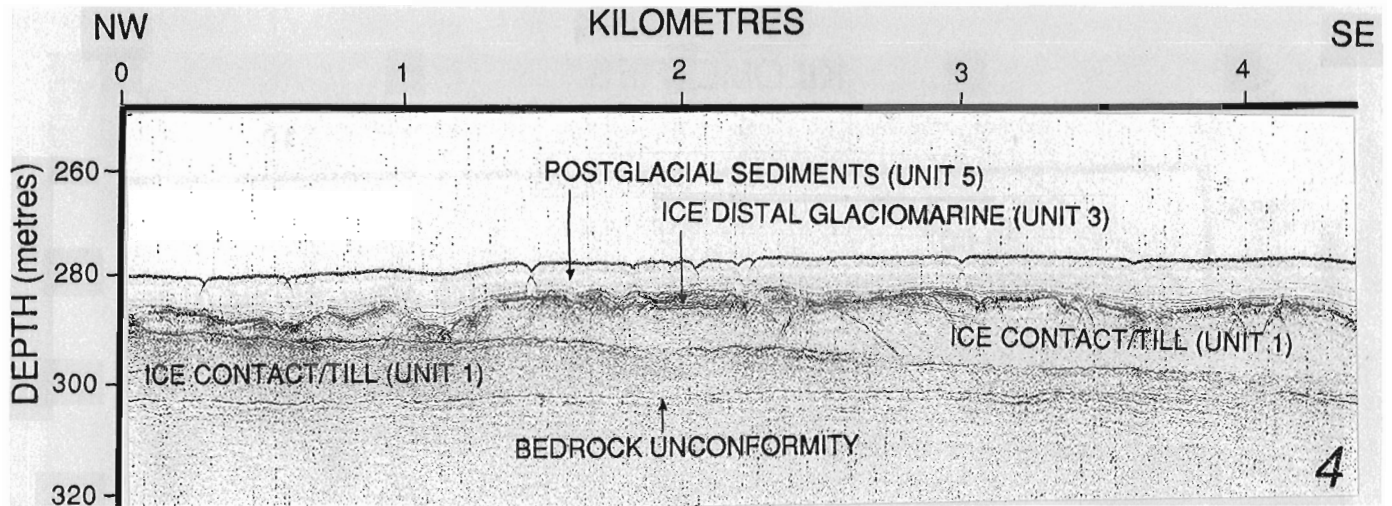
Section 1. Hunttec DTS profile showing thick sequences of unit 1 (glacial till), units 2 and 3 (glaciomarine sediments), and unit 4 (postglacial sediments) at core site 89-007-111 (Vilks et al, 1990) in Cabot Strait. The profile is representative of the seismic type section within the Laurentian Channel. See Figure 1 for location.



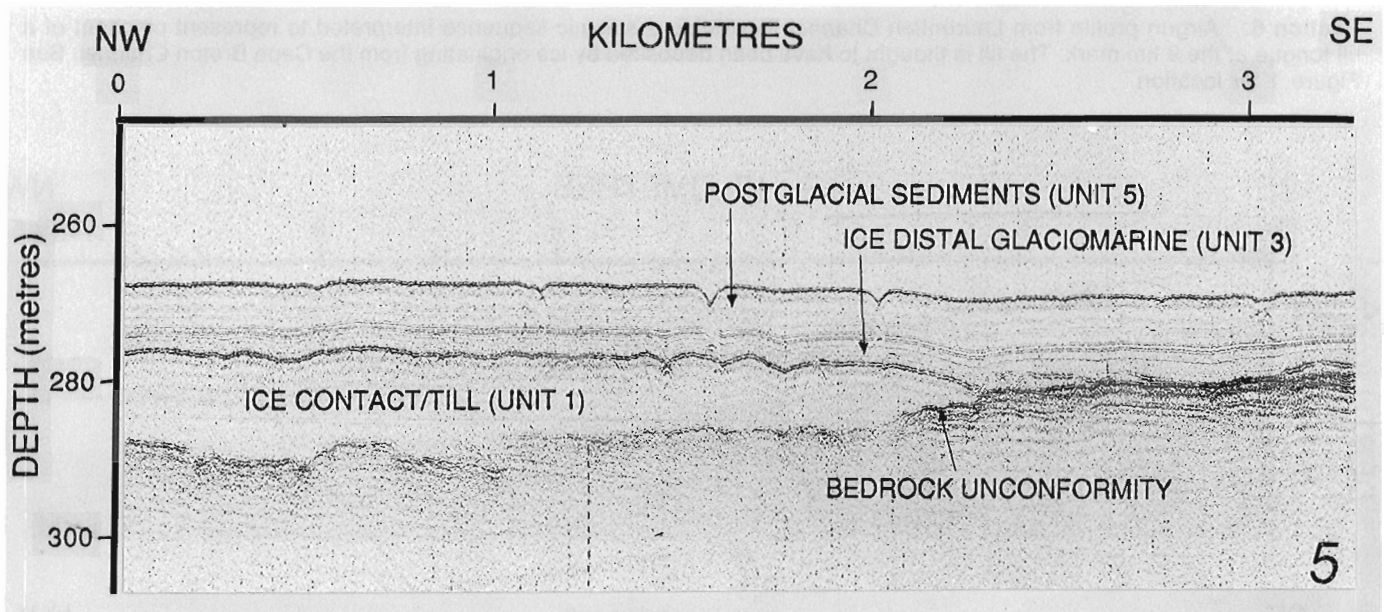
Section 2. Hunttec DTS profile located between the eastern tip of Gaspésie and Anticosti Island, illustrating seismic units interpreted as multiple tills (up to 60 m thick) overlain by glaciomarine and postglacial sediments. The well stratified horizons between tills suggest that interglacial/interstadial sediments may have been preserved. See Figure 1 for location.



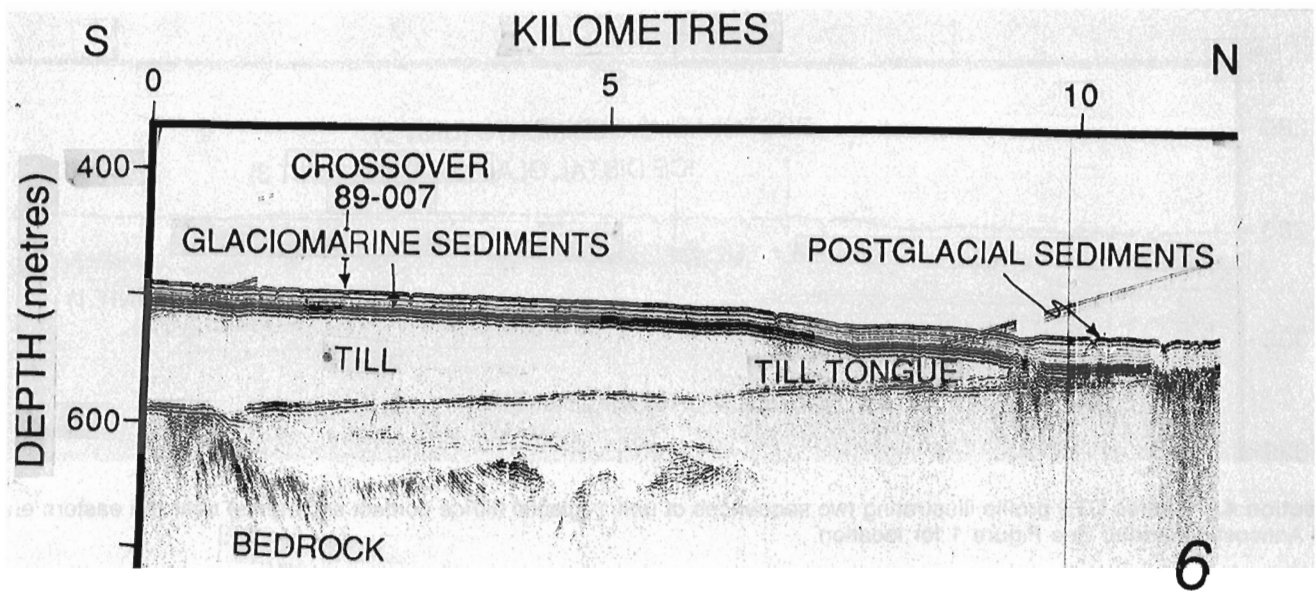
Section 3. Airgun profile extending from the Magdalen Plateau at Banc De L'Orphelin to the bottom of the Laurentian Channel illustrating up to six seismic sequences of unstratified material interpreted as successive deposits of glacial tills. The well stratified horizons between some of these units may represent interglacial/interstadial horizons. See Figure 1 for location.



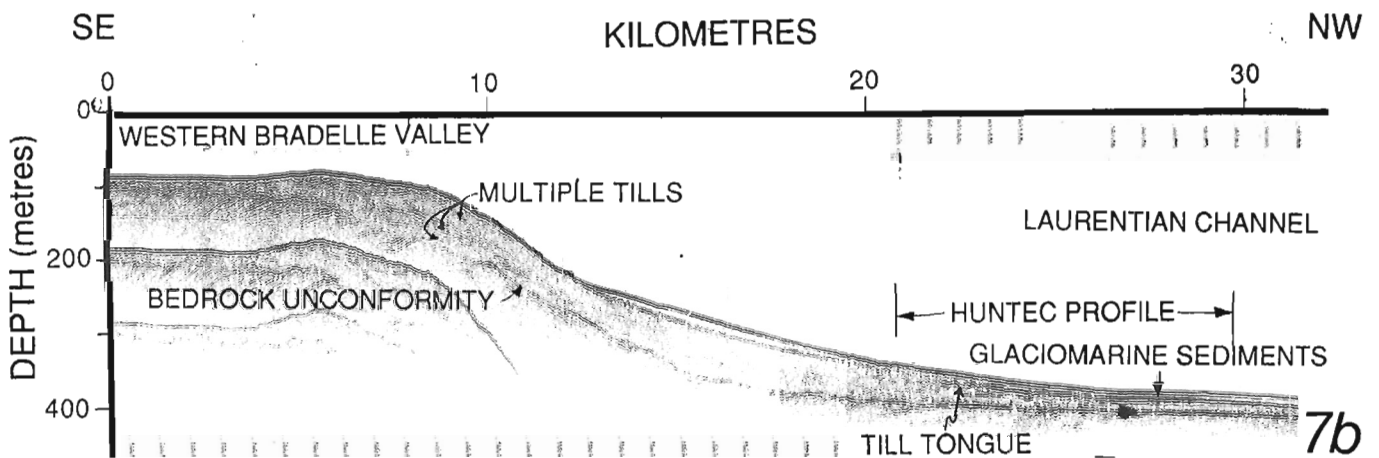
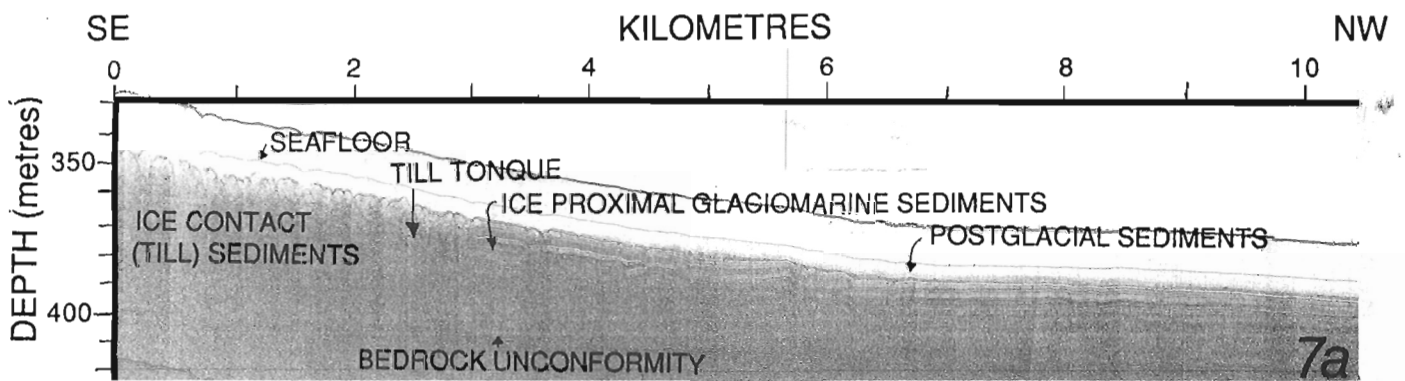
Section 4. Hunttec DTS profile illustrating two sequences of unit 1 (glacial till/ice contact sediments) near the eastern end of Anticosti Channel. See Figure 1 for location.



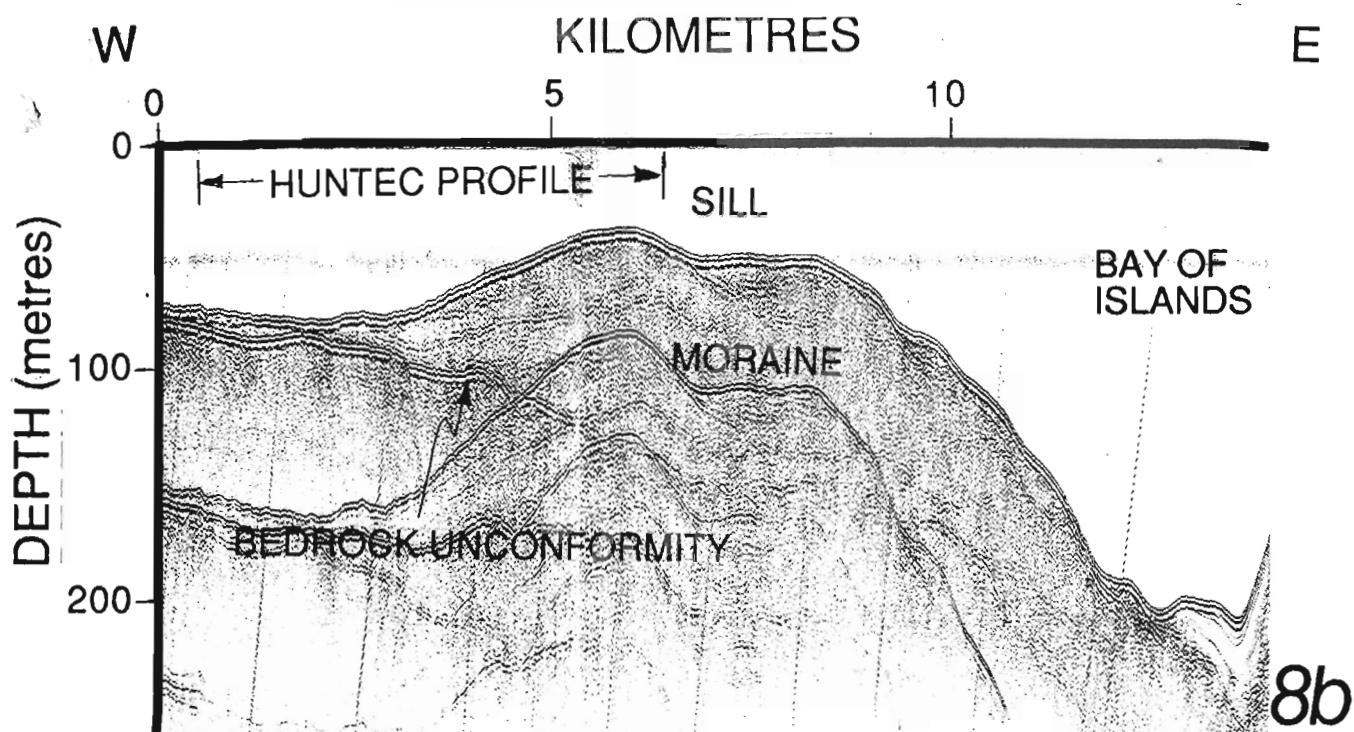
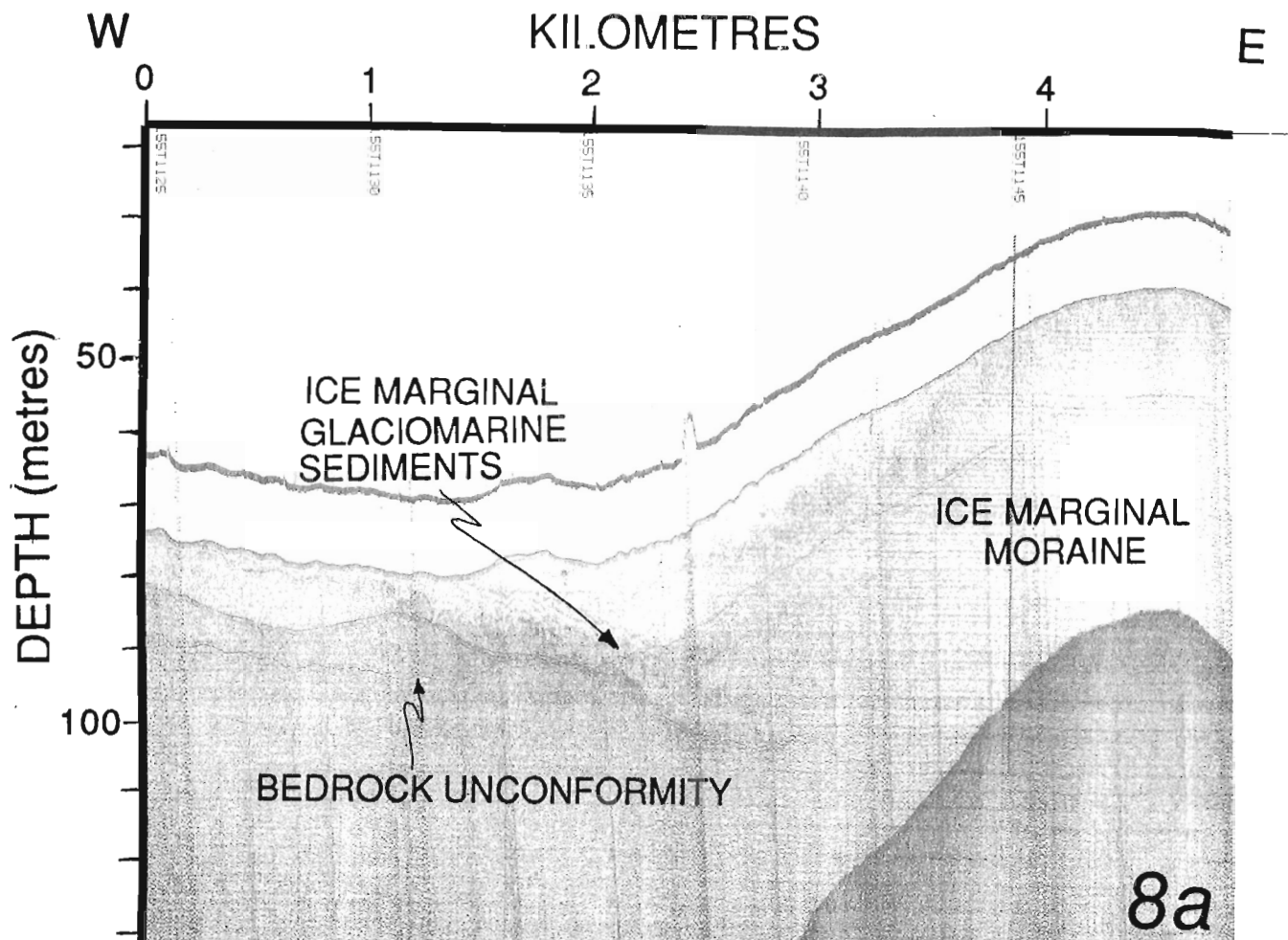
Section 5. Hunttec DTS profile from eastern Anticosti Channel illustrating the eastern margin of the upper sequence of unit 1 (glacial till/ice contact) illustrated in section 4; the lower sequence terminated 24 km to the northwest. See figure 1 for location.



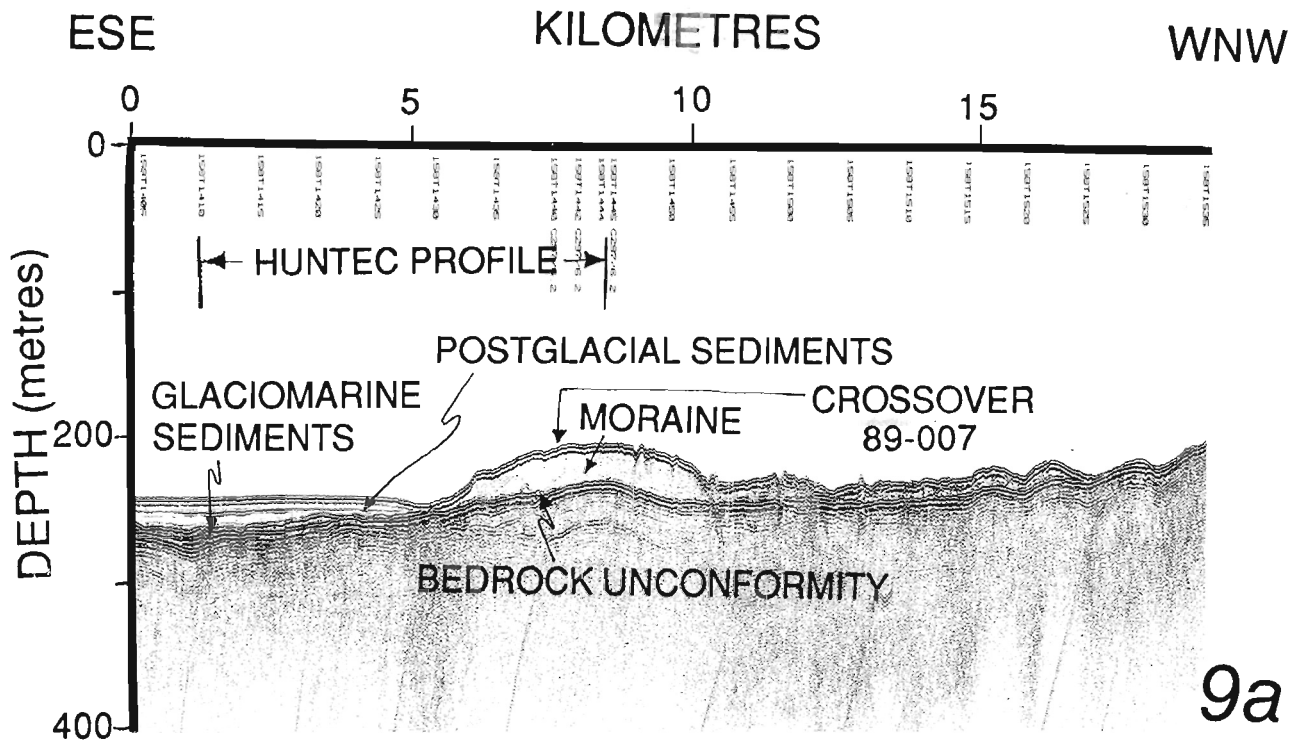
Section 6. Airgun profile from Laurentian Channel illustrating a seismic sequence interpreted to represent pinchout of a till tongue at the 9 km mark. The till is thought to have been deposited by ice originating from the Cape Breton Channel. See Figure 1 for location.



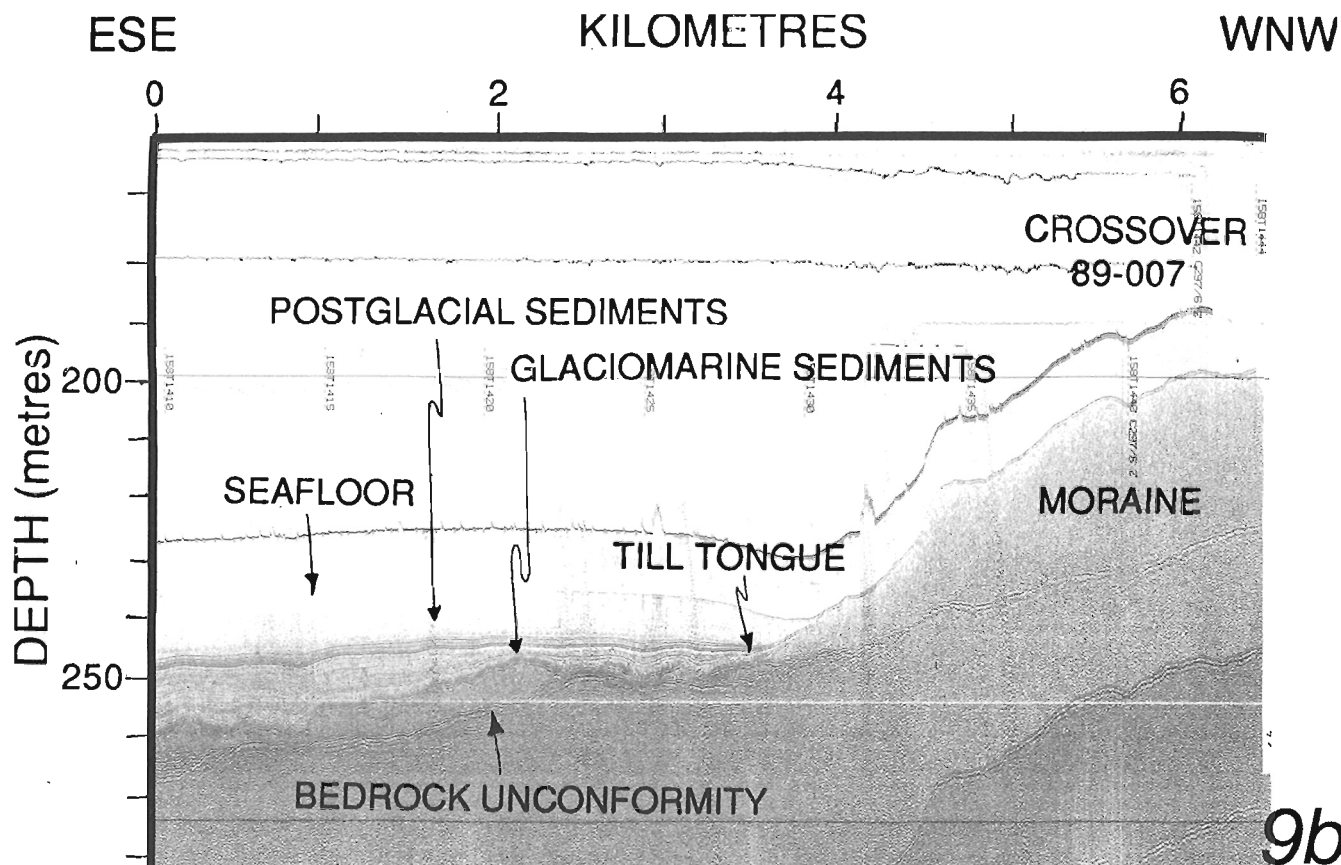
Section 7. Airgun (below) and corresponding Huntect DTS profiles from the western flank of the Laurentian Channel (see Fig. 1) illustrating seismic sequences interpreted as multiple tills, lift off moraines and ice marginal deposits. The Huntect DTS profile illustrates the depth dependent transition from ice contact (till) deposits in shallow water to well stratified ice proximal glaciomarine sediments down slope.



Section 8. Hunttec DTS and corresponding airgun profile from the southern entrance to the Bay of Islands showing an ice marginal terminal moraine overriding previously deposited glaciomarine ice contact sediments. The airgun profile indicates a moraine sequence up to 100 m thick. The sill is entirely composed of morainal material. See Figure 1 for location.

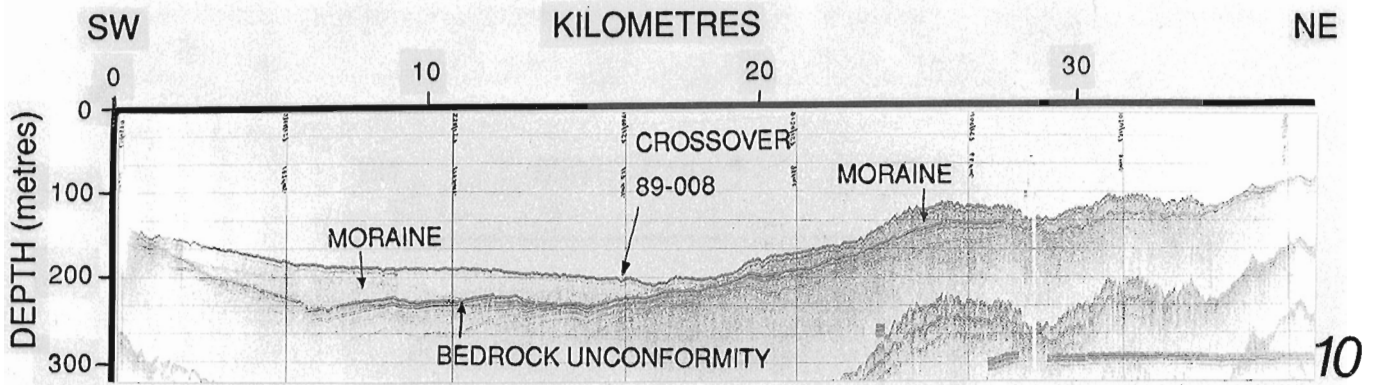


9a

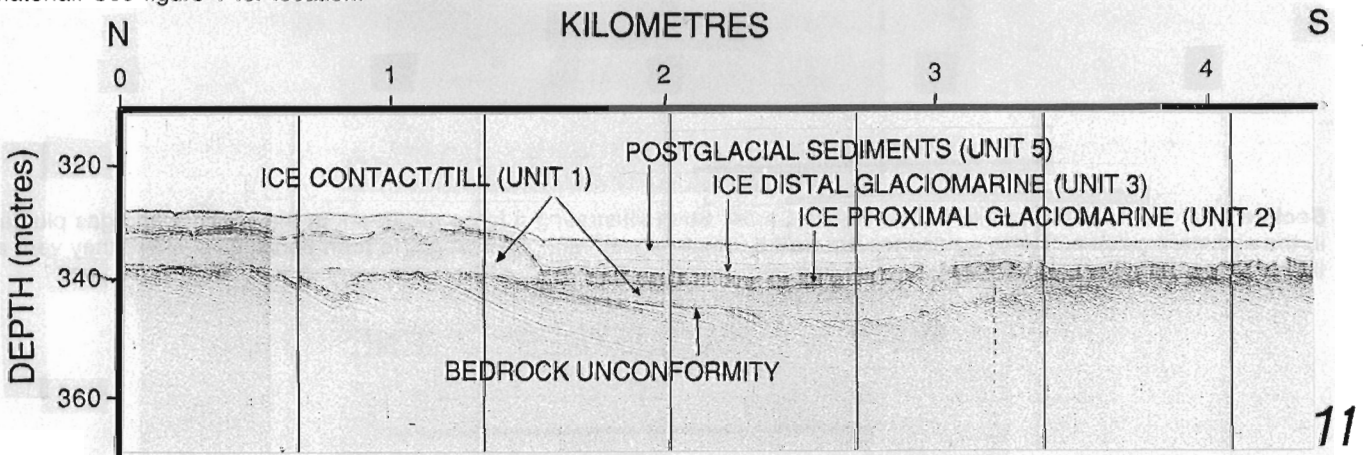


9b

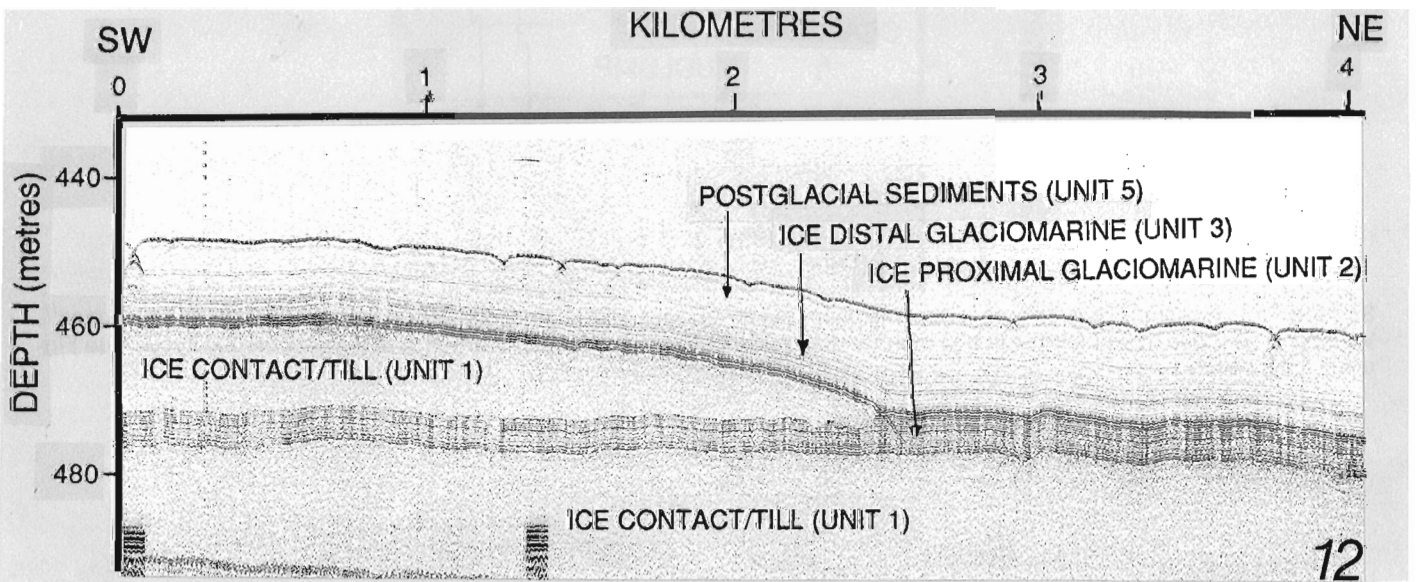
Section 9. Airgun and Hunttec DTS profiles illustrating a large moraine and associated till tongue and glaciomarine sediments. The moraine forms a major topographic feature that connects the north shore of Anticosti Island with the Quebec North Shore. This moraine may correlate with the maximum extension of Late Wisconsinan ice on Anticosti Island, dated at approximately 14.5 ka. (Dyke and Prest 1987) See figure 1 for location.



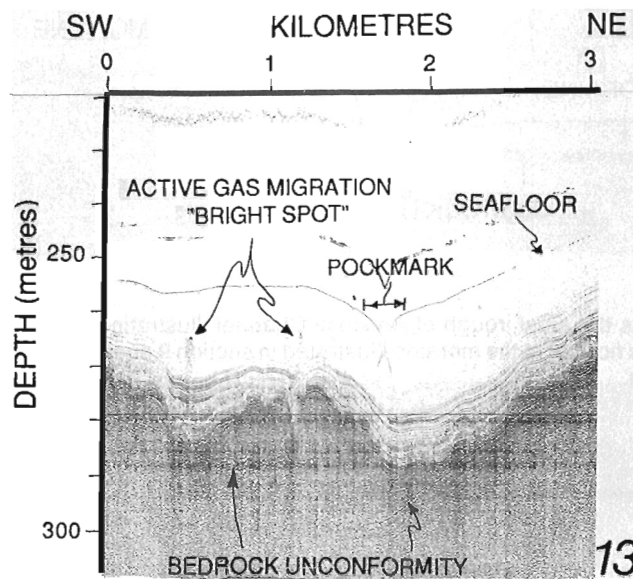
Section 10. Airgun profile across the axial trough of Anticosti Channel illustrating unit 1 (glacial till) sediments up to 50 m thick in the trough. This profile runs normal to the moraine illustrated in section 9 and illustrates the lateral extent of the morainal material. See figure 1 for location.



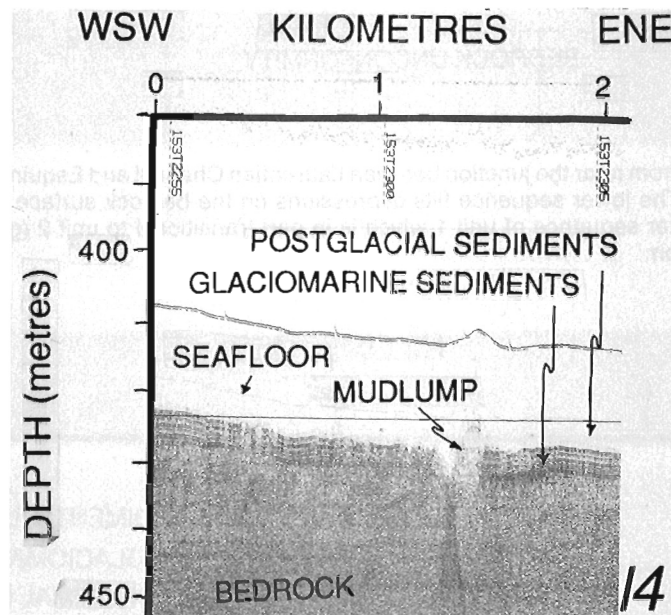
Section 11. Huntex DTS profile from near the junction between Laurentian Channel and Esquiman Channel showing multiple sequences of unit 1 (glacial till). The lower sequence fills depressions on the bedrock surface in the center of the diagram. This sequence is overlain by a later sequence of unit 1 which is in part transitional to unit 2 (glaciomarine sediments) at its terminus. See Figure 1 for location.



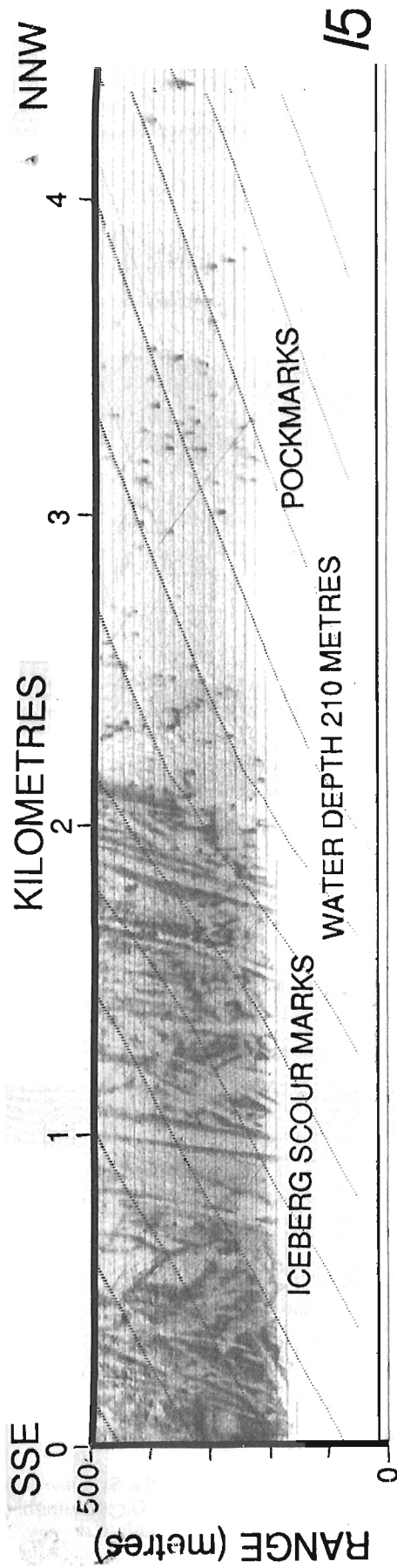
Section 12. Huntex DTS profile illustrating tonguing relationships northeast of St Paul Island between sediments of the upper part of unit 1 (glacial till) and the acoustically stratified sediments of unit 2 (glaciomarine sediments). Also note the pockmarks which indent the seabed in unit 5 (postglacial sediments). See Figure 1 for location.



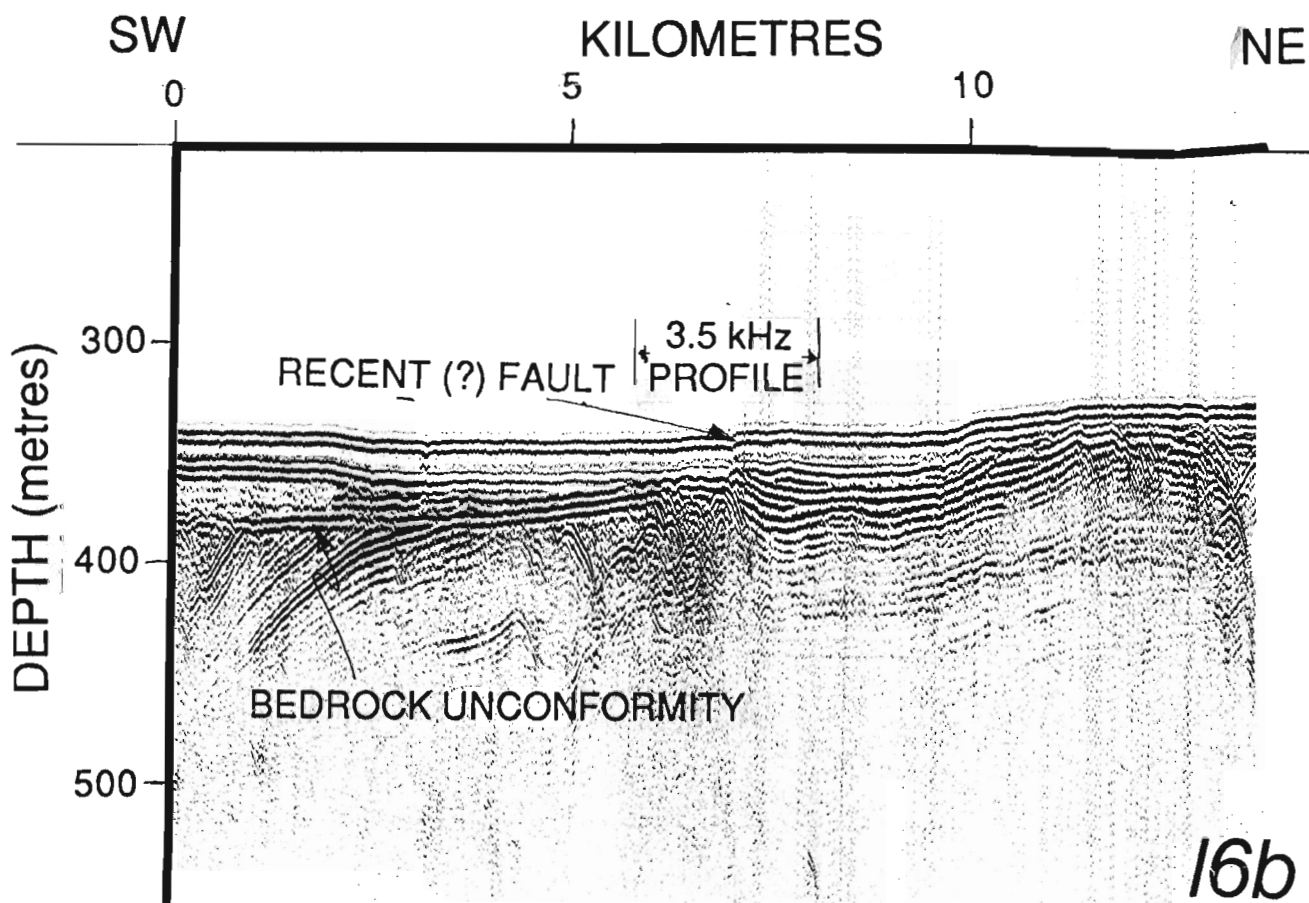
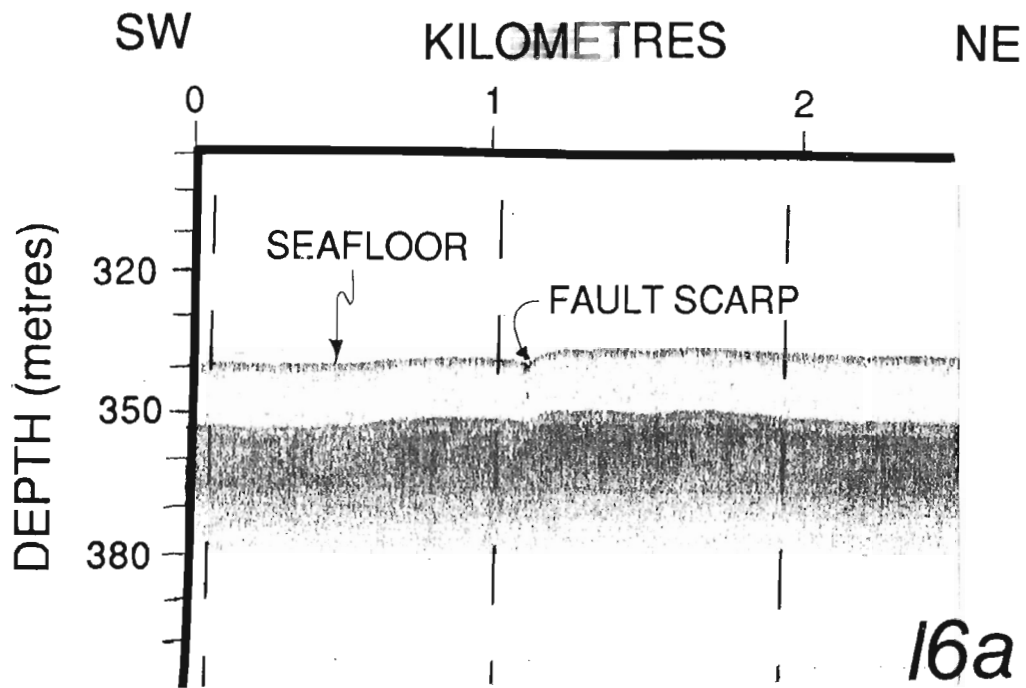
Section 13. Huntect DTS profile from Jacques Cartier Strait illustrating a large pockmark at the seafloor and gas plumes in the sediment column. These gas zones are called "bright spots" and are thought to form pockmarks where they vent at the seafloor. See Figure 1 for location.



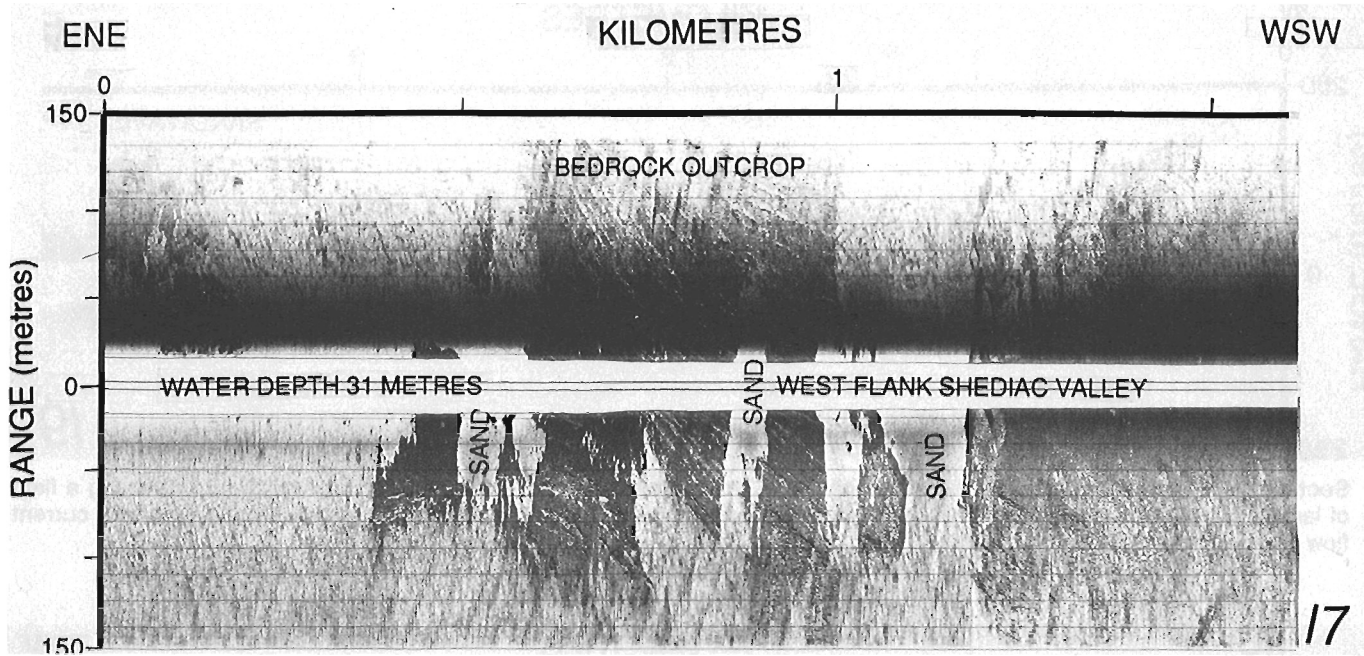
Section 14. Huntect DTS profile of sediments disturbed by upward migration of gas. Such features are called "mudlumps". Venting of gaseous hydrocarbons in this manner may add significant amounts of carbon to the global carbon cycle. See Figure 1 for location.



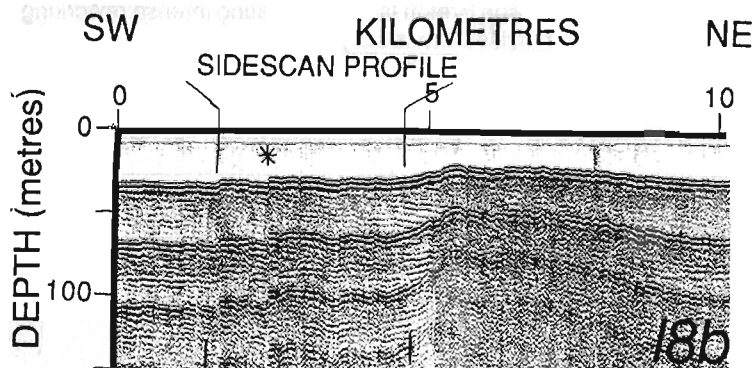
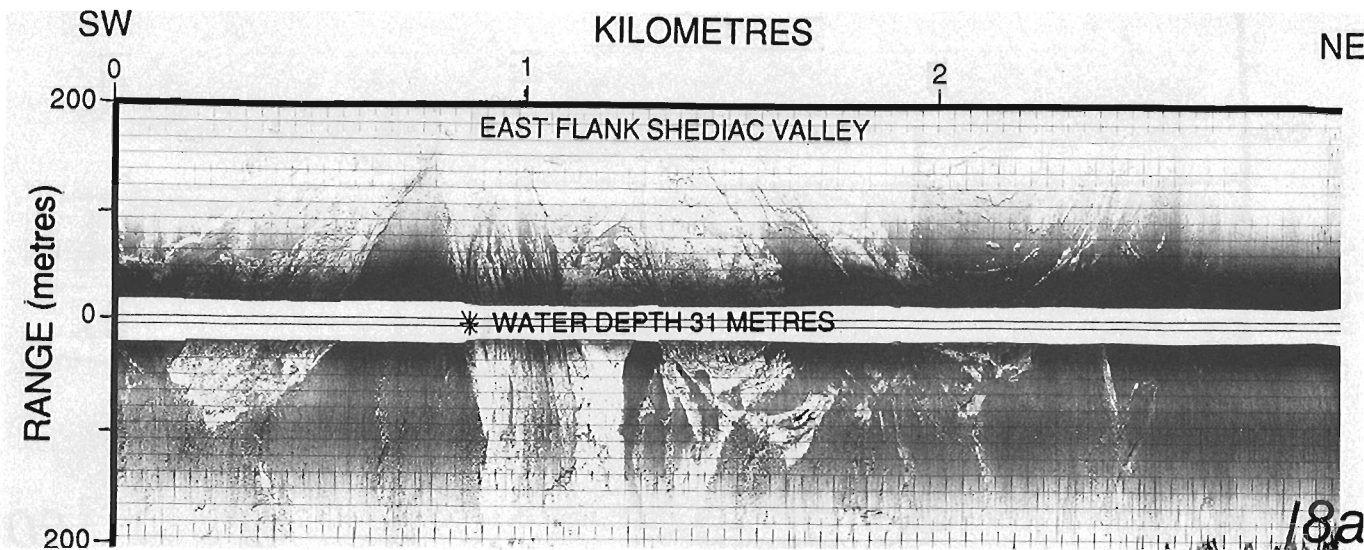
Section 15. 50 KHz sidescan sonogram showing circular gas venting features called pockmarks and linear paleo-iceberg scour marks. The pockmarks are formed in the postglacial clays which have partially buried the paleo iceberg scour marks. See Figure 1 for location.



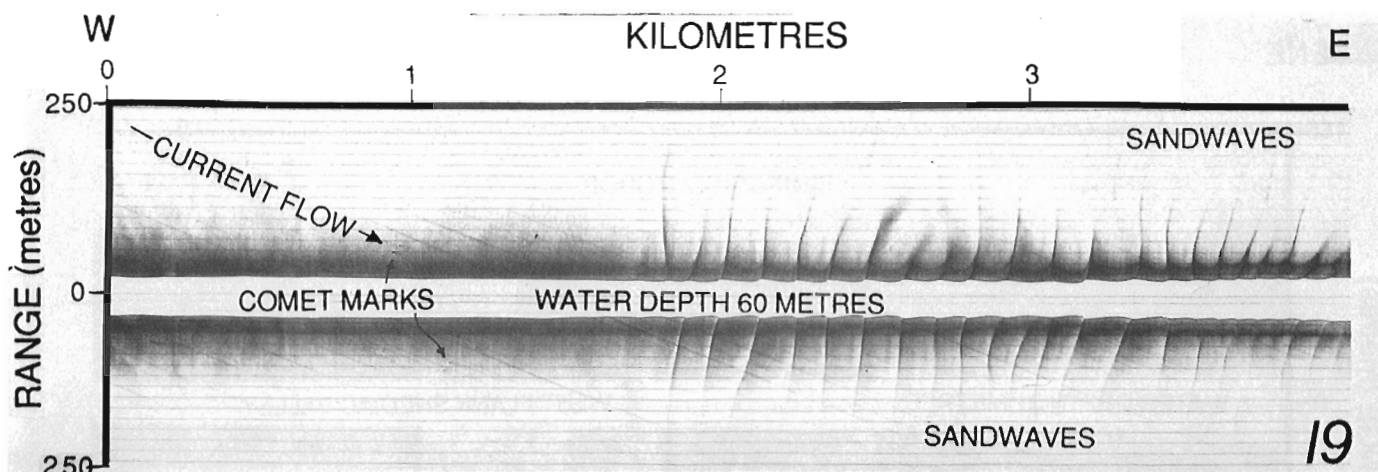
Section 16. Airgun and associated 3.5 kHz subbottom profiles from the St. Lawrence Estuary showing faulted bedrock and a fault scarp extending through the modern sediments to the seafloor. Displacement of approximately 3 m within the modern sediments indicates that this is a recent feature. See Figure 1 for location.



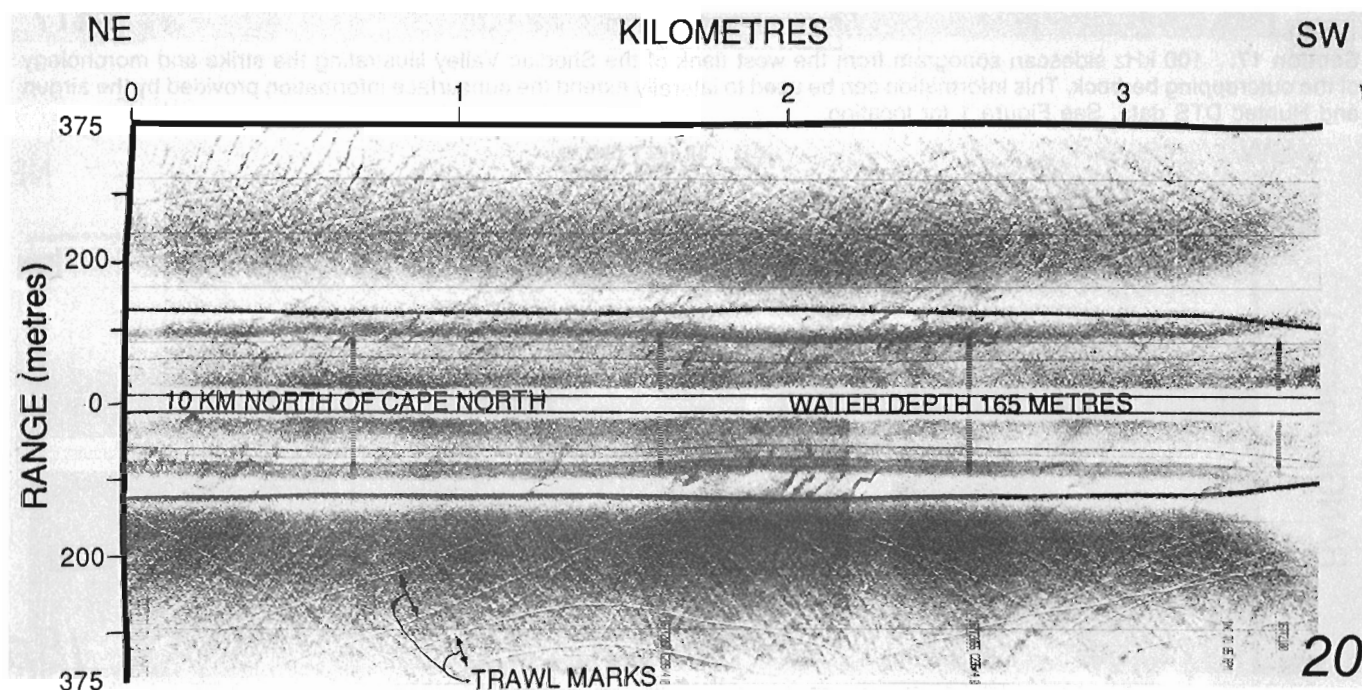
Section 17. 100 kHz sidescan sonogram from the west flank of the Shediac Valley illustrating the strike and morphology of the outcropping bedrock. This information can be used to laterally extend the subsurface information provided by the airgun and Hunttec DTS data. See Figure 1 for location.



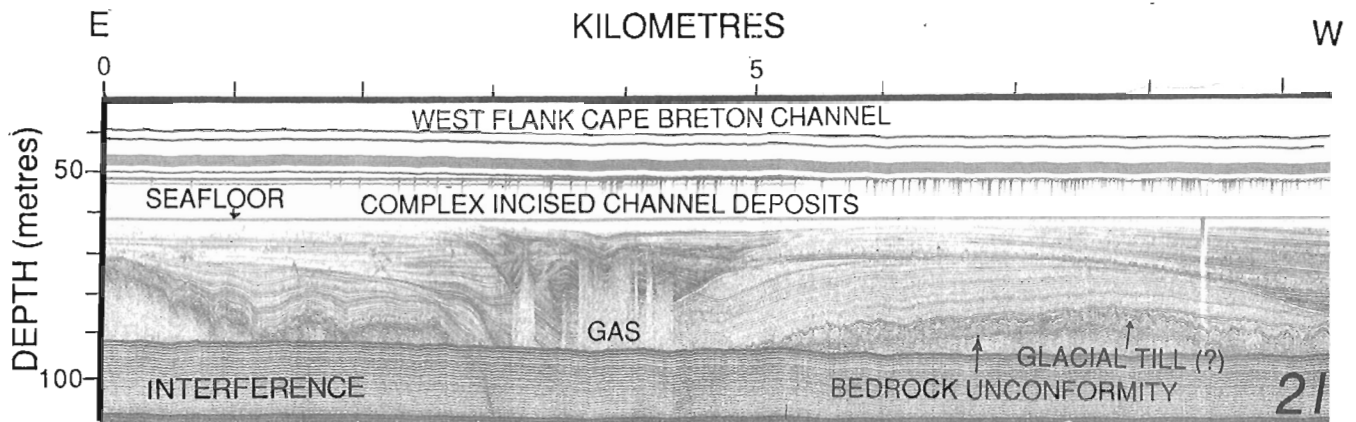
Section 18. Airgun profile and corresponding 100 kHz sidescan sonogram illustrating step faulted bedrock outcropping at the seafloor. The sidescan sonogram illustrates the lateral complexity and orientation of the faulted bedrock blocks. See Figure 1 for location.



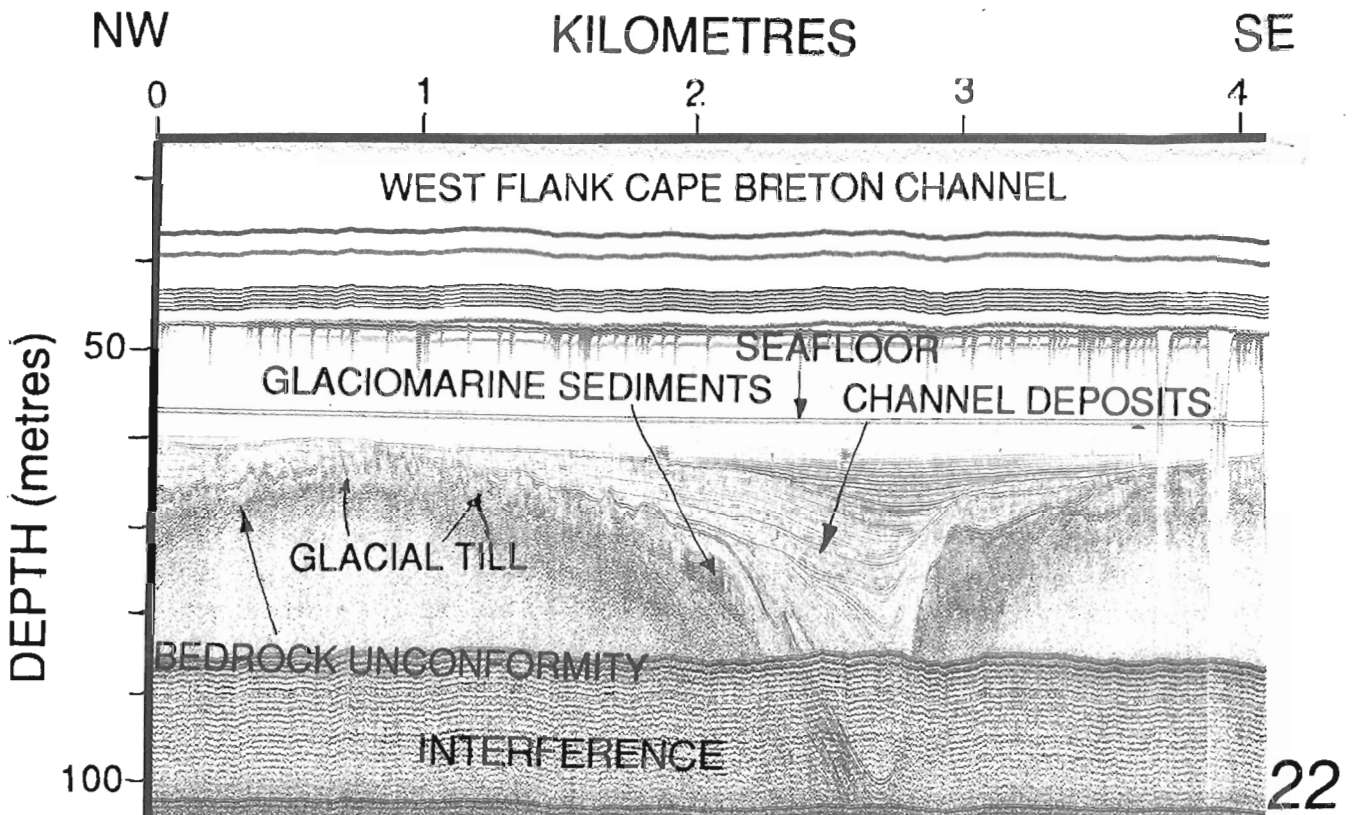
Section 19. 100 kHz sidescan sonogram located 30 km northwest of East Point, Prince Edward Island illustrating a field of large asymmetric sand waves with a maximum crest to trough height of 11 m. The comet marks indicate dominant current flow to the east-southeast. See Figure 1 for location.



Section 20. 75 kHz sidescan sonogram located 10 km north of Cape North, Cape Breton Island illustrating intense reworking of the seafloor by bottom trawling activity. Many of these trawl marks have incised the muddy seafloor to a depth of 1.5 m. See Figure 1 for location.



Section 21. Huntex DTS profile of part of a 50 km wide and 200 km long paleo-channel(?) system located between Prince Edward Island, Cape Breton Island and the Magdalen Islands. Much of the extensive channel system has been eroded by glacial activity and bottom currents, but isolated remnants of channel deposits up to 50 m thick which are cut to a base level 140 m below present day sea level, occur in places throughout this large paleodrainage system. See Figure 1 for location.



Section 22. Huntex DTS profile of an isolated channel deposit which is part the same paleochannel(?) complex shown in section 21. Note that the channel deposits are conformably draped over seismic units interpreted as glacial till and glaciomarine sediments. The conformable relationship suggests that the channel is associated with glacial activity. The channel may have formed subglacially. See Figure 1 for location.

A preliminary report on contrasting structural styles of gold-only deposits in western Newfoundland

Benoît Dubé
Quebec Geoscience Centre, Quebec

Dubé, B. A preliminary report on contrasting structural styles of gold-only deposits in western Newfoundland; in *Current Research, Part B, Geological Survey of Canada, Paper 90-1B*, p. 77-90, 1990.

Abstract

Preliminary field investigations suggest that western Newfoundland gold-only deposits can be morphologically divided into two main types: i) Disseminated stratabound sulphide gold deposits (DSSG); and ii) Mesothermal vein type. The former is subdivided into two subtype: 1) DSSG in silicified rocks (Hope Brook); and 2) DSSG in sedimentary rocks (Nugget Pond); and the latter is subdivided into 1) quartz vein type (Cape Ray) and 2) altered wallrocks type (Stog'er tight). The influence of structural control on gold mineralization varies from deposits which do not exhibit any significant structural control (Nugget Pond), to deposits which seem more deformed by a major fault zone then genetically related to it (Hope Brook mine), and to deposits genetically related to shear zone (Cape Ray). The latter appear to be located in second order structures or Splays associated with major fault zones.

Résumé

Des travaux de terrain préliminaires indiquent que les gîtes aurifères de la partie ouest de Terre-Neuve peuvent être morphologiquement répartis en deux principaux types: 1) gîtes aurifères stratoides de sulfures disséminés (OSSD); et ii) gîtes mésothermaux de type filonien (GMTF). Le premier type se subdivise en: i) OSSD encaissé dans des roches silicifiées (Hope Brook) et 2) OSSD encaissé dans des roches sédimentaires (Nugget Pond), tandis que le second se subdivise en: 1) GMTF compris dans des veines de quartz (Cape Ray) et 2) GMTF compris dans les épontes altérées (Stog'er tight). L'influence du contrôle structural sur les minéralisations aurifères varie de dépôts qui ne montrent pas de contrôle structural significatif (Nugget Pond), à des dépôts qui semblent plutôt déformés par une zone de faille majeure que génétiquement liés à celle-ci (mine Hope Brook), ainsi qu'à des dépôts qui sont liés à des zones de cisaillement (Cape Ray). Ces derniers sont situés dans des structures de deuxième ordre associées à des zones de failles importantes.

INTRODUCTION

Historically, gold in the Canadian Appalachians was synonymous with quartz veins hosted in Meguma sedimentary rocks in Nova Scotia (Graves and Zentilli, 1982) and auriferous placers in the Quebec Eastern Townships (Gauthier et al., 1989). Recent significant new gold deposits have been found elsewhere in the Canadian Appalachians (Fig. 1, Table 1). In Newfoundland, these include the Hope Brook Mine (the 12th largest Canadian gold producer in

Table 1. Major gold-only deposits and occurrences in the Canadian Appalachians.

NOVA SCOTIA		
<u>Major past producers</u>	Million tonnes (rock crushed)	Grade g/t Au
Goldenville district	0,55	12
Upper Seal Harbour	0,44	4,07
Caribou district	0,19	17
Waverley Gold district	0,16	15,43
Montague Gold district	0,13	17,14
Oldham district	0,12	25
Renfrew Gold district	0,07	27
<u>Major Prospects</u>	Million tonnes	Grade g/t Au
Mooseland	1,86	13,37
Golboro	5.06	6,50
NEWFOUNDLAND		
<u>Deposits</u>	Million tonnes	Grade g/t Au
Hope Brook mine	11,2	4,54
Cape Ray	0,89	7,54
Nugget Pond	0,51	14,13
<u>Major Prospects</u>	Examples of results	
Stog'er tight	DDH : 6,86 g/t over 8,2m	
Deer Cove	Adit : 16,1 g/t across 1,5m over 30m.	
Lightning zone	DDH : 11,14 g/t over 6,3m	
Rendall-Jackman	Trench 12,87 g/t across 3,7m over 70 m	
Rattling Brook	1,23 g/t across 54,5m over 250m	
NEW BRUNSWICK		
<u>Deposits</u>	Million tonnes	Grade Au g/t
Elmtree	0,35	4,46
Cape Spencer mine	0,55 (proven)	2,50
	0,23 (possible)	2.26
QUEBEC		
<u>Placer</u>		
Estimated production from the Beauceville placer is 1,5 tons of gold (Gauthier et al., 1989)		
<u>Prospects and showings</u>	Example of results	
Bellechasse-Timmins	Bulk sample: 2,06 g/t Au over 34m	
Lac Arsenault	DDH : 48 g/t Au over 1,2m	

1988; Northern Miner, July 24, 1989), the Cape Ray deposit, the Nugget Pond deposit and many significant gold prospects in the Baie Verte and Springdale peninsulas. In Nova Scotia, the former producing Mooseland and Golboro properties are promising and Inco Gold is exploring an interesting auriferous quartz vein system on Cape Breton Island. In New Brunswick, the Cape Spencer mine and the Elmtree deposit are the most important discoveries to date. In Québec, the lac Arsenault (Roy and Valiquette, 1987) and especially the quartz vein Bellechasse-Timmins gold prospect represent important gold occurrences.

In 1989, the author initiated a long-term project on structure and gold deposits in the Canadian Appalachians with emphasis on Newfoundland. The project is integrated in a Geological Survey of Canada team effort studying gold mineralizing processes and their relationships to major fault zones in various regions of Canada. This paper summarizes some of the results of fieldwork by the author during the summer of 1989 on gold deposits and occurrences in Western Newfoundland. Particular emphasis is given to the Hope Brook mine and the Cape Ray deposit. The different styles and types of gold mineralization and the major structural characteristics of the gold deposits are presented along with a preliminary morphological classification.

GOLD DEPOSITS IN NEWFOUNDLAND

Historically, the primary source of gold in Newfoundland was the volcanogenic massive sulphide deposits (Tuach et al., 1988), but, following the recent discoveries of many significant gold occurrences of different types and the recognition that many of those are associated with major faults (Tuach, 1987), systematic exploration for gold-only type of deposits is now underway. Gold-only deposits in Newfoundland show contrasting structural characteristics and can be morphologically divided into two major types: i) disseminated stratabound sulphide gold deposits; and ii) mesothermal vein type.

Dissiminated stratabound sulphide-gold deposits (DSSG)

In this type of deposit the mineralized zone is stratabound, not related to adjacent veins and contains disseminated gold associated with relatively abundant sulphide (pyrite) (5-20 %). On the basis of host rock characteristics, this type of deposit can be subdivided into: 1) DSSG in silicified host rocks; and 2) DSSG in sedimentary rocks.

1) Dissiminated stratabound sulphide-gold in silicified rocks: The Hope Brook mine

The Hope Brook mine, the only producing gold mine in Newfoundland, is located at the northeast end of the Cinq Cerf fault zone (CCFZ), in the southwestern part of Newfoundland (Fig. 2). The CCFZ is a 5 km long and 500 m wide high strain zone which separates the Silurian La Poile Group (mainly felsic pyroclastic and conglomerates) from Precambrian- Cambrian unnamed phyllitic units that host the gold mineralization (Fig. 3) (O'Brien, 1989). The Devonian Chetwynd granite truncates all the units, postdates the alteration zone and has a thermal metamorphic aureole

MAJOR GOLD-ONLY DEPOSITS AND OCCURRENCES IN THE CANADIAN APPALACHIANS

NEWFOUNDLAND

1. Baie Verte Gold Deposits
2. Nugget Pond
3. Rendell-Jackman (Hammer Down)
4. Browning Mine, Unknown Brook
5. Rattling Brook
6. Hope Brook (Chetwynd)
7. Cape Ray

NOVA SCOTIA (GOLD DISTRICT)

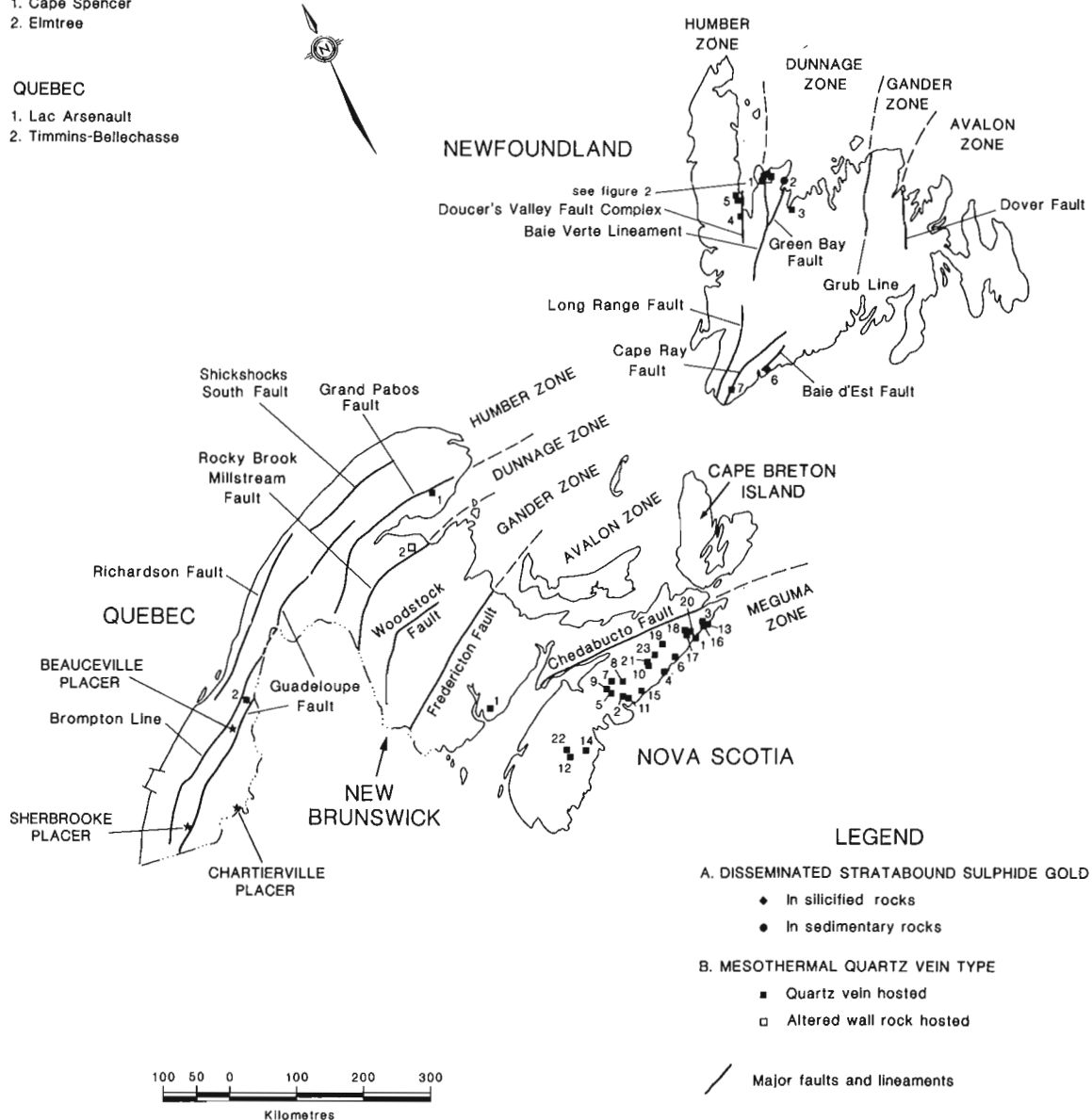
- | | | | |
|-----------------------|-----------------------|-----------------------|----------------|
| 1. Wine Harbour | 8. Oldham | 15. Lake Catcha | 22. Brookfield |
| 2. Waverly | 9. Mount Uniacke | 16. Isaacs Harbour | 23. Beaver Dam |
| 3. Upper Seal Harbour | 10. Moose River | 17. Goldenville | |
| 4. Tangler | 11. Montague | 18. Forest Hill | |
| 5. South Uniacke | 12. Molega | 19. Fifteen Mile Str. | |
| 6. Salmon River | 13. Lwr. Seal Harbour | 20. Cochrane Hill | |
| 7. Renfrew | 14. Leipsigate | 21. Caribou | |

NEW BRUNSWICK

1. Cape Spencer
2. Elmtree

QUEBEC

1. Lac Arsenaault
2. Timmins-Bellechasse



Modified from Map No. 4 (1982), Memorial University of Newfoundland (Duncan Keppie, coordinator; and 1989 revised version of Map 87-04 by Tuach, Newfoundland Department of Mines.

Figure 1. Major fault zones and spatial distribution of gold-only deposits and major occurrences in Canadian Appalachians. Modified from map No 4, 1982, Memorial University of Newfoundland, Duncan Keppie coordinator and from a 1989 revised version of Tuach's Map 87-04 of Newfoundland Department of Mines.

TYPES OF GOLD DEPOSITS AND MAJOR OCCURRENCES
IN NEWFOUNDLAND

LEGEND

- 1- GOLD-ONLY DEPOSITS
- A. DISSEMINATED STRATABOUND SULPHIDE GOLD
- 1) IN SILICIFIED ROCKS
- ◆ Major
 - ♦ Prospect
- 2) IN SEDIMENTARY ROCKS
- Major
- B. MESOTHERMAL QUARTZ VEIN TYPE
- 1) QUARTZ VEIN HOSTED
- Major
 - Prospect
- 2) ALTERED WALLROCK HOSTED
- Major
- x Unclassified significant occurrences
- 2- BYPRODUCT FROM MASSIVE SULPHIDE DEPOSITS
- ▲ Major deposit with significant Au
 - △ Accessory Au with base metals; deposits and occurrences

- Ultramafic rocks
- Faults, fractures, thrusts
- Lineaments and major faults

Modified from 1989 revised version of Map 87-04 by Tuach, Newfoundland Department of Mines.

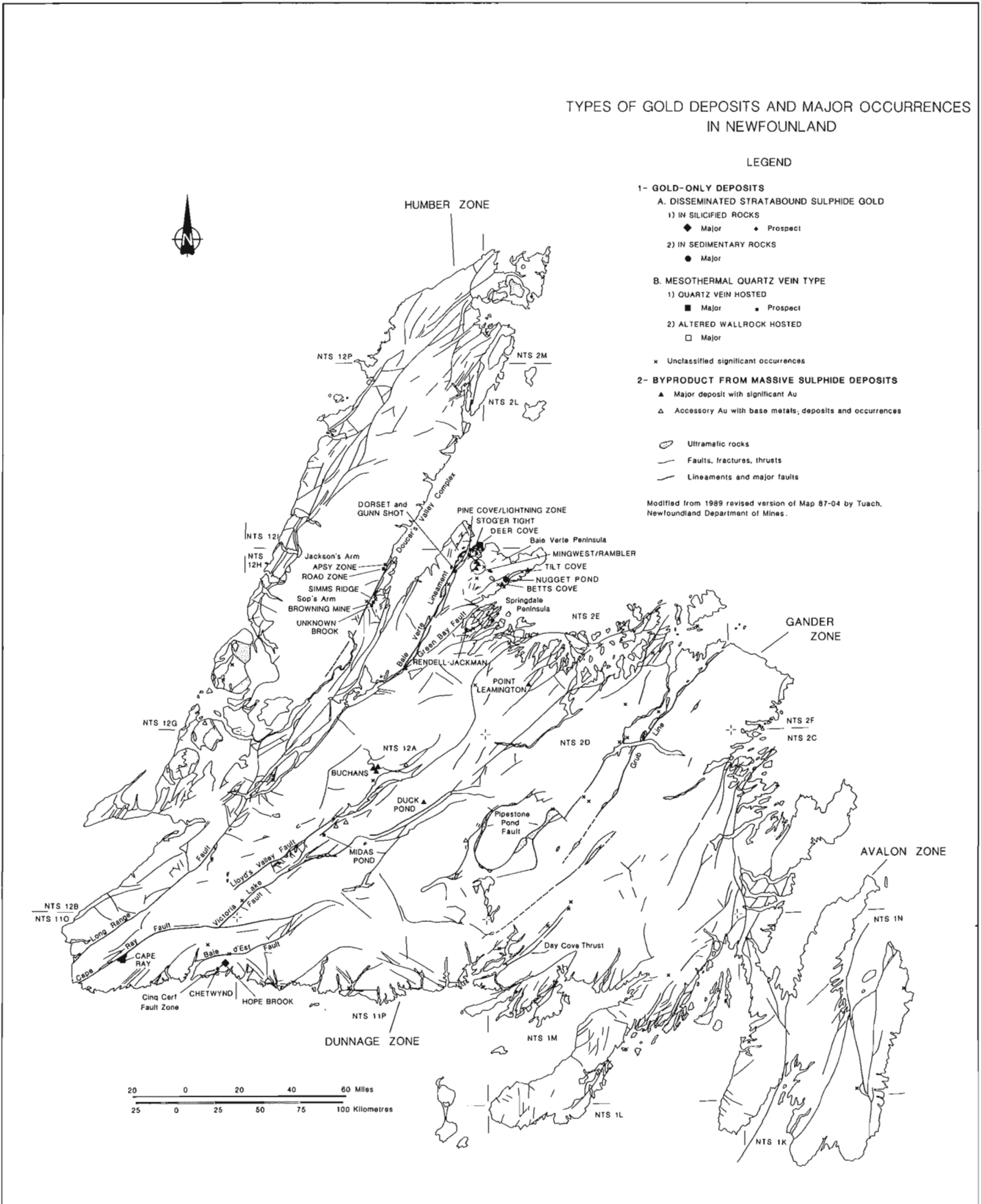


Figure 2. Distribution and classification of gold-only deposits and occurrences in Newfoundland, with emphasis on their relation to major fault zones. Modified from a 1989 revised version of Tuach's Map 87-04 of Newfoundland Department of Mines.

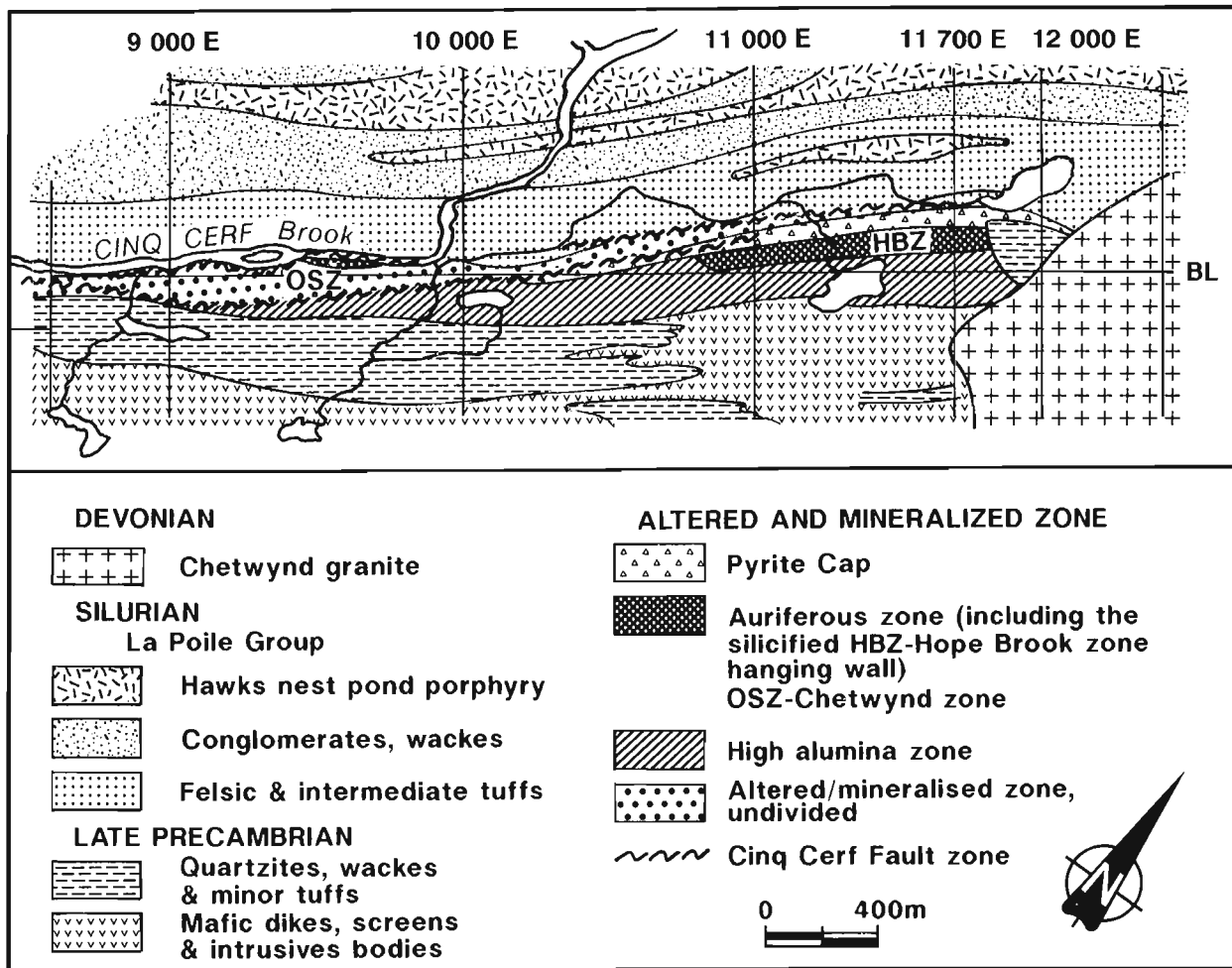


Figure 3. Geology of the Hope Brook area. Modified from McKenzie (1986) using data available from Dunning and O'Brien (1989) and from P.W. Stewart and others (pers. comm.)

which has produced hornfels. The Hope Brook deposit has been studied, among others, by McKenzie (1986), Yule (1988), and Stewart and Stewart (1988) using data from drill core, outcrop and trenches. The descriptions below summarize two weeks of detailed underground mapping.

Deposit stratigraphy

Five different units have been observed underground: the silicified and pyritized unit, the altered aluminous hanging-wall, the footwall mylonite, the Chetwynd granite and various mafic dykes (Fig. 4). The silicified and pyritized unit has a lateral extent of at least 1 km, an average width of 120 m and a minimum thickness of 400 m. This unit can be subdivided into three sub-units: 1) the ore zone (30-35 m), 2) the so-called footwall "pyritic cap" (50-60m), and 3) the silicified hangingwall (25-30m) (Fig. 3, 4). Underground, it is relatively difficult to visually recognize these different units without prior knowledge of the gold cut off grade of 2 g/t which defines the limit of the ore zone. The three relatively massive grey to light grey-beige sub-units are characterized by the presence of blue quartz eyes (1-5%), small rutile grains (2-3%), and a generally weak foliation. Pyrite is present in all of the sub-units, but is more abundant in the ore zone (1-10%) and in the pyritic cap (1-25%). The pyrite occurs as fine disseminated grains or, more commonly, in millimetre wide veinlets sub-parallel to the folia-

tion. Small vugs are present in all the silicified rocks but they are more abundant in the ore zone. Chalcopyrite occurs locally in the ore zone associated with pyrite or in small aggregates. White to beige "fragments", are present in the ore zone but they are more abundant in the pyritic cap. These "fragments" comprise 5 to 25% of the rock and contain common blue quartz eyes. The original nature of the "fragments" is unknown but some resemble pumice, suggesting a felsic pyroclastic protolith as presented by McKenzie (1986). Alternatively they may result from different intensities or types of alteration as proposed by Yule (1988).

The footwall mylonite is in fault contact with the pyritic cap (Fig. 4). This mylonite zone contains a relatively well defined tectonic banding characterized by metre to millimetre scale bands of different lithologies varying from mafic to intermediate to felsic quartz-sericite-pyrite schists. Some quartz-feldspar porphyry and mafic dykes or sills are also present. Elongate blue quartz eyes (2-3 mm, $\leq 3\%$) are common. Metre- to centimetre-scale silicified and pyritized fragments of the pyritic cap have been tectonically incorporated into the mylonite and are observed as far as 20 m from the contact with the base of the pyritic cap (Fig. 4). Many metre-wide quartz-sericite-pyrite schist bands, present over a thickness of 40 m, are thought to represent strongly deformed, silicified and pyritized equivalents of the main silicified-pyritized zone. The latter schists bands are

HOPE BROOK

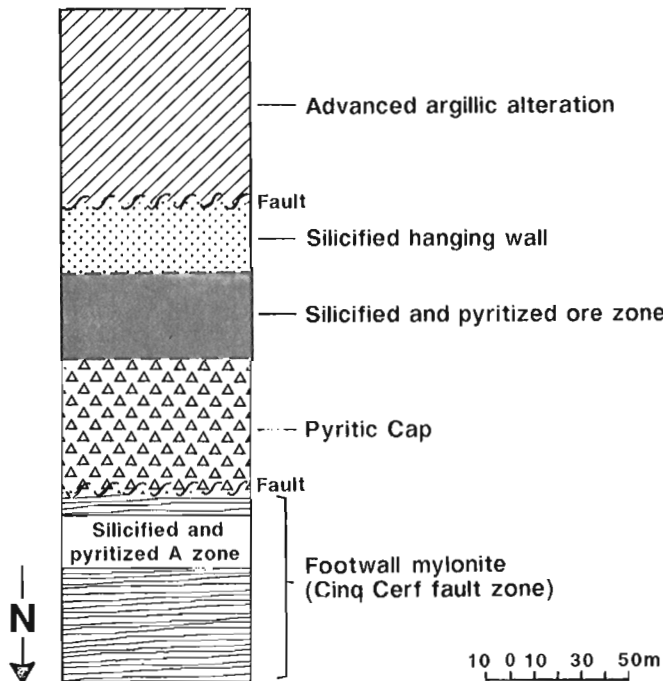


Figure 4. Schematic section showing the distribution of the alteration zone at Hope Brook.

equivalent to the "A" zone (Swinden, 1984) which hosts the Chetwynd showings located farther west.

Structure

The structural features observed underground suggest, as proposed by McKenzie (1986), that all the rocks, except the Chetwynd granite, have been strongly deformed under coaxial strain by the CCFZ. This was followed by an oblique to strike slip movement along pre-existing discontinuous planes and by late discordant oblique brittle faults. A strong NE-trending foliation is present in the mylonite footwall (Fig. 5a). Whereas the silicified rocks are more competent and the foliation is generally weak or absent except near the contacts with the mylonitic footwall and the aluminous hangingwall where a good foliation is commonly present. In the silicified rocks, the orientation of pyrite veinlets is also sub-parallel to the main NE foliation (Fig. 5b). The "fragments" present in the "pyritic cap" have been flattened and are sub-parallel to the foliation. All the mafic dykes observed have been deformed such that the contacts between the dykes and the silicified rocks are always sheared or faulted, and oblique to sub-horizontal striations are commonly present (Fig. 5c). These sheared contacts are sub-parallel to the main foliation (Fig. 5c). The ductility of the mafic dykes and the competency contrast with the surrounding silicified rocks have favored the localization of high strain shears and faults in the dykes. Local mineral lineations measured on the foliation planes have a shallow NE plunge and are related to an oblique movement (Fig. 5d). The contact between the pyritic cap and the footwall mylonite is a discrete ductile fault whereas the contact between the silicified and the aluminous altered hangingwall is a fault breccia 1 m wide. Both tectonic contacts are sub-parallel to the main NE foliation.

Centimetre to metre scale folding has been observed in the mylonite footwall. These folds generally have a southward vergence, although some with northward vergence are also present. The poles to folded NE foliation are distributed along a poorly defined great circle (Fig. 5e) having a pole with a northeast plunge of 60° . The measured plunge of the folds is also to the east but is shallow and sub-parallel to the lineation measured on the foliation (Fig. 5f). On the 4960 level these folds are located in the immediate vicinity (2-3 m) of the Chetwynd granite, suggesting that, locally, the emplacement of the granite may have been responsible for the folding. However, other folds are spatially and genetically associated with local normal faults.

In the mylonite zone an early crenulation sub-parallel to lineation in the foliation and plunging to the east is commonly cut by a younger crenulation lineation plunging to the west (Fig. 5d). Ductile-brittle faults are common in the mylonite zone and also occur locally in the silicified-pyritized altered rocks (Fig. 5g). These faults are mainly sub-parallel to the NE foliation, but a major discordant fault, oriented at $250^\circ/78^\circ$, and minor E-W faults are also present locally. The faults are strike-slip to oblique-slip and steps observed on them suggest an overall sinistral movement on the NE faults and a dextral one on the E-W faults. Measured striations on the fault planes are sub-parallel to the measured hinge and to the lineations measured on the NE foliation (Fig. 5g) suggesting that they are related to the same oblique to strike-slip structural event. Late joints and brittle faults are present in all the units. The main joint set is oriented at $113^\circ/78^\circ$, another set is oriented at $354^\circ/76^\circ$ and a few others at 200° with shallow to steep dip (Fig. 5h). Striations and steps observed on the minor brittle fault planes suggest oblique dextral and sinistral movement (Fig. 5i).

Various genetic models have been suggested to explain the genesis of the Hope Brook deposit. Yule (1988) is in accord with McKenzie (1986) that this is an epithermal type of deposit, whereas Stewart and Stewart (1988) proposed that the mineralization and the alteration are fault controlled and related to the CCFZ. P.W. Stewart with others (pers. comm.) suggested that thermal and hydrothermal processes associated with the Chetwynd granite have probably played an important role in the formation of economic gold mineralization. The Hope Brook deposit shows similarities with Romberger's (1986) disseminated gold sub-type of epithermal deposit. The size and the grade of the deposit fits relatively well as do typical geological characteristics such as finely dispersed gold in rocks where little or no fabric control on mineralization is apparent, a strong silicification, a close association between gold and pyrite and a low abundance of base metals. The present rock sequence (apparent stratigraphy) cannot be used with full proof to reconstruct the geological environment of formation of the deposit and to fit the asymmetrical alteration pattern with the theoretical epithermal model. All the rocks, except the Chetwynd granite, have been deformed and possibly transposed, so the actual geometric relationships are probably less influenced by primary or secondary hydrothermal processes than by subsequent tectonic events.

2) Disseminated stratabound sulphide gold in sedimentary rocks

The Nugget Pond deposit (Bitech and Equity Silver Mines) is the only significant example of this type in the Canadian

HOPE BROOK Mine

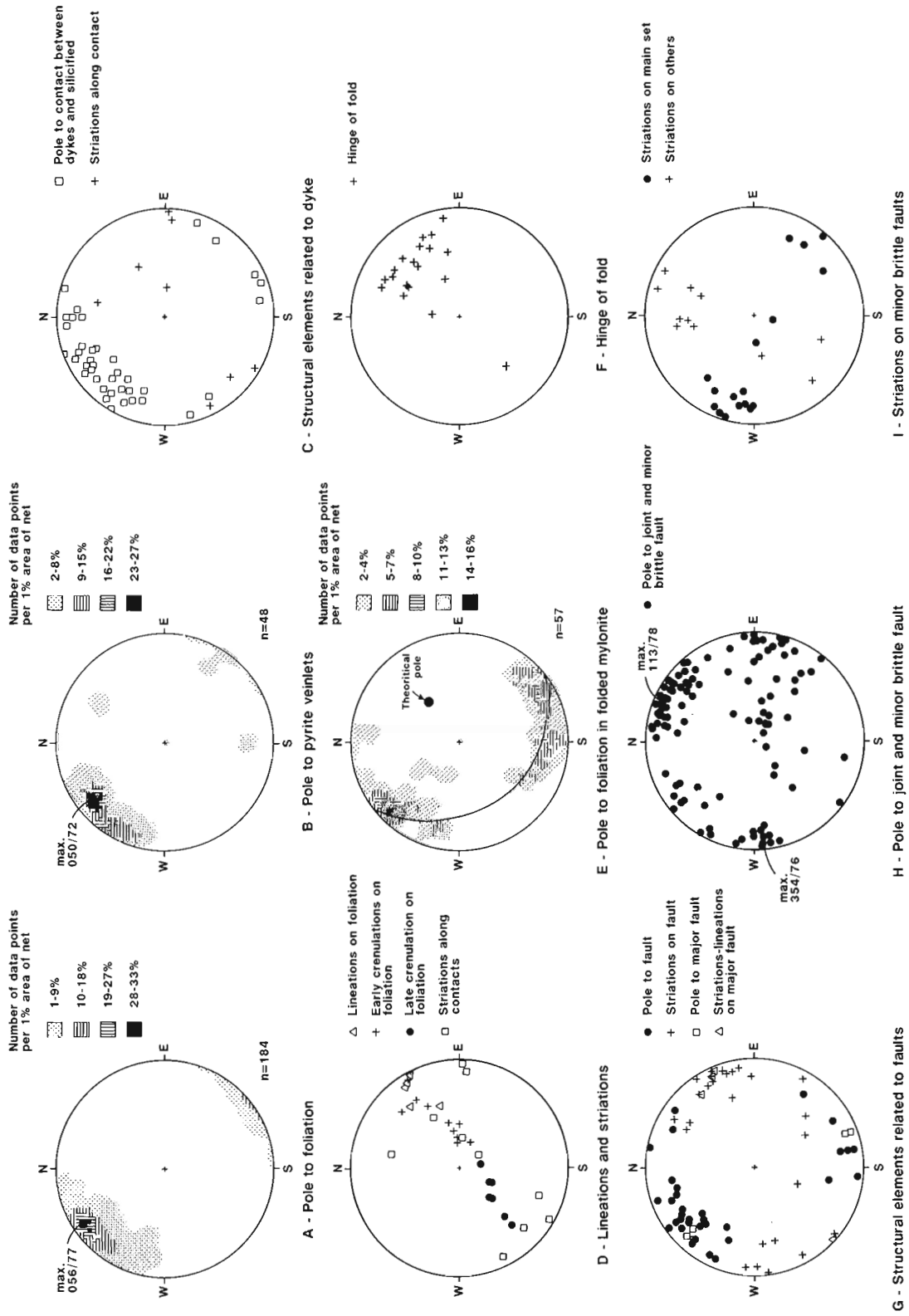


Figure 5. Equal area projections (lower hemisphere) of structural elements from Hope Brook.

Appalachians (Fig. 1). Geological reserves are reported to be 513 744 tonnes grading 14,13 g/t Au (Northern Miner, 4/09/89).

The mineralization at Nugget Pond occurs in a clastic sedimentary interval within pillow lavas of the Betts Cove (ophiolitic) Complex. The sedimentary sequence comprises, in ascending stratigraphic order, undeformed red siltstone (3 to 5 m), banded sediments (3 m) characterized by centimetre-scale beds of red siltstone alternating with green sandstone, an undeformed green sandstone containing traces of pyrite grains (3 m), a dark green to black "shaly" siltstone overlain by an undeformed banded sequence (10 to 15 m thick) of green, locally cherty, sandstone-siltstone and graded greywacke. Overlying the latter sedimentary sequence is a medium-grained green unit containing feldspar phenocrysts.

Gold mineralization occurs in two different zones. A lower grade zone in the red-green siltstone located near the base of the sedimentary sequence and containing coarse (2-5mm) pyrite cubes and, a higher grade zone in the dark green to black bedded "shaly" siltstone (McBride, 1989). The latter zone contains 20 to 25 % pyrite as veinlets sub-parallel to the bedding and also cross-cutting it locally. Small millimetre scale folds were locally noted in the pyrite veinlets. Locally, the mineralized zone is unusually chloritized, contains 25 % pyrite veinlets, and its host rocks are locally deformed with a relatively intense schistosity. It is not yet known whether this deformation is local or widespread, or whether it is synchronous with the gold mineralization or a later event superimposed on it.

The Nugget Pond deposit has been interpreted by McBride (1989) as syngenetic and associated with volcanogenic exhalative processes related to circulating seawater. According to this model, the gold was leached by the circulating hydrothermal fluid and deposited as a sedimentary exhalite. More information is needed in order to present a definite genetic model for the Nugget Pond deposit, but there is no doubt that the mineralization is stratabound, hosted by an undeformed sedimentary sequence and associated with pyrite grains, veinlets and layers. It is interesting to note that minor occurrences of pyritized black shale with anomalous gold values located at the base of a clastic sediment sequence (the Ordovician Beauceville Formation) are also reported in the Eastern Townships, Quebec (Castle Brook and Rapides du Diable) (Gauthier et al., 1989).

Mesothermal vein type

The mesothermal vein deposits are the most common type of gold-only mineralization in Newfoundland and are similar to many lode gold deposits in the Archean Abitibi greenstone belt. This type of deposit is genetically related to structural deformation. The mesothermal vein type of deposit can be subdivided into 1) a quartz vein type in which the gold mineralization occurs mostly in quartz veins (Cape Ray, Deer Cove) and 2) an altered wallrock type in which the mineralization occurs as disseminations in adjacent altered wallrocks (Stog'er tight).

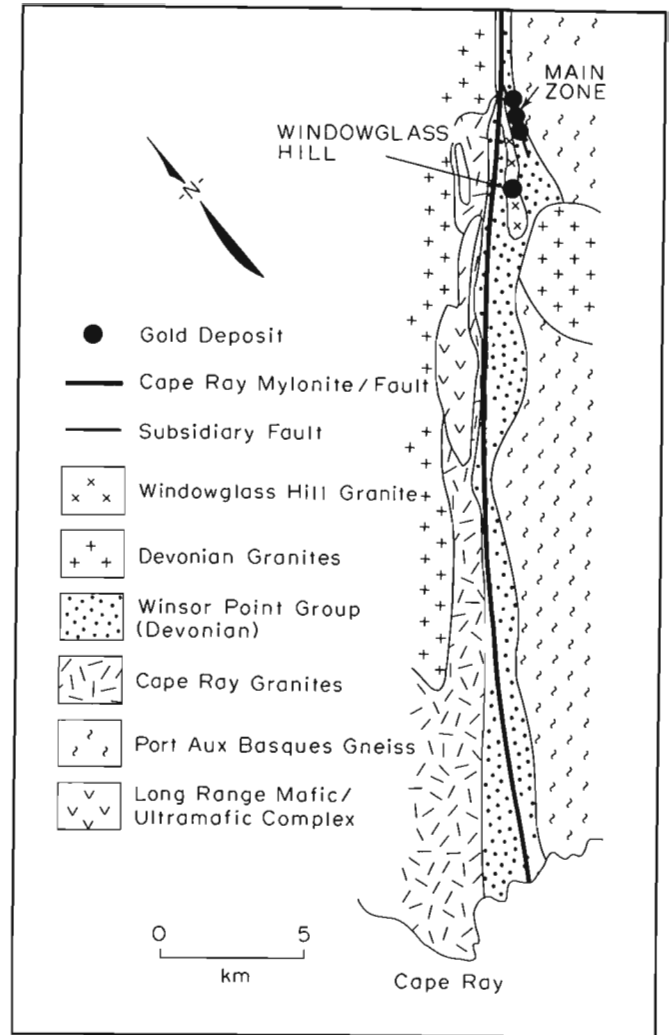


Figure 6. Simplified geological map of the Cape Ray Fault Zone showing location of the gold deposits. From Tuach et al. (1988); after Wilton (1983) and Tuach (1986).

1) Quartz vein type of mesothermal gold deposit

Cape Ray deposit

The Cape Ray deposit is located within the Cape Ray fault zone in the southwest part of Newfoundland. The Cape Ray fault is a 100 km long fault zone which juxtaposes extensive terranes of Ordovician tonalite, isolated remnants of the Long Range ophiolitic complex, the Cape Ray granite, and Devonian granite to the northwest of the fault zone with the Port Aux Basques Complex (gneiss) and the Windowglass Hill granite to the southeast (Wilton, 1983) (Fig. 6). The Devonian Windsor Point Group is located between these two terranes and has been strongly deformed. The mineralization occurs in galena and chalcopyrite-rich quartz veins most of which are hosted by shear zones within the Windsor Point Group. The deposit consists of three mineralized zones (4, 41 and 51) occupied in the same structure and known as the main zone. Other significant auriferous quartz veins and stockworks occur in the Windowglass Hill granite (Wilton, 1983).

CAPE RAY SCHEMATIC SECTION

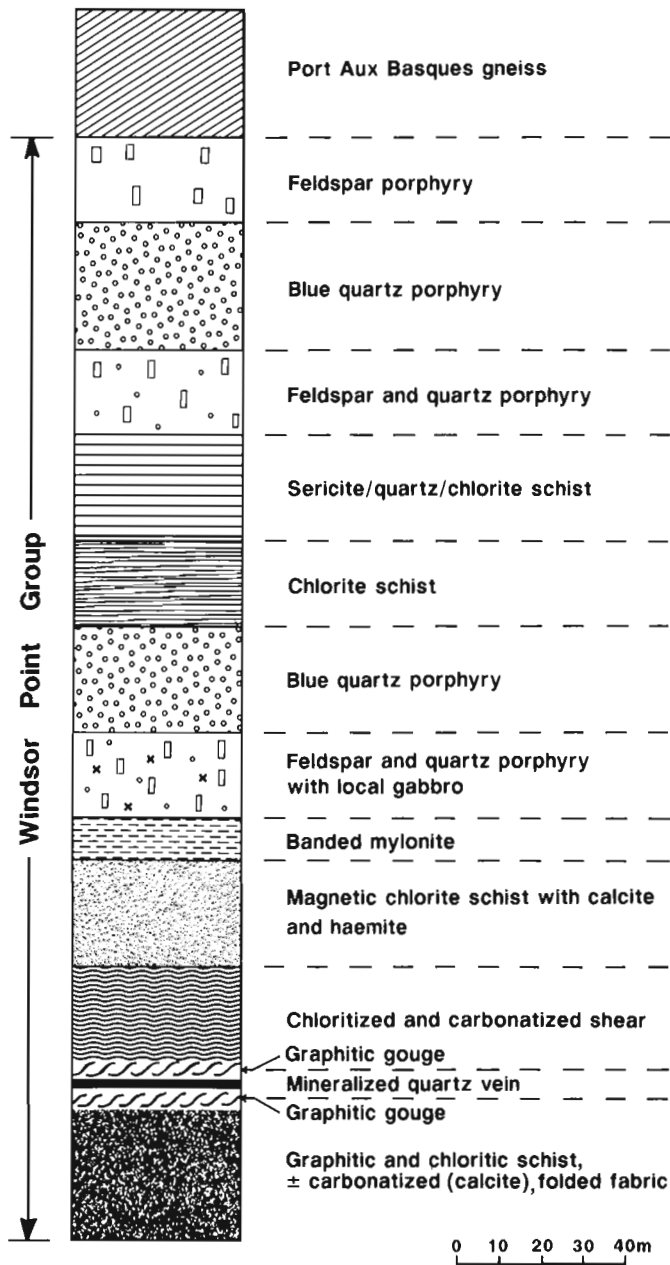


Figure 7. Schematic section of the main mineralized zone at the Cape Ray deposit. Based on this study and discussions with Bud James (Dolphin Explorations). Thicknesses may vary.

Deposit stratigraphy

A schematic section across the main mineralized zone shows a relatively gradual transition from the deformed amphibolitic Port aux Basques gneiss to greenschist metamorphosed rocks of the Windsor Point Group (Fig. 7). The Windsor Point Group consists of various porphyry units, sericite-chlorite schists and chloritic shear zones containing various proportions of calcite, magnetite and graphite. Carbonatization (calcite) typically increases close to the ore zone. A green to pale green-grey pervasively carbonatized chlorite shear zone, that commonly contains leucoxene (suggesting a gabbroic protolith), is in contact with a brittle graphitic

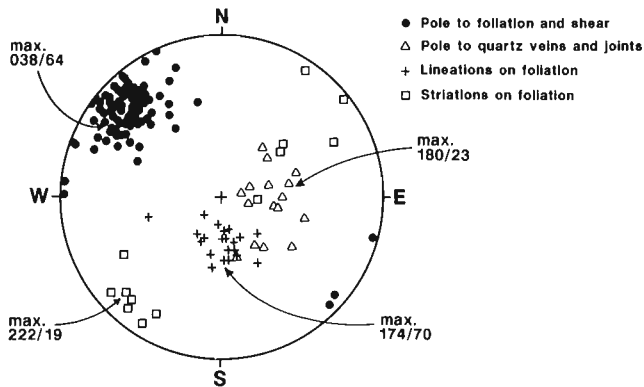
and chloritic fault gouge. This brittle gouge fault marks the boundary between the mineralized quartz vein with both the hangingwall and the footwall. The fault gouge ($\leq 2\text{m}$) contains small fragments of quartz veins and chloritized-carbonatized rock. The mineralized quartz vein (known as the A vein) contains variable proportions of sulphides (3-5%), mainly galena and chalcopyrite, and is strongly fractured and deformed. The footwall rocks are mainly composed of banded, folded and locally brecciated black graphitic and chloritic schist, with local quartz \pm sulphide veins, chloritic and carbonatized sheared mafic rocks containing local leucoxene and local beige (sericite-rich) bands. At least three mineralized quartz veins (a few centimetres to 1m) are present in the footwall of the 41 zone. These veins are discontinuous and located above, or below, millimetre-scale brittle faults (gouge) oriented at $065^\circ/35^\circ$. They are sub-parallel to the faults and spatially associated with locally mineralized quartz stockwork or breccia zones.

Structural setting

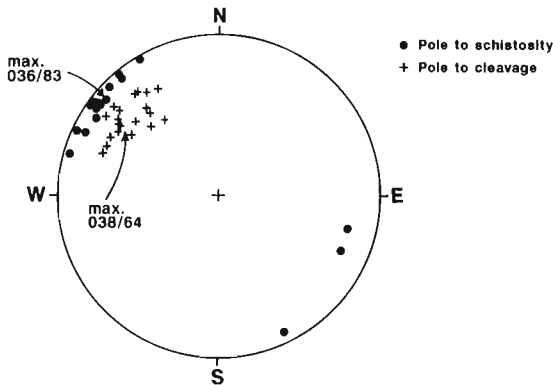
Detailed underground structural mapping reveals that the hangingwall of the mineralized fault zone is characterized by an oblique-reverse ductile high strain zone with layer-parallel overthrusting to the northwest, followed by late brittle oblique to strike slip movements. The high strain zone is typified by an intense foliation oriented $038^\circ/64^\circ$ (Fig. 8a) and many sub-parallel metre scale shear zones hosting quartz veinlets (Fig. 8a). Non-coaxial deformation is suggested by C-S fabrics in the highly deformed quartz/sericite schist and the chlorite schist. The angular relationship shows that the schistosity (S) planes dip more steeply than the C planes (Fig. 8b). Poorly developed mineral elongation lineations are locally present on the foliation plane. Their steep plunge ($174^\circ/70^\circ$) combined with the C-S fabric confirm the oblique-reverse movement. Also, local, probably syn-shearing, micro-folding of the foliation shows a northwest vergence. Sub-horizontal to shallowly dipping quartz-calcite veins and joints (Fig. 8a) oriented at $180^\circ/23^\circ$ are also compatible with the oblique-reverse movement. These are approximately normal to the main northeast foliation but not perfectly perpendicular to the lineations in the foliation. Local down-dip crenulation lineations are sub-parallel to the mineral lineations. Numerous brittle faults characterized by millimetre-scale gouge planes are also present in the high strain hangingwall. Some are oriented sub-parallel to the foliation but most are oblique to it and dip at shallow angles to the east, or to the west (Fig. 8c). Movement along these faults is generally small ($\leq 1\text{m}$) and reverse. The faults disrupt the foliation but are also disrupted by it, suggesting their contemporaneous relationship to the high strain zone. Local shallow plunging SW or NE striations (average at $222^\circ/19^\circ$) present on the fabric and shear planes are probably related to late oblique to strike slip movement in the high strain zone.

The mineralized fault zone (zone "A") shows a 6m wide zone of intense faulting characterized by numerous graphitic and/or chloritic gouge zones and sheared chloritic rocks. Like the high strain zone, the fault zone is characterized by an oblique-reverse movement followed by an oblique to strike slip displacement which probably is responsible for the deformation of the shear hosted mineralized veins. The contact with the hangingwall and the footwall is sharp and the main orientation of the fault zone is $045^\circ/57^\circ$, but

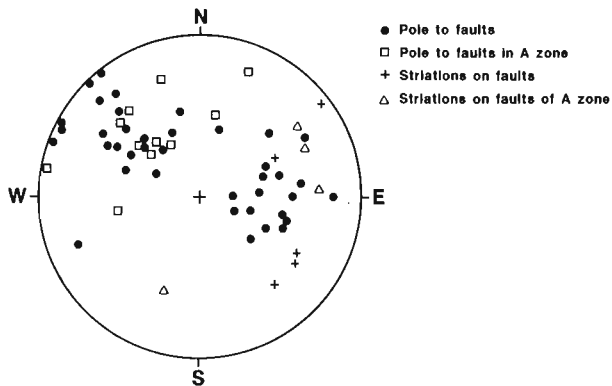
CAPE RAY DEPOSIT



A - Structural elements of the high strain hanging wall



B - C-S fabrics observed in the hanging wall



C - Faults measured in the hanging wall and in the mineralized A zone

Figure 8. Equal area projections (lower hemisphere) of the high strain hangingwall and the mineralized fault zone at Cape Ray.

numerous oblique shallowly-dipping reverse brittle faults oriented $350^{\circ}/30^{\circ}$ and $050^{\circ}/30^{\circ}$ are also present within the fault zone. Inside the fault zone, the material is chaotic but locally a consistent schistosity oriented $040^{\circ}/85^{\circ}$ suggests a reverse movement. In the study area, the fault zone contains local centimetric fragments of deformed and fragmented quartz veins oriented sub-parallel to the fabric and containing traces of chalcopyrite. Centimetre-scale folds located along the discrete fault planes observed within the fault zone have NE moderately plunging hinges ($040^{\circ}/50^{\circ}$, $045^{\circ}/56^{\circ}$) and show a westward vergence compatible with

the reverse component of movement. A few striations on the schistosity or fault plane plunge moderately to weakly to the east or to the west suggesting that the latest movement was oblique to strike-slip. These striations are sub-parallel to the striations measured in the high strain zone.

Two different fold generations have been observed in the footwall of the "A" vein in the 41 zone. The first generation (F_1) is characterized by tight centimetre to metre-scale folds with axial plane sub-parallel to the main NE foliation. They correspond to the D_1 folds described by Wilton (1983). These folds have been refolded by metre-scale gentle to open folds (F_2) with sub-vertical E-W axial planes having fold axes plunging gently to moderately to the east or the west. In the studied area, the mineralized quartz veins and the gouge plane have been folded only by the F_2 folds. Thus the mineralization observed in the 41 zone footwall seems to have been emplaced after F_1 and before F_2 . The relationship between these mineralized veins and the folds with the main mineralized vein observed in the A zone is unknown.

The main mineralized zone of the Cape Ray deposit is located in an oblique splay of the Cape Ray Fault (Tuach, 1986) (Fig. 6). The auriferous mineralization is enclosed in sulphide rich quartz veins mostly hosted by ductile oblique-reverse shear zones located at the boundary between chloritized mafic rocks in the hangingwall and graphitic and chloritic schist in the footwall. Hydrothermal alteration associated with the auriferous fluid has produced a typical strong chloritization and carbonatization of the hangingwall with the formation of secondary magnetite. In the footwall, the alteration is mainly characterized by calcite, and chlorite, with graphite. Late brittle oblique to strike-slip movements have strongly deformed the shear hosted mineralized veins and has resulted in boudinage and brecciation of them.

Other mesothermal quartz vein gold prospects and showings

Several other quartz vein hosted gold prospects have been discovered in Western Newfoundland (Fig. 2, Table 2) particularly in the Baie Verte Peninsula, the Springdale Peninsula and the western White Bay area. All of the prospects are close to major geological structures, but localize in second or third-order structures sub-parallel to the main structure. The mineralized zones are hosted by extension veins or stockwork-breccias enclosed in lower strain rocks, and/or sheared quartz veins enclosed in high angle shear zones with vertical to oblique movement. In general, these veins are hosted by structures showing brittle to brittle-ductile behavior. These variations in ductility are, in part, related to the variation in host rock composition and corresponding competency as suggested by the Table 2. The veins are not sulphide rich like those at Cape Ray. They are mainly composed of quartz with traces of carbonate and feldspar; generally, no more than 1 or 2 % of pyrite is present. Although, the proportion of pyrite in the Lightning zone varies from trace to locally semi-massive, whereas at Rattling Brook the proportion of pyrite and arsenopyrite can reach 10 % (Saunders et Tuach., 1988). In some areas, traces of galena, chalcopyrite or specularite are also present. However, the gold content is in general directly related to the amount of sulphide, and especially, in the Baie Verte Peninsula, to the presence of coarse pyrite cubes

Table 2. Major characteristics of mesothermal quartz vein sub-type of gold-only deposits and major occurrences in western Newfoundland.

PROSPECTS AND SHOWINGS	TYPE OF QUARTZ VEIN	ALTERATION	TYPE OF DEFORMATION	SPATIAL RELATIONSHIP WITH A MAJOR FAULT	SULPHIDE	HOST ROCKS
BAIE VERTE PENINSULA						
Deer Cove	Extension vein	chlorite, \pm Fe carbonate \pm sericite, traces of green micas	Brittle-ductile	Deer Cove Thrust	\leq 1-2 % pyrite	basalt of Point Rousee Ophiolitic Complex
Dorset	Sheared vein	chlorite, \pm sericite	brittle-ductile	Baie Verte Brompton Line	\leq 1-2 % pyrite	basalt and gabbro of FlatWater Pond Group
Gunn Shot	sheared vein	chlorite, \pm Fe carbonate \pm sericite and green micas	ductile-brittle	Baie Verte Brompton Line	\leq 1 % pyrite	gabbro of FlatWater Pond Group
Lightning Zone	extension, breccia sheared veins	silicification, chlorite Fe carbonate	brittle-ductile	Scrape thrust	trace to semi- massive pyrite	tuff and mafic volcanic of Point Rousee Complex
SPRINGDALE PENINSULA						
Rendall-Jackman	sheared veins	chlorite, \pm Fe carbonate	brittle-ductile	Green Bay fault	\leq 1-2 % of pyrite	Felsic dyke and basalt
WESTERN WHITE BAY AREA						
Rattling Brook	stockwork and sheared veins	albite, K feldspar, Fe carbonate sericite	brittle-ductile	Doucers Valley Fault Complex	\leq 10 % pyrite	Proterozoic granite
Simms Ridge	sheared and extension veins	sericite, Fe carbonate green micas	ductile-brittle	Doucers Valley Fault Complex	\leq 1 % pyrite galena, chalcocopyrite	felsic dyke and calcareous slate
Unknown Brook	extension veins	sericite, Fe carbonate chlorite	Brittle	Doucers Valley Fault Complex	\leq 1 % pyrite	conglomerate
West Corner Brook	extension (en echelon)	potassic alteration Fe carbonate	brittle	Doucers Valley Fault Complex	\leq 1 % pyrite and specularite	rhyolite, porphyry tuff
Browning Mine	extension (en echelon)	Fe carbonate, sericite chlorite	brittle-ductile	Doucers Valley Fault Complex	\leq 1 % pyrite	shale and carbonate beds

(5mm-1cm). In the Baie Verte and Springdale peninsulas, the wallrock hydrothermal alteration is generally relatively weak and characterized by chloritization and carbonatization with local and small amounts of sericite, pyrite and green micas. Silicification is also present at the Lightning Zone prospect. No well-defined alteration zoning, as described in Archean examples of this type of deposits (Dubé et al., 1987), has been observed. The prospects in the White Bay area show a stronger hydrothermal alteration characterized by carbonatization (Fe-carbonate), sericitization, and potassium metasomatism. Secondary albite is also important at Rattling Brook (Saunders and Tuach, 1988).

2) Mesothermal altered wallrock gold deposits

In the altered wallrock type of gold deposit, quartz veins are a minor component (5%) and the ore zones consist mostly of altered rock containing secondary minerals such as iron carbonate, sericite, albite and pyrite replacing or growing in the host rocks. Typical examples of this type of gold deposit elsewhere include the Archean Golden Mile deposits in Kalgoorlie, Australia (Phillips, 1986). In Newfoundland, the best example is the Stog 'er tight prospect (Noranda Exploration Company Ltd and International Impala Resources) on the Baie Verte Peninsula (Fig. 2).

Because this is a relatively new discovery, few data are available. The Stog 'er tight prospect is mainly located in a differentiated gabbroic sill of the Ordovician Point Rouse Ophiolite Complex. The gold mineralization forms lenses possibly disposed in "en echelon" pattern (Huard, pers. comm. 1989). It is enclosed in slightly deformed and strongly altered gabbro flanked by sheared gabbro located in a small thrust zone (Huard, pers. comm. 1989). The typical alteration assemblage comprises up to 45% pink albite (the colour is produced by disseminated hematite), 10-15% coarse (1mm to 2cm) euhedral pyrite crystals or millimetre-sized grains in centimetre aggregates, a strong iron carbonate alteration, and the presence of sericite, chlorite and quartz. Locally, green mica (fuchsite?) associated with quartz veinlets is present. The pyrite forms coarse (recrystallized?) grains commonly spatially related to titanomagnetite grains which are altered to leucoxene (Huard, pers. comm. 1989). This relationship is typical of gold environments and has been explained elsewhere (Dubé et al., 1987). It shows the strong influence of the host rock on the formation of the alteration assemblages. According to A. Huard of Noranda Exploration (pers. comm., 1989) there is an iron carbonate-quartz alteration zone surrounding the albite-pyrite halo. Titanomagnetite, when present, can occur in the footwall and the hanging wall. It is not clear if the titanomagnetite is primary, a product of crystallization of the sill, or secondary and related to the hydrothermal alteration, but observed partial replacement of titanomagnetite by leucoxene suggests a primary origin. Quartz-carbonate extension and shear veins are present but they are generally barren. These veins are commonly located in the iron carbonate alteration zone and, in lower proportions, in the mineralized zone, where strongly albitized and pyritized wallrock fragments are inclusions in quartz veins (Huard, pers. comm. 1989). The hydrothermal alteration is spatially and genetically related to the occurrence of these quartz-carbonate veins. Evidence of folding in the mineralized zone, at least on a small scale, has been locally observed.

According to A. Huard (pers. comm., 1989), the gold mineralization is spatially associated with a small scale E-W, north dipping, south verging thrust zone, injected by quartz veins, and sub-parallel to the major Scrape thrust and to the Deer Cove thrust. The mineralization is apparently located in the hangingwall of the thrust at the contact between the mineralized host gabbro and volcanics footwall.

Thus, the gold mineralization is not directly located in a major structure. It is associated with a second-order shear or thrust, and it is obvious that the gabbroic host rock has played a key role both chemically, in the formation of the secondary alteration minerals because of its primary iron content and structurally, because of its competency. From an alteration point of view and its relationship with the gabbroic host rocks, the Stog 'er tight prospect is an analog of Archean gold mineralization described, among others, by Phillips (1986) and Dubé et al (1987).

DISCUSSION

Although the Nugget Pond deposit does not exhibit any significant structural control, and the Hope Brook mine seems to be more deformed by the major Cinq Cerf Fault Zone than genetically related to it, most other significant western Newfoundland gold-only discoveries appear, as proposed by Tuach et al. (1988), to be located in second order structures or splays associated with major fault zones. The complex deformation history of these fault zones, including probable reactivation during Paleozoic orogenic events, and/or Acadian and Carboniferous transcurrent movements, resulted in deformation of most of mineralized zones. At the district and deposit scales, gold mineralization occurs in different rock types. The disseminated stratabound sulphide gold type is associated with Precambrian felsic and aluminous altered rocks or with Ordovician clastic sedimentary sequences. The mesothermal vein type of deposits in the Baie Verte area are mainly associated with Ordovician ophiolitic mafic flows and gabbros whereas at Cape Ray, the main deposit is located at or near the boundary between Devonian altered and sheared mafic rocks and sheared graphitic rocks.

Multiple gold mineralizing events are suggested by the different types of deposits, ages of the hosting rocks and intensities of deformation. For examples, if the epithermal model for Hope Brook is correct, the mineralization is of Precambrian age, whereas the Cape Ray mineralization is probably Late Devonian (Wilton and Strong, 1986). In most cases, the gold mineralization seems to have occurred prior to end of the major orogenic events since most of the occurrences display evidence of deformation after their formation. This later deformation has also probably produced the recrystallized coarse grained euhedral pyrite observed in the Baie Verte area.

The style of deformation hosting gold mineralization in the Baie Verte area, is brittle-ductile to brittle and suggests a shallower depth of formation than in the Archean mesothermal ductile-brittle quartz vein deposits of the Canadian Shield (Poulsen and Robert, 1989). The intensity of the alteration is also generally relatively weak compared to the Abitibi Archean gold deposits. Different genetic models have been previously proposed for these deposits:

the epithermal model (Mckenzie, 1986), the granite-related model (Wilton and Strong, 1986), the listwaenite alteration model (Tuach et al., 1988) and, for the Baie Verte Peninsula, the model of sudden decompression of H₂O-CO₂ fault-zone fluids by hydrofracturing of the hanging wall (Lydon et al., 1988). With the exception of Hope Brook and Nugget Pond, most gold-only zones are related to the ascension of hydrothermal fluids in faults or sheared rocks. At a regional scale, the ultramafic altered rocks (listwaenite) located in or near major fault zones (e.g. Baie Verte Brompton Line) seem to be related to gold mineralization. But at the deposit scale, very few deposits or occurrences are spatially directly related to or hosted by listwaenites. However, the listwaenites are good indicators of the presence of major fault zones and they provide evidence that the hydrothermal fluids are the CO₂ rich which are so characteristic of Archean mesothermal gold deposits. From a regional exploration perspective, these gold-only deposits are not only of the typical quartz vein type. Gold mineralization has also been found as disseminations hosted in clastic sediments and silicified rocks. Also, the recognized relationships between gold and major lineaments is emphasized by recent gold discoveries made by the Noront/Noranda joint venture along the Gander River Ultramafic Belt (Northern Miner, 18/09/89).

This preliminary report on gold-only deposits in Western Newfoundland shows the contrasting structural influence on the genesis of the gold mineralization. It varies from deposits which do not appear to be related to any significant structural control (Nugget Pond), to shear zone hosted type deposits (Cape Ray) and to deformed deposits (Hope Brook). The impressive number of significant gold discoveries made in the last 10 years suggests a great potential for gold in Newfoundland and for geologically equivalent areas elsewhere in the Canadian Appalachians.

ACKNOWLEDGMENTS

The author expresses his thanks to I. MacWilliams and J. Harris of Hope Brook Mine, J. Thompson, B. James, T. Lever, H. Dekker and L. McNeill of Dolphin Explorations, D. MacInnis, S. Walker, A. Huard, C. MacDougall and P. Andrews of Noranda Exploration Company Ltee, D. E. McBride and G.D. Ovens of James Wade Engineering, P. Dimmell, C Hartley and D. Hoy of Corona Corporation, C. McKenzie of BP-Selco, D. R. Duncan of MPH Consulting, D. A. Sawyer of Petromet Ressources Ltee and A. Sheito and M. Slauenwhite of Inco Gold for their great collaboration, helpful comments, field trips and permission to publish. Dave Duncan of MPH Consulting, Ivor McWilliams of Hope Brook Mine and John Thompson of Dolphin Explorations are specially thanked for their logistic support. Special acknowledgments to H.S. Swinden of the Newfoundland Department of Mines and Energy for his great collaboration and help. Thanks are also due to Derek Wilton, Cindy Saunders and Steve McCutcheon for leading field trips and to P. W. Stewart and A.L. Sangter for their co-operation. Donald Watanabe provided dedicated field assistance and contributed to mapping. Thanks are also due to Luce Dubé and Kim Nguyen for drafting the diagrams and to Robert Godue for the preparation of some of them. The manuscript has benefited from the constructive criticism of K. H. Poulsen, H.S. Swinden, T. Birkett and D.G. Richardson.

REFERENCES

- Dubé, B., Guha, J. and Rocheleau, M.,**
1987: Alteration pattern related to gold mineralization and their relation to CO₂-H₂O ratios; *Contribution to Mineralogy and Petrology*, v. 37, p. 267-291.
- Dunning, G.R. and O'Brien, S.J.,**
1989: Late Proterozoic-Early Paleozoic crust in the Hermitage Flexure, Newfoundland, Appalachians: U/Pb ages and tectonic significance; *Geology*, v. 17, p. 548-551.
- Gauthier, M., Auclair, M., Bardoux, M., Boisvert, D., Brassard, B., Chartrand, F., Dupuis, L., Godue, R., Jébrak, M., Trottier, J.,**
1989: Synthèse métallogénique de l'Estrie et de la Beauce; Ministère de l'Énergie et des Ressources du Québec, MB 89-20. 631 p.
- Graves, M.C. and Zentilli, M.,**
1982: A review of the geology of gold in Nova Scotia; in Hodder, R.W. and Petruk, W., ed., *Geology of Canadian Gold Deposits*, Canadian Institute of Mining and Metallurgy Special Volume 24, p. 233-242.
- Lydon, J.W., Al, T., Richardson, D. G., and Lancaster, R.D.,**
1988: Magmatic and hydrothermal processes of precious metal enrichment in Newfoundland Ophiolites; *Geological Survey of Canada Current Activities Forum*, January 1988, Poster Sessions abstracts, p 22.
- McBride, D.E.,**
1989: The Nugget Pond deposit; Oral presentation given at the Baie Verte Mining meeting, June, 24, 1989.
- McKenzie, C.B.,**
1986: Geology and mineralization of the Chetwynd deposit, southwestern Newfoundland, Canada; *In Proceedings on Gold 86*, an International Symposium on the Geology of Gold, edited by A.J. MacDonald, p. 137-148.
- O'Brien, B.H.,**
1989: Summary of the geology between La Poile bay and Couteau Bay (11 O/9 and 11 O/16), southwestern Newfoundland; *in Current Research, Newfoundland Department of Mines and Energy*, Report 89-1, p. 105-119.
- Phillips, G.N.,**
1986: Geology and alteration in the Golden Mile, Kalgoorlie; *Economic Geology*, v 81, p. 779-808.
- Poulsen, K.H. and Robert, F.,**
1989: Shear zones and gold: Practical examples from the Southern Canadian Shield; *in Mineralization and shear zones*, Short courses notes, Volume 6, edited by J.T. Bursnell, Geological Association of Canada, p. 239-266.
- Romberger, S. B.,**
1986: Disseminated gold deposits; *Geoscience Canada*, v. 13, no 1, p. 23-34.
- Roy, A. and Valiquette, G.,**
1987: Étude des minéralisations aurifères de la région du Lac Arsenault-Gaspésie; Ministère de l'Énergie et des Ressources du Québec, MB 87-01.
- Saunders, C.M. and Tuach, J.,**
1988. K-feldspathization, albitization and gold mineralization in granitoid rocks: the Rattling Brook alteration system; *in Current Research, Newfoundland Department of Mines and Energy*, Mineral Development Division, Report 88-1. p. 307-318.
- Stewart, P.W. and Stewart, J.W.,**
1988: The relative timing of gold mineralization at Hope Brook, NFLD (abstract); *in Program with abstracts*, Geological Association of Canada-Mineralogical Association of Canada, v. 13, p. 188.
- Swinden, H.S.,**
1984: The Chetwynd prospect, southwestern Newfoundland; Newfoundland Department of Mines and Energy, Open File (11 O/09/148), 10 p.
- Tuach, J.,**
1986: Metallogeny of Newfoundland granites-studies in the western White Bay area and on the southwest coast; *in Current Research, Newfoundland Department of Mines and Energy*, Report 86-1, p. 27-38.
1987: Mineralized environments, metallogenesis, and the Doucers Valley fault complex, Western White Bay. A philosophy for gold exploration; *in Current Research, Newfoundland Department of Mines and Energy*, Report 87-1, p. 129-144.

Tuach, J., Dean, P.I., Swinden, H.S., O'Driscoll, C.F., Kean, B.F. and Evans, D.T.W.,

1988: Gold mineralization in Newfoundland: A 1988 review; *in* Current Research, Newfoundland Department of Mines and Energy, Mineral Development Division, Report 88-1. p. 279-306.

Wilton, D.H.C.,

1983: The geology and structural history of the Cape Ray Fault Zone in southwestern Newfoundland; Canadian Journal of Earth Sciences v. 20, p. 1119-1133.

Wilton, D.H.C., and Strong, D.F.,

1986: Granite-related gold mineralization in the Cape Ray fault zone of southwestern Newfoundland; Economic Geology, v. 81, p. 281-295.

Yule, A.,

1988: The Hope Brook gold deposit, Newfoundland, Canada: surface geology, representative lithochemistry and styles of hydrothermal alteration; M. Sc. thesis, Dalhousie University, Halifax, Nova Scotia, 249 p.

Characterizing vegetation response to an alteration halo using LANDSAT Thematic Mapper imagery and aeromagnetic data in the Murdochville area, Gaspésie, Québec¹

A.N. Rencz and D.F. Sangster
Mineral Resources Division

Rencz, A.N. and Sangster, D.F. Characterizing vegetation response to an alteration halo using LANDSAT Thematic Mapper imagery and aeromagnetic data in the Murdochville area, Gaspésie, Québec; in Current Research, Part B, Geological Survey of Canada, Paper 90-1B, p. 91-94, 1989.

Abstract

The analysis of LANDSAT Thematic Mapper (TM) imagery illustrate that spectral reflectance patterns of vegetation around the Gaspé copper deposit are quite specific to that area, possibly caused by a stress response in the vegetation. A TM imagery 'halo' around the mine site corresponds in position to, but is larger than, alteration zones defined by various geological/geochemical indicators. Furthermore, the anomalous TM spectral signature extends beyond an aeromagnetic anomaly associated with the Copper Mountain intrusion. Within a larger area (40 x 30 km), centred on Murdochville, the two anomalies overlap at only one other locality.

Résumé

L'analyse de l'imagerie LANDSAT réalisée à l'aide de l'appareil de cartographie thématique montre que les configurations créées par la réflexion spectrale de la végétation autour du gisement de cuivre de Gaspé sont particuliers à cet endroit et qu'ils résultent probablement d'une réaction de la végétation dans des conditions difficiles. Un halo dans l'imagerie ainsi obtenu autour de l'emplacement de la mine correspond à des zones d'altération qui sont plus petites que le halo et qui sont définies par différents indicateurs géologiques et géochimiques. En outre, la signature spectrale anormale s'étend au-delà d'une anomalie aéromagnétique associée à l'intrusion de Copper Mountain. Au sein d'une région plus grande (40 km × 30 km), centrée sur Murdochville, les deux anomalies se chevauchent seulement à un autre endroit.

¹ Contribution to the 'Plan de développement économique Canada/Gaspésie et Bas Saint-Laurent, Volet Mines 1983-1988'. Project carried by the Geological Survey of Canada.

INTRODUCTION

Theoretically, vegetation response to geochemical anomalies manifests itself in reflectance changes, sometimes in the absence of significant metal uptake in plants (Horler, 1985). Researchers have attempted to use this relationship, particularly reflectance changes along the 'red edge' (a zone of plant reflectance between 680-800 nm of rapid reflectance increase), to characterize stress (Collins et al., 1983). Typically, data from airborne scanners are required to measure this response as the systems can be configured with a relatively small pixel size (from <1 to 10 m) and a large number of wavelength choices. It is more difficult to use reflectance data from LANDSAT Thematic Mapper (TM) because of the relatively large pixel size (30 m) and wide spectral band widths. Interpretation of the results is also complicated by the variety of factors, in addition to those caused by the local soil and rock chemistry, that affect plant reflectance. Keeping these limitations in mind, satellite data can be used as a tool in mineral exploration. To enhance the information content in LANDSAT data, an ancillary data source, such as geophysics, could 'mask out' unlikely areas and 'confirm' other likely patterns.

The Murdochville district in eastern Québec, Canada is currently being exploited for copper and molybdenum. In the immediate vicinity of the mine, several studies have characterized alteration zones associated with mineralization and intrusion (Allcock, 1982; Williams-Jones, 1986). Such studies are useful in determining the origin of the deposit and could provide insights into locating other deposits of similar epigenetic origin. The dimensions of the alteration zone have been defined using different mineral indicators and are contained within 2 km of the deposit (Allcock, 1982). Williams-Jones (1986) presented an illite crystallinity survey which increased the zone of thermal effects over that of previous work. He illustrated an envelope of anomalous illite crystallinity that extends to a maximum diameter of around 3.3 km. Stevens (1989) described a mineral zoning pattern with a diameter of 15-20 km centred roughly on the copper deposit.

One objective of this project was to determine if there was an anomalous spectral signature in LANDSAT TM imagery associated with any of the zones noted above. If a unique spectral response was in fact determined, then could other zones with similar characteristics be identified in the surrounding area and could these zones be further isolated by incorporating geophysical data?

STUDY AREA

The study area is centred around Les Mines Gaspé near Murdochville, Québec (Fig. 1). The area is underlain by shallow marine Siluro-Devonian sedimentary rocks. During the late Devonian Acadian orogeny the sedimentary rocks were folded along northwest trending axes and were subsequently intruded by quartz monzonitic to granitic igneous rocks. The mine is within the Copper Brook aureole, a zone of calc-silicate minerals produced during contact metasomatism and metamorphism of the calcareous host rocks. The skarn and porphyry copper orebodies yield both copper and molybdenum. Initial reserves of the skarn orebody have been estimated at 62 million tons grading 1.2 %

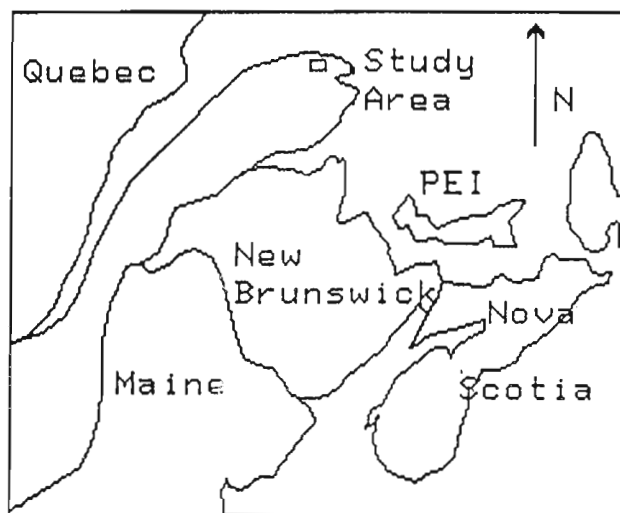


Figure 1. Location map for Murdochville, Quebec and the two study sites.

Cu and 0.03 % Ni; the porphyry initially contained 275 million tons of 0.4 % Cu and 0.03 % Mo (Williams-Jones, 1986).

METHODS

The LANDSAT TM image was recorded on 26 June 1986. In this study TM bands 1-5 and 7 were used but not the thermal band (band 6). Initially a subscene of 600 × 600 pixels was downloaded from a computer compatible tape. This image was geometrically corrected using 24 ground control points from a 1:50 000 scale topographic map. From this image a subscene of 512 × 512 pixels, centred on Murdochville, was selected as the study area. The original pixel size of 30 × 30 m was retained. The image processing was done on a 386 microcomputer using EASI/PACE software (Anon, 1989).

The aeromagnetic data were provided by the Geophysical Data Centre of the Geological Survey of Canada. The data were recorded with a 1/2 mile line spacing and this was gridded to provide 100 m pixels. The data were downloaded to the microcomputer and merged with the georeferenced LANDSAT data.

RESULTS

a. LANDSAT TM Data

Several features could readily be identified on the TM image, such as water bodies, roads, and the open pit operations. Obvious colour changes, associated with these features, represent significant differences in the radiance values on the TM digital tape. The visible symptoms associated with vegetation stress, however, would be considerably more subtle than these 'gross' features. Notwithstanding this limitation, it is possible to discern a 'halo' around the open pit (Fig. 2). Although the halo corresponds approximately in position with the illite crystallinity zonation defined by Williams-Jones (1986), its radius is about 2 km larger. The halo is evident on a variety of band combinations on the colour monitor, particularly TM bands 4, 5 and

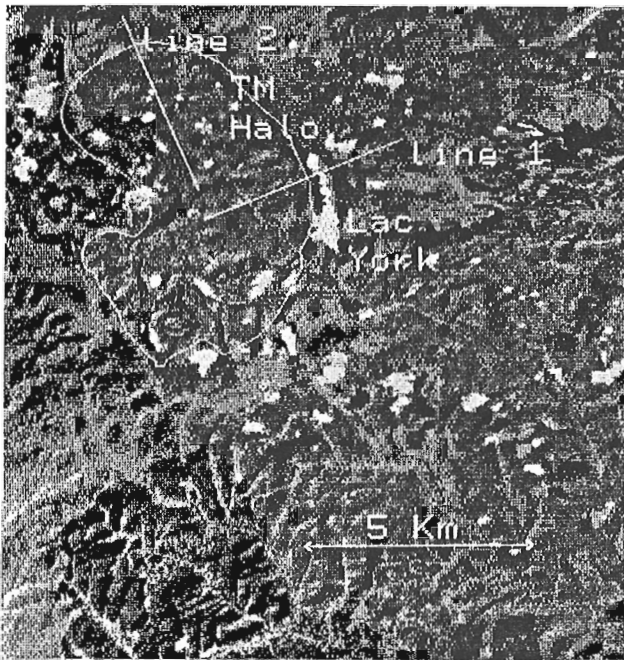


Figure 2. Band 4 image from Thematic Mapper illustrating the outline of the 'TM halo' and the location of the two transect lines.

7. It is not as evident on the single channel (band 4) reproduction in Figure 2.

To determine the magnitude and significance of this colour change it was first necessary to analyze the actual reflectance data. Table 1 illustrates the mean reflectance values plus standard deviations in vegetation for six bands of TM along two transects which extend across the halo into a 'background' region (Fig. 2). The table illustrates that the reflectance values in TM bands 4 and 5 are highest at the centre of the anomaly and gradually decrease outward. This pattern was evident in LINE 1 but was not as consistent in LINE 2. Although the values varied along LINE 2, the highest values in bands 4 and 5 were found at the centre and the lowest were detected outside the halo. The increased reflectance in this mid-infrared part of the electromagnetic spectrum has been attributed to lower absorption by chlorophyll and a changing leaf morphology (Horler et al., 1983). Both of these phenomena are characteristic of vegetation under stress, although this conclusion must be interpreted with caution. The reflectance pattern is attributed by us, in part, to the copper mineralization. However, other secondary influences such as contamination from the mining operation contribute to the overall response.

The next step was to determine if the reflectance patterns within the halo were found at other locations in the immediate vicinity and in the surrounding region. It was found that reflectance values falling within the range of the mean \pm two standard deviations of radiance values in AREA 1, LINE 1 occurred in only 0.17 % of the total 225 km² area, mainly in the areas surrounding the open pit. This suggests that the reflectance patterns are unique. In this comparison only pixels with values of 71-75 on band 1 and 28-31 on band 2 were included. This was done to limit the comparisons between vegetation of similar types.

Table 1. Reflectance values on LANDSAT TM imagery across two transects of forested land in the Murdochville area, Québec

Transect 1					
Area*	Mean and standard deviation				
	1	2	3	"Back"	water
1	72 0.8	72 0.9	72 0.8	71 0.9	68 1.2
B 2	29 0.7	29 1.0	29 0.6	28 0.7	21 0.6
A 3	23 0.6	23 0.7	23 0.6	22 0.7	16 0.7
N 4	103 4.5	98 3.5	94 3.9	91 5.9	11 1.6
D 5	66 3.7	63 2.4	61 2.0	52 3.0	5 1.2
7	16 1.2	16 1.1	15 1.1	13 0.9	2 .6

Transect 2					
Area*	Mean and standard deviation				
	1	2	3	"Back"	
1	75 4.1	73 3.2	73 3.1	74 3.6	
B 2	31 2.1	29 1.4	28 2.1	31 2.0	
A 3	26 1.7	24 1.3	22 1.2	26 1.9	
N 4	98 4.4	90 5.3	85 5.6	91 5.1	
D 5	68 3.8	58 3.2	43 3.1	57 3.8	
7	18 1.2	15 1.0	12 0.6	18 1.2	

"Back" refers to background.
*See Figure 2 for locations of transect lines.

b. Geophysical Data

The contour map of the classified aeromagnetic data is presented in Figure 3. The original aeromagnetic data represented a range from -243 to 465 gammas but these were converted to a range of 1 to 256 to facilitate manipulation on the image analysis system. This was done by placing an equal number of pixels within each of the 256 classes. The image, classified into 13 levels, illustrates a 'bulls eye' pattern with the highest levels corresponding to the mineralized zone at Les Mines Gaspé. (Fig. 3). This anomaly is likely caused by pyrrhotite developed during each of the several stages of mineralization (Allcock, 1982).

c. Data Integration

Within the area represented by Figures 2 and 3, the only place where the geophysical anomaly and the TM anomaly overlap is in the Murdochville area (Fig. 3). Although this was expected, because the geophysical anomaly only occurs in the Murdochville area, it illustrates that the aeromagnetic data are useful in eliminating several 'TM anomalies' that are probably not related to mineralization. When the investigation area is enlarged (Fig. 4) an aeromagnetic anomaly coincided with a TM anomaly in the northwest corner of Figure 4, placing it in the southeastern corner of Boisbuisson Township.

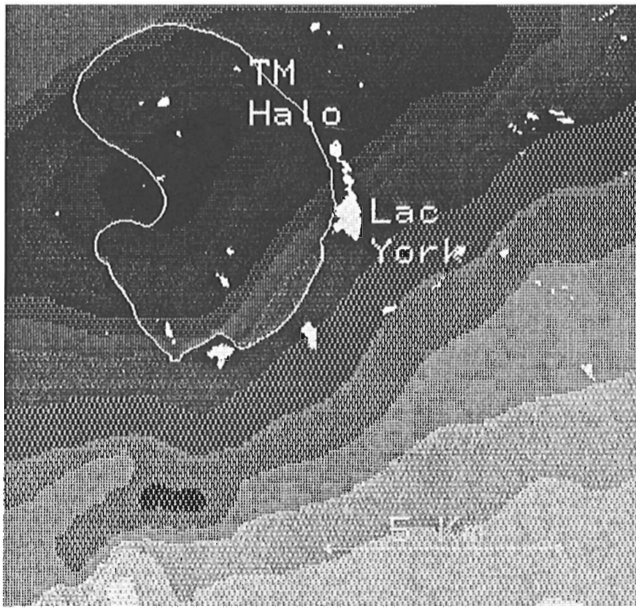


Figure 3. Image of the airborne aeromagnetic survey for the Murdochville area, Québec. The range from high to low aeromagnetic response is represented by the black to white gradient.

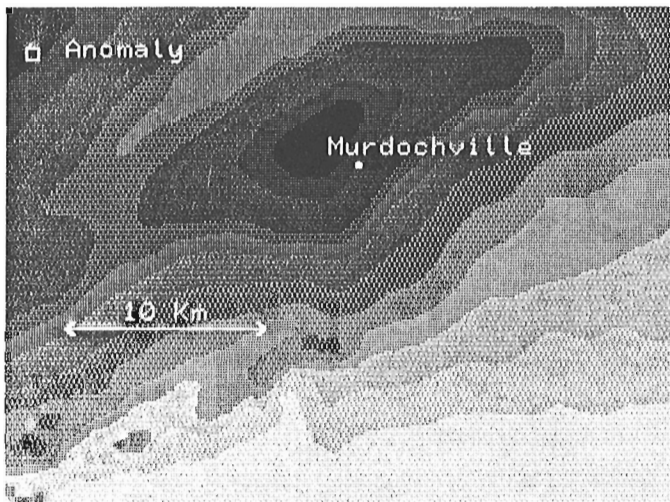


Figure 4. Image of the aeromagnetic survey for an enlarged study area, illustrating the location of an anomaly where a high geophysical response coincides with a spectral anomaly in the LANDSAT TM data. The range from high to low aeromagnetic response is represented by the black to white gradient.

CONCLUSIONS

The LANDSAT TM data reveal a spectral reflectance halo corresponding to a geological anomaly based on geochemistry and mineralogy. The TM halo was similar in shape to, but larger than, an alteration halo that had been defined by previous workers.

The LANDSAT TM data appear effective in identifying other sites indicative of mineralization. In this study the prediction was improved by including airborne magnetic data. The two sets of data provided complimentary information that helped to restrict the prediction to a smaller zone than would have been achieved by using the maps separately. In other areas TM data could make similar contributions by integrating ancillary data sets that would eliminate artifacts in the predicted map.

ACKNOWLEDGMENTS

We thank K. Stevens for comments and G. Watson for review of the paper.

REFERENCES

- Allcock, J.B.**
1982: Skarn and porphyry copper mineralization at Mines Gaspé, Murdochville, Quebec; *Economic Geology*, v. 77, p. 971-999.
- ANON**
1989: PACE Image Analysis Kernel Manual, Version 4.1, November, 1988; PCI Incorporated, Toronto.
- Collins, W., Chang, S., Raines, G., Canney, F., and Ashley, R.**
1983: Airborne biogeochemical mapping of hidden mineral deposits; *Economic Geology*, v. 78, p. 737-749.
- Horler, D.N.H.**
1985: Geobotany: The state of the art in Canada; DSS Contract NO. 19SR.23413-4-8150. May 1985, 90 p.
- Horler, D.N.H., Dockray, M., and Barber, J.**
1983: The red edge of plant leaf reflectance; *International Journal of Remote Sensing*, v. 4, p. 273-288.
- Stevens, K.**
1989: Vein mineral zoning in the Mines Gaspé ore system, Gaspé, Quebec; *Geological Survey of Canada, Open File 1890*, 39 p.
- Williams-Jones, A.E.**
1986: Low-temperature metamorphism of the rocks surrounding Les Mines Gaspé, Quebec: Implications for mineral exploration; *Economic Geology*, v. 81, p. 466-470.

Rare-earth-bearing apatite near Benjamin River, northern New Brunswick

W.D. Sinclair and D.M. Kingston¹
Mineral Resources Division

Sinclair, W.D. and Kingston, D.M. Rare-earth-bearing apatite near Benjamin River, northern New Brunswick; in *Current Research, Part B, Geological Survey of Canada, Paper 90-1B*, p. 95-104, 1990.

Abstract

Rare-earth-bearing apatite near Benjamin River in northern New Brunswick is associated with small plutons and dykes of feldspar porphyry that have intruded Silurian mafic volcanic rocks. The feldspar porphyry may be related to a nearby gabbroic to granitic intrusive complex of probable Devonian age. The apatite occurs with pyroxene, magnetite and minor epidote in small pegmatitic bodies and in veins and veinlet stockworks in adjacent rocks. Electron-microprobe analyses indicate that the apatite contains 1 to 2 % rare-earth elements (REEs) unevenly distributed both within individual grains and from grain to grain. REEs are also present in monazite and allanite inclusions in apatite. The abundance and distribution of REEs in the Benjamin River apatite are comparable to those in apatites associated with ultramafic and alkaline rocks, including carbonatites, and some apatite-bearing iron deposits.

Résumé

De l'apatite renfermant des terres rares, relevée près de la rivière Benjamin, dans le nord du Nouveau-Brunswick, est associée à de petits plutons et dykes de porphyre feldspathique qui ont pénétré des roches volcaniques mafiques du Silurien. Le porphyre feldspathique peut être lié à un complexe intrusif de nature gabbroïque à granitique et d'âge dévonien probable situé à proximité. L'apatite est associée à du pyroxène, de la magnétite et un peu d'épidote contenus dans de petits massifs pegmatitiques et des veines et des stockwerks au sein de roches adjacentes. Des analyses par microsonde électronique indiquent que l'apatite renferme de 1 à 2 % d'éléments de terres rares, répartis inégalement à l'intérieur des grains et d'un grain à l'autre. Les ÉTR sont également présents dans des inclusions de monazite et d'allanite à l'intérieur de l'apatite. L'abondance et la répartition des ÉTR dans l'apatite de la rivière Benjamin sont comparables à celles des apatites associées à des roches ultramafiques et alcalines, y compris des carbonatites et des gisements de fer contenant de l'apatite.

¹ Department of Geology, The University of Western Ontario, London, Ontario N6A 5B7

INTRODUCTION

The Benjamin River apatite-rare-earth occurrence is approximately 23 km south-southeast of Dalhousie and about 8 km west-southwest of the settlement of Benjamin River on the south coast of Chaleur Bay (Fig. 1). Access is by gravel road and narrow bush roads from Benjamin River.

The occurrence of apatite near Benjamin River has been known since the 1930s. It was explored for its phosphate potential in 1969 by Doral Mining Exploration Ltd. (Marleau, 1969). At that time, "above normal" concentrations of yttrium oxide were noted (Canadian Mining Journal, v. 90, p. 13, 1969). G.E. Schrock examined the

property in 1987 and collected grab samples that contained 0.5 to 2.7% combined La+Ce (Schrock, 1987). In 1988, Long Lake Gold Ltd. conducted surface exploration on the property, including bulldozer trenching and extensive sampling of the apatite occurrence. The results indicated rare-earth element (REE) contents of up to 1100 ppm La, 3000 ppm Ce and 1345 ppm Y (Whaley, 1989). The first author examined the apatite occurrence during a one-day visit in August 1988 and completed one week of mapping and sampling in June 1989. The second author carried out electron-microprobe analyses of selected samples in order to determine the distribution of REEs within the occurrence.

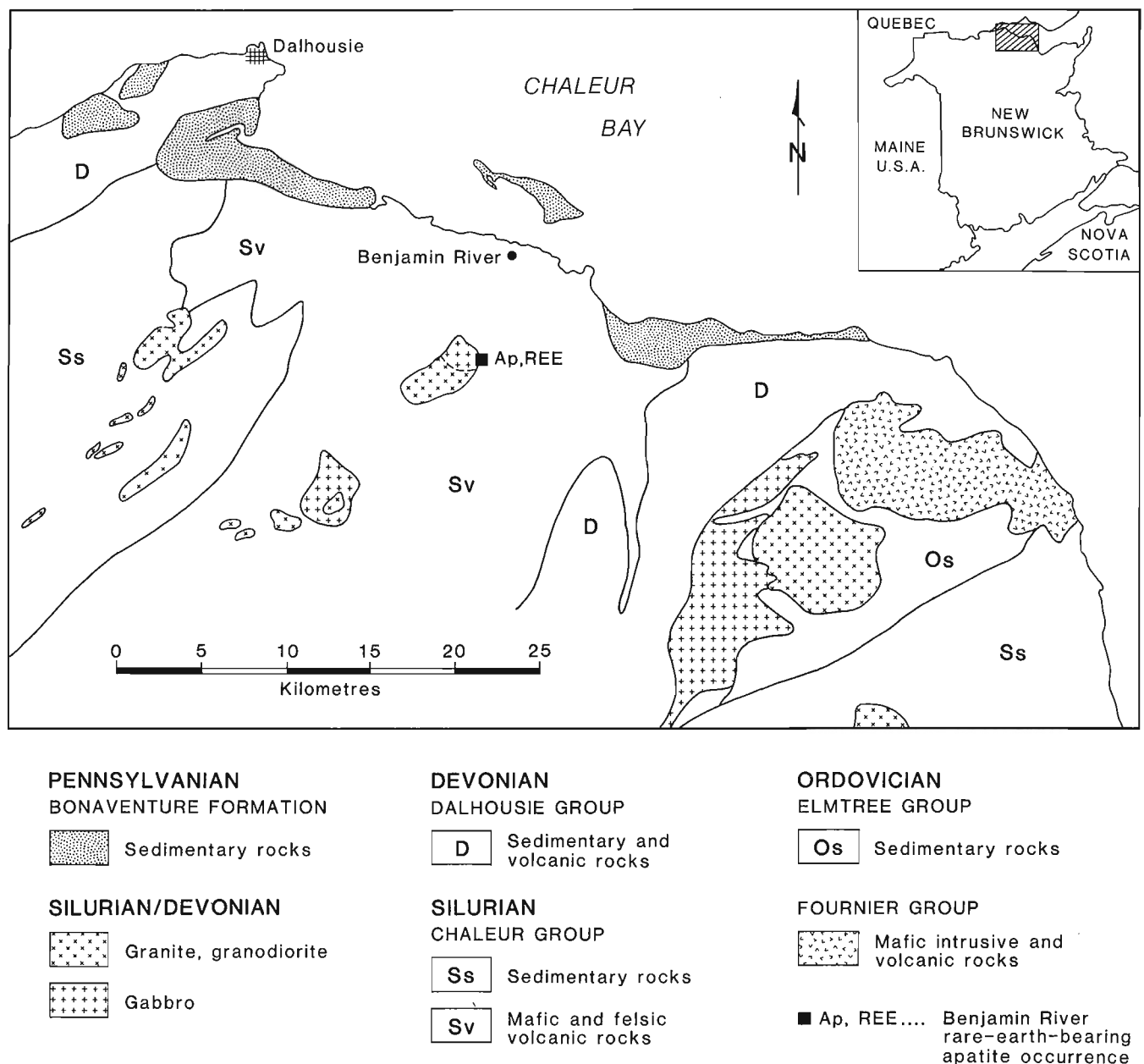


Figure 1. Regional geology and location of the Benjamin River rare-earth-bearing apatite occurrence (after Davies, 1979).

GENERAL GEOLOGY

The Benjamin River apatite-REE occurrence lies within the Dunnage zone of New Brunswick as defined by Van Staal and Fyffe (in press). The area is underlain mainly by Silurian volcanic rocks of the Chaleur Group which have been intruded by a small gabbro — granite plutonic complex of probable Devonian age (Fig. 1). The volcanic rocks have also been intruded by small stocks and dykes of feldspar porphyry which may or may not be related to the gabbro-granite complex. Apatite concentrations appear to be most closely associated with the feldspar porphyry (Fig. 2, 3).

The volcanic rocks in the area were assigned by Greiner (1970) to the Bryant Point Formation of the Chaleur Group. They consist mainly of thick flows of dark green, fine grained basalt, in places sparsely porphyritic, in places amygdaloidal. No pillows were observed. In the vicinity of the apatite occurrence the rocks are fractured and silicified to varying degrees.

The Devonian intrusive rocks form an irregular elliptical, northeast-trending body 5 km long and 2.5 km wide. The northeast end of the complex consists of gabbro composed of approximately 60 to 70 % plagioclase, 20 to 30 % clinopyroxene and 10 to 20 % biotite and chlorite. Magnetite (up to 1 % or more) is also present. The gabbro is medium-to coarse-grained except near its contact with basalt where it is fine grained. It is typically massive with no evidence of internal layering or foliation.

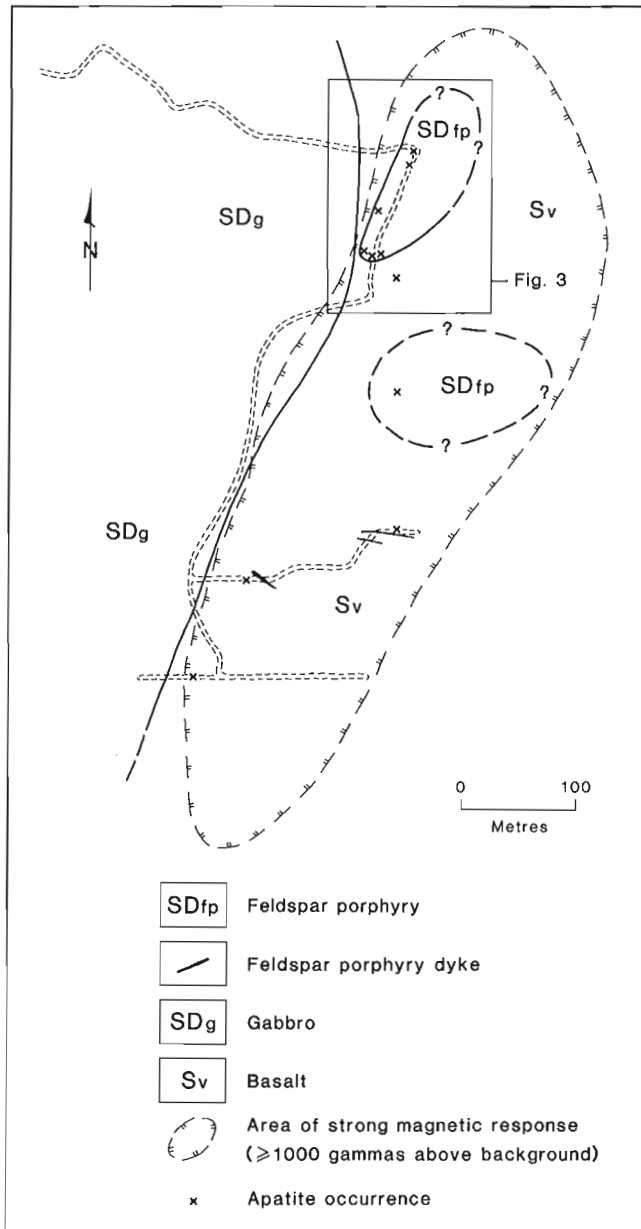


Figure 2. Geological map of Benjamin River property with location of apatite occurrences.

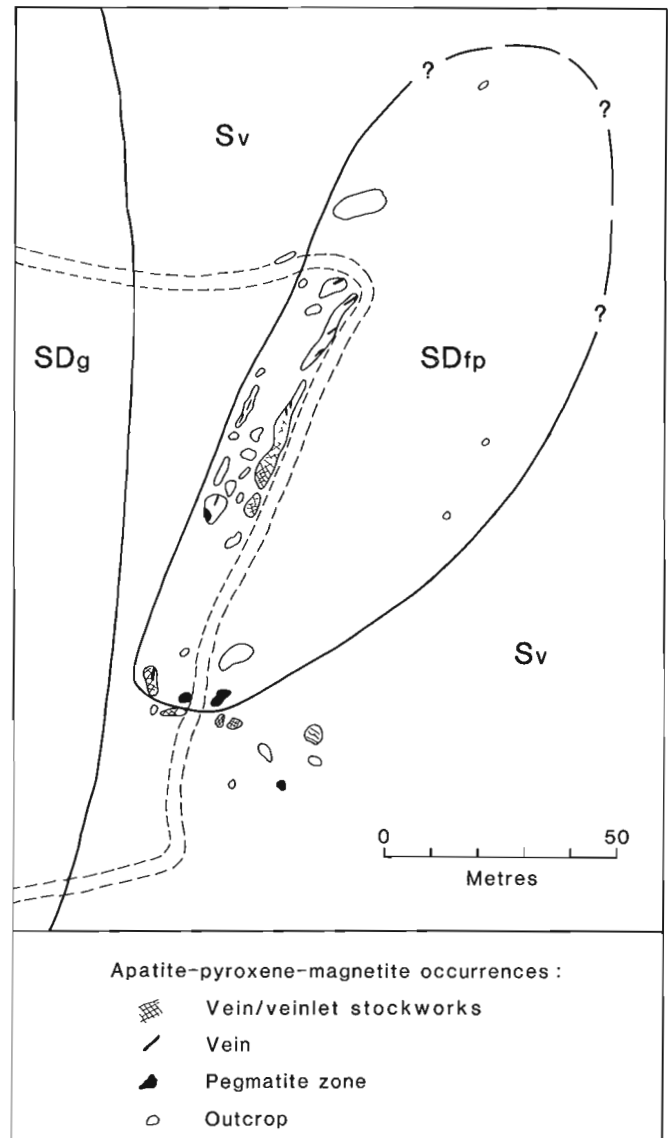


Figure 3. Detailed map of area outlined in Figure 2. Rock units are the same as in Figure 2.

Rocks in the southwest end of the plutonic complex consist mainly of pink, fine grained granite. Between the gabbro and granite are mafic-rich granitic and granodioritic rocks that are transitional in composition between gabbro and granite. Contacts generally appear to be gradational but, in places, dykes of more felsic rocks cut more mafic phases.

The plutonic complex has not been dated radiometrically but is probably Devonian or older. Plutonic rocks of similar composition to the southwest yielded a Devonian Rb-Sr isochron age of 370 ± 30 Ma and initial $^{87}\text{Sr}/^{86}\text{Sr}$ of 0.0746 ± 0.0011 (Stewart 1978). Granitoid plutons in the extension of the Elmtree Terrane in northern Maine are also considered to be Devonian (Ayuso, 1986).

Feldspar porphyry consists of 40 to 50 % white to pink, medium-sized albite phenocrysts in a reddish-grey, fine grained to aphanitic matrix. Outcrops of feldspar porphyry associated with the apatite occurrences are exposed over areas up to 160 m long by 100 m wide and are probably part of small stocks (Fig. 2). Dykes of feldspar porphyry 0.5 to 3 m wide are also present. Although it appears to have intruded mainly the Silurian volcanic rocks, the feldspar porphyry locally contains xenoliths of gabbro.

GENERAL FEATURES OF THE APATITE OCCURRENCE

Apatite occurs along with pyroxene and magnetite in small pegmatitic bodies and in associated veins and veinlets. The apatite is pink to reddish-brown and ranges from very fine- to coarse-grained (crystals in the pegmatitic zones are as much as 6 cm long). The pyroxene is dark green to nearly black and, like apatite, ranges from very fine- to coarse-grained. X-ray diffraction and petrographic studies indicate clinopyroxene of diopsidic composition.

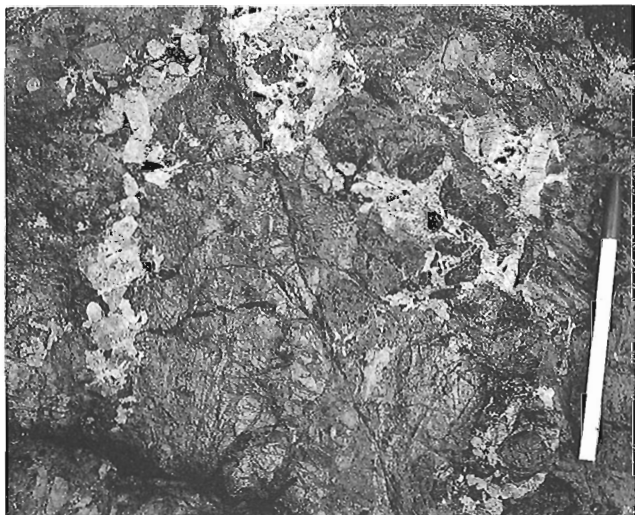


Figure 4. Pegmatitic apatite and pyroxene; apatite crystals are light-coloured, the dark grey areas are mainly pyroxene. GSC 204983-E.

Zones of pegmatitic apatite, pyroxene and magnetite are present locally along the margin of the northernmost feldspar porphyry stock and in adjacent volcanic rocks (Fig. 3). Contacts are not well exposed but these zones appear to be relatively small pods or lenses measuring 5 to 10 m long and 2 to 5 m wide. In addition to pyroxene, apatite and magnetite, minor amounts of epidote are present and trace amounts of chalcopyrite occur locally. Apatite and pyroxene range from fine- to coarse-grained; magnetite and epidote occur as smaller, interstitial grains. Magnetite- and apatite-bearing veinlets crosscut the pegmatitic zones locally. The apatite content of the pegmatitic zones overall is 20 to 30 %.

Apatite within the pegmatitic zones in most places is irregularly distributed and apatite crystals are randomly oriented (Fig. 4). In places, however, it is concentrated in layers in which apatite crystals are subparallel and appear to have grown from one side of a layer, roughly at right angles to the layer (Fig. 5). The apatite crystals are tapered at their base and to some degree resemble (morphologically) elongate feldspar crystals oriented normal to layering in asymmetric pegmatite-aplite bodies (e.g. Fig. 4 in Jahns and Tuttle, 1963). The apatite crystals in these layers thus appear to be a type of unidirectional solidification texture (cf. Shannon et al., 1982; Kirkham and Sinclair, 1988).

Veins and veinlets containing apatite are widely distributed but are best developed within an area about 100 m long and 50 m wide centred over the southern portion of the northernmost stock of feldspar porphyry (Fig. 3). Within this area, zones of veinlet stockworks cut pervasively silicified host rocks (Fig. 6). Outside this area, veinlets are more widely spaced and alteration is restricted to thin selvages in the adjacent host rocks.

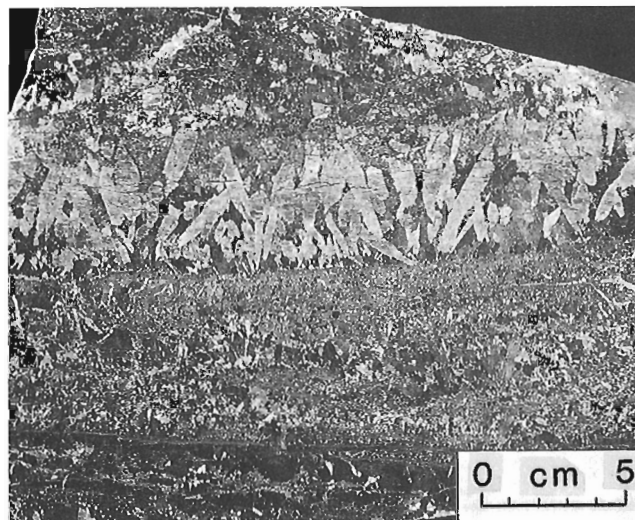


Figure 5. Layered pegmatitic apatite-pyroxene-magnetite; coarse grained apatite crystals (white) are oriented roughly perpendicular to the lower contact of the apatite-rich layer, the upper contact of which is irregular. Pyroxene is light grey, magnetite is dark grey. GSC 204983-D.



Figure 6. Stockwork zone of pyroxene and magnetite veinlets cut by apatite-pyroxene-magnetite vein (bottom) GSC 204983A.

At least two stages of fracturing and vein development are indicated by crosscutting relationships. The earliest stage consists of veinlets 1 to 2 mm wide and containing mainly pyroxene and/or magnetite with lesser amounts of apatite. These veinlets are cut by veins ranging from 1 to 10 cm in width. The veins are similar to the pegmatitic zones in that they consist mainly of apatite, pyroxene and magnetite. Apatite generally makes up 10% or less of the vein material but is irregularly distributed and locally ranges up to 40%. The apatite content of the veins and veinlet stockwork zones overall, including host rock, is about 1 to 2%.

The distribution of magnetite associated with the apatite occurrence is defined by ground magnetic surveys carried out by Doral Mining Ltd. and Long Lake Gold Ltd. These surveys have outlined an area of strong magnetic response 800 m long and 200 m wide adjacent to the contact of the gabbro (Fig. 2). All of the known apatite concentrations occur within this area.

GEOCHEMISTRY OF THE APATITE-BEARING ZONES

The analytical results of the sampling program carried out by Long Lake Ltd. are summarized in the plots of La, Ce and Y versus PO_4 shown in Figure 7. Although there is some scatter in the data, there is good correlation between REEs and phosphate content in the apatite-bearing rocks. This correlation suggests that apatite may be an important host for the REEs but does not preclude the presence of other phosphate minerals such as monazite, nor of other REE-bearing minerals associated with apatite. The maximum content of REEs in the samples analyzed was 1100 ppm La, 3000 ppm Ce and 1345 ppm Y; in general, total REE contents (La+Ce+Y) ranged from about 100 to 2000 ppm.

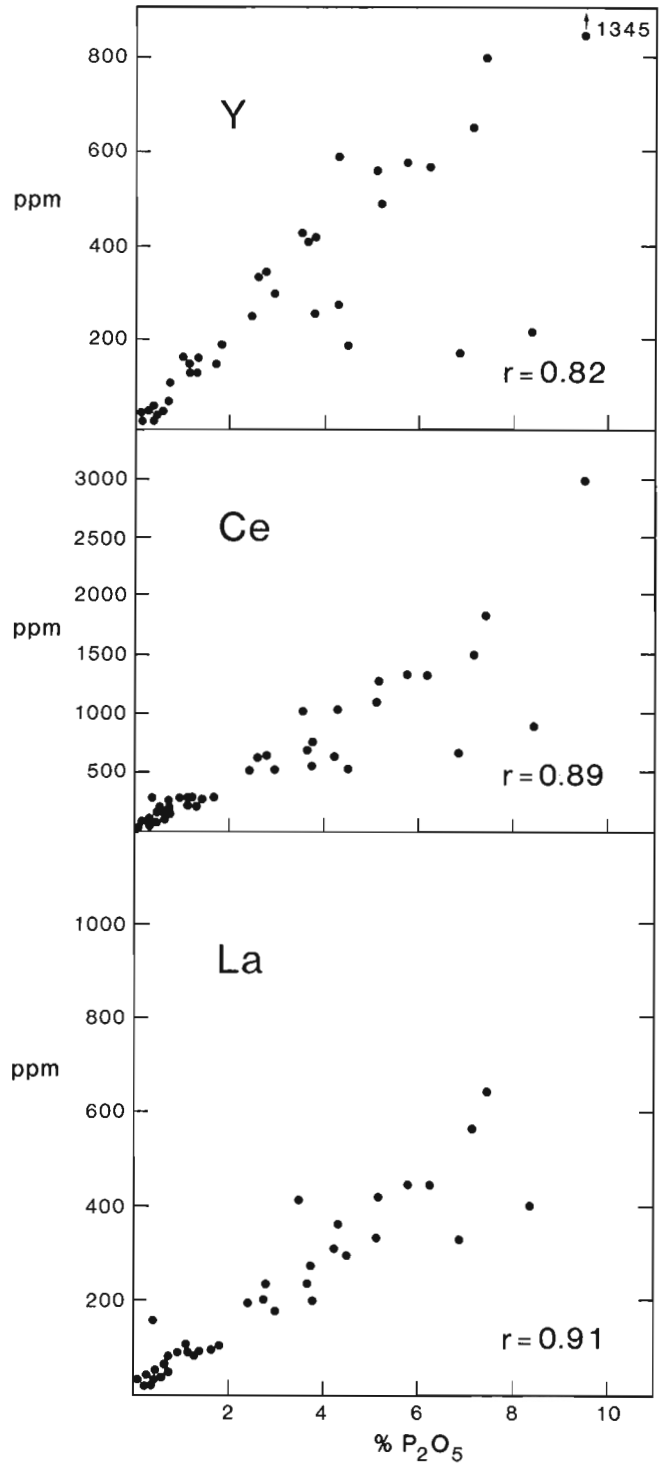


Figure 7. Plots of La, Ce and Y versus PO_4 . (data from Whaley, 1989); r = linear correlation coefficient.

Table 1. Rare-earth element composition (ppm) of selected host rocks and apatite-bearing rock samples, Benjamin River, New Brunswick.

Sample	La	Ce	Nd	Sm	Eu	Gd	Dy	Yb	Y	% ap*
Pegmatitic apatite-pyroxene-magnetite										
SYA88-37F	400	730	270	45	6.0	51	42	22	250	10
SYA89-14	1200	2800	1400	250	17	270	200	71	1100	40
SYA89-20	850	2000	1100	200	14	210	170	65	940	30
Apatite-pyroxene-magnetite veins/veinlet stockworks										
SYA88-37A	760	1500	590	89	10	100	72	31	420	25
SYA88-37B	270	620	300	53	4.9	56	47	22	270	5
SYA88-37C	350	840	430	74	6.3	78	64	27	360	10
SYA89-16	77	200	130	28	2.4	32	31	14	170	<5
Gabbro										
SYA88-41	21	46	30	5	1.8	6	5	2	26	0
SYA89-36	29	64	40	7	2.6	8	7	4	39	0
Granite										
SYA88-44	62	130	61	11	2.3	12	13	8	76	0
Feldspar Porphyry										
SYA89-12	7	16	10	2	1.3	2	2	3	17	0
SYA89-13	5	10	7	1	1.0	1	2	2	13	0

* % apatite estimated visually

REE analyses by ICP-ES after pre-concentration and separation using ion exchange resins, Analytical Chemistry Section, GSC

The REE concentrations of selected apatite-bearing samples and associated intrusive rocks analyzed as part of this study are presented in Table 1. Compared to associated intrusive rocks, the apatite-bearing samples have significantly higher REE contents, which vary in proportion with apatite content; the highest content of REEs (including 1200 ppm La, 2800 ppm Ce, 1400 Nd and 1100 ppm Y) are in the sample which has the highest apatite content.

Chondrite-normalized REE plots of the apatite-bearing samples from both vein/veinlet stockwork and pegmatitic zones (Fig. 8A) have almost identical patterns. They display negative slopes reflecting greater enrichment of light rare-earth elements (LREEs) relative to heavy rare-earth elements (HREEs) and have negative europium anomalies of similar magnitudes.

Chondrite-normalized REE plots for the associated intrusive rocks (Fig. 8B) are typical of gabbro and granite. The patterns for gabbro have a slightly negative but uniform trend with no significant anomalies. The granite sample has a similar trend but displays a slight negative europium anomaly. The patterns for feldspar porphyry, on the other hand, are concave upward and display positive europium anomalies. With the exception of ytterbium and to some degree europium, individual REE contents of the feldspar porphyry are much lower than in the granite and gabbro samples. The positive europium anomaly in the feldspar porphyry complements that of the apatite-bearing zones and may reflect a genetic relationship between them.

COMPOSITION OF APATITE

Apatite, represented by the general formula $A_5(MO_4)_3X$, can accommodate a considerable variety of elements in its crystal structure (Roy et al., 1978). The A site, for example, may contain divalent Ca, Mg, Ni, Mn, Fe, Sn, Cd, Rb, Ba, Eu; trivalent REEs as well as Sc, Tl, Y, Bi, V; monovalent Na, K, Tl, Rb, Cs; and tetravalent Ce. The M site may be occupied by P^{5+} , Si^{4+} , S^{6+} , As^{5+} , Ge^{4+} , Cr^{5+} , Mn^{6+} , V^{5+} , Al^{3+} , B^{3+} and OH. The X site most frequently

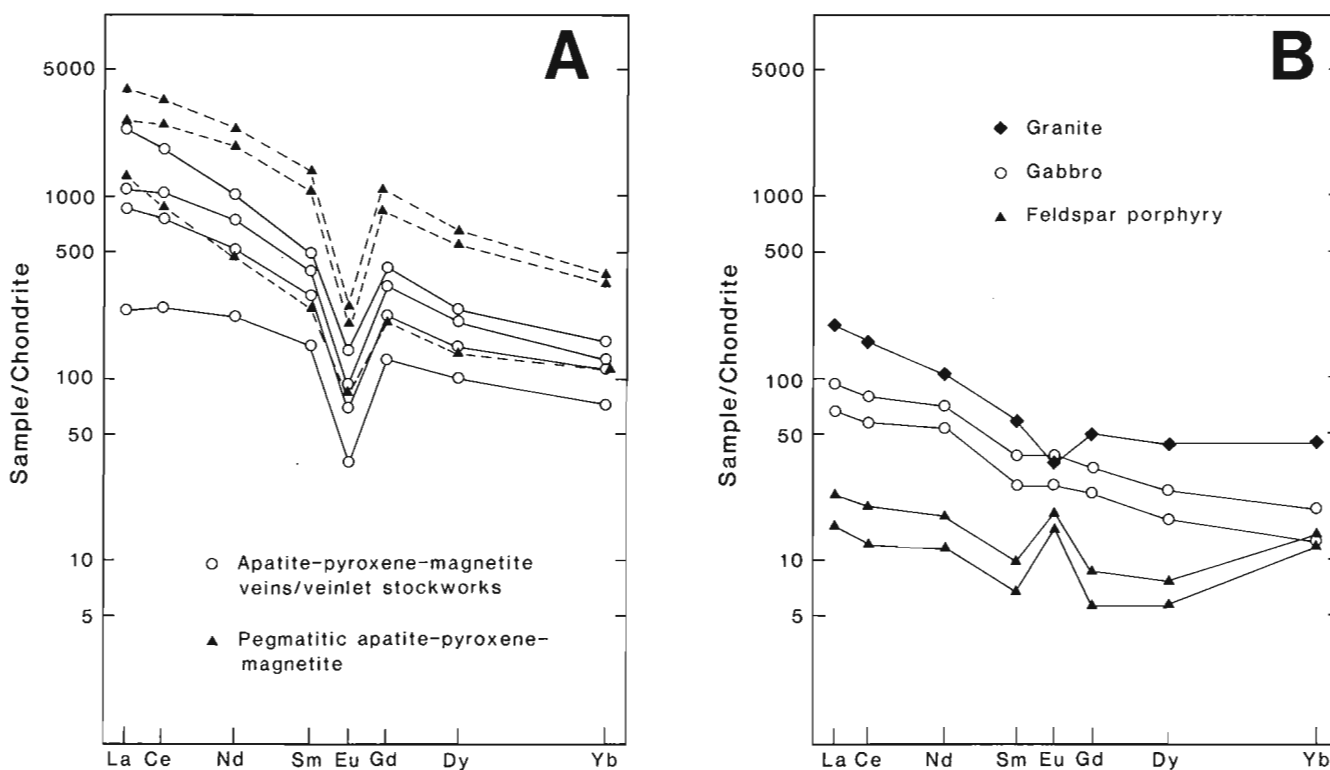


Figure 8. Chondrite-normalized plots of REE data in Table 1. A: Apatite-bearing samples. B: Intrusive rocks. Chondrite values used were those recommended by Taylor and Gorton (1977).

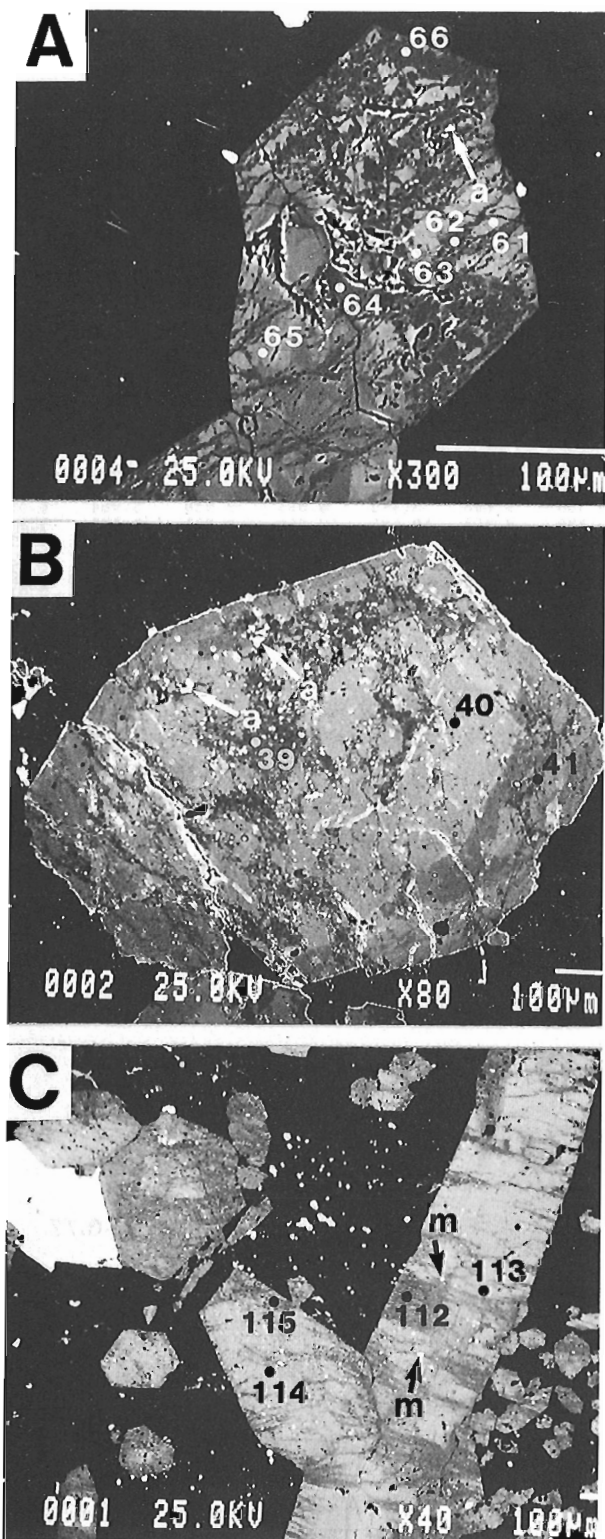


Figure 9. Electron-backscatter images of apatite grains; numbered points refer to electron-microprobe analyses in Table 2. Note allanite (a) inclusions in apatite in A and B, and monazite (m) inclusions in C. White areas outside apatite grains are magnetite grains; black background is pyroxene. GSC 205028.

occupied by F, Cl and OH; however, Br, I, CO_3 , S, N and possibly H_2O may also be present. To determine the nature and extent of REE^{3+} substitution in the Benjamin River apatite, the compositions of selected samples were determined by electron-microprobe analysis. The instrument used was a JEOL JXA 8600 electron-microprobe with Tracor Northern TN 5500 automation. Analyses were performed at an accelerating voltage of 25 KV, beam current of 20 na measured with a Faraday cup and a beam diameter of $5\mu\text{m}$. Data were corrected on-line using Tracor Northern's ZAF correction program. The REE standards used were synthetic glasses prepared by Drake and Weill (1972). X-ray lines were selected to minimize peak overlaps as outlined by Roeder (1985).

REE compositions of typical apatite grains determined by electron-microprobe analysis are given in Table 2; these compositions are for spot analyses of apatite grains shown in Figure 9. Complete compositions of these grains are given in Table 3. The analyses indicate that the REE content is highly varied, both within individual apatite grains and from one grain to another. Overall, lanthanum ranges from 0.01 to 0.89% La and cerium ranges from 0.01 to 1.65% Ce. The average of 131 spot analyses of 42 apatite grains is 0.15% La, 0.50% Ce, 0.21% Nd, 0.06% Sm, 0.03% Eu and 0.07% Gd. Based on this, the REE content of the apatite consists primarily of LREEs and probably averages about 1%. Fluorine content ranges from 2.03 to 4.83% overall and averages 3.09% F.

In most apatite grains compositional variation with respect to REEs appears to be irregular. Dark grey zones in backscatter-electron images (Fig. 9) have lower contents of REEs relative to light grey zones and appear to be associated with microfractures in the apatite; some of the REE content thus appears to have been lost or redistributed after the apatite had crystallized. In some grains, however, compositional variation may be related to primary zoning. The apatite grain in Figure 9B, for example, has a light grey core rimmed by a slightly darker grey zone that appears to conform to the crystal boundary and possibly represents a growth zone. Dark grey, REE-poor zones in Figure 9B appear to be superimposed on the lighter grey zones.

Table 2. Electron-microprobe analyses (wt.%) of apatite grains from the Benjamin River apatite-rare-earth occurrence, New Brunswick.

	La	Ce	Nd	Sm	Eu	Gd	F
Apatite grain in Figure 9A							
Spot 61	0.38	1.24	0.65	0.22	0.02	0.21	2.57
Spot 62	0.19	0.56	0.27	0.12	0.01	0.11	2.60
Spot 63	0.55	1.40	0.62	0.20	0.06	0.23	2.38
Spot 64	0.40	0.65	0.35	0.13	0.02	0.11	2.38
Spot 65	0.72	1.40	0.47	0.16	0.02	0.20	2.87
Spot 66	0.03	0.14	0.07	0.01	0.01	0.01	3.19
Apatite grain in Figure 9B							
Spot 39	0.01	0.17	0.06	0.07	0.01	0.01	3.01
Spot 40	0.40	0.75	0.15	0.08	0.01	0.03	3.07
Spot 41	0.06	0.31	0.06	0.06	0.01	0.01	3.13
Apatite grains in Figure 9C							
Spot 112	0.01	0.03	0.06	0.06	0.01	0.01	2.79
Spot 113	0.53	1.16	0.55	0.20	0.01	0.13	2.82
Spot 114	0.58	1.25	0.57	0.17	0.01	0.14	3.10
Spot 115	0.23	0.35	0.19	0.09	0.01	0.03	3.37

Table 3. Chemical composition (wt.%) of apatite grains from the Benjamin River apatite-rare-earth occurrence, New Brunswick.

	39 ^a	40	41	61	62	63	64	65	66	112	113	114	115
SiO ₂	0.01	0.01	0.01	0.41	0.01	0.47	0.01	0.45	0.01	0.01	0.18	0.45	0.01
Al ₂ O ₃	0.01	0.01	0.01	0.03	0.03	0.05	0.01	0.03	0.03	0.01	0.03	0.01	0.03
CaO	55.46	54.82	55.48	52.36	54.25	52.20	53.93	52.20	55.95	55.73	52.53	52.22	54.64
P ₂ O ₅	42.09	40.81	41.06	39.09	40.92	39.02	39.89	38.79	41.47	42.85	40.21	40.74	42.53
La ₂ O ₃	0.01	0.47	0.07	0.45	0.22	0.65	0.47	0.84	0.03	0.01	0.62	0.68	0.27
Ce ₂ O ₃	0.20	0.88	0.36	1.46	0.66	1.64	0.76	1.64	0.14	0.03	1.36	1.46	0.41
Sm ₂ O ₃	0.08	0.09	0.07	0.26	0.14	0.23	0.15	0.18	0.07	0.07	0.23	0.20	0.10
Nd ₂ O ₃	0.07	0.18	0.07	0.76	0.31	0.72	0.41	0.55	0.01	0.07	0.64	0.66	0.22
Eu ₂ O ₃	0.01	0.01	0.01	0.02	0.01	0.07	0.02	0.02	0.01	0.01	0.01	0.01	0.01
Gd ₂ O ₃	0.01	0.04	0.01	0.24	0.13	0.26	0.13	0.23	0.01	0.01	0.15	0.16	0.03
Cl	0.14	0.65	0.56	0.74	0.65	0.76	0.51	0.70	0.06	0.04	0.77	0.76	0.23
F	3.01	3.07	3.13	2.57	2.60	2.38	2.38	2.87	3.19	2.79	2.82	3.10	3.37
-O=F ₂ +Cl	1.30	1.44	1.44	1.25	1.24	1.17	1.12	1.37	1.36	1.18	1.36	1.48	1.47
Total	99.80	99.60	99.40	97.14	98.69	97.28	97.55	97.13	99.62	100.45	98.19	98.97	100.38
Number of ions based on 26 O													
Si	0.002	0.002	0.002	0.073	0.002	0.084	0.002	0.080	0.002	0.002	0.032	0.078	0.002
Al	0.002	0.002	0.002	0.006	0.006	0.011	0.002	0.006	0.006	0.002	0.006	0.002	0.006
P	6.031	5.931	5.941	5.888	5.994	5.888	5.953	5.848	5.965	6.085	5.958	5.964	6.051
Ca	10.057	10.082	10.159	9.982	10.058	9.968	10.186	9.961	10.185	10.016	9.851	9.675	9.838
La	0.001	0.030	0.004	0.030	0.014	0.043	0.031	0.055	0.002	0.001	0.040	0.043	0.017
Ce	0.012	0.055	0.023	0.095	0.042	0.107	0.049	0.107	0.009	0.002	0.087	0.092	0.025
Sm	0.005	0.005	0.004	0.016	0.008	0.014	0.009	0.011	0.004	0.004	0.014	0.012	0.006
Nd	0.004	0.011	0.004	0.048	0.019	0.046	0.026	0.035	0.001	0.004	0.040	0.041	0.013
Eu	0.001	0.001	0.001	0.001	0.001	0.004	0.001	0.001	0.001	0.001	0.001	0.001	0.001
Gd	0.001	0.002	0.001	0.014	0.007	0.015	0.008	0.014	0.001	0.001	0.009	0.009	0.002
F	1.611	1.667	1.692	1.446	1.423	1.342	1.327	1.617	1.714	1.480	1.561	1.695	1.791
Cl	0.040	0.189	0.162	0.223	0.191	0.230	0.152	0.211	0.017	0.011	0.228	0.223	0.066

^aNumbers refer to spots analyzed as indicated in Fig 9.

Most workers consider that the REEs substitute in apatite as trivalent cations in Ca²⁺ sites, coupled with substitution of Si⁴⁺ for P⁵⁺ to provide a charge balance (e.g. Watson and Green, 1981; Roeder et al., 1987; Rønbro, 1988). A reasonable degree of correlation between Ca²⁺ + P⁵⁺ and REE³⁺ + Si⁴⁺ (Fig. 10) suggests that this is likely the case for the Benjamin River apatite. In strongly peralkaline environments, REE³⁺ cations may substitute for Ca²⁺ with a complementary substitution of Na⁺ for Ca²⁺ providing charge balance (Rønbro, 1988). Such a substitution in the Benjamin River apatite is unlikely as Na contents are below detection levels of the electron-microprobe (<0.01% Na).

LREEs are also present in monazite and allanite inclusions in the Benjamin River apatite (Fig. 9). These grains are minute; allanite grains are up to 20 μm in diameter, monazite grains are generally 5 μm or less in diameter. They appear to be concentrated to some degree in REE-poor zones in the apatite. They account for probably about 10 to 20% of the REEs at Benjamin River.

DISCUSSION

REE content of the apatite-bearing zones at Benjamin River ranges from several hundred to seven thousand ppm total REEs. Even the higher levels are well below those in currently exploited REE deposits. The Mountain Pass deposit in California, for example, has an average grade of 8.86% total rare-earth oxides (O'Driscoll, 1988) and the Bayan Obo deposit in China contains 1 to 6% rare earths (Argall, 1980).

At both Mountain Pass and Bayan Obo, the principal REE-bearing mineral is bastnaesite; REEs at Benjamin River are concentrated primarily in apatite. Although it is unlikely that REEs could be produced from Benjamin River apatite as primary products under current economic conditions, they may have some potential as byproducts. Apatite

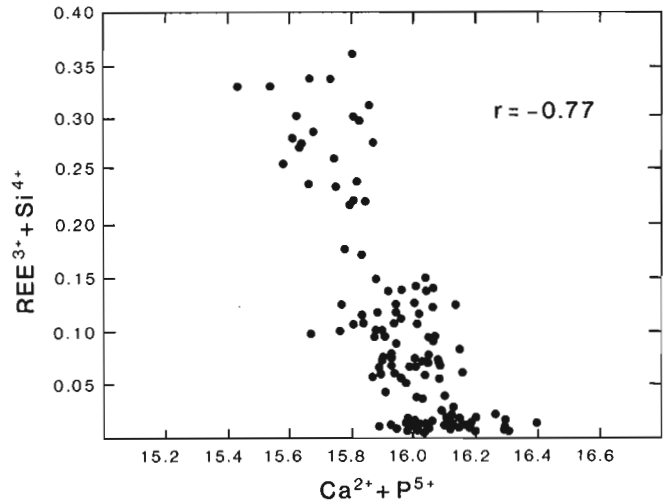


Figure 10. Plot of Ca²⁺ + P⁵⁺ versus REE³⁺ + Si⁴⁺; r = linear correlation coefficient.

concentrates from deposits associated with the Khibiny alkalic igneous complex in the Kola Peninsula, U.S.S.R., for example, contain 0.85 % rare-earth oxides (Notholt, 1979); the rare-earths are apparently recovered as byproducts from the processing of the phosphate to produce fertilizer. Preliminary tests by the New Brunswick Department of Natural Resources and Energy have had some success in upgrading apatite from Benjamin River by phosphate floatation techniques and extracting REEs with dilute sulphuric acid (D. Thibault, pers. comm., 1988).

The Benjamin River apatite occurrence has some similarities with apatite-bearing iron deposits. At Mineville, New York, apatite is associated with magnetite deposits related to Proterozoic gabbroic and granitic rocks (McKeown and Klemic, 1956). REE content of the Mineville apatite, however, is significantly higher than in Benjamin River apatite. According to electron-microprobe analysis by Roeder et al. (1987), Mineville apatite is highly enriched in LREEs, including 1.376 % La, 2.717 % Ce, 1.359 % Nd and 1.487 % Y. In 1985, Rhône-Poulenc acquired the ore reserves and tailings at Mineville as a potential source of yttrium and europium (O'Driscoll, 1988), but there has since been no report of production.

Other iron deposits that contain REE-bearing apatite include Kiruna, Sweden, and Avnik, Turkey. Apatites from Kiruna-type deposits in northern Sweden contain 0.15 to 0.67 % total REEs (Parák, 1973); those from the Avnik region in southeastern Turkey contain 0.20 to 0.41 % total REEs (Helvacı, 1984). Furthermore, the REEs are generally enriched in LREEs with the exception of significant europium depletion at Avnik. In this regard, the REE patterns from Avnik ores in particular are strikingly similar to those from the Benjamin River occurrence.

Kiruna-type iron deposits have long been considered to be magmatic (e.g. Geijer, 1931; Frietsch, 1978) although this hypothesis has frequently been challenged (e.g. Parák, 1973, 1975, 1985; Hildebrand, 1986). According to Parák (1973), the REE contents of Kiruna-type ores and associated apatite are similar to those found in sedimentary and metamorphic rocks and therefore do not support a magmatic origin. Fleischer (1983, 1986), however, showed that Parák's (1973) REE data, as well as REE data from other apatite-bearing iron ores, have no affinities with sedimentary rocks; instead they are comparable to REE compositions of apatites from ultramafic and alkaline rocks, including carbonatites. He concluded that the REE data support a magmatic origin for Kiruna-type ores. Helvacı (1984) also favoured a magmatic origin for the apatite-rich iron ores of the Avnik region, based to a large extent on the REE data.

REE data for the Benjamin River apatite are thus consistent with a magmatic origin for the occurrence. The negative europium anomaly in the apatite-bearing samples probably reflects the strong preference of apatite for trivalent REEs (cf. Watson and Green, 1981). In this case the iron- and phosphorus-rich silicate melt from which the apatite crystallized was either depleted in europium, or had a low fO_2 that favoured Eu^{2+} over Eu^{3+} . Depletion of europium in the melt may have resulted from fractional crystallization in the parent magma from which the melt was derived. Feldspar porphyry, which is characterized by a positive europium anomaly, may represent a fraction of the parent magma in which europium was enriched.

SUMMARY

The Benjamin River apatite-REE occurrence consists of pegmatitic apatite-pyroxene-magnetite zones and apatite-bearing veins and veinlet stockwork zones that are most closely associated with small intrusions of feldspar porphyry. The occurrence of pegmatitic zones and particularly the presence of apatite with unidirectional solidification textures within them suggests that apatite crystallized directly from an iron- and phosphorus-rich silicate melt. The chondrite-normalized REE patterns are consistent with a magmatic origin.

REEs are concentrated mainly in apatite; total REE content is about 1 to 2 %, with LREEs predominating over HREEs. Distribution of REEs in apatite is irregular except in some grains that have apparent growth zones. A small proportion of REEs occur in monazite and allanite inclusions in apatite.

The REE contents of the Benjamin River apatite are comparable to those in apatites associated with ultramafic and alkaline rocks, including carbonatites, and some apatite-rich iron deposits of supposed magmatic origin. Under current economic conditions, recovery of REEs from the apatite is unlikely except as possible byproducts if the apatite were to be processed for phosphate. The potential for magnetite deposits at Benjamin River, with possible byproduct phosphate and REEs, should be considered in exploration.

ACKNOWLEDGMENTS

Long Lake Gold Ltd. gave permission to conduct this study and provided data from their sampling program. K.D.A. Whaley provided logistical and historical information on the Benjamin River property. K.K. Nguyen assisted in the mapping and sampling program and drafted the figures. T.C. Birkett, D. Richardson and J.B. Whalen reviewed the paper and provided helpful comments.

REFERENCES

- Argall, G.O.**
1980: Three iron ore bodies of Bayan Obo; *World Mining*, January, 1980, p. 38-41.
- Ayuso, R.A.**
1986: Lead-isotopic evidence for distinct sources of granite and for distinct basements in the northern Appalachians, Maine; *Geology*, v. 14, p. 322-325.
- Davies, J.L.**
1979: Geology map of northern New Brunswick; New Brunswick Department of Natural Resources, Map NR-3.
- Drake, M.J. and Weill, D.F.**
1972: New rare earth element standards for electron microprobe analysis; *Chemical Geology*, v. 10, p. 179-181.
- Fleischer, M.**
1983: Distribution of the lanthanides and yttrium in apatites from iron ores and its bearing on the genesis of ores of the Kiruna type; *Economic Geology*, v. 78, p. 1007-1010.
1986: The lanthanides and yttrium in minerals of the apatite group – an analysis of the available data; *Neues Jahrbuch für Mineralogie Monatshefte*, v. 1986, no. 10, p. 467-480.
- Freitsch, R.**
1978: On the magmatic origin of iron ores of the Kiruna type; *Economic Geology*, v. 73, p. 478-485.
- Geijer, P.**
1931: The iron ores of the Kiruna type: geographical distribution, geological characters, and origin; *Sveriges Geologiska Undersökning, Ser. C*, no. 367, 39 p.
- Greiner, H.R.**
1970: Geology of the Charlo area 21-O/16, Restigouche County, New Brunswick; New Brunswick Department of Natural Resources, Map Series 70-2, 18 p.
- Helvacı, C.**
1984: Apatite-rich iron deposits of the Avnik (Bingöl) region, southeastern Turkey; *Economic Geology*, v. 79, p. 354-371.
- Hildebrand, R.S.**
1986: Kiruna-type deposits: their origin and relationship to intermediate subvolcanic plutons in the Great Bear Magmatic Zone, northwest Canada; *Economic Geology*, v. 81, p. 640-659.
- Jahns, R.H. and Tuttle, O.F.**
1963: Layered pegmatite-aplite intrusives; *Mineralogical Society of America, Special Paper 1*, p. 78-92.
- Kirkham, R.V. and Sinclair, W.D.**
1988: Comb quartz layers in felsic intrusions and their relationship to porphyry deposits; *in Recent Advances in the Geology of Granite-Related Mineral Deposits*, ed. R.P. Taylor and D.F. Strong, The Canadian Institute of Mining and Metallurgy, Special Volume 39, p. 50-71.
- Marleau, R.A.**
1969: Magnetic and geochemical surveys on the Colborne Property, N.B.; Doral Mining Exploration Ltd., report #471986 in assessment files of the Geological Surveys Branch, New Brunswick Department of Natural Resources and Energy, Fredericton.
- McKeown, F.A. and Klemic, H.**
1956: Rare-earth-bearing apatite at Mineville, Essex County, New York; U.S. Geological Survey, Bulletin 1046-B, p. 9-26.
- Notholt, A.J.G.**
1979: The economic geology and development of igneous phosphate deposits in Europe and the USSR; *Economic Geology*, v. 74, p. 339-350.
- O'Driscoll, M.**
1988: Rare earths — enter the dragon; *Industrial Minerals*, no. 254, p. 21-55.
- Parák, T.**
1973: Rare earths in the apatite iron ores of Lappland together with some data about the Sr, Th and U content of these ores; *Economic Geology*, v. 68, p. 210-221.
1975: Kiruna iron ores are not "intrusive-magmatic ores of the Kiruna type"; *Economic Geology*, v. 70, p. 1242-1258.
1985: Phosphorus in different types of ore, sulfides in the iron deposits, and the type and origin of ores at Kiruna; *Economic Geology*, v. 80, p. 646-665.
- Roeder, P.L.**
1985: Electron-microprobe analysis of minerals for rare-earth elements: Use of calculated peak-overlap corrections; *Canadian Mineralogist*, v. 23, p. 263-271.
- Roeder, P.L., MacArthur, D., Ma, X.-P., Palmer, G.R., and Mariano, A.N.**
1987: Cathodoluminescence and microprobe study of rare-earth elements in apatite; *American Mineralogist*, v. 72, p. 801-811.
- Rønsbro, J.G.**
1988: Coupled substitutions involving REEs and Na and Si in apatites from the Ilfmaussaq intrusion, South Greenland, and the petrological implications; *American Mineralogist*, v. 74, p. 896-901.
- Roy, D.M., Drafall, L.E., and Roy, R.**
1978: Crystal chemistry, crystal growth, and phase equilibria of apatites; *in Phase Diagrams, Materials Science and Technology, Volume V*, ed. A.M. Alper, Academic Press, New York, p. 185-239.
- Schrock, G.E.**
1987: Property examination report, Benjamin River; private report.
- Shannon, J.R., Walker, B.M., Carten, R.B., and Geraghty, E.P.**
1982: Unidirectional solidification textures and their significance in determining relative ages of intrusions at the Henderson Mine, Colorado; *Geology*, v. 10, p. 293-297.
- Stewart, R.D.**
1978: Geology of the Benjamin River intrusive complex; unpublished M.Sc. thesis, Carleton University, Ottawa, 126 p.
- Taylor, S.R. and Gorton, M.P.**
1977: Geochemical application of spark source mass spectrography—III. Element sensitivity, precision and accuracy; *Geochemica et Cosmochimica Acta*, v. 41, p. 1375-1380.
- Van Staal, C.R. and Fyffe, L.R.**
in press: Dunnage zone of New Brunswick; *in Canadian Appalachian Volume, Decade of North American Geology*.
- Watson, E.B. and Green, T.H.**
1981: Apatite/liquid coefficients for the rare earth elements and strontium; *Earth and Planetary Science Letters*, v. 56, p. 405-421.
- Whaley, K.D.A.**
1989: Report on the Benjamin River Property, Restigouche County, New Brunswick; Long Lake Gold Ltd., private company report.

An earthquake doublet in the Charlevoix seismic zone, Québec

R.J. Wetmiller and John Adams
Geophysics Division

Wetmiller, R.J. and Adams, J., An earthquake doublet in the Charlevoix seismic zone, Québec; in Current Research, Part B, Geological Survey of Canada, Paper 90-1, p. 105-113, 1990.

Abstract

In March 1989 an earthquake doublet occurred in the highly-active Charlevoix seismic zone. The pair of earthquakes (m_{bLg} 4.3 on 9 March and m_{bLg} 4.4 on 11 March, forty-seven hours apart) were co-located and had very similar waveforms and focal mechanisms, suggesting a repeated rupture on a common fault plane that may be evidence of weakening of the rocks in a critical part of the seismic zone. They occurred a) close to the hypocentre of the damaging 1925 Charlevoix earthquake, b) at one edge of an aseismic slab which has persisted since at least 1977, and c) at the depth of the strongest part of the crust. This is the first time that an earthquake doublet has been identified in the Charlevoix seismic zone with any confidence. It has not been followed by a larger earthquake in the subsequent six months.

Résumé

En mars 1989, un double séisme s'est produit dans la zone sismique fortement active de Charlevoix. Les deux séismes (m_{bLg} 4,3 le 9 mars et m_{bLg} 4,4 le 11 mars, à 47 heures d'intervalle) étaient situés au même endroit et avaient des formes d'onde et des mécanismes focaux très similaires, laissant supposer une rupture répétée sur un plan de faille commun qui peut être l'indice d'une faiblesse des roches dans une partie critique de la zone sismique. Les deux séismes se sont produits a) près de l'hypocentre du désastreux séisme de Charlevoix de 1925, b) à une arête d'une dalle asismique qui persiste depuis au moins 1977 et c) à la profondeur de la partie la plus résistante de la croûte. Il s'agit de la première fois qu'un double séisme est reconnu avec certitude dans la zone sismique de Charlevoix. Il n'a pas été suivi d'un plus grand séisme dans les six mois suivants.

INTRODUCTION

In March 1989 an unusual and unique earthquake doublet took place in the Charlevoix seismic zone (CSZ), source of five large earthquakes during historical times. The events of the doublet were the largest earthquakes in the CSZ in a decade and were widely felt in the Charlevoix and Kamouraska regions of Québec, causing a great deal of public concern. At the time, the seismological staff of the Geological Survey of Canada were aware of the unique character of the doublet and the fact that similar waveforms had been identified by some studies as a characteristic of foreshocks, so there was naturally some concern that the doublet might have been precursory to a large, damaging earthquake in the Charlevoix seismic zone. However it was concluded that the doublet, while certainly unusual, was not sufficient evidence that a larger earthquake was imminent and, in fact, no larger earthquake occurred in the six months following the doublet.

The doublet event in the CSZ occurred at a time of unusual earthquake activity throughout eastern Canada which followed the Saguenay earthquake of 25 November, 1988 (magnitude m_b 6.0) which was the largest earthquake in southeastern Canada since the m_b 6.2. Timiskaming earthquake of 1935. The Saguenay earthquake, the strong ground motion records it produced, and the damage it caused are already documented by numerous papers (North

et al., 1989; Du Berger et al., 1990; Munro and Weichert, 1989; Hough et al., 1989; Mitchell et al., 1989; Tuttle et al., 1989). A coincident or related effect of the Saguenay earthquake was a dramatic increase in the number of larger earthquakes in eastern Canada for a period of about four months. It was during this notable four-month period of increased earthquake activity that the earthquake doublet occurred in the CSZ.

The anomalous nature of the seismic activity in eastern Canada in this period has spurred our thinking about the nature of the larger earthquakes in the CSZ and the type of precursory seismic activity that might be expected to precede them. It is not our intention here to predict the next large earthquake in CSZ. In fact, we do not believe that that event is necessarily imminent nor do we believe that there is sufficient information at this time to make a reliable prediction. Instead, we present an overview of the Charlevoix seismicity, document the parameters of the doublet and speculate how the doublet may relate to the pattern of activity in the CSZ. We conclude by suggesting that the prediction of the next large event in the CSZ on the basis of seismicity patterns alone will not be at all easy.

THE CHARLEVOIX SEISMIC ZONE

The Charlevoix seismic zone (CSZ; *see* Fig. 1 for location) is one of the few locations in eastern North America where

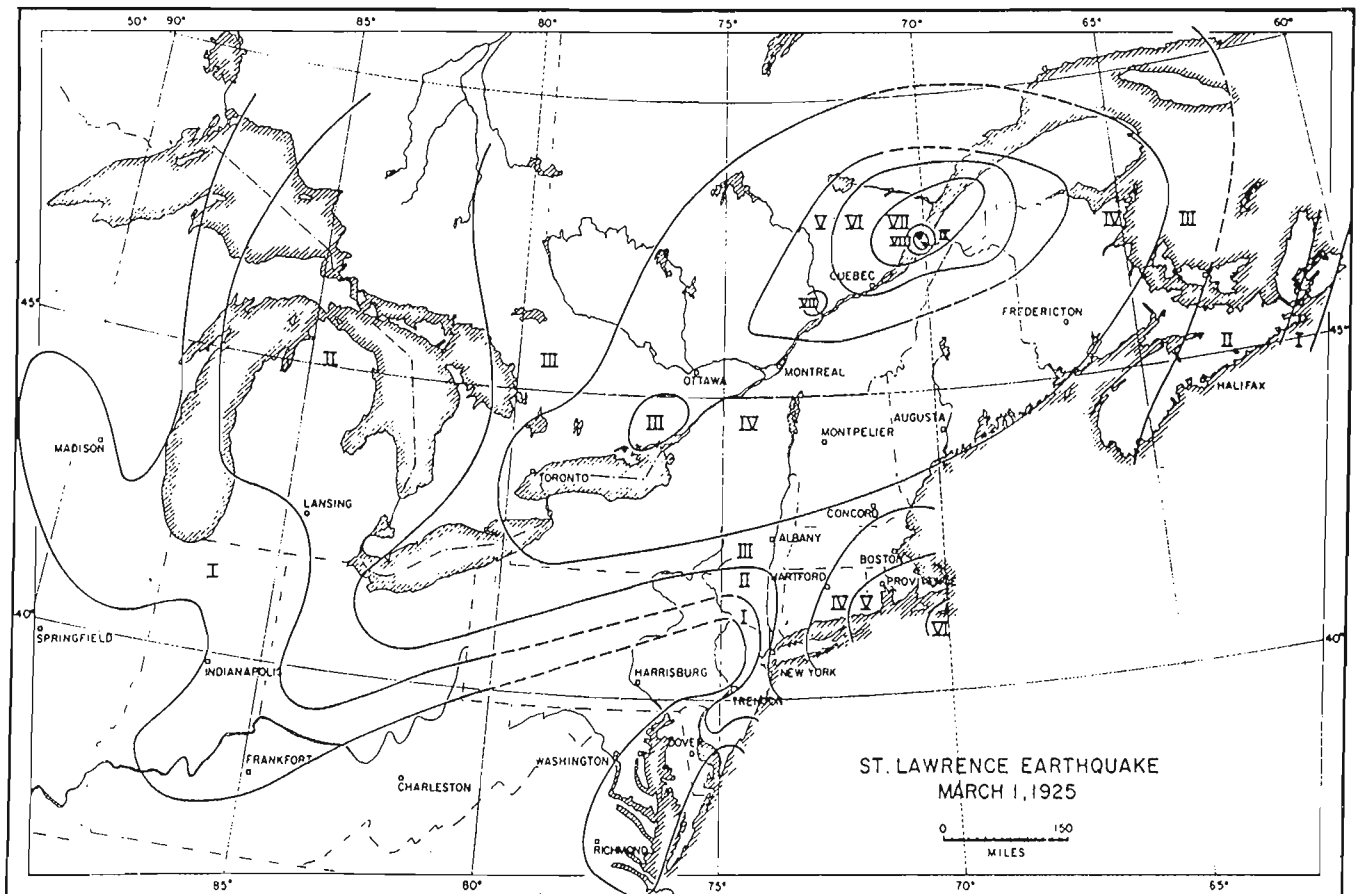


Figure 1. Isoseismal map of the 1925 Charlevoix earthquake (Smith, 1962), showing the large felt area of the earthquake and the general location of the CSZ.

large earthquakes have repeated. Smith (1962) showed that earthquakes of about magnitude 6 or greater have occurred in the St. Lawrence valley northeast of Québec City at least five times, in 1663, 1791, 1860, 1870 and 1925. The 1925 event had a magnitude (M_s) of 6.5 (Ebel et al., 1986), was felt very widely (Fig. 1), and caused much property damage in communities along both shores of the St. Lawrence River adjacent to the epicentre and in the lower town of Québec City (Hodgson, 1925, 1950; Smith, 1962). It is now over 60 years since that last large event and therefore not at all unreasonable to consider what the consequences might be of a comparable CSZ earthquake sometime in the future.

Given the significant development and population growth in Quebec since 1925 another large event in the zone seems certain to produce severe consequences in terms of property damage and public trauma. For this reason the Canadian Government carried out extensive geophysical monitoring of the CSZ from 1974 to 1985 (Buchbinder et al., 1988) with the longterm aim of determining the background level and fluctuations in activity, recognizing (probably after the fact) precursory phenomena to a large earthquake, and so developing the capability to predict subsequent large earthquakes and hence perhaps mitigate their effects in ways not currently possible. Many aspects of the monitoring were discontinued in 1985 as a cost-cutting measure and because the results had been negative. Current research is restricted to determining the microseismicity with one analogue seismograph station, one Eastern Canada Telemetered Network station and a 6-station telemetered network which has operated continuously since late 1977

(Anglin and Buchbinder, 1981; Anglin, 1984). The original analogue network was converted to a wide dynamic range digital network in October 1987.

To date, the Charlevoix studies have identified no reliable precursors to the small-to-moderate (M 5.0 or less) events that have occurred in the zone since the program began. However, they have established accurate baselines against which any possible precursory activity in the future can be judged. These baselines included seismicity, seismic travel-times, electrical impedance, vertical movement, horizontal movement, tilt, gravity changes, and strain through well-water fluctuations (Buchbinder et al., 1988).

DETAILED STRUCTURE OF THE CHARLEVOIX SEISMIC ZONE

The extent of the CSZ has been defined by the distribution of microseismicity determined by the local seismic network which has operated continuously since late 1977, and by a number of short-term field experiments, notably in 1970 and 1974 (Leblanc et al., 1973; Leblanc and Buchbinder, 1977; Lamontagne, 1987). Figure 2 shows the distribution of the microseismicity which occupies an area approximately 35 by 85 km mostly under the St. Lawrence River. Focal depths of these events vary from less than 3 to over 30 km, which places them within the crystalline Precambrian rocks of the Canadian Shield. Seismic activity appears to be absent within the Appalachian sedimentary rocks which form the southern shore of the St. Lawrence River in this area. Apparently, earthquakes in the CSZ can occur deeper than 25 km



Figure 2. Stereo pair of overhead view of earthquakes in the Charlevoix Seismic Zone (similar to Anglin, (1984), but updated to include earthquakes until March 1989).

because the old Precambrian crust is water-saturated (Kirsch et al., 1987) and has a heat flow of only 30 mW/m² (Mareschal et al., 1989), and so behaves in a brittle fashion even at such depths (Hasegawa, 1986). However, in profile the most stressed, and probably strongest, part of the crust is from 7 — 15 km, as evidenced by the strong peak around 10 km in the depth distribution of the CSZ micro-earthquakes (Fig. 3).

The boundaries of the seismicity distribution in the CSZ appear to be controlled by steeply dipping faults running parallel to the river (Anglin and Buchbinder, 1981). These faults were originally rift faults that formed the ancient continental margin of the Iapetus Ocean and were last active during a period of continental rifting in post-Silurian times, perhaps as recently as the Mesozoic (Kumarapeli and Saull, 1966; Kumarapeli, 1985). In the current tectonic regime they behave as thrust faults reactivated by the high horizontal compressive stress field that is prevalent in eastern North America (Adams, 1989). The influence of the rift faults on the CSZ seismicity is best seen on the north shore of the St. Lawrence where the Gouffre Fault clearly forms the northwest boundary to the seismic zone. Elsewhere the correlation between the rift faults and seismicity is obscured by the river or by sediment cover, but in cross-sections across the trend of the river Anglin (1984) recognized that the seismicity was controlled by a framework of northeast-striking rift faults and northwest-striking transverse faults (Fig. 4).

A number of reports (Hasegawa and Wetmiller, 1980; Lamontagne, 1987; Adams et al., 1988a, b) have shown P-nodal mechanisms for recent small-magnitude Charlevoix earthquakes that support reverse movement on these high-angle faults being the dominant earthquake mechanism, although from the nodal planes as many of the earthquakes seem to occur on the transverse faults as the rift faults.

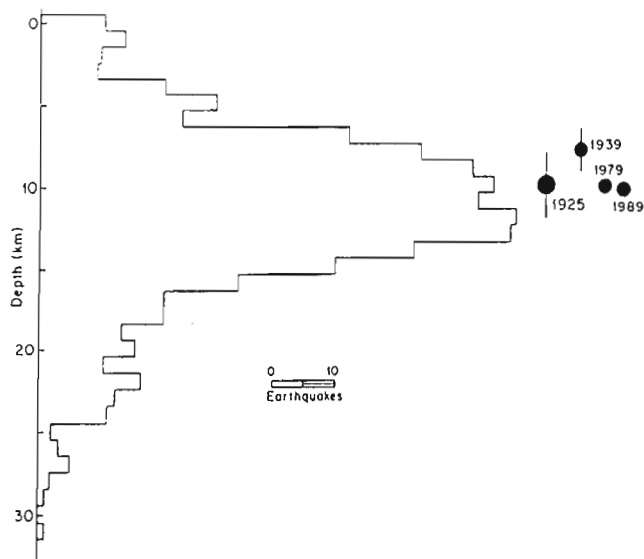


Figure 3. Histogram of depths for microearthquakes in CSZ from 1977 to March 1989, together with the focal depths of some of the larger earthquakes in the zone as discussed in the text.

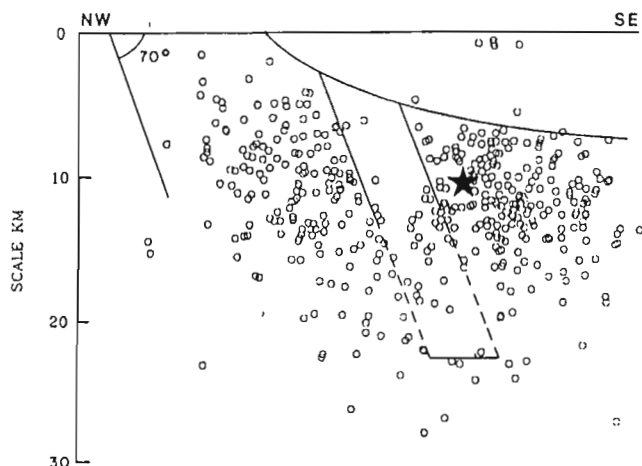


Figure 4. Section taken normal to the St. Lawrence River of earthquake hypocentres for the middle half of the CSZ showing the aseismic slab and the truncation of activity at the base of the overthrust Appalachian rocks. Star represents the location of the 1979 earthquake.

Anglin and Buchbinder (1981) first noted that the microseismicity was not uniformly distributed within the CSZ, but that there were persistent aseismic volumes within the seismic zone. Two distinct aseismic volumes within the seismic zone are visible on Figure 2; one is near Ile aux Coudres at the south-western end of the zone, the other is off La Malbaie about halfway between Ile aux Lièvres and Ile aux Coudres (see Fig. 5 for the locations of the islands). These two volumes are in fact part of a long contiguous aseismic volume which runs almost the entire length of the CSZ. However, at depths below 15 km the aseismic volume is parted in the middle by a transverse trend of micro-earthquakes. In sections taken normal to the river (e.g. Fig. 4) the volume can be seen to have the form of a slab, about 5 km thick that dips 70° to the southeast. It is bounded to the northwest by a seismically active slab of twice the thickness and to the southeast by a cloud of activity that is truncated at the top by the contact with the Appalachian rocks. The slab extends down dip (“width”) from the base of the Appalachian rocks to about 15 km in the middle, deeper at the ends, and has a length of over 40 km. Although projected sections suggest closure at the ends, various stereo views suggest that the closure is apparent rather than real.

The microseismic monitoring has confirmed that the aseismic slab has been almost completely devoid of seismic activity since 1977. Therefore it may represent a localized part of the seismic zone which is: a) weak, and strain is dissipated aseismically; b) strong, and strain is transmitted without generating microseismicity; or c) strong, and lies about a strained fault within which microseismicity is suppressed during some parts of the earthquake cycle. We do not favour a) because the evidence for such weak rocks in the Grenville Province is lacking, but are unable to choose between b) and c), though c) seems more plausible.

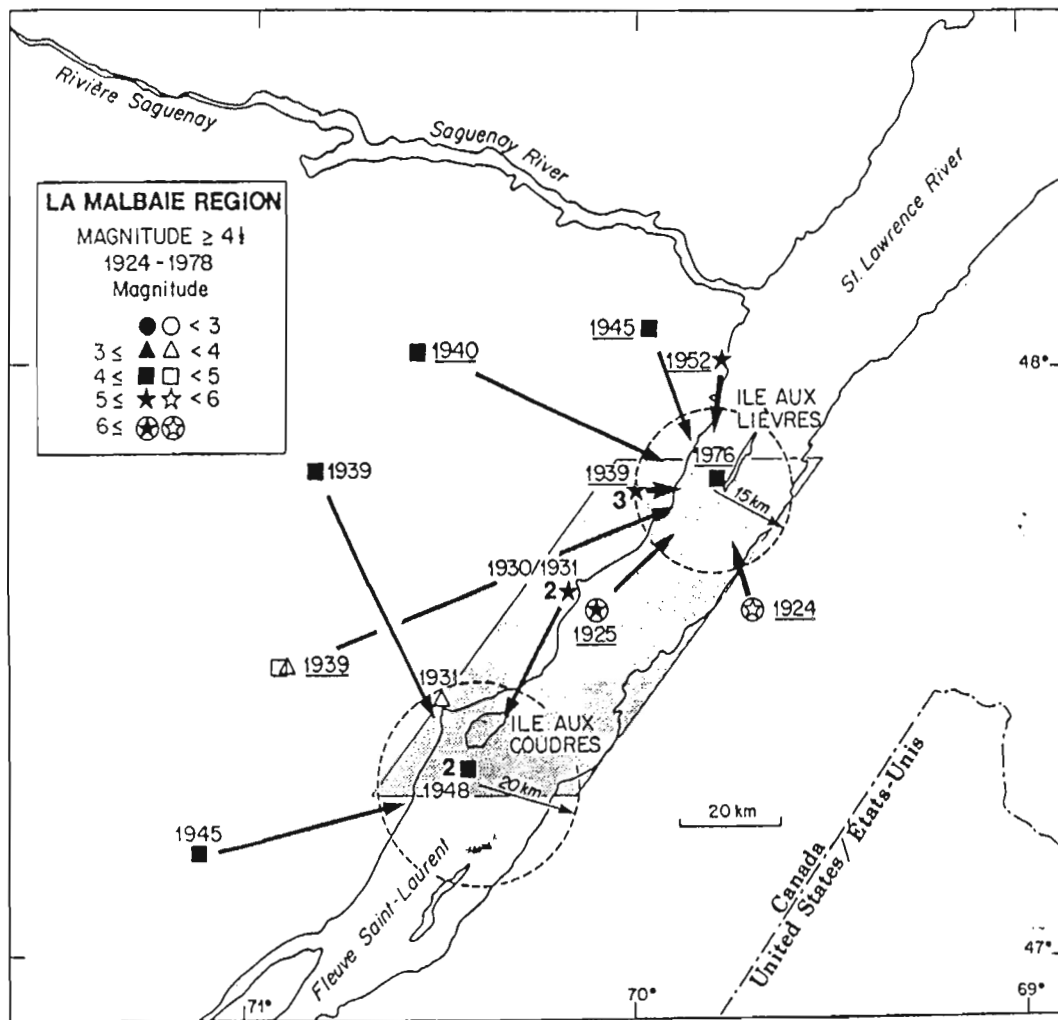


Figure 5. Areas in the CSZ where large events in this century have nucleated. Arrows show relocations from former epicentres to the two source areas determined by Stevens (modified after Stevens, 1980).

RELATIONSHIP OF LARGE EARTHQUAKES TO THE SEISMIC ZONE

Stevens (1980) relocated some of the larger Charlevoix earthquakes of this century and showed that all the larger events nucleated at one end or the other of the seismic zone (Fig. 5). In particular, the 1925 earthquake appeared to have nucleated at the northeastern end of the zone as did a magnitude M5.5 event which occurred 5 months prior to the 1925 event. We follow Stevens (1980, p. 554) and interpret the distribution of the large earthquakes to represent the sites of stress concentrations (asperities) at each end of the seismic zone, asperities which trigger large earthquakes when they fail. The rupture zone of the large events presumably extends into the main part of the seismic zone, modifying or extending it, possibly releasing the strain accumulated in the aseismic volume in the process.

The depth of the largest earthquake for which we have a reliable computed depth (1979, M 5.0) was 10 ± 2 km. The 1979 earthquake occurred on the upper boundary of the seismic slab (star on Fig. 4). Ebel et al. (1986) showed that the 1925 event initiated at a depth of 10 ± 2 km, but it is not possible to locate the 1925 epicentre relative to the end of the aseismic slab with any confidence. The 1939 m_{bLg} 5.6 occurred at 8 ± 1 km (Ebel et al., 1986). Because of the strength profile of the lithosphere, we consider that a

seismic failure at depths near 10 km is most likely to trigger the release of the accumulated strains throughout the entire zone, thereby resulting in a large earthquake.

In summary, we consider that it is activity towards the ends of the seismic zone, close to the boundary of the aseismic slab, and at a depth of about 10 km, which should be of most concern to anyone who wishes to anticipate the next big earthquake.

EARTHQUAKE DOUBLET ON 9-11 MARCH 1989

The earthquake doublet occurred at $47.718 \pm 0.005^\circ\text{N}$, $69.865 \pm 0.01^\circ\text{W}$ near the northeastern end of the CSZ at a depth of 10.5 ± 0.5 km. The first event (m_{bLg} 4.3) took place on 9 March at 09:40 UT and the second (m_{bLg} 4.4) forty-seven hours later on 11 March at 08:31 UT. The doublet events are the largest seismic events in the CSZ since the M 5.0 event in 1979. They were not followed by unusual seismic activity within the zone, and no larger events have occurred in the six months since.

The location of the doublet (Fig. 6) is within the more northeasterly of the two areas where large events have nucleated (as identified by Stevens, 1980), at the northerly end of the aseismic slab identified by Anglin (1984), and at the depth of the strongest part of the crust. The doublet also

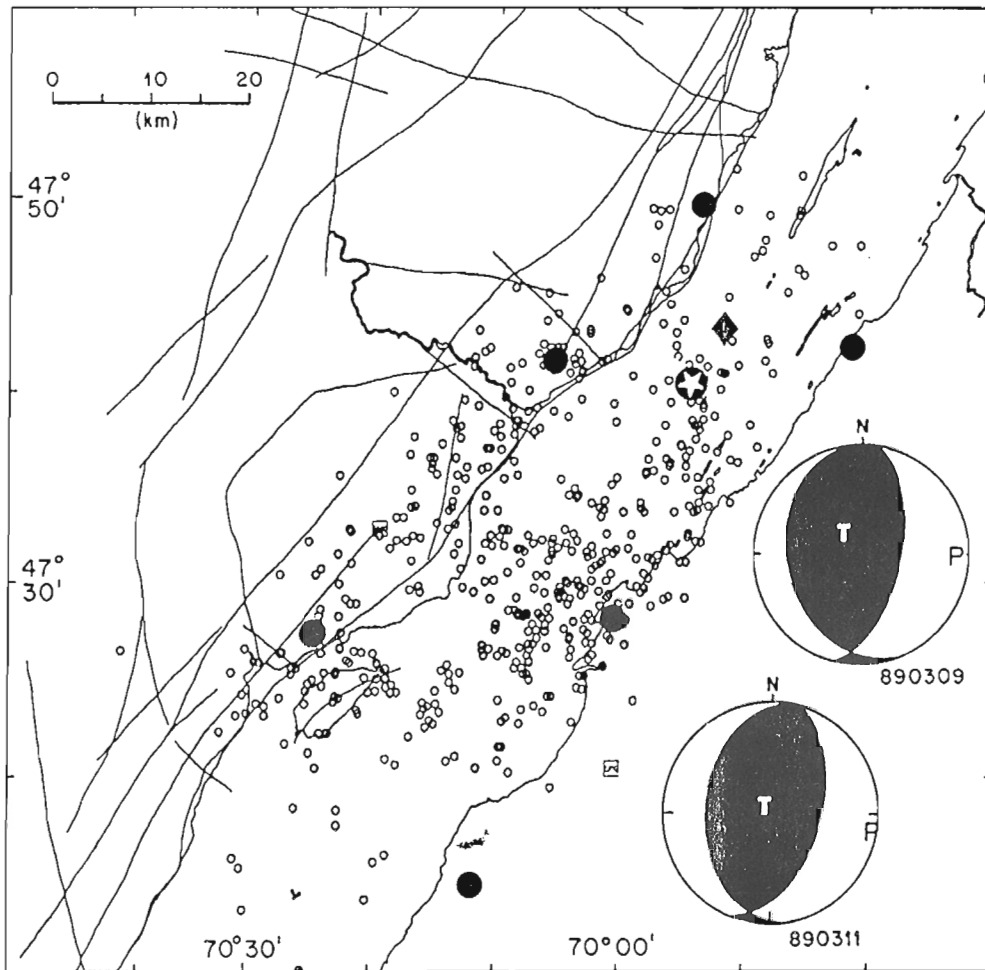


Figure 6. Location of the earthquake doublet of 9 and 11 March 1989 in the CSZ (diamond), and of the 1979, M5 earthquake (star), together with the microseismicity as in Figure 2. Focal mechanisms (lower hemisphere projections with P and T axes marked) for the two 1989 earthquakes are shown in the lower right corner. Location of the 6 seismograph stations of the local network are shown by solid circles.

occurred close (≈ 10 km) to the epicentre of the 1925 earthquake (47.8°N , $69.8^{\circ}\text{W} \pm 15$ km), and at a similar focal depth.

Three-component waveforms of the doublet events on a typical station of the Charlevoix network are shown on Figure 7. The high degree of similarity between the waveforms of the two events is obvious. As might be expected, the focal mechanisms of the two events are similar, representing thrust faulting on north-trending planes (inset to Fig. 6). From the trend of nearby epicentres and the southeasterly dip of the rift faults we favour the steep, east-dipping nodal plane as the probable fault plane.

Earthquake doublets of any size have been rare in CSZ and none of this magnitude have occurred since detailed monitoring began in 1977. An examination of Smith's 1962 and 1966 catalogues and the Geophysics Division earthquake database also reveals only one other possible pair of felt or instrumentally-located earthquakes of this size, a pair of m_{blg} 3.6 earthquakes 80 minutes apart in April 1969 at the southwestern end of the seismic zone. The 1969 pair occurred before the advent of digital seismographs in Canada, and before detailed monitoring of CSZ began, so it is unclear whether their waveforms were similar.

Ishida and Kanamori (1978) first noted such similarity of waveforms could be a powerful diagnostic tool for identifying foreshock sequences. They studied five small events

($M < 3$) which had very similar (to each other) waveforms that occurred in the year preceding the 1971 San Fernando earthquake in California. The events were located within a small area around the mainshock epicentre and had remarkably similar waveforms from event to event. Ishida and Kanamori (1978) concluded that these events were in fact foreshocks to the San Fernando event, which were unrecognized at the time of the mainshock. Subsequent studies (Pechman and Kanamori, 1982) have shown that similar waveforms are neither a necessary nor a unique characteristic of foreshocks generally, but that the significance of earthquakes with repeated waveforms must be evaluated within the context of each unique seismotectonic environment. We propose to examine the waveforms of other pairs of CSZ microearthquakes to ascertain their degree of waveform similarity and temporal significance.

Thus, the doublet earthquakes in the CSZ in March 1989 satisfy many of the conditions that one would expect for foreshocks to a large Charlevoix event; they are located in one of the asperities that has nucleated large events, at the end of the aseismic slab where strain may be accumulating, and at the depth of the strongest part of the crust. In addition, their similar waveforms may be the first evidence of a systematic weakening of the critical asperity. However, they have not been followed (in six months) by a larger event and hence doublet events in general cannot be considered a reliable basis by themselves for a short-term prediction of a larger event in the CSZ.

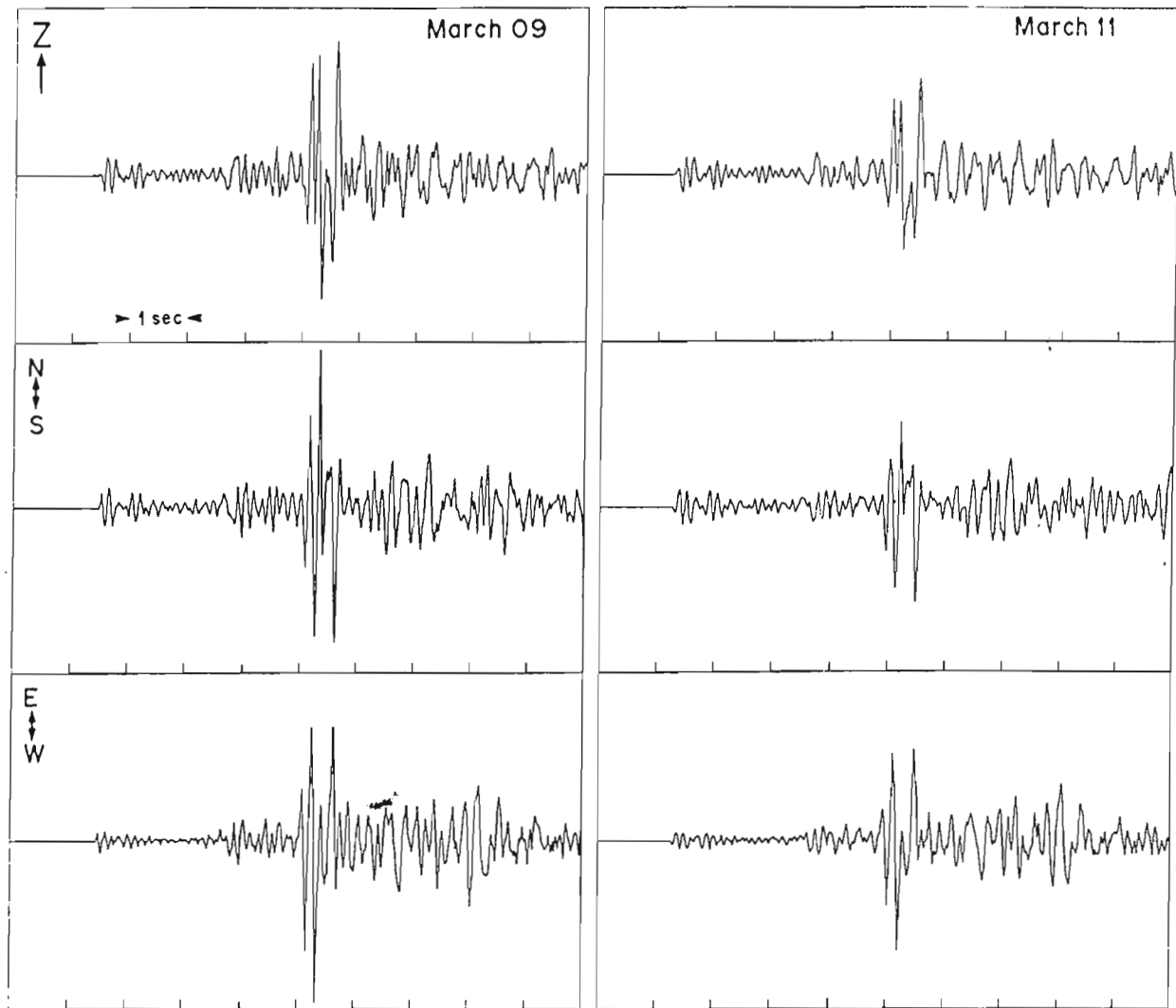


Figure 7. Three-component waveforms from seismograph station A16 for the doublet events of 9 and 11 March 1989. The vertical and horizontal scales are the same for each trace.

THE ROLE OF MICROSEISMICITY IN PREDICTING THE NEXT CHARLEVOIX EARTHQUAKE

The geophysical monitoring that has been carried out to date in the CSZ has not provided any clear examples of what type of precursory activity might be expected prior to a large ($M > 6$) earthquake, simply because no large earthquake has occurred during the period of the program. However at the present time, the seismicity monitoring by the Charlevoix Network is the only geophysical monitoring program routinely carried out continuously and therefore the only practical means for a short-term (hours to weeks) prediction of large events in the CSZ. Thus, any credible short-term prediction of a large CSZ event will have to be based on exceptional seismic activity being recognized within the zone, exceptional by rate or magnitude or style. However, we suggest it will also be essential to include other phenomena that might reasonably be expected for precursory activity. Two examples serve to illustrate why corroboration is essential.

In 1977 a tripling of the rate of small-magnitude seismic activity (largest earthquake was m_{bLg} 3.1) in the CSZ over a period of a few months caused considerable concern at the time that a large event was imminent (Buchbinder et al., 1988). A large event did not occur and the rate of small earthquakes eventually declined to normal values (about 12 events per month, of which one-half can be located by the local network). Subsequent monitoring has shown that variations of a factor of 2 or 3 in the rate of activity in the CSZ as a whole are not uncommon and do not necessarily represent precursory activity. This experience suggests that a three-fold increase in micro-earthquake activity is not sufficient by itself for a reliable short-term prediction.

In September, 1924 a m_{bLg} 5.5 earthquake occurred at the northeast end of the zone near where the 1925 rupture began five months later. We have no information whether any other unusual seismic activity occurred in the intervening months but, apparently, there were no felt earthquakes ($M > 4$) in the zone between September 1924 and March

1925 (Smith, 1962. Hodgson, 1950). Thus, the 1924 earthquake, while it might have been related to the 1925 mainshock in some fashion, was not immediately followed by the large event and was not sufficient by itself for a short-term prediction of the event. Comparable earthquakes, m_{bLg} 5.6 in 1939 and m_{bLg} 5.0 in 1979, were followed by localized smaller aftershocks but not a larger earthquake, despite (in the case of the 1979 earthquake at least) being located at 10 km depth on the edge of the aseismic slab. We are tantalized by thoughts of what the level and pattern of microearthquake activity was between the 1924 and 1925 earthquakes, but have only the lack of felt reports for crude advice.

Thus the physical significance of changes in seismic activity by itself can often be difficult to ascertain. The next large CSZ earthquake might be preceded by activity so unusual that it was immediately recognizable as foreshock activity. However, doublet events, a high rate of microearthquake activity and single magnitude 5 events have from experience been shown to be unreliable evidence on their own of the imminence of a larger event. It is more likely that there will be only subtle seismicity changes, the significance of which may be appreciated only in hindsight. In such circumstances, prompt information from other geophysical phenomena, such as seismic velocities or tilt, will be essential to confirm the seismicity anomaly before any warning could be contemplated.

CONCLUSIONS

The magnitude 4 earthquakes which occurred in the CSZ on 9 and 11 March 1989 were an earthquake doublet. The events had identical waveforms and therefore had the same hypocentre and fault rupture. They are the largest events to occur in the seismic zone in a decade and are the only obvious example of moderate-sized, repeated events that have been identified in the activity of the CSZ since detailed monitoring began in 1977, or (with less confidence) in the historical record. They are certainly unique for the magnitude 4.0 or greater events. The doublet was located in the CSZ at

- one of two asperities where many of the larger events in this century have initiated
- one edge of an aseismic slab which has persisted since at least 1977 and
- at the depth of the strongest part of the crust.

The earthquakes of the doublet therefore possess many of the characteristics that one might reasonably expect for foreshocks to a large CSZ event, together with the waveform similarity characteristic that was identified after-the-fact as typical of foreshocks to the 1971 San Fernando earthquake. In addition they occurred during a period of increased earthquake activity on a regional scale. However, they have not been followed by larger events (in six months) and therefore it seems that doublets are not sufficient evidence by themselves for a short-term prediction of a large event in the CSZ. We are not aware of any other information at this time that would allow a credible prediction of such an event to be made.

ACKNOWLEDGMENTS

We thank F.M. Anglin for diligence in locating the hundreds of CSZ micro-earthquakes necessary for us draw our conclusions, and P. Basham, G.G.R. Buchbinder, J. Drysdale, H. Hasegawa, M. Lamontagne, R. North, and A. Stevens for valuable comments on drafts of the paper.

REFERENCES

- Adams, J.**
1989: Crustal stresses in eastern Canada; in S. Gregersen and P.W. Basham, ed. Earthquakes at North Atlantic Passive Margin: Neotectonics and Postglacial Rebound; Kluwer Academic Publishers, p. 289-297.
- Adams, J., Sharp, J., and Stagg, M.**
1988a: New focal mechanisms for southeastern Canadian earthquakes; Geological Survey of Canada, Open File 1892, 109 p.
- Adams, J., Vonk, A., Pittman, D., and Vatcher, H.**
1988b: New focal mechanisms for southeastern Canadian earthquakes Volume II; Geological Survey of Canada, Open File 1955, 97 p.
- Anglin, F.M.**
1984: Seismicity and faulting in the Charlevoix zone of the St. Lawrence Valley; Seismological Society of America, Bulletin, v. 74, p. 595-603.
- Anglin, F.M., and Buchbinder, G.**
1981: Microseismicity in the mid St. Lawrence Valley Charlevoix zone, Quebec; Seismological Society of America, Bulletin, v. 71, p. 1553-1560.
- Buchbinder, G.G.R., Lambert, A., Kurtz, R.D., Bower, D.R., Anglin, F.M., and Peters, J.**
1988: Twelve years of geophysical research in the Charlevoix seismic zone; Tectonophysics, v. 156, p. 193-224.
- Du Berger, R., Roy, D. W., Lamontagne, M., Woussed, G., North, R.G., and Wetmiller, R.J.**
1990: The Saguenay (Quebec) earthquake of November 25, 1988: Seismological data and geological setting; Tectonophysics.
- Ebel, J.E., Somerville, P.G., and McIver, J.D.**
1986: A study of the source parameters of some large earthquakes in northeastern North America; Journal of Geophysical Research, v. 91, p. 8231-8247.
- Hasegawa, H.S.**
1986: Seismotectonics in eastern Canada, an overview with emphasis on the Charlevoix and Miramichi regions; Earthquake Notes, v. 57, p. 83-94.
- Hasegawa, H.S. and Wetmiller, R.J.**
1980: The Charlevoix earthquake of 19 August 1979 and its seismotectonic environment; Earthquake Notes, v. 51, p. 23-37.
- Hodgson, E.A.**
1925: The St. Lawrence earthquake, February 28, 1925; Seismological Society of America, Bulletin, v. 15, p. 84-99.
1950: The Saint Lawrence earthquake March 1, 1925; Publications of the Dominion Observatory, Ottawa, v. 7, no. 10, p. 367-436.
- Hough, S.E., Jacob, K.H., and Friberg, P.A.**
1989: The 11/25/88, M=6 Saguenay earthquake near Chicoutimi, Quebec: Evidence for anisotropic wave propagation in northeastern North America; Geophysical Research Letters, v. 16, p. 645-648.
- Ishida, M. and Kanamori, H.**
1978: The foreshock activity of the 1971 San Fernando earthquake, California; Seismological Society of America, Bulletin, 68, p. 1265-1279.
- Kirsch, R., Lambert, A., and Buchbinder, G.G.R.**
1987: The seismic travel-time drop in the Charlevoix region from 1979 to 1980: evidence for aligned saturated cracks in the crust; Tectonophysics, v. 140, p. 145-154.
- Kumarapeli, P.S.**
1985: Vestiges of Iapetan rifting in the west of the northern Appalachians; Geoscience Canada, v. 12, p. 55-59.
- Kumarapeli, P.S. and Saull V.A.**
1966: The St. Lawrence Valley system: a North American equivalent of the east African rift valley system; Canadian Journal of Earth Sciences, v. 3, p. 639-658.

- Lamontagne, M.**
1987: Seismic activity and structural features in the Charlevoix region, Quebec; Canadian Journal of Earth Sciences, v. 24, p. 2118-2129.
- Leblanc, G. and Buchbinder, G.**
1977: Second microearthquake survey of the St. Lawrence Valley near La Malbaie, Quebec; Canadian Journal of Earth Sciences, v. 14, p. 2778-2789.
- Leblanc, G., Stevens, A.E., Wetmiller, R.J., and DuBerger, R.**
1973: A microearthquake survey of the St. Lawrence valley near La Malbaie, Quebec; Canadian Journal of Earth Sciences, v. 14, p. 2778-2789.
- Mareschal, J. C., Pinet, C., Gariépy, C., Jaupart, C., Bienfait, G., Dalla Coletta, G., Jolivet, J., and Lapointe, R.**
1989: New heat flow density and radiogenic heat production data in the Canadian Shield and the Quebec Appalachians; Canadian Journal of Earth Sciences, v. 26, p. 845-852.
- Mitchell, D., Tinawi, R., and Law, T.**
1989: The 1988 Saguenay Earthquake — a site visit report; Geological Survey of Canada, Open File 1999, 92 pp.
- Munro, P.S. and Weichert, D.H.**
1989: The Saguenay earthquake of November 25, 1988; Processed strong motion records: Geological Survey of Canada Open File 1996, 145 pp.
- North, R.G., Wetmiller, R.J., Adams, J., Anglin, F.M., Hasegawa, H.S., Lamontagne, M., Du Berger, R., Seeber, L. and Armbruster, J.**
1989: Preliminary results from the November 25, 1988 Saguenay (Quebec) earthquake; Seismological Research Letters, v. 60, p. 89-93.
- Pechman, J.C. and Kanamori, H.**
1982: Waveforms and spectra of preshocks and aftershocks of the 1979 Imperial Valley, California, earthquake: evidence for fault heterogeneity; Journal of Geophysical Research, v. 87, p. 10, 579-10,597.
- Smith, W.E.T.**
1962: Earthquakes of eastern Canada and adjacent areas 1534-1927; Publications of the Dominion Observatory, v. 26, p. 271-301.
1966: Earthquakes of eastern Canada and adjacent areas 1928-1959; Publications of the Dominion Observatory, v. 32 p. 87-121.
- Stevens, A.**
1980: Reexamination of some larger La Malbaie, Quebec, earthquakes (1924-1978); Seismological Society of America, Bulletin, v. 70, p. 529-557.
- Tuttle, M., Such, R., and Seeber, L.**
1989: Ground failure associated with the November 25, 1988 Saguenay earthquake in Quebec Province, Canada: *in* The Saguenay earthquake of November 25, 1988, Quebec, Canada: strong motion data, ground failure observations, and preliminary interpretations; ed. K. Jacobs; National Center for Earthquake Engineering, Buffalo, New York, Preliminary Report, February 1989.

Some results from the 25 November, 1988 Saguenay, Québec, earthquake

M. Lamontagne, R.J. Wetmiller and R. Du Berger¹
Geophysics Division

Lamontagne, M., Wetmiller, R.J. and Du Berger, R., Some results from the 25 November, 1988 Saguenay, Québec, earthquake; in Current Research, Part B, Geological Survey of Canada, Paper 90-1B, p. 115-121, 1990.

Abstract

On 25 November, 1988 the largest earthquake (m_{bLg} 6.5) to take place in eastern North America in over 50 years occurred in the Laurentide Provincial Park of the Saguenay region, some 35 km south of Chicoutimi, Québec. The location of this event in a hitherto relatively aseismic region, its depth, its large component of high-frequency seismic waves, its remarkably mild aftershock activity and the difficulty in defining the reactivated structure, pose several problems for existing models of seismic zoning and hazard assessment for eastern North America. The analysis of airborne radar images improves understanding of the geological features of the area, and of their possible connections with the earthquake activity.

Résumé

Le 25 novembre 1988, le plus grand séisme (m_{bLg} 6,5) à se produire dans la partie est de l'Amérique du Nord au cours des 50 dernières années a eu lieu au Saguenay, dans le parc provincial des Laurentides, à quelque 35 km au sud de Chicoutimi, au Québec. L'emplacement de ce séisme dans une région relativement asismique jusqu'à présent, sa profondeur, la forte proportion d'ondes sismiques de haute fréquence, l'intensité très moyenne de sa réplique et la difficulté de définir la structure réactivée, posent plusieurs problèmes quant à la précision des modèles existants de zonation sismique et d'évaluation des risques de la partie est de l'Amérique du Nord. L'analyse d'images radar obtenues par levé aérien aide à mieux comprendre les structures géologiques de la région et leur relation possible avec l'activité sismique.

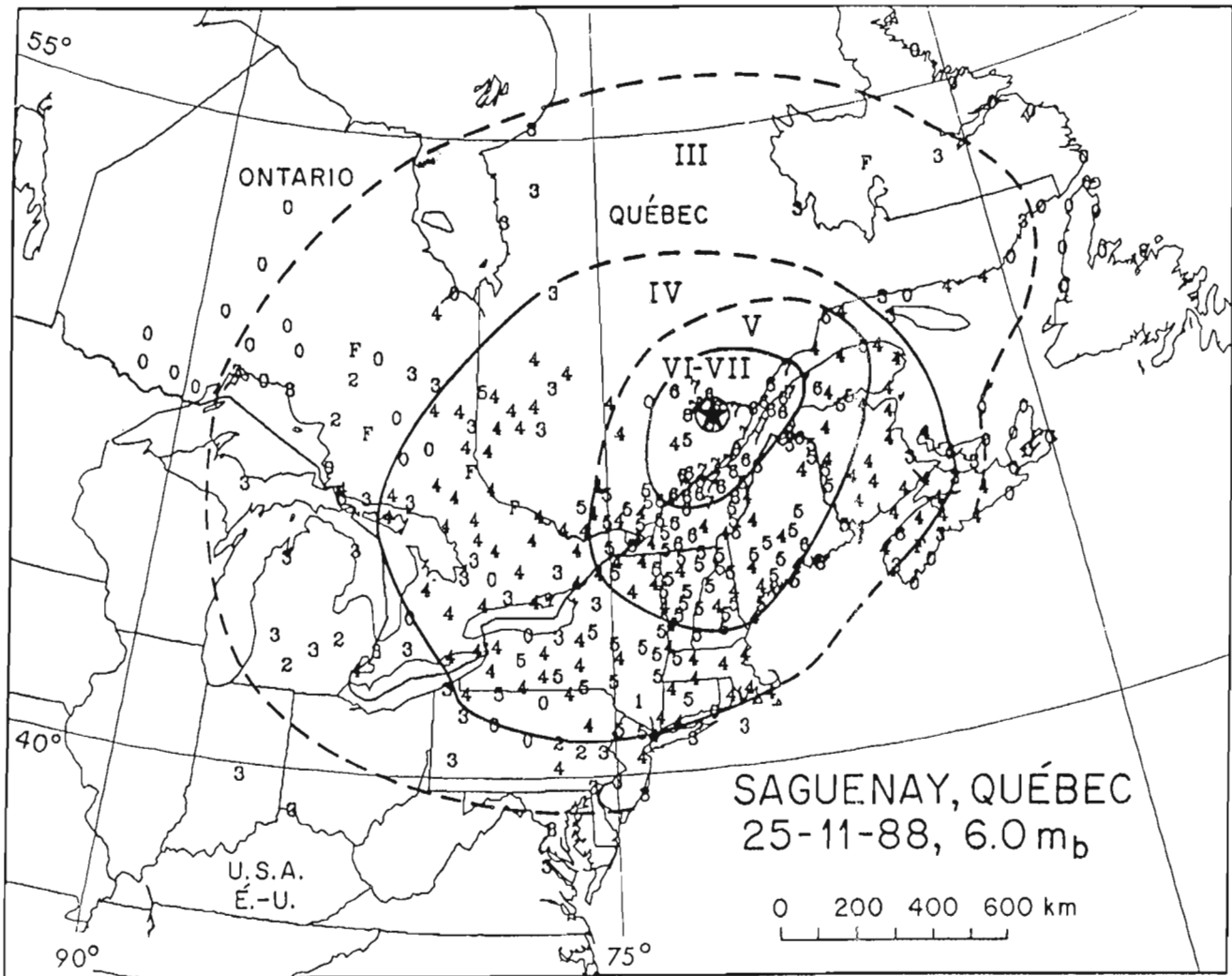
¹ Département des sciences de la Terre, Université du Québec à Chicoutimi

INTRODUCTION

On 25 November, 1988 the Saguenay earthquake, the largest earthquake to take place in Eastern North America in over 50 years, occurred in the Laurentide Fauna Reserve, about 35 km to the south of the city of Chicoutimi, Québec and 100 km north of Québec City. The earthquake, its sequence of aftershocks, and some preliminary interpretation were described by North et al. (in press). This event has provided a large amount of new information for seismic hazard estimation in eastern North America, previously based largely on questionable data from earthquakes which took place early this century. The location of the Saguenay event in a hitherto relatively aseismic region, its depth in the lower crust, its large component of high-frequency seismic waves, its remarkably mild aftershock activity and the difficulty in defining the reactivated structure, pose several problems for existing models of seismic zoning and hazard assessment for eastern North America.

Immediately following the event, the Geophysics Division distributed about 2000 questionnaires to rural postmasters in Quebec, Ontario, the Maritimes and

Newfoundland to determine the intensity distribution of the earthquake. Response rate is estimated to be about 75 %, a figure considered high for broadly-based mail surveys. The Canadian data were combined with similar data collected and interpreted by the National Earthquake Information Center in the United States in order to produce an isoseismal map (Fig. 1). In total, 1924 communities in Canada and the United States were assigned an intensity value based on the Modified Mercalli Intensity scale and then plotted on a large-scale map. The isoseismal contours were hand-contoured taking into account the most typical responses for a region. The Saguenay earthquake was felt with maximum intensity MM VII in the Chicoutimi-Jonquière-La Baie area, was felt strongly by most people within 500 km, was felt by many within 1000 km and was perceptible by some people, under special circumstances, beyond 1000 km. Although many people were badly frightened, and there were numerous reports of articles being thrown from shelves in the epicentral area, there was in fact, little serious damage. Isolated cases of property damage in the Saguenay region and parts of Québec City and Montréal, consisted primarily of cracked or partially collapsed unreinforced



Drysdale and Cajka,
Geological Survey of Canada

Figure 1. Preliminary intensity map of the 25 November, 1988 Saguenay earthquake. Only 350 points have been plotted, for clarity, but all the data were used during contouring (after Drysdale and Cajka, pers. comm.).

masonry walls which in some cases were obviously as much due to the unstable soil conditions on which the damaged structure was constructed as to the initial strength of the ground shaking (Mitchell et al., 1989). Hydro-Québec suffered some significant damage at some of their transformer stations in locations where topographical and/or soil conditions made the ground shaking particularly strong. There were a few minor injuries but no direct casualties. In all, the total expense for damage caused by the earthquake in the province of Québec has been estimated to be a few tens of million dollars.

The total felt area exceeded 3 million square kilometres and approached that of the magnitude 6.7 (approx.) 1925 Charlevoix-Kamouraska earthquake. For the Saguenay, the extent of the intensity IV and greater areas were consistent with the instrumental magnitude of 6.5 based on the high frequency Lg waves. The magnitudes based on body and surface waves were 5.9 a half magnitude lower. The Saguenay earthquake produced unexpectedly large amounts of high frequency seismic energy, as evidenced by the value m_{bLg} 6.5, by the intensity data, and by the high accelerations observed at distances ranging from 40 to 800 km (Munro and Weichert, 1989).

Focal mechanisms for the foreshock, main shock and two aftershocks all indicate thrust faulting (Figure 2) with some strike slip movement, which is quite consistent with the idea of reactivation of existing faults by the regional stress field presently active in eastern Canada.

The Saguenay event was preceded 62 hours earlier by a foreshock (mb 4.4) which allowed the GSC to deploy field equipment in the epicentral area before the unexpected main

shock. The depth of the main shock could thus be well determined at 29 km which is deeper than 95 % of all the other earthquakes in eastern Canada. One area in which some seismic activity does occur at comparable depth is the Charlevoix seismic zone where some micro-earthquake activity occurs below 25 km. While almost all earthquakes in stable continental areas around the world are shallow, similar or greater depths have been reported for occasional earthquakes in Brazil and Fennoscandia (Chen, 1989), indicating that deep crustal events are a rare but well-documented seismic phenomena. The seismic hazard implications for such deep events in stable continental areas have never been fully appreciated.

The field network showed that no small magnitude activity occurred in the epicentral area in the 24 hours prior to the mainshock. The absence of continuous low-level activity preceding the main shock may represent a characteristic of these deep events.

The Saguenay main shock was followed by over 85 aftershocks (as of 31 October, 1989), of which only two have been larger than magnitude 3. Since the main shock, the activity has been monitored by a network of two GSC seismograph stations (one telemetered to Ottawa and one to the Université du Québec à Chicoutimi (UQAC) and four field stations operated by the UQAC. The stations are located within 50 km of the epicentre of the main shock, providing a detection threshold of approximately magnitude 0.5. The aftershock activity decreased very rapidly (Fig. 3) unlike the 1982 Miramichi, N.B., and 1985 Nahanni earthquake sequences and is currently almost absent with only three shocks of magnitude 2 or greater since the end of January.

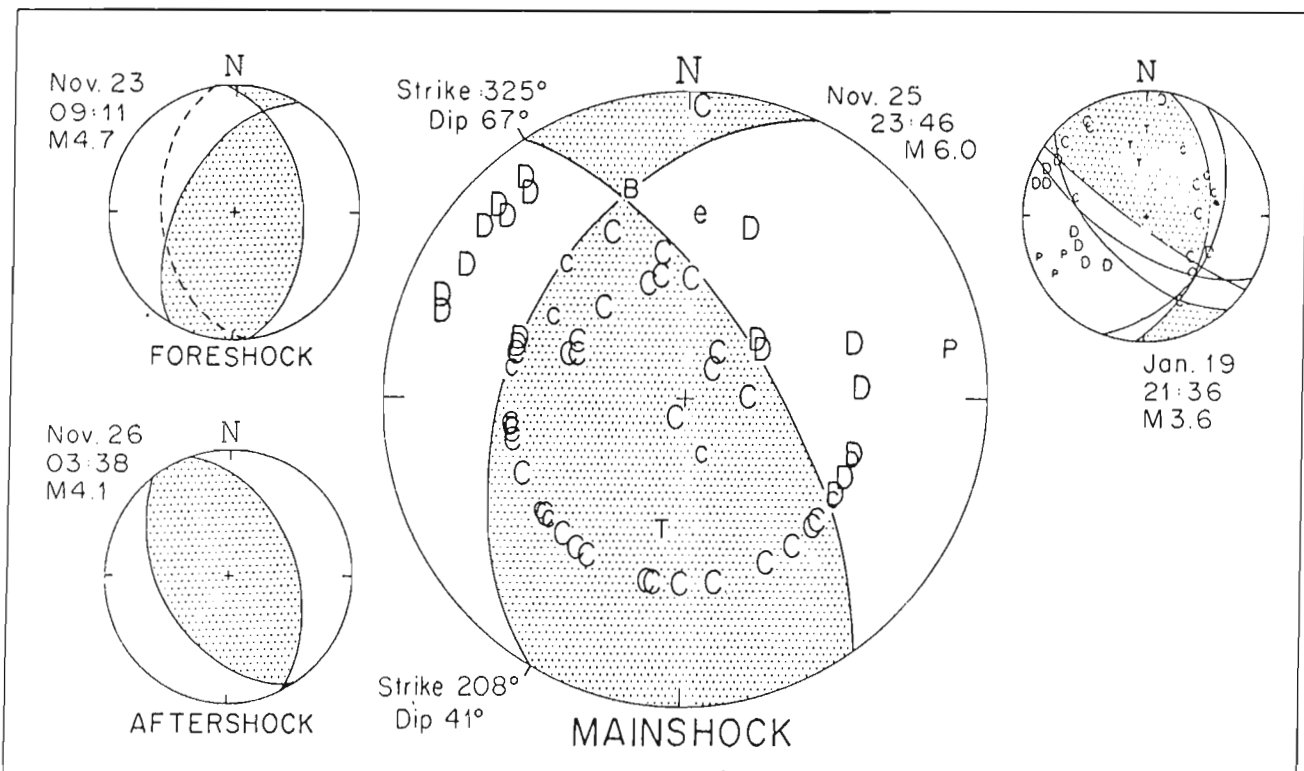


Figure 2. Focal mechanisms of the foreshock, the main shock and two aftershocks.

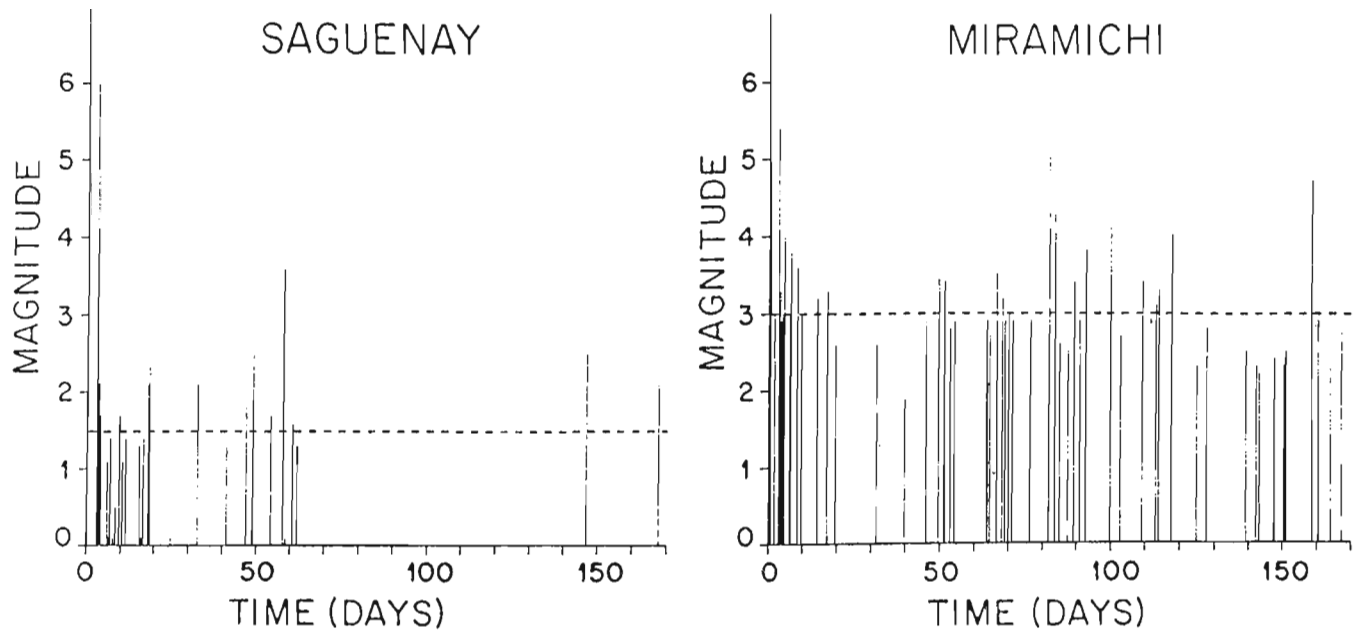


Figure 3. Time-histories of the Saguenay (A) and the Miramichi, N.B. (B) earthquake sequences for the first 170 days of recording. Considering the similar Mb magnitude values (5.9 and 5.8), the difference in the levels of seismic activity is striking between the two sequences.

For zoning purposes, it is very difficult to delineate and define a “Saguenay source zone” from the present level of aftershock activity, even though it is less than a year since the event. By contrast the aftershock zones of the Miramichi and Nahanni events are still clearly identifiable by their continuing activity. The greater depth of the Saguenay activity may be the key factor controlling its unusual quiescence.

Nearly all of the aftershock activity was located above the main shock which would seem to indicate that the rupture propagated upwards. The aftershock activity spread out over a wide area, more than 10 km from the main shock (Figure 4) but we feel that much of this spread-out activity was caused by secondary stress/strain adjustments and does not represent the true dimensions of the rupture. Three-dimension analysis of the hypocentres has not yielded any orientation that unambiguously indicates the main shock rupture plane, but a clustering of very small events around the main shock hypocentre could represent a rupture plane with dimension of a few kilometres.

Seismo-tectonically, the epicentral region lies between the Saguenay Graben to the north and the St. Lawrence valley to the southeast, within the Jacques Cartier tectonic block of the Grenville province (Du Berger et al., in press). It is some 75 km from the outer boundary of the Charlevoix seismic zone which has been a source of several large earthquakes (magnitude up to 7) over the last 300 years, most recently in 1925. The Saguenay region was not previously considered to be particularly seismically active as only a few small events of magnitude less than 3 had been located within 50 km of the November 1988 epicentre during the last ten years and there were no historical accounts of large events in the past 150 years. It is thought that, since the mid

1970s, any earthquake exceeding magnitude 2 should have been seen on the permanent seismograph station LMQ, located approximately 100 km to the southeast. Interestingly, a re-examination of these earthquakes has shown that a magnitude 2.7 event had occurred 10 months prior to and fewer than 15 km from the November 1988 shock. However, this small shock cannot be linked directly to the main shock since small earthquakes in this magnitude range are recorded sporadically throughout the Grenville province outside the well-defined active regions.

As a first step towards a better definition of the geological characteristics of the area, a synthesis of previous geological works has been conducted (Du Berger et al., in press). Currently, it appears that the Saguenay earthquake occurred some 20 km south of the most southerly of the previously faults mapped as part of the Saguenay Graben (the Lake Kénogami lineament). There has been considerable controversy whether the earthquake was associated with the Graben in some manner. The relationship is especially difficult to assess, considering the depth of the earthquake, which makes a correlation with surface geology difficult to establish.

In order to bring more constraints on our geological models, an airborne synthetic aperture radar survey has been conducted by the Canada Centre for Remote Sensing over the epicentral region. In addition to emphasizing lineaments that were not as evident on either air photographs or available LANDSAT images, the radar scenes put surface features in their regional context (Fig. 5). The high resolution of these scenes allows the characterization of structural patterns and their spatial variations over the Saguenay region as a whole.

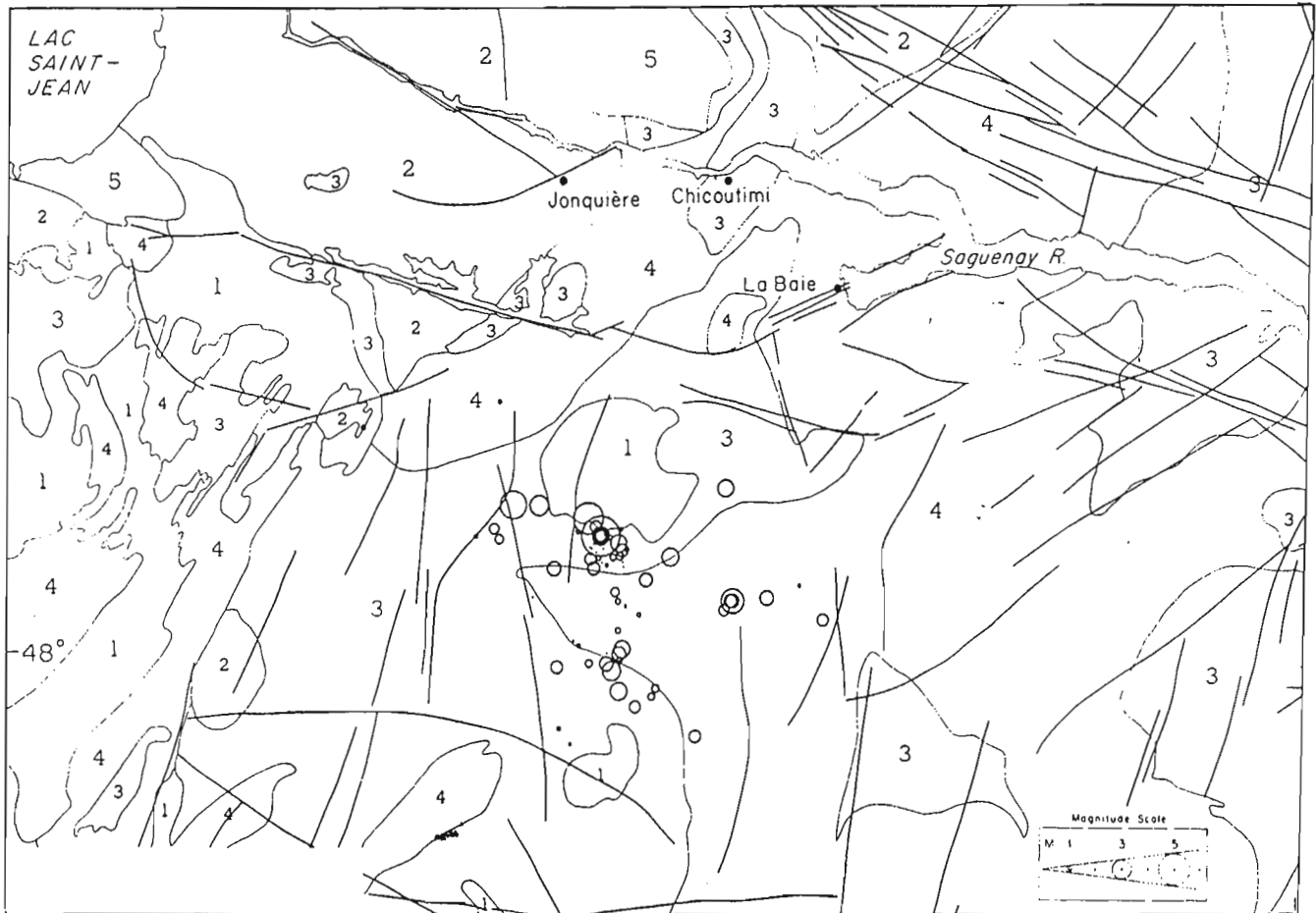


Figure 4. Geological map of the Saguenay region with some interpreted lineaments from an analysis of LANDSAT pictures by P. St-Julien, of Université Laval. The earthquake activity scaled by magnitude is also indicated. The units are 1- Granite, 2- Anorthosite, 3- Mangerite, 4- Other Precambrian rocks, 5- Limestones. This map is modified from the map of the Ministère Énergie et ressources, Québec, and does not take into account the most recent works by geologists of the UQAC.

In all of the lineaments, the most striking set is the NW—SE oriented faults north of the Saguenay graben and the similarly oriented major lineament in the centre of the picture (for which we proposed the name Lac Ha! Ha! lineament). Between the faults and the Lac Ha! Ha! lineament, many smaller scale features of similar orientation can be seen, which may represent a second order structural pattern inside the Graben structure. The parallelism between the Graben faults and Lac Ha! Ha! lineament suggests may that Saguenay Graben faults may extend farther south than previously assumed. Interestingly, the Lac Ha! Ha! lineament splays out into a fan of at least three other lineaments oriented NNW (splay faults?). The Lac Ha! Ha! lineament is a continuation of lineaments located farther east which are interpreted as Graben faults by Rondot (1979). The analysis of the E-W line of the radar survey may shed more light on the southern extension of this set of lineaments.

The next step will be to define the different structural patterns, to characterize them in terms of orientation, spatial distribution and origin (faults, joint systems, ductile deformation zones, glacial features). This analysis will be carried out with geoscientists of the UQAC who are already much

involved in the geological mapping of the area and who will make correlations between field observations and radar images possible.

The radar images represent an important contribution to the study of the surface geology of the area. As a preliminary interpretation, epicentre of the main shock is within 10 km of the Lac Ha! Ha! lineament, and most of the seismic activity is distributed between 5 and 25 km of it. This would place the activity outside of the expected depth extension of the Saguenay Graben. Any interpretation of the seismic activity is made difficult by the large depth of the event which makes correlations with surface geology uncertain. However, until a LITHOPROBE survey is conducted in the region to define the crustal structure at depth, putting the geological information together represents the most important step in characterizing the geological environment of this very special earthquake sequence.

ACKNOWLEDGMENTS

The authors are indebted to people who analyzed the seismological and intensity data at the Geological Survey of

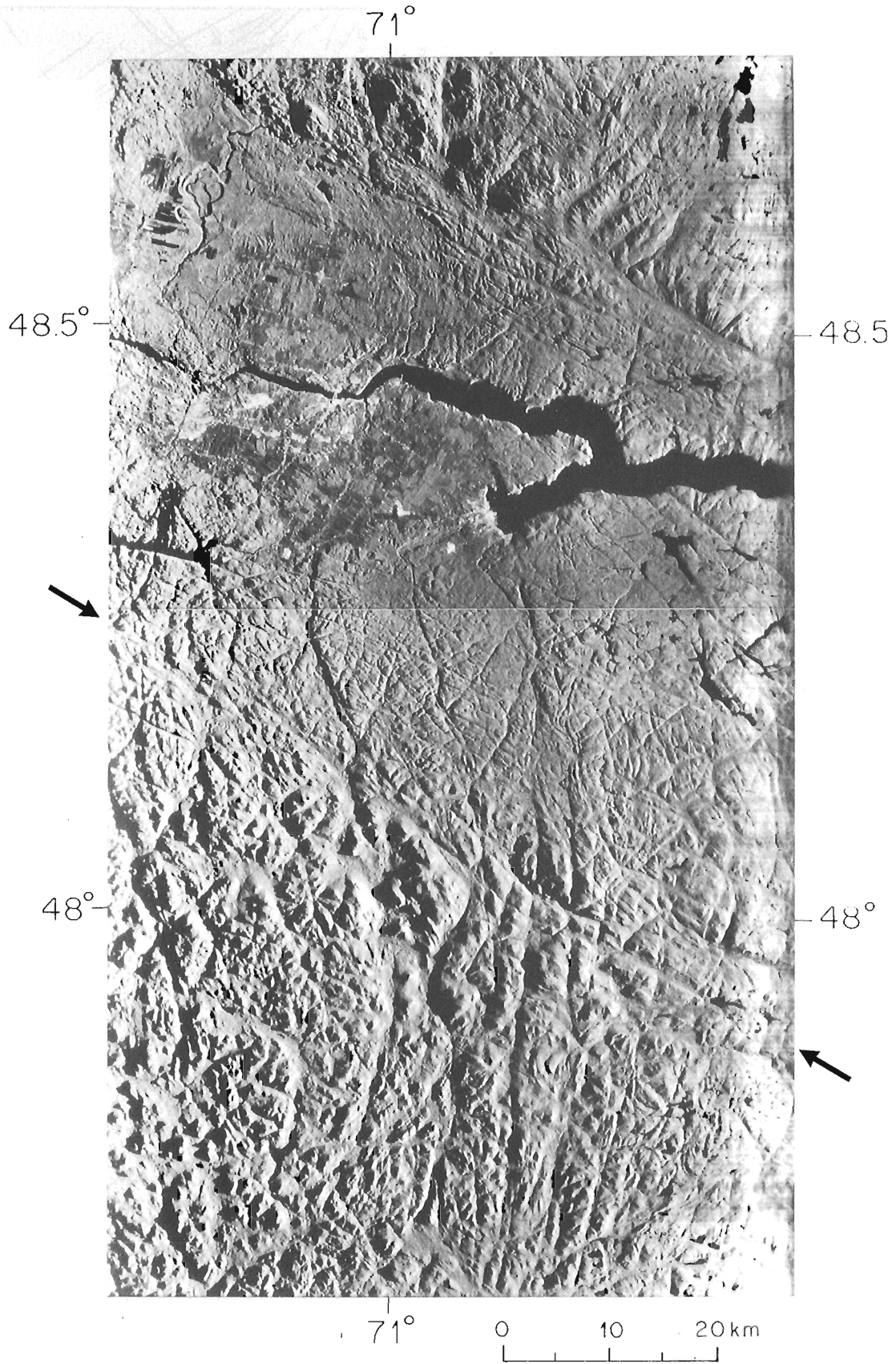


Figure 5. Radar images representing the epicentral region of the Saguenay earthquake. The Lac Ha! Ha! lineament is indicated by arrows.

Canada: J.E. Adams, F.A. Anglin, M.G. Cajka, J.A. Drysdale and R.G. North, and to the scientists of the Canada Centre for Remote Sensing for their interest in this project.

REFERENCES

Chen, W.-P.

1989: A brief update on the focal depths of intracontinental earthquakes and their correlations with heat flow and tectonic age, *Seism. Res. Lett.*, (in press).

Du Berger, R., D.W. Roy, M. Lamontagne, G. Woussen, R.G. North, R.J. Wetmiller

1989: The Saguenay (Québec) earthquake of November 25, 1988: seismological data and geological setting; Submitted to *Tectonophysics*, in press.

Lamontagne, M.

1989: Earthquake in the Saguenay: More fear than harm; *GEOS*, v. 18, no. 4, p. 9-14.

Mitchell, D., R. Tinawi and T. Law

1989: The 1988 Saguenay earthquake — a site visit report; Geological Survey of Canada, Open File 1999.

Munro, P.S. and D.H. Weichert

1988: The Saguenay earthquake of November 25, 1988: processed strong motion records; Geological Survey of Canada, Open File 1996.

North, R.G., R.J. Wetmiller, J.E. Adams, F.M. Anglin, H.S. Hasegawa, M. Lamontagne, R. Du Berger, L. Seeber and J. Armbruster

1989: Preliminary results from the November 25, 1988, Saguenay (Québec) earthquake, Submitted to *Seism. Res. Lett.*, in press.

Rondot, J.

1979: Reconnaissances géologiques dans Charlevoix-Saguenay; Ministère des Richesses Naturelles du Québec, DPV-682, pp. 44.

In situ stress magnitudes at Whiterose, Jeanne d'Arc Basin, Grand Banks of Newfoundland

R.E. McCallum and J. S. Bell
Institute of Sedimentary and Petroleum Geology, Calgary

McCallum, R.E. and Bell, J.S., In situ stress magnitudes at Whiterose, Jeanne d'Arc Basin, Grand Banks of Newfoundland, ; in Current Research, Part B, Geological Survey of Canada, Paper 90-1B, p. 123-130, 1990.

Abstract

Principal stress magnitudes describe the present-day compression that rocks are subject to in the sub-surface. Smaller principal stresses, S_{Hmin} , have been calculated from well documented formation leak-off tests from three wells in the Whiterose area. In conjunction with other exploration well data, estimates of the magnitudes of the larger principal stress, S_{Hmax} , have been made. The vertical principal stress, S_v , is equated with the overburden load, and has been derived from density measurements of well cuttings and density logs. Mud weights and pressure tests for the three wells studied do not indicate significant overpressuring.

Résumé

Les valeurs des contraintes principales décrivent les forces actuelles qui agissent en profondeur sur les roches. Des enregistrements bien documentés d'essais d'intégrité de formation, effectués dans la région de Whiterose, ont permis le calcul de S_{Hmin} , la petite contrainte horizontale. On a également estimé les valeurs de S_{Hmax} , la grande contrainte horizontale, grâce à d'autres données de sondages. Le poids de la couverture de sédiments, interprété comme la contrainte verticale (S_v), a été obtenu par l'intégration des valeurs de densité. Ces valeurs proviennent de mesures d'échantillons et de diagraphies mécaniques. Les pressions de boues et les essais aux tiges indiquent l'absence de pressions anormales significatives dans les trois puits étudiés.

INTRODUCTION

This paper describes the estimation of in situ stress magnitudes at three well locations in the Whiterose area of the Jeanne d'Arc Basin on the Grand Banks of Newfoundland (Fig. 1). Whiterose is a gas discovery made by the Husky-Bow Valley Group in 1984. It is located 360 km east of St. John's, where the water depth is approximately 125 m. It has not yet been placed on production. Very detailed drilling records were released for the first three wells drilled on the Whiterose structure and analyses of them have yielded unusually good estimates of the subsurface principal stress magnitudes. They provide an excellent case history for the approach used.

NEED FOR STRESS MAGNITUDE INFORMATION

Principal stress magnitudes describe the present-day compression to which rocks are subject in the subsurface. Together with the principal stress directions, they permit predictions of how rocks will respond to natural and induced changes of pressure. Stress magnitudes are, therefore, essential measurements for predicting and understanding secondary recovery programs for hydrocarbons that involve increasing fluid pressures and propagating hydraulic fractures through reservoirs. Understanding how local stress fields change within reservoirs during hydrocarbon extraction has taken on added urgency following the subsidence of the Ekofisk Field in the North Sea, and the very costly modifications required for its production platforms (Teufel, 1989). Since the stress regime exercises the major control over how, and under what conditions, a rock will deform,

contemporary stress magnitude information is essential for understanding recent tectonism and for estimating future earthquake risk (e.g., Bell, in press, a).

At present, there are only a few methods for measuring stress magnitudes in deeply buried sediments. Hydraulic fracturing (Haimson and Fairhurst, 1970) is the most widely used technique, but is also the most difficult and expensive to apply. It involves initiating a fracture in open, or cased, holes by pumping fluids down the wellbore. The fracture is opened and closed several times until a reliable measure of its closure pressure is obtained, and this value is equated with the least principal stress. In most cases, what is measured is the smaller horizontal principal stress, and the larger horizontal principal stress magnitude is then calculated. The vertical principal stress is obtained by using rock density measurements to estimate the overburden load (e.g., Bredehoeft et al., 1976). Stress magnitudes also have been determined from measurements of core expansion due to stress release (anelastic strain recovery) and from laboratory reversals of this process (differential strain analysis). These methods have been used successfully on samples from oil fields (McLellan, 1988), but they have some constraints and are not yet applied widely (Montgomery and Ren, 1983; Teufel and Warpinski, 1984). Holographic stress measurements show promise, but are still in the development phase (Bass et al., 1986). Strain release methods involving overcoring or flatjack techniques, that are used in mines or on open rock faces, are not suitable for well bores.

Fortunately, certain measurements that are made routinely while drilling oilwells can be used to estimate principal stress magnitudes at depth in sedimentary basins. Density logs run for reservoir evaluation can be used to determine the overburden load (vertical principal stress, S_v). Leak-off tests can constrain estimates of the magnitude of the smallest principal stress. If this is horizontal (as it usually is), it is also possible to calculate the larger horizontal principal stress. Methods for doing this have been described by Breckels and Van Eekelen (1981), by Ervine and Bell (1987) and elaborated by Bell (in press, b). These methods are applied here to data from three wells drilled in the Whiterose area of the Grand Banks of Newfoundland. All elevations are listed in metres below sea level unless otherwise stated.

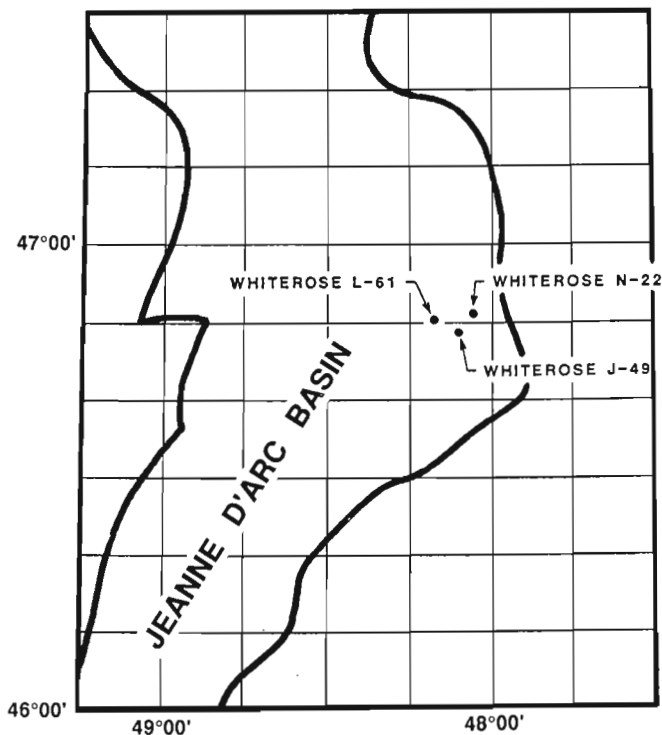


Figure 1. Location of Whiterose wells.

STRESS MAGNITUDES AT WHITEROSE

Leak-off tests are run during drilling to measure the maximum mud weight a well can sustain (Dickey, 1986). A test involves pumping drill mud down the wellbore to create a small fracture in the borehole wall below casing. Leak-off, or fracture initiation, is diagnosed when pressure build-up ceases to be linear.

Figure 2 is a record of a leak-off test run in a 29.6 m interval of indurated shale and siltstone below casing at 3679.1 m below sea level at the Whiterose J-49 well (Table 1). Eleven barrels (1.8 m³) of mud were pumped down the well bore. As the first 9.5 barrels were pumped, surface pressure increased linearly from zero to 4250 psi

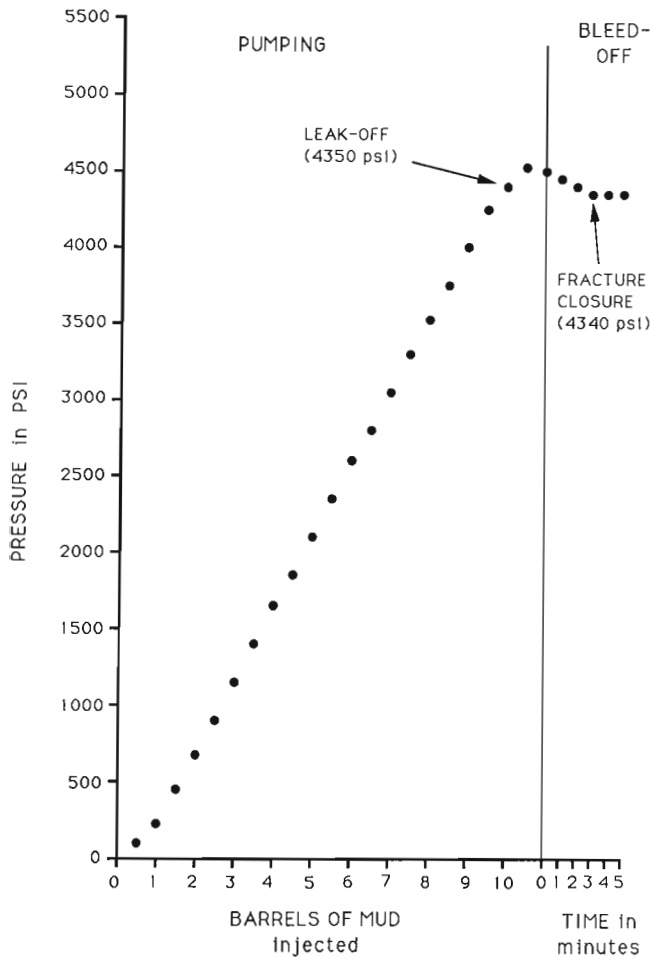


Figure 2. Record of pressure buildup and decline during a leak-off test run over a 29.6 m interval of shale and siltstone below a casing shoe set at 3679.1 m below sea level in Whiterose J-49. Linear pressure buildup ceased at a surface pressure of 4350 psi, at which point a fracture was initiated in the well bore. After pumping ended, the pressure declined rapidly to 4340 psi and then remained at this level. The fracture is interpreted to have closed at this latter pressure, which is equated with S_{Hmin} .

(29.3 MPa). Linear pressure increase was not maintained, and leak-off is interpreted to have occurred when 10 barrels of mud had been pumped and the pressure had reached 4350 psi (30.0 MPa). At this pressure the drilling mud began to initiate a fracture in the borehole wall. Continued pumping increased pressure to 4525 psi (31.2 MPa) and extended the fracture. However, this pressure could not be maintained and, by the time 11 barrels had been added, it had fallen to 4500 psi (31.0 MPa). In other words, the fracture propagation pressure was between 4350 and 4500 psi. At this point, pumping ceased, and pressure was allowed to decline naturally. During the first two minutes pressure dropped to 4400 psi (30.3 MPa) and then remained at 4340 psi (29.9 MPa) for the next three minutes, at which point record keeping ended. The initial rapid pressure drop is interpreted to have occurred while the fracture was still open. After it had closed, pressure decline was too small to measure. Hence, the minimum pressure required to keep this fracture open (instantaneous shut-in pressure) is inter-

preted as 4340 psi plus the weight of the column of mud in the well. Mud weight was 9.6 lbs/gallon and column height (i.e., K.B. depth in feet to base casing) was 12 146 ft., so bottom hole pressure is calculated as follows:

$$4340 + (9.6 \times 12,146 \times 0.052) = 10,403.3 \text{ psi (71.7 MPa)}$$

We equate 71.7 MPa with the smallest principal stress at a depth of 12 146 ft. K.B. (3679.1 m below sea level). Is this stress horizontal or vertical? To answer this question we calculate the weight of overburden at the same depth.

When Whiterose J-49 was drilled, density measurements were made on cuttings on the rig (Husky-Bow Valley, 1986). From these data, overburden pressure gradients were estimated (Fig. 3). At a depth of 3679.1 m the overburden load, S_v , was calculated to be 81.1 MPa. Density logs were run in Whiterose J-49 below 2152 m to the bottom of the well. These values were integrated to depth (Fig. 3). This involved estimating the densities of the unlogged interval between the seafloor (116 m) and 2152 m. Clearly there is room for some error in the latter procedure. This approach gave an overburden value, S_v , of 84.1 MPa at 3679.1 m. Both figures are significantly greater than 71.7 MPa, so this value must refer to the smaller horizontal principal stress.

In the test illustrated in Figure 2, leak-off (formation breakdown) occurs at a slightly greater pressure than fracture closure (71.8 MPa vs. 71.7 MPa). The pressure required to initiate the fracture is barely greater than that required to hold it open. In other words, the rock's tensile strength is negligible (0.1 MPa). In this case, if pressure decline (bleed-off) records had not been available, the leak-off pressure could have been used to give a good estimate of the smaller horizontal principal stress. Where good leak-off data are available in Whiterose and other Jeanne d'Arc Basin wells (Bell and McCallum, studies in progress) tensile strengths are characteristically low, particularly in shales. There are, however, some ambiguous tests. Figure 4 is a record of a leak-off test run in Whiterose L-61 at a depth of 722.6 m (Table 1). Leak-off occurs at a surface pressure of approximately 450 psi (3.1 MPa), which represents a bottom hole pressure of 10.9 MPa. Bleed-off was recorded for 7 minutes, during which time the surface pressure declined to 260 psi. There is a slight kink in the pressure decline curve at 300 psi, but it is not clear whether this is the pressure at which the fracture closed. The test was run in a 33.3 m interval where the dominant lithology was weakly consolidated siltstone, so the pressurised mud could have continued to flow relatively rapidly through the borehole wall after the fracture had closed. If this is what happened, the smallest principal stress at this depth would be given by 300 psi (2.1 MPa) plus the weight of the mud column (8.0 MPa) for a total of 10.1 MPa. Alternatively, surface pressure leakage may have occurred, or it is possible that the fracture closed abnormally slowly and that pressure decline was not monitored long enough. In the latter case, the smallest principal stress would be less than 9.9 MPa. For this test, the most reliable estimate of the smallest principal stress has to be the leak-off pressure, although it is appreciated that it will overestimate the magnitude (Table 1).

The smallest principal stresses have been estimated from 10 leak-off tests run in the Whiterose N-22, J-49 and L-61

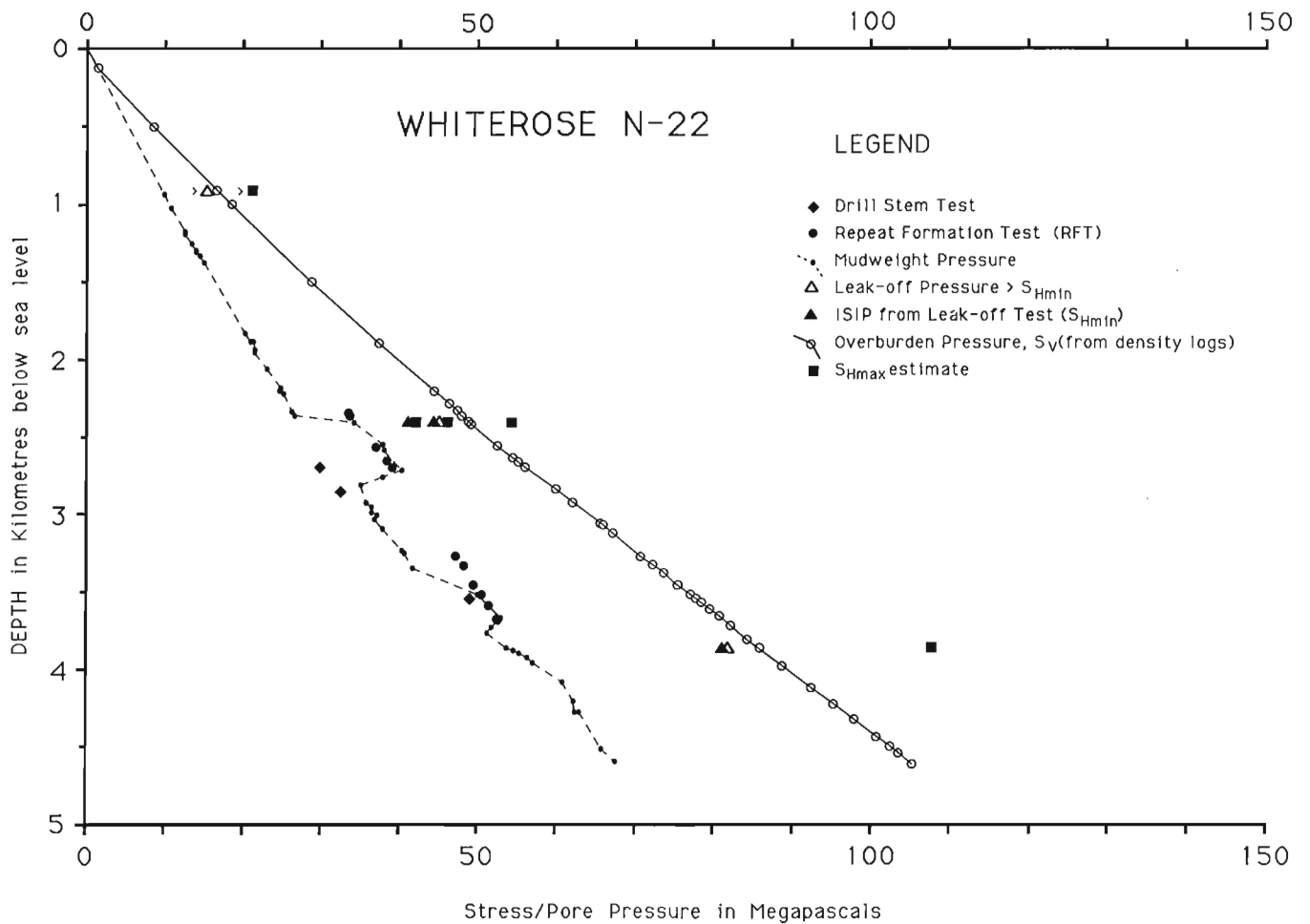


Figure 3. Pressure/depth plot of pore pressures and estimated principal stresses at Whiterose J-49. Note the two S_v profiles from samples and logs. Mud weight pressures were maintained slightly higher than pore pressures at around 3000 m, according to the repeat formation tests results. Leak-off tests indicate $S_{Hmin} < S_v$ and suggest that $S_{Hmax} > S_v$, except possibly above 1000 m depth.

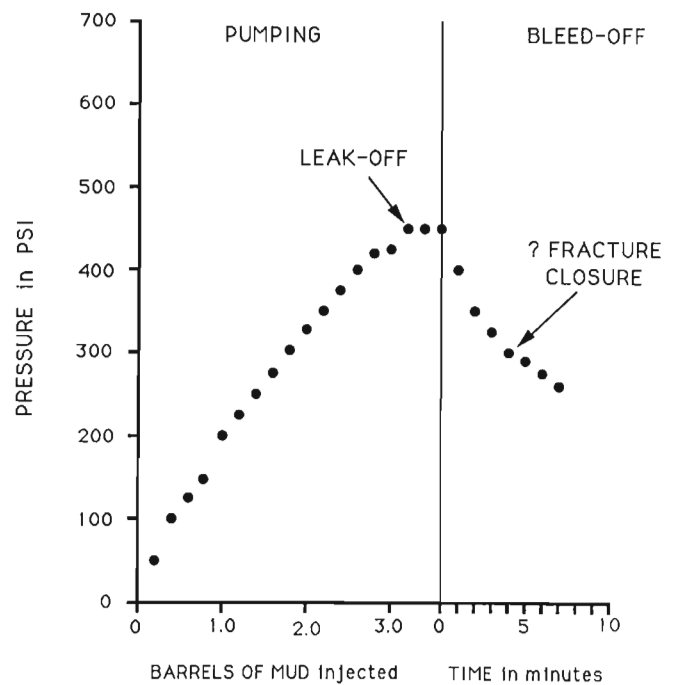


Figure 4. Record of pressure build-up and decline during a leak-off test run in a 33.3 m thick siltstone-rich interval below casing at 722.6 m subsea at Whiterose L-61. Leak-off, or fracture initiation, occurs at a surface pressure of approximately 450 psi, but the fracture closure record is ambiguous, as discussed in the text.

Table 1. Whiterose in situ stress magnitude estimates from leak-off tests, pore pressures and rock density measurements. Pore pressure data sources: H - hydrostatic, MW - mud weight. Equations 1-3 used to calculate S_{Hmax} are given in the text.

Well Name Location K.B. (m above sea level) Water Depth (m)	Depth to base casing in (m) below sea level	Open Interval Thickness in (m)	Dominant Lithology in Open Interval	Pore Pressure at base casing in MPa (data source)	First Leak-off Test Pressure at base casing in MPa	Repeat Leak-off Test Pressure at base casing in MPa	Instantaneous Shut-in Pressure in MPa S_{Hmin}	Overburden Pressure at base casing in MPa Sv	Calculated S_{Hmax} at base casing in MPa Sv	Data Quality S_{Hmax} and S_{Hmin}
WHITEROSE L-61 46.843°N 48.175°W K.B. 22.9 m W.D. 114.3	722.6	33.3	Siltstone	8.0 (MW)	10.9		?	13.1	13.8 (3)	C
	2644.0	34.1	Shale	32.3 (MW)	46.8		45.9	57.3	58.6 (2)	B
	750.4	14.6	Claystone	8.2 (H,MW)	11.7		11.1	13.6	13.1 (2)	B
WHITEROSE J-49 46.809°N 48.108°W K.B. 22.9 m W.D. 115.8 m	750.4	14.6	Claystone	8.2 (H,MW)		11.5	10.8	13.6	12.7 (1)	A
	2464.6	28.0	Shale	29.3 (MW)	43.6		43.0	50.5	56.1 (2)	B
	3679.1	29.6	Shale	41.8 (MW)	71.8		71.7	81.1	101.6 (2)	B
	902.6	10.1	Claystone	9.4 (MW)	> 15.3			16.6	>21.2 (3)	D
WHITEROSE N-22 46.863°N 48.066°W K.B. 27.4 m W.D. 122.0 m	2401.4	20.1	Shale	35.7 (MW)	45.2		41.0	48.9	42.1 (2)	B
	2401.7	27.4	Shale	35.7 (MW)		40.8	40.8	48.9	45.9 (1)	A
	2401.7	27.4	Shale	35.7 (MW)		40.9	40.9	48.9	46.1 (1)	A
	2401.7	32.0	Shale	35.7 (MW)		45.0		48.9	54.3 (3)	B
	3862.3	17.7	Silty Shale	54.9 (MW)	81.8		81.5	85.9	107.8 (2)	B

wells (Husky-Bow Valley, 1985, 1986, 1987). As Table 1 indicates, it was usually possible to obtain both bottom hole leak-off pressures and instantaneous shut-in pressures. In every case, their magnitudes were less than the overburden pressure, or vertical principal stress, so the instantaneous shut-in pressures represent the smaller horizontal principal stresses.

No direct measurements were made of the larger horizontal principal stress. Bredehoeft et al. (1976) showed that, for isotropic rocks:

$$S_{H_{max}} = 3(S_{H_{min}}) - \text{Reopening pressure} - \text{Pore pressure} \quad (1)$$

This equation can be used when more than one leak-off test has been run below the same casing shoe and the pressure decline has been recorded as discussed above (Bell, in press b). At Whiterose J-49, two leak-off tests were run

below casing at 750.4 m. The two tests were run over the same 14.6 m interval of claystone (Table 1). In the first test, leak-off occurred at a bottom hole pressure of 11.7 MPa and fracture closure is interpreted to have taken place at 11.1 MPa. In the second test, leak-off occurred at 11.5 MPa, followed by fracture closure at 10.8 MPa. No actual measurement of pore pressure was made, but the mud weight while drilling was 9.4 lbs/gallon. Drilling with mud of such density implies that the section was hydrostatically pressured. This inference is confirmed by examining the mud weight record for the entire well, together with the drillstem test and repeat formation test results (Fig. 3). There is no sign of significant overpressuring in this well. Therefore we can apply the sea water pore pressure gradient of 0.465 psi/ft. At 750.4 m this amounts to a pore pressure of 8.2 MPa. The Bredehoeft et al. (1976) relationship thus gives:

$$S_{H_{max}} = 3(10.8) - 11.5 - 8.2 = 12.7 \text{ MPa}$$

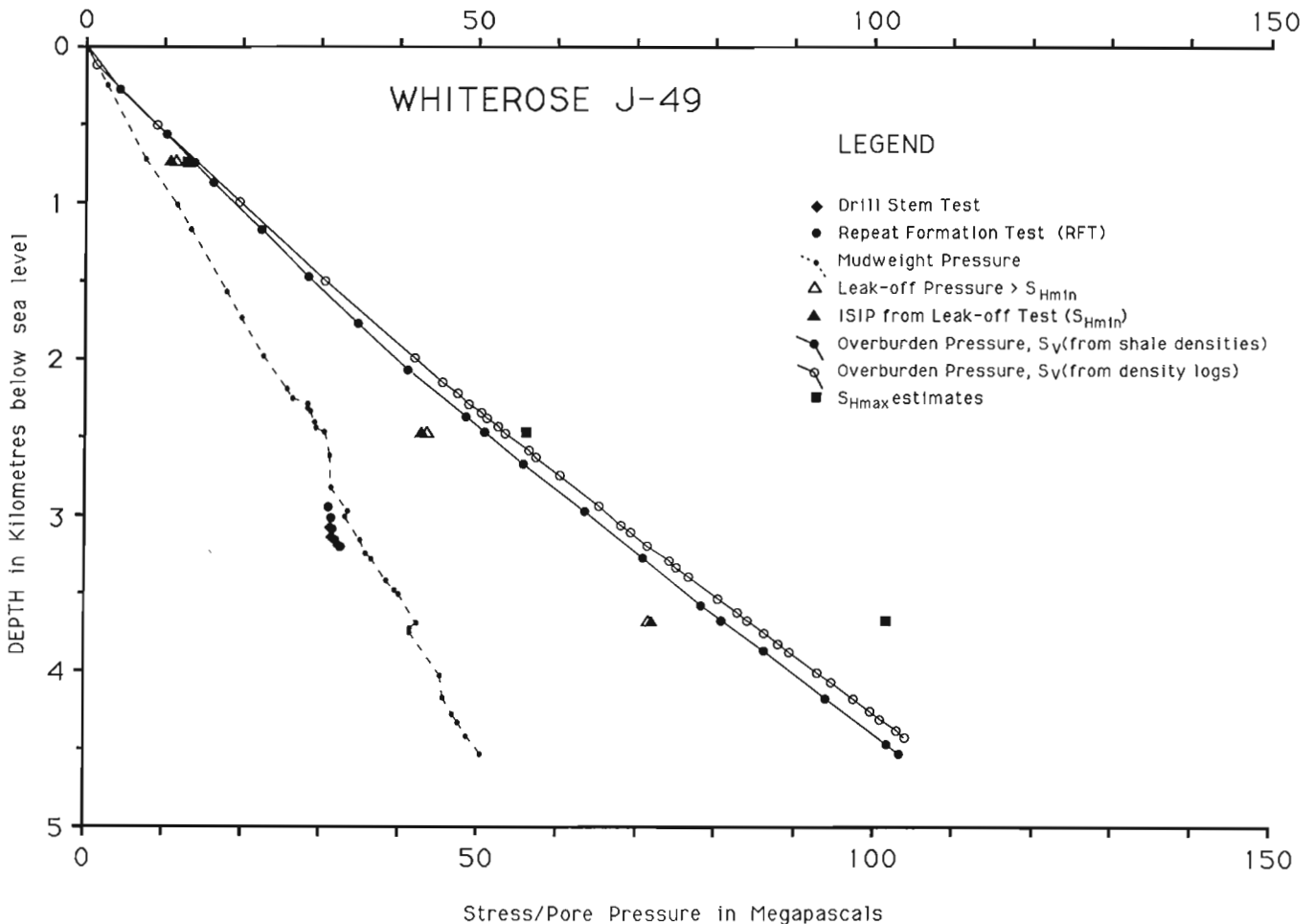


Figure 5. Pressure/depth plot of pore pressures and estimated principal stresses at Whiterose N-22. Mud weight pressures were raised above hydrostatic levels at 2408 m depth and again at 3523 m. Repeat formation tests suggest that the section below approximately 2400 m may be mildly overpressured. Four leak-off tests were run at 2401.4 m. Test 1 fractured shale at a pressure of 45.2 MPa. Tests 2 and 3 reopened and closed this fracture at, respectively, 40.8 and 40.9 MPa. These are good values for $S_{H_{min}}$ and indicate an original tensile strength of 4.4 MPa. A stress regime where $S_{H_{max}} > S_v > S_{H_{min}}$ appears to exist at all depths in Whiterose N-22.

If the mud weight were exactly equal to the pore pressure, the latter would be 8.6 MPa and S_{Hmax} would calculate to 12.3 MPa. Both values are less than the calculated overburden pressure at 750.4 m below sea level at Whiterose J-49.

If a second leak-off test had not been run, but the single test had a suitable pressure decline record, the next best approach would be to substitute the leak-off pressure itself for the reopening pressure, as follows:

$$S_{Hmax} = 3(\text{ISIP}) - \text{Leak-off Pressure} - \text{Pore Pressure} \quad (2)$$

This equation will underestimate S_{Hmax} , especially if the rock interval has significant tensile strength, but it is likely to give reasonable results for shales. It has been used to estimate S_{Hmax} for all the other leak-off test data suites reported here (Table 1, Fig. 3, 5, 6), except for the leak-off

test run in claystone at 902.6 m below sea level at Whiterose N-22. In this test, bottom hole pressures were raised to 15.3 MPa, but leak-off was not achieved. All that can be concluded was that S_{Hmin} is probably greater than 15.3 MPa.

In cases where only a leak-off pressure is reported, we can make the simplifying assumption that the leak-off pressure is of similar magnitude to both the reopening pressure and the instantaneous shut in pressure for rocks with minimal tensile strengths, so that the Bredehoeft et al. (1976) relationship reduces to:

$$S_{Hmax} = 2(\text{Leak-Off Pressure}) - \text{Pore Pressure} \quad (3)$$

This equation offers a means of making a crude estimate of the magnitude of the larger horizontal principal stress (Ervine and Bell, 1987). Since the leak-off pressure will inevitably be larger than the smaller horizontal principal

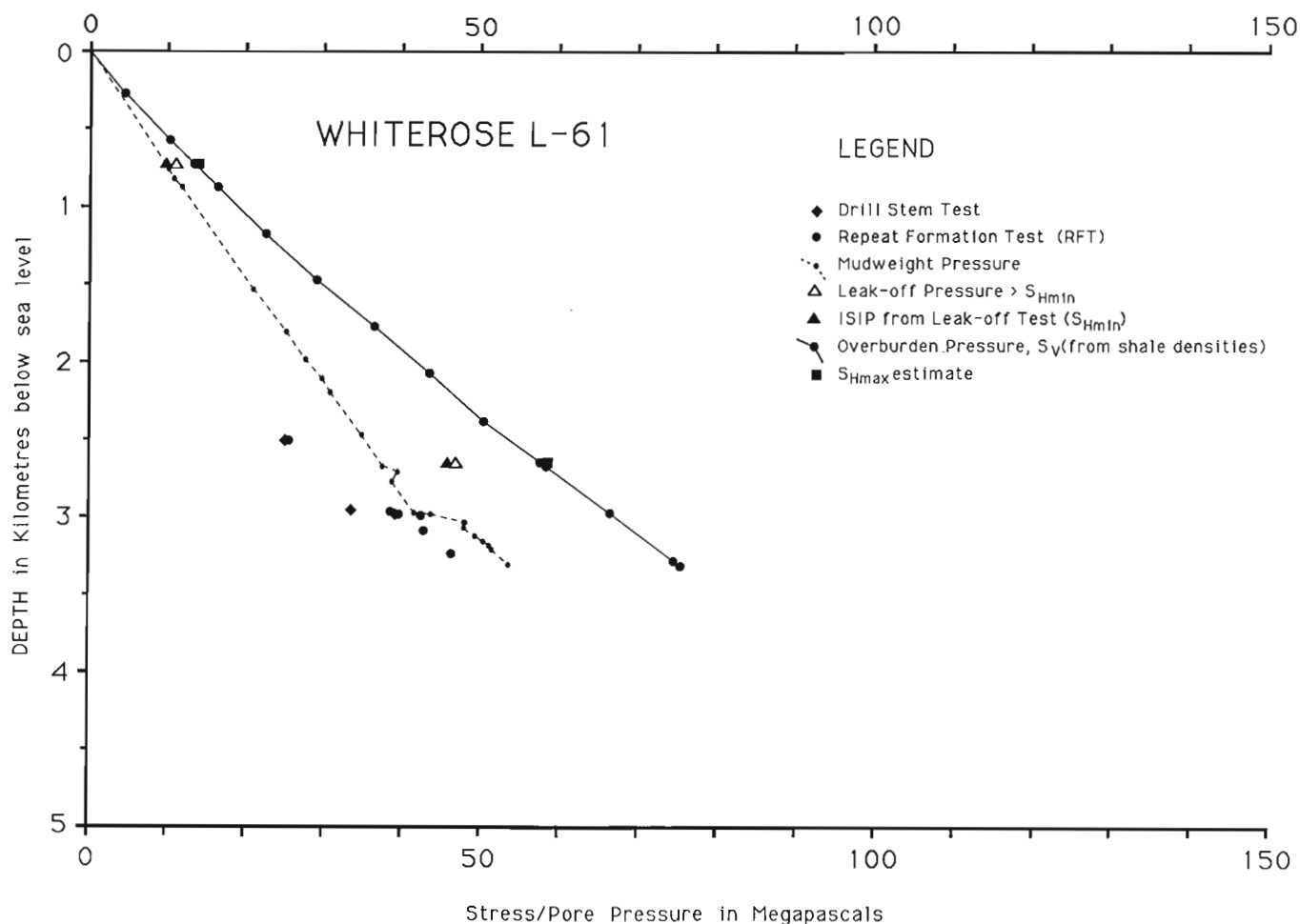


Figure 6. Pressure/depth plot of pore pressures and estimated principal stresses at Whiterose L-61. The well was drilled with mud weights in excess of hydrostatic pressure although drill stem tests and a repeat formation test suggest that the well is normally pressured above 2977 m depth. Below this level, the mud weights were raised due to concern about overpressuring, which is supported by repeat formation tests. Leak-off pressure levels are similar to N-22 and J-49, suggesting a similar S_{Hmin} profile. The apparently low S_{Hmax} values in L-61 result from using overbalanced mud weights for pore pressures in equations 2 and 3. The true values are likely to exceed S_v as in Whiterose N-22.

stress, it will overestimate S_{Hmax} . In the above example, using this relationship suggests that S_{Hmax} is greater than 21.2 MPa.

Stress magnitude calculations for all three wells are portrayed graphically in Figures 3, 5 and 6 and listed in Table 1. The data point to a stress regime where $S_{Hmax} > S_v > S_{Hmin}$ at all depths except locally above 1000 m, where S_v may be the greatest principal stress. Also shown on the figures are the mud pressure profiles and fluid pressures measured during drill stem and repeat formation tests. These data suggest that significant overpressures were not encountered in Whiterose N-22, J-49 or L-61. There are indications of mild overpressuring below 2400 m in Whiterose N-22 (Fig. 5) and, possibly, below approximately 3000 m in Whiterose L-61 (Fig. 6).

SUMMARY AND CONCLUSIONS

Leak-off tests open small fractures in the sides of well bores and can be used to measure the magnitudes of the smallest principal stresses acting on rocks at a specific depth. The most accurate measurements are those where the fracture is opened and a record of pressure bleed-off is obtained. Ideally, bleed-off should be monitored until there is a clear indication that the fracture has closed (i.e., for a sufficient time to identify a marked reduction in the rate of pressure decline). Clearly it is also worth repeating a leak-off test, so that the fracture reopening pressure can be measured, because this permits a more accurate assessment of S_{Hmax} .

This case history shows how well-documented leak-off test information, together with other exploration well data, can yield excellent in situ stress magnitude information. Such records are very valuable because they can be treated like hydraulic fracture pressure/time plots and used to infer both formation breakdown pressures and the pressure at which the fracture closes (i.e., the smallest principal stress). If reliable pore pressure measurements are also available for the depths in question, good estimates of the larger horizontal principal stress magnitudes can be obtained as well. The Whiterose well history reports contain such information and provide an excellent case history for stress magnitude estimation in an offshore sedimentary basin where virgin geomechanical conditions (i.e., no hydrocarbon production) still prevail. Unfortunately, such data suites are rarely recorded. More often, leak-off test results are merely reported as single pressures, thus much valuable information is lost.

ACKNOWLEDGMENTS

The authors are most grateful to M. Labonté and D. N. Skibo, who reviewed the manuscript and suggested improvements, and to Husky Oil Ltd. for the loan of well history reports.

REFERENCES

- Bass, J. D., Schmitt, D. R., and Ahrens T. J.**
1986: Holographic in-situ stress measurements; Royal Astronomical Society, *Geophysical Journal*, v. 85, p. 13-41.
- Bell, J. S.**
in press a: Investigating stress regimes in sedimentary basins using information from oil industry wireline logs and drilling records; in *Geological Applications of Wireline Logs*, ed. A. Hurst, Geological Society of London, Special Publication.
in press b: The stress regime of the Scotian Shelf, offshore eastern Canada, to 6 kilometres depth and implications for rock mechanics and hydrocarbon migration; in *Rock at Great Depth*, Victor Maury and D. Fourmaintraux; A. A. Balkema, Rotterdam, v. 3.
- Breckels, I. M. and Van Eekelen, H. A. M.**
1981: Relationship between horizontal stress and depth in sedimentary basins; Paper SPE10336, 56th Annual Fall Technical Conference, Society of Petroleum Engineers of AIME, San Antonio, Texas, October 5-7, 1981.
- Bredehoeft, J. D., Wolff, R. G., Keys, W. S., and Shuter, E.**
1976: Hydraulic fracturing to determine the regional in-situ stress field, Piceance Basin, Colorado; *Geological Society of America, Bulletin*, v. 87, p. 250-280.
- Dickey, P. A.**
1986: *Petroleum Development Geology*, 3rd Edition; Pennwell Books, Oklahoma, 530 p.
- Ervine, W. B., and Bell, J. S.**
1987: Subsurface in-situ stress magnitudes from oil well drilling records: an example from the Venture area, offshore Eastern Canada; *Canadian Journal of Earth Sciences*, v. 24, p. 1748-1759.
- Haimson, B. C., and Fairhurst, C.**
1970: In-situ stress determination at great depth by means of hydraulic fracturing; in *Rock Mechanics - Theory and Practice*; Proceedings of the 11th Symposium on Rock Mechanics, ed. W. Somerton; American Institute of Mining Engineers, New York, p. 559-584.
- Husky-Bow Valley**
1985: Whiterose N-22 Well History Report, 179 p. plus Appendices, (available from COGLA).
1986: Whiterose J-49 Well History Report, 65 p. plus Appendices, (available from COGLA).
1987: Whiterose L-61 Well History Report, 66 p. plus Appendices, (available from COGLA).
- McLellan, P.**
1988: In situ stress prediction and measurement by hydraulic fracturing, Wapiti, Alberta; *Journal of Canadian Petroleum Technology*, v. 27, no. 2, p. 85-95.
- Montgomery, C. T., and Ren, N-K.**
1983: Differential strain curve analysis: does it work? in *Hydraulic Fracture Stress Measurements*, ed. M.D. Zoback and B.C. Haimson; National Academy Press, Washington, D.C., p. 239-245.
- Teufel, L. W.**
1989: On recent in situ stress measurements in Ekofisk Gas Field. Paper presented at International Society of Rock Mechanics - Society of Petroleum Engineers Symposium "Rock at Great Depth", Pau, France, August 28-31, 1989.
- Teufel, L. W. and Warpinski, N. R.**
1984: Determination of in situ stress from anelastic strain recovery measurements of oriented core: comparison to hydraulic fracture stress measurements in the Piceance Basin, Colorado. Paper presented at 25th U. S. Symposium on Rock Mechanics, Evanston, Illinois, June 1984.

Lithostratigraphy of upper Middle Ordovician sedimentary rocks, lower Ottawa Valley, Ontario and Quebec

H.M. Steele-Petrovich¹
Institute of Sedimentary and Petroleum Geology, Calgary

Steele-Petrovich, H.M., Lithostratigraphy of upper Middle Ordovician sedimentary rocks, lower Ottawa Valley, Ontario and Quebec; in Current Research, Part B, Geological Survey of Canada, Paper 90-1B, p. 131-134, 1990.

Abstract

The Middle Ordovician carbonate rocks of this study occur in the eastern part of the Ottawa Valley, and are traditionally assigned to the Hull, Sherman Fall and Cobourg formations of the Trenton Group. These rocks are subdivided here on the basis of the recurring interbedded lithofacies that are defined in this study. The carbonate rocks appear to have been deposited on offshore shoals, in environments associated with the shoals, and in deeper water offshore environments.

Résumé

Les roches carbonatées de l'Ordovicien moyen de la présente étude se trouvent dans la partie est de la vallée de l'Outaouais, et on les rattache généralement aux formations de Hull, de Sherman Fall et de Cobourg du groupe de Trenton. On les divise dans cette région en fonction de leurs lithofaciès interstratifiés cycliques, définis dans la présente étude. Elles avaient été mises en place sur des hauts fonds marins, dans des milieux associés à des hauts fonds et dans des milieux marins profonds.

¹ 1463 Valley Rd., Bartlesville, Oklahoma 74003, U.S.A.

INTRODUCTION

This report, based on fieldwork carried out during the summers of 1987 and 1988, deals with the Middle Ordovician carbonate rocks that occur in a highly faulted terrane (Wilson, 1946; Sanford et al., 1979) in the eastern part of the Ottawa Valley, between Ottawa and Hawkesbury (Fig. 1). These rocks include the units that have been assigned traditionally to the Hull, Sherman Fall, and Cobourg formations (or members) of the Trenton Group (or Formation) (e.g., Wilson, 1946), or, more recently, to the Bobcaygeon, Verulam, and Lindsay formations (or members) of the Ottawa Group (or Formation) (Liberty, 1967, 1981; Williams and Rae, 1983; Williams and Telford, 1986, 1987, Table 1). Stratigraphically, these carbonate rocks occur immediately above the sequence discussed in a previous report (Steele-Petrovich, 1989).

Table 1. Relationships between the lithostratigraphic classifications used by different authors for the rocks of this study.

TRADITIONAL CLASSIFICATION (SEE WILSON 1946)		LIBERTY 1967, 1981	WILLIAMS & TELFORD 1986	THIS STUDY
TRENTON	COBOURG	LINDSAY	LINDSAY	η
	SHERMAN FALL	VERULAM	VERULAM	ζ
	HULL		BOBCAYGEON	ε

Table 2. Lithostratigraphic units and their lithofacies composition. Lithofacies listed in order of dominance.

Lithostratigraphic Units	Lithofacies
η	<ol style="list-style-type: none"> 1. Fine grained, somewhat recrystallized, commonly laminated limestone. Fossils unusually rare. Local occurrences of small chert nodules. Beds regular, well defined, 5-30 cm thick. 2. Medium grained, somewhat recrystallized, bioclastic, intraclastic, fossiliferous, commonly shaly limestone. Nodular structure rare. 3. Thin, relatively unfossiliferous, calcareous shale partings and interbeds (up to 7 cm thick).
ζ	<ol style="list-style-type: none"> 1. Fine to medium grained, somewhat recrystallized, highly fossiliferous, shaly limestone. Beds 5-8 cm thick. 2. Grey fossiliferous, calcareous shales. Beds 2-5 cm thick.
ε	<ol style="list-style-type: none"> 1. Fine grained, commonly laminated, unfossiliferous, slightly to highly recrystallized limestone. Beds well defined, 5-40 cm thick. Chert nodules and lenses common locally. 2. Medium to very coarse grained, bioclastic, fossiliferous, slightly to highly recrystallized limestone. Sorting and rounding generally poor. Occurs as lenses, or beds up to 1 m thick. Conspicuous crosslaminae and crossbedding common. 3. Medium grained, highly recrystallized, unfossiliferous, stylonitic limestone. Horizontal laminae, crosslaminae, and crossbeds present locally. Beds massive. 4. Thin calcareous shale partings and interbeds. Generally unfossiliferous. 5. Sublithographic limestone.

Definitions
 Very fine grained: individual grains not distinguishable with hand lens (10x).
 Fine grained: individual grains visible with hand lens but not identifiable.
 Medium grained: individual particles visible to naked eye but not identifiable.
 Coarse grained; particles identifiable to naked eye but generally smaller than 1 cm.
 Very coarse grained: particles generally larger than 1 cm.

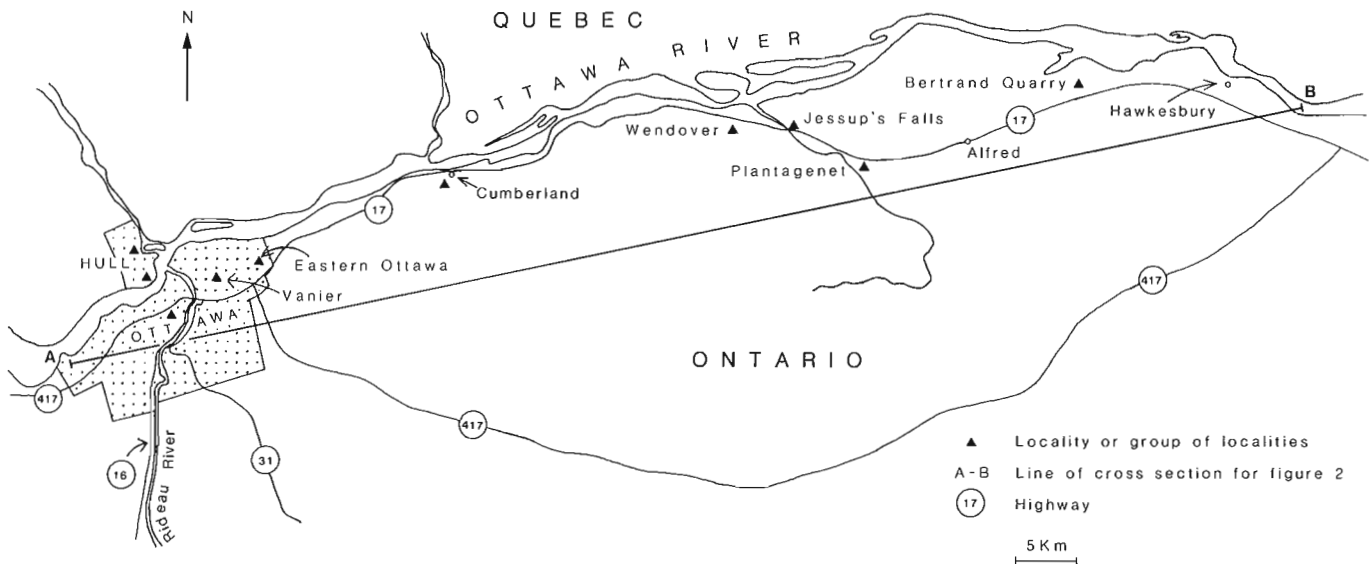


Figure 1. Locality map.

METHOD OF STUDY

Stratigraphic sections were studied in the field at 13 localities. The different lithofacies were identified, their geographic and stratigraphic positions were noted, and the physical characteristics of each occurrence were recorded. At least one rock sample from each occurrence and as many of the contained fossils as possible were collected for future laboratory studies.

LITHOSTRATIGRAPHIC UNITS

As noted previously (Steele-Petrovich, 1984, 1986, 1989), certain lithofacies of Middle Ordovician age from the Ottawa Valley are highly interbedded, making correlation of individual lithofacies impossible; however, sets of interbedded lithofacies form well delineated lithostratigraphic units that can be correlated and should have formation (or possibly member) status. The lithostratigraphic

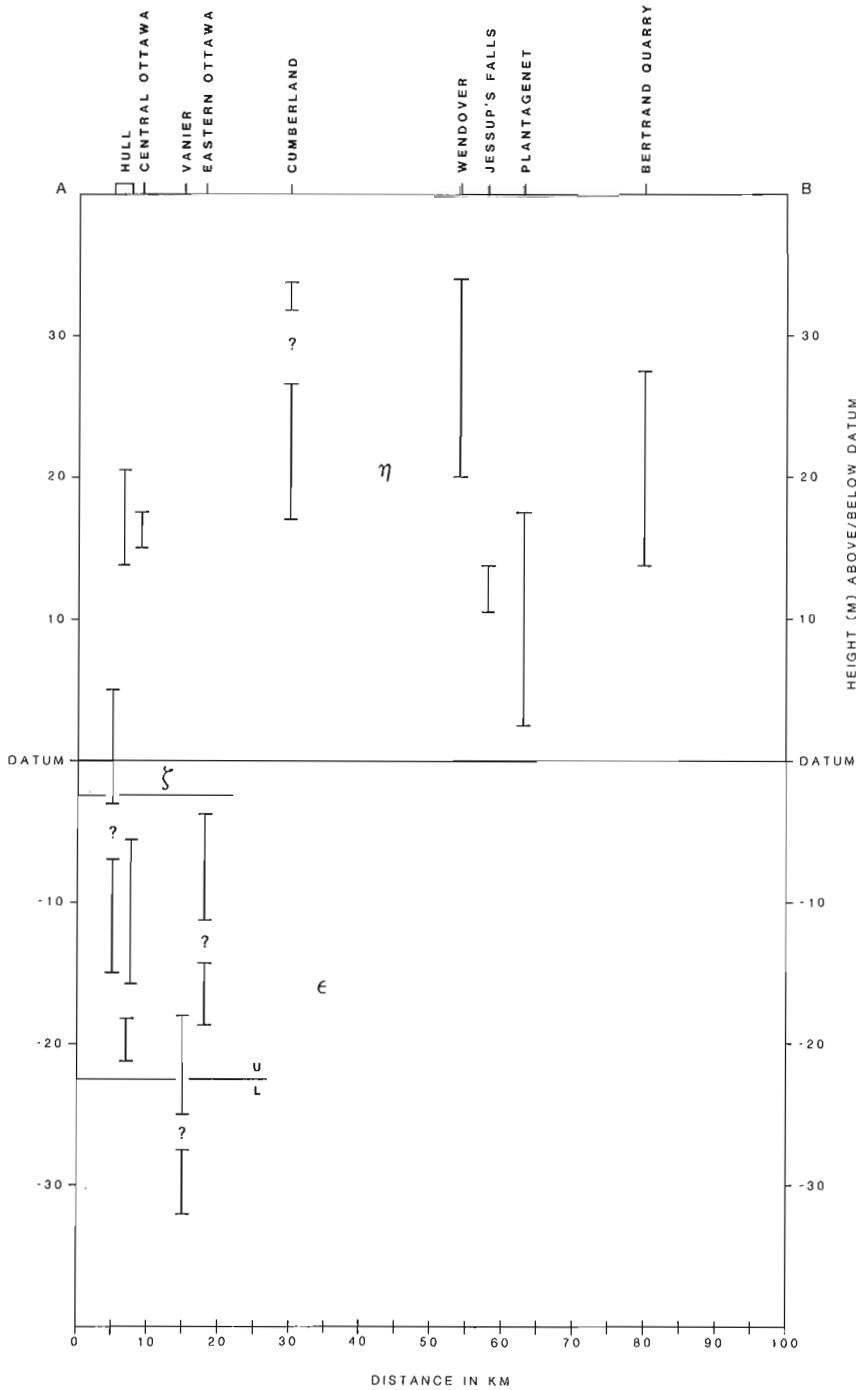


Figure 2. Measured sections, projected onto AB of Figure 1. ϵ , ζ , η : provisional names of proposed lithostratigraphic units. Datum: base of unit η . ?: covered interval of unknown thickness. Stratigraphic positions of outcrops that do not include the datum are estimated from lithological evidence. Thickness of the upper part of unit is taken from Uyeno (1974).

units of this study are called here, provisionally, and in ascending order, ϵ (epsilon), ζ (zeta), and η (eta); the constituent lithofacies are described in Table 2. A comprehensive study of the stratigraphy, including consideration of the names of the different units, is being prepared for the Middle Ordovician rocks of the whole of the Ottawa Valley.

No obvious contact between units δ (the top unit of the previous study) and ϵ (the lowest unit of this study) is exposed today in the field area, although the laminated and crosslaminated packstone at the top of the Rockland quarry (Steele-Petrovich, 1989) may indicate a transition into unit ϵ . The contact between units ϵ and ζ is sharply defined at the only locality where it is exposed. A contact between units ζ and η appears to occur at one locality and appears to be sharp; however, a fault contact cannot be ruled out at this stage of the work. Fieldwork has not been completed at the top of unit η and the upper boundary of that unit has not been determined.

Units ϵ , ζ , and η of this study do not occur in the western part of the Ottawa Valley (cf. Steele-Petrovich, 1984, 1986) and, in the east, units ϵ and ζ occur only in the vicinity of Ottawa. Unit ϵ (Table 2) consists of two parts: the lower part is composed of fine grained, commonly laminated, unfossiliferous, somewhat recrystallized limestone (1) with thin shale partings and interbeds (4); the upper part is composed mainly of medium- to very coarse-grained, bioclastic, fossiliferous, slightly to highly recrystallized limestone (2), and commonly includes thin interbeds of (1) and (4); more rarely (1) and (2) are interbedded subequally. Medium grained, highly recrystallized, unfossiliferous, massive, stylolitic limestone (3) occurs locally in the upper part of unit ϵ . Thin beds of sublithographic limestone (5) occur rarely in the upper part of unit ϵ . Unit ζ consists of interbeds of fossiliferous shaly limestone (1) and fossiliferous calcareous shale (2); at one time this unit was exposed at several localities in Hull, but only one unusually thin exposure remains today. Unit η is commonly dominated by either the fine grained, laminated, unfossiliferous limestone (1), or the coarser grained, bioclastic, intraclastic, fossiliferous limestone (2), with each lithofacies incorporating lenses and thin interbeds of the other; however, there are also localities where (1) and (2) are interbedded subequally. Interbeds of relatively unfossiliferous, calcareous shale and thin shaly partings (3) are found at irregular intervals throughout unit η .

PALEOENVIRONMENTS

Preliminary interpretations are as follows: the coarse grained bioclastic packstone that comprises the upper part of unit ϵ , formed in offshore shoal deposits; the finer grained, laminated sediments that form the lower part of unit ϵ , were probably deposited in the lee of the shoals; and the shaly limestones and shales of unit ζ were deposited in quiet, deeper water, protected regions in front of the shoals. It is generally considered that units ϵ and ζ occur throughout the eastern part of the Ottawa Valley; the absence of outcrops of these units east of Ottawa (Fig. 2) is usually

attributed to differential exposure, due, at least in part, to intense faulting (e.g., Wilson, 1946; Williams et al., 1985a, b). However, since shoal deposits commonly have only a local distribution, units ϵ and ζ originally may have been restricted to the vicinity of the present city of Ottawa. Unit η occurs throughout the field area and appears to have been deposited in deeper water, offshore environments.

ACKNOWLEDGMENTS

I thank M.J. Copeland and T.E. Bolton for logistical assistance and helpful discussions, S.N. Petrovich for help in the field, and R. Petrovich for editorial comments. GSC contract nos. 23233-7-0179/01-SZ and GSC 23233-8-0119/01-SZ.

REFERENCES

- Liberty, B.A.**
1967: Ordovician stratigraphy of Southern Ontario: the Ottawa Valley problem; Abstracts, Geological Association of Canada and Mineralogical Association of Canada, International Meeting, p. 49, 50.
1981: Lower and Middle Ordovician stratigraphy of the Ottawa area; Brock University Department of Geological Sciences, Research Report Series 25, Studies in Paleozoic Stratigraphic Investigations no. 1, p. 19-33.
- Sanford, B.V., Grant, A.C., Wade, J.A., and Barss, M.S.**
1979: Geology of Eastern Canada and adjacent areas; Geological Survey of Canada, Map 1401A.
- Steele-Petrovich, H.M.**
1984: Stratigraphy and paleoenvironments of Middle Ordovician carbonate rocks, Ottawa Valley, Canada; unpublished Ph.D. thesis, Yale University, New Haven, Connecticut, 477 p.
1986: Lithostratigraphy and a summary of the paleoenvironments of the lower Middle Ordovician sedimentary rocks, upper Ottawa Valley, Ontario; *in* Current Research, Part B, Geological Survey of Canada, Paper 86-1B, p. 493-506.
1989: A preliminary report on the lithostratigraphy of lower Middle Ordovician sedimentary rocks, lower Ottawa Valley, Ontario; *in* Current Research, Part B, Geological Survey of Canada, Paper 89-1B, p. 121-125.
- Uyeno, T.T.**
1974: Conodonts of the Hull Formation, Ottawa Group (Middle Ordovician), of the Ottawa-Hull area, Ontario and Quebec; Geological Survey of Canada, Bulletin 248, 31 p.
- Williams, D.A. and Rae, A.**
1983: Paleozoic geology of the Ottawa-St. Lawrence Lowland, Southern Ontario; Ontario Geological Survey, Miscellaneous Paper 116, p. 107-110.
- Williams, D.A., Rae, A., and Wolf, R.R.**
1985a: Paleozoic geology of the Russel-Thurso area, Southern Ontario; Ontario Geological Survey, Map 2717, Geological Series-Preliminary Map.
1985b: Paleozoic geology of the Hawkesbury-Lachute area, Southern Ontario; Ontario Geological Survey, Map 2718, Geological Series-Preliminary Map.
- Williams, D.A. and Telford, P.G.**
1986: Paleozoic geology of the Ottawa area; Geological Association of Canada, Mineralogical Association of Canada, and Canadian Geophysical Union, Joint Annual Meeting, 1986, Ottawa, Ontario; Field Trip 8, Guidebook, p. 1-25.
1987: Structure and Ordovician stratigraphy of the Ottawa area, Southern Ontario; Geological Society of America Centennial Field Guides-Northeastern Section, p. 349-352.
- Wilson, A.E.**
1946: Geology of the Ottawa-St. Lawrence Lowland, Ontario and Quebec; Geological Survey of Canada, Memoir 241, 65 p.

AUTHOR INDEX

Adams, J.	105	McCallum, R.E.	123
Asselin, E.	17	Moran, K.	29
Banke, E.	43	Paradis, S.	1
Bell, J.S.	123	Parrott, D.R.	43
Birkett, T.C.	1	Piper, D.J.W.	29
Dubé, B.	77	Rencz, A.N.	91
Du Berger, R.	115	Rodrigues, C.	49
Fader, G.B.J.	43	Sanford, B.V.	33
Gipp, M.R.	29	Sangster, D.F.	91
Godue, R.	1	Sinclair, W.D.	95
Grant, A.C.	33	Sonnichsen, G.V.	43
Josenhans, H.	59	Steele-Petrovich, H.M.	131
Kingston, D.M.	95	Tassé, N.	17
Lamontagne, M.	115	Vilks, G.	49
Lavoie, D.	17	Wetmiller, R.J.	105, 115
Lewis, C.F.M.	43	Zevenhuizen, J.	59
MacLean, B.	49, 59		

Geological Survey of Canada, Paper 90-1, Current Research is published as six parts, listed below, that can be purchased separately.

Recherches en cours, une publication de la Commission géologique du Canada, Étude 90-1, est publiée en huit parties, énumérées ci-dessous; chaque partie est vendue séparément.

Part A, National and general programs
Partie A, Programmes nationaux et généraux

Part B, Eastern and Atlantic Canada
Partie B, Est et région atlantique du Canada

Part C, Canadian Shield
Partie C, Bouclier canadien

Part D, Interior Plains and Arctic Canada
Partie D, Plaines intérieures et région arctique du Canada

Part E, Cordillera and Pacific Margin
Partie E, Cordillère et marge du Pacifique

Part F, Frontier Geoscience Program, Cordilleran and offshore basins, British Columbia
Partie F, Programme géoscientifique des régions pionnières, bassins de la Cordillère et extracôtiers, Colombie-Britannique.